Classification and Birational Equivalence of Dimer Integrable Systems for Reflexive Polygons

Minsung Kho,[a] **Norton Lee,**[b] **Rak-Kyeong Seong**[a,c]

[a]*Department of Mathematical Sciences, and* [c]*Department of Physics,*
  Ulsan National Institute of Science and Technology,
  50 UNIST-gil, Ulsan 44919, South Korea

[b]*Center for Geometry and Physics, Institute for Basic Science (IBS),*
  Pohang 37673, South Korea

  E-mail: minsung@unist.ac.kr, norton.lee@ibs.re.kr,
  seong@unist.ac.kr

ABSTRACT: Brane tilings are bipartite periodic graphs on the 2-torus and realize a large family of $4d$ $\mathcal{N} = 1$ supersymmetric gauge theories corresponding to toric Calabi-Yau 3-folds. We present a complete classification of dimer integrable systems corresponding to the 30 brane tilings whose toric Calabi-Yau 3-folds are given by the 16 reflexive polygons in 2 dimensions. For each dimer integrable system associated to a reflexive polygon, we present the Casimirs, the single Hamiltonian built from 1-loops, the spectral curve, and the Poisson commutation relations. We also identify all birational equivalences between dimer integrable systems in this classification by presenting the birational transformations that match the Casimirs and the Hamiltonians as well as the spectral curves and Poisson structures between equivalent dimer integrable systems. In total, we identify 16 pairs of birationally equivalent dimer integrable systems which combined with Seiberg duality between the corresponding brane tilings form 5 distinct equivalence classes. Echoing phenomena observed for brane brick models realizing a family of $2d$ $(0, 2)$ supersymmetric gauge theories corresponding to toric Calabi-Yau 4-folds, we illustrate that deformations of brane tilings, including mass deformations, correspond to the birational transformations we discover in this work, and leave invariant the number of generators of the mesonic moduli space as well as the corresponding $U(1)_R$-refined Hilbert series.

Contents

---

1 Introduction

Brane tilings [1–3] as bipartite periodic graphs on a 2-torus form a large family of $4d$ $\mathcal{N} = 1$ supersymmetric gauge theories corresponding to toric Calabi-Yau 3-folds. The $4d$ $\mathcal{N} = 1$ supersymmetric gauge theories are worldvolume theories of a stack of D3-branes probing the associated toric Calabi-Yau 3-folds. By Goncharov and Kenyon, brane tilings have also been shown to correspond to an equally large family of integrable systems, now known as **dimer integrable systems** [4, 5]. The bipartite graph on the 2-torus, also known as a dimer in the literature [6, 7], not only encodes the $4d$ $\mathcal{N} = 1$ theory as well as the Type IIB brane configuration in string theory that realizes it, but also the Casimirs, Hamiltonians, the spectral curve and the Poisson commutation relations of the underlying dimer integrable system.

    Various aspects of dimer integrable systems have been studied [8–14] since the initial work by Goncharov and Kenyon. However, there has not been a systematic attempt in classifying dimer integrable systems as it is the case for brane tilings and corresponding $4d$ $\mathcal{N} = 1$ supersymmetric gauge theories [15]. For brane tilings, one of the largest collections has been obtained through the classification based on toric

Calabi-Yau 3-folds whose toric diagrams [16–21] are one of the **16 reflexive polygons** in $\mathbb{Z}^2$. Reflexive polytopes [22, 23] are convex lattice polytopes with a single interior point as the origin and have been classified up to dimension 4 by Kreuzer and Skarke in [24–26]. The classification in [15] is based on the 16 reflexive polygons in dimension 2 shown in Figure 1 that correspond to 16 toric Calabi-Yau 3-folds, including the zeroth Hirzebruch surface [1, 2, 27], the del Pezzo surfaces [27–30] and certain abelian orbifolds of $\mathbb{C}^3$ [31, 32]. The classification in [15] resulted in 30 brane tilings associated to these 16 toric Calabi-Yau 3-folds. There are more brane tilings and associated $4d$ $\mathcal{N} = 1$ supersymmetric gauge theories than toric Calabi-Yau 3-folds due to the fact that some brane tilings and $4d$ $\mathcal{N} = 1$ theories correspond to the same toric Calabi-Yau 3-fold due to Seiberg duality [33], which is also known as toric duality in this context [27, 28, 30, 34, 35].

Based on this classification of brane tilings for toric Calabi-Yau 3-folds with reflexive polygons as toric diagrams, the following work has the aim to identify the corresponding dimer integrable systems. For the 30 brane tilings, we identify 30 dimer integrable systems with their corresponding Casimirs and Hamiltonians, the spectral curve and the Poisson commutation relations. Here we note that because these dimer integrable systems correspond to toric Calabi-Yau 3-folds with reflexive toric diagrams, the dimer integrable systems possess only one Hamiltonian associated to the single interior point of the toric diagrams.

As part of this classification, we also identify the complete collection of birational equivalences between dimer integrable systems corresponding to the reflexive polygons in 2 dimensions. As observed in [13], when two toric Calabi-Yau 3-folds with their corresponding toric varieties are related by a birational transformation [36–42], then the associated brane tilings define dimer integrable systems, which are birationally equivalent to each other. Under what is now known as **birational equivalence** between dimer integrable systems, the birational transformation identifies the Casimirs and Hamiltonians as well as the spectral curve and the Poisson commutation relations between the two birationally equivalent dimer integrable systems. In the following work, we identify out of the 30 dimer integrable systems in our classification in total 16 pairs of birationally equivalent dimer integrable systems.

We note here that besides birational equivalence, dimer integrable systems can also be equivalent when the corresponding brane tilings and the $4d$ $\mathcal{N} = 1$ supersymmetric gauge theories are related by Seiberg duality [27, 28, 30, 33–35]. Under Seiberg duality, the bipartite period graph of the brane tiling undergoes a local deformation also referred to as a spider move or urban renewal [4, 43, 44]. Under this local mutation of the periodic bipartite graph, the associated dimer integrable system undergoes a canonical transformation that leaves the integrable system and the corresponding Pois-
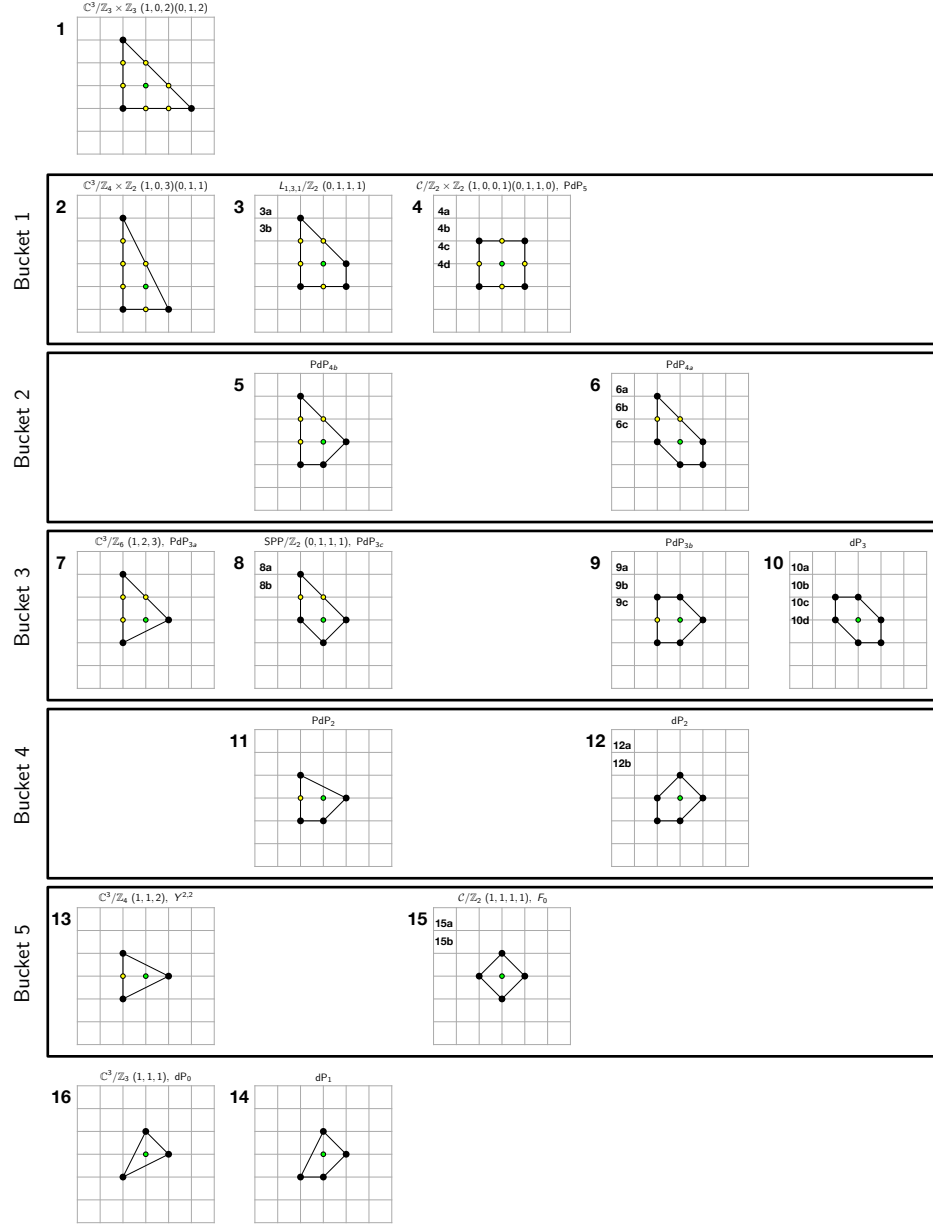
Figure 1: The 16 reflexive polygons in 2 dimensions with labels corresponding to the associated 30 brane tilings classified in [15]. Birational transformations between toric Calabi-Yau 3-folds correspond to birational equivalence between the associated dimer integrable systems. Combined with Seiberg duality, we identify 5 equivalence classes called buckets amongst the 30 brane tilings and dimer integrable systems classified in this work.

son moduli space invariant [4]. When equivalence due to Seiberg duality is combined with birational equivalence between dimer integrable systems, we are able to identify 5 distinct equivalence classes amongst the 30 dimer integrable systems classified in this work. We refer to these equivalence classes as **buckets** [38]. These are illustrated with the corresponding reflexive toric diagrams in Figure 1.

Birational transformations between toric Calabi-Yau 4-folds and associated $2d$ $(0,2)$ supersymmetric gauge theories given by brane brick models [45–50] have been studied extensively in [41, 42]. In particular, it has been shown that mass deformation between brane brick models [51] realizing $2d$ $(0,2)$ supersymmetric gauge theories can be identified with a birational transformation between the corresponding toric Calabi-Yau 4-folds. This result has been recently extended to relevant deformations of brane brick models in [52]. In this work, we see that brane tilings related by deformations [53–55], including mass deformations [56–58], correspond to birationally equivalent dimer integrable systems.

As observed for brane brick models corresponding to toric Calabi-Yau 4-folds [41, 42] as well as in the context of generalized toric polygons (GTPs) [59], we observe as part of our classification that brane tilings and dimer integrable systems that are related by a birational transformation have the same Hilbert series [60–64] of the mesonic moduli space of the associated abelian $4d$ $\mathcal{N} = 1$ supersymmetric gauge theory [28], when the Hilbert series is refined under a $U(1)_R$ symmetry that gives generators of the mesonic moduli space the same $U(1)_R$ charge and gives the superpotentials of the brane tilings $U(1)_R$ charge 2. Moreover, as observed for brane brick models in [41, 42], we also confirm in this work that the mesonic moduli spaces have the same number of generators for brane tilings and dimer integrable systems that are related by a birational transformation.

Our work is organized as follows. Section §2 gives a brief overview about brane tilings and the corresponding family of $4d$ $\mathcal{N} = 1$ supersymmetric gauge theories. The section also reviews the moduli spaces of the abelian $4d$ $\mathcal{N} = 1$ theories, including the mesonic moduli space [28] and the master space [65–67], and then summarizes the family of toric Calabi-Yau 3-folds whose toric diagrams are reflexive polygons. While discussing the moduli spaces, the section also gives an overview of Seiberg duality that preserves the mesonic moduli space, also referred to as toric duality [27, 28, 30, 33–35], as well as specular duality [68] which preserves the master space. The section then gives a detailed review on how brane tilings define dimer integrable systems and the observation in [13] on how dimer integrable systems can be equivalent under birational transformations between the corresponding toric Calabi-Yau 3-folds. Sections §3 to §18 summarize the 30 brane tilings and the corresponding dimer integrable systems

corresponding to the 16 reflexive polygons, giving explicit expressions for the Casimirs, Hamiltonians, the spectral curve and the Poisson commutation relations for each of the dimer integrable systems. Sections §19 to §23 summarize the birational transformations that map between equivalent dimer integrable systems in the classification. The sections explicitly show the mapping between the Casimirs, Hamiltonians, the spectral curve and the Poisson commutation relations of the birationally equivalent dimer integrable systems. Moreover, the sections are organized in terms of buckets containing dimer integrable systems that are birationally equivalent and also dimer integrable systems that are equivalent under Seiberg duality of the corresponding brane tilings. For completeness, these sections also summarize how within the buckets brane tilings that are related by birational transformations all share the same number of generators of the mesonic moduli space of the associated $4d$ $\mathcal{N} = 1$ theories. Moreover, the sections illustrate how the Hilbert series of the mesonic moduli space refined only under the $U(1)_R$ symmetry is invariant within each of the buckets. We conclude our work in section §24 with an overview of our results as well as an overview on the correspondence between birational transformations of toric Calabi-Yau 3-folds, deformations of brane tilings, birational equivalence between dimer integrable systems, and Hanany-Witten moves for (p, q) webs and corresponding $5d$ $\mathcal{N} = 1$ theories.

2   Background

2.1   Brane tilings and $4d$ $\mathcal{N} = 1$ Quiver Gauge Theories

A **brane tiling** [1–3], also known as a **dimer model** [6, 7], is a periodic bipartite graph on a 2-torus T^2. The bipartite graph consists of black and white nodes where edges connect nodes of opposite color. Brane tilings realize a family of $4d$ $\mathcal{N} = 1$ gauge theories, which are worldvolume theories of D3-branes probing a toric Calabi-Yau 3-fold [27, 28, 69, 70].

	0	1	2	3	4	5	6	7	8	9
D3	×	×	×	×	·	·	·	·	·	·
CY3	·	·	·	·	×	×	×	×	×	×

Table 1: The D3-branes probing a toric Calabi-Yau 3-fold. The worldvolume theory on the probe D3-branes is a $4d$ $\mathcal{N} = 1$ supersymmetric gauge theory given by a brane tiling.

The probe D3-branes at the Calabi-Yau singularity, as summarized in Table 1, become under T-duality D5-branes suspended between a NS5-brane wrapping a 2-torus T^2. In this Type IIB brane configuration, the D5-branes extend along the (012345) directions, and the NS5-brane extends along the (0123) directions and wraps a holomorphic curve Σ defined in terms of directions (4567) as summarized in Table 2. The holomorphic curve Σ is given by,

$$\Sigma : P(x,y) = 0 \text{ for } x, y \in \mathbb{C}^* \ , \tag{2.1}$$

where the complex coordinates x and y come from the directions (45) and (67), respectively. $P(x,y)$ in (2.1) is known as a **Newton polynomial** given by the toric diagram Δ of a toric Calabi-Yau 3-fold. The Newton polynomial for a toric diagram Δ is defined as follows,

$$P(x,y) = \sum_{(n_x, n_y) \in \Delta} c_{(n_x, n_y)} x^{n_x} y^{n_y} \ , \tag{2.2}$$

where the sum is over vertices in Δ with coordinates $(n_x, n_y) \in \mathbb{Z}^2$. The coefficients are associated to complex structure moduli in the corresponding mirror Calabi-Yau and are chosen to be in $c_{(n_x, n_y)} \in \mathbb{C}^*$ [71–73].

	0	1	2	3	4	5	6	7	8	9
D5	×	×	×	×	×	·	×	·	·	·
NS5	×	×	×	×	——Σ——				·	·

Table 2: The Type IIB brane configuration given by a brane tiling, consisting of D5-branes suspended between a NS5-brane wrapping a holomorphic curve Σ.

The brane tiling as a bipartite graph on a 2-torus T^2 represents the Type IIB brane configuration in Table 2. In the following paragraph, we summarize the dictionary that translates between the bipartite graph on T^2 and the corresponding 4d $\mathcal{N} = 1$ quiver gauge theory:

- **Faces** correspond to $U(N)_i$ gauge groups of the 4d $\mathcal{N} = 1$ gauge theory. The faces are all even-sided because of the bipartite nature of the brane tiling on T^2. This also implies that the number of fundamental and anti-fundamental chiral multiples X_{ij} associated to a gauge group $U(N)_i$ is always the same.

- **Edges** correspond to bifundamental chiral multiplets X_{ij} of the 4d $\mathcal{N} = 1$ supersymmetric gauge theory. Every chiral field X_{ij} in the brane tiling transforms

under the bifundamental representation of associated gauge groups $U(N)_i$ and $U(N)_j$, which correspond to the adjacent faces of the edge associated to X_{ij} in the bipartite graph on T^2.

- **White (Black) nodes** correspond to positive (negative) monomial terms in the superpotential of the associated $4d$ $\mathcal{N} = 1$ gauge theory. The monomial terms corresponding to white (black) nodes are given by products of chiral fields, which are associated with the edges that connect to the given white (black) nodes in a clockwise (anti-clockwise) orientation. This orientation along white (black) nodes determines the bifundamental representation of chiral fields associated to the connected edges. This ensures that the monomial product of chiral fields corresponding to the white (black) node is gauge-invariant.

The Newton polynomial of Δ is also given by the permanent of the **Kasteleyn matrix** [74] of the brane tiling. The Kasteleyn matrix K for a brane tiling is a $n \times n$ square matrix, where n is the number of white nodes which is the same as the number of black nodes in a brane tiling. Here, white nodes w_j and black nodes b_k are labelled by $j, k = 1, \ldots, n$. The colouring of nodes in the brane tiling allows us to assign also an orientation *along* the edges from a white node to a black node. Under this orientation, an edge $e_{jk} = (w_j, b_k)$ can be assigned a winding number $h(e_{jk}) = (h_1, h_2) \in \mathbb{Z}^2$ along the two independent S^1 cycles on T^2. Based on the winding number assignment on edges of the brane tiling, the elements of the Kasteleyn matrix are given by,

$$K_{w_j, b_k}(x, y) = \sum_{e_{jk} = (w_j, b_k)} e_{jk} \, x^{h_1(e_{jk})} y^{h_2(e_{jk})} \ , \tag{2.3}$$

where x and y are the fugacities for the winding numbers. The permanent of the Kasteleyn matrix,

$$\text{perm } K(x, y) = P(x, y) \ , \tag{2.4}$$

gives the Newton polynomial defined in (2.2). We note here that the particular form of the Newton polynomial depends on the $GL(2, \mathbb{Z})$ frame chosen for the toric diagram Δ, or equivalently the choice of the fundamental domain in the brane tiling that determines the winding number of edges. We also note that the coefficients $c_{(n_x, n_y)}$ in the Newton polynomial in (2.4) correspond to products of edge variables e_{jk}, which themselves are associated to chiral fields in the $4d$ $\mathcal{N} = 1$ supersymmetric gauge theory. These products of edge variables correspond to a particular subset of edges in the brane tiling associated to each vertex in the toric diagram Δ, which are known as perfect matchings.

A **perfect matching** p_a [1–3, 6, 7] is a collection of edges in a brane tiling that covers all white and black nodes in the bipartite graph precisely once. All perfect matchings for a brane tiling are summarized in a $|E| \times c$ matrix, which we call the perfect matching matrix P. Here, $|E|$ and c indicate the number of edges and perfect matchings, respectively. For simplicity, we label here the edges e_k and the corresponding chiral fields X_k in the brane tiling with a single index $k = 1, \ldots, |E|$. Then, the entries in a perfect matching matrix P are given by,

$$
P_{ka} = \begin{cases} 1 & \text{if } e_k \in p_a \\ 0 & \text{if } e_k \notin p_a \end{cases} .
$$

The perfect matchings correspond to gauged linear sigma model (GLSM) fields [75], and can be used to express each bifundamental chiral field X_k as a product of perfect matchings as follows,

$$
X_k = \prod_a (p_a)^{P_{ka}} , \tag{2.5}
$$

We note here that the F-term constraints from the superpotential W of the $4d\ \mathcal{N} = 1$ theory automatically satisfy the relations in (2.5).

The space of gauge invariant operators satisfying the F- and D–terms of the $4d$ $\mathcal{N} = 1$ supersymmetric quiver gauge theory is known as the **mesonic moduli space** [27, 28]. For an abelian $4d\ \mathcal{N} = 1$ theory with $U(1)$ gauge groups, the mesonic moduli space is precisely the probed toric Calabi-Yau 3-fold. It is defined as follows,

$$
\mathcal{M}^{mes} = \text{Spec}\left(\mathbb{C}[X_{ij}]/\mathcal{I}_{\partial_W}\right)//U(1)^{G-1} , \tag{2.6}
$$

where $\mathbb{C}[X_{ij}]$ is the coordinate ring formed by the chiral fields X_{ij} of the $4d\ \mathcal{N} = 1$ theory and $\mathcal{I}_{\partial_W}$ is the irreducible component of the ideal formed by the F-terms of the form $\partial_{X_{ij}} W = 0$. The F-terms are binomial due to the bipartite nature of the brane tiling and $\mathcal{I}_{\partial_W}$ forms a binomial ideal giving a **toric variety** [16, 17]. We also note that G is the total number of $U(1)$ gauge groups in the abelian $4d\ \mathcal{N} = 1$ theory, where an overall $U(1)$ decouples, and $i, j = 1, \ldots, G$ are the gauge group labels. When we remove the quotient by the $U(1)$ gauge groups in (2.6), we remain with the space of chiral fields X_{ij} subject to the F-terms of the $4d\ \mathcal{N} = 1$ theory,

$$
\mathcal{F}^{\flat}_{\text{Irr}} = \text{Spec } \mathbb{C}[X_{ij}]/\mathcal{I}_{\partial_W} , \tag{2.7}
$$

which is known as the **master space** [65–67] of the brane tiling.

In terms of the GLSM fields corresponding to perfect matchings of the brane tiling, we can express the master space and the mesonic moduli space as the following symplectic quotients,

$$\mathcal{F}^{\flat}_{\mathrm{Irr}} = \mathrm{Spec}\ \mathbb{C}[p_1, \ldots, p_c]//Q_F \ ,$$
$$\mathcal{M}^{mes} = \mathrm{Spec}\left(\mathbb{C}[p_1, \ldots, p_c]//Q_F\right)//Q_D \ , \tag{2.8}$$

where the F-term and D-term constraints are given as $U(1)$ charges on the GLSM fields p_a, which are summarized in the Q_F and Q_D charge matrices, respectively. The computation of the Q_F and Q_D charge matrices using the perfect matching matrix P follows what is known as the forward algorithm for brane tilings [27, 28].

2.2 Reflexive Polygons, Toric Duality and Specular Duality

In this paper, we mainly focus on a special family of brane tilings associated to **reflexive polygons** in $\mathbb{Z}^2$. It is known based on the classification in [15] that there are 30 distinct brane tilings corresponding to the toric Calabi-Yau 3-folds whose toric diagrams [16–21] are one of the 16 reflexive polygons in $\mathbb{Z}^2$. There are more brane tilings because some of them correspond to the same toric Calabi-Yau 3-fold due to **Seiberg duality** between the corresponding $4d\ \mathcal{N} = 1$ theories [33]. This correspondence in the context of toric Calabi-Yau 3-folds associated to $4d\ \mathcal{N} = 1$ theories is also known as **toric duality** [27, 28, 30, 34, 35].

d	number of reflexive polytopes
1	1
2	16
3	4319
4	473800776

Table 3: The number of reflexive polytopes in dimension $d \leq 4$ [24–26].

A convex d-dimensional lattice polytope Δ is **reflexive** if its dual polytope Δ° defined as

$$\Delta^\circ = \{\mathbf{u} \in \mathbb{Z}^d \mid \mathbf{u} \cdot \mathbf{v} \geq -1, \ \forall \mathbf{v} \in \Delta\} \ , \tag{2.9}$$

is also a convex lattice polytope in $\mathbb{Z}^d$ [22, 23]. Due to a classification by Kreuzer and Skarke [24–26], it is known up to lattice dimension 4 that there are finitely many reflexive polytopes up to $GL(d, \mathbb{Z})$ equivalence. Table 3 summarizes the number of reflexive
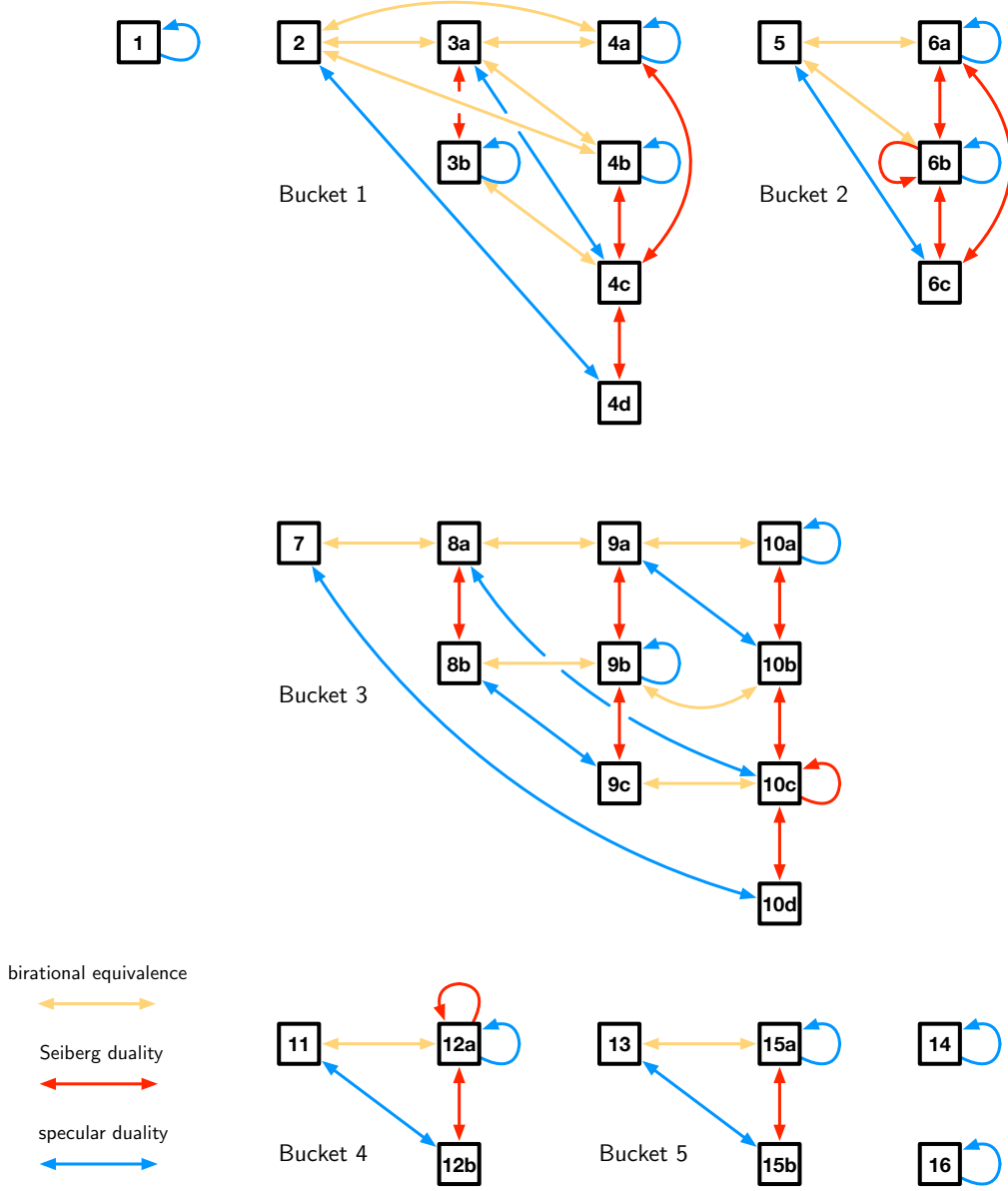
Figure 2: The 30 brane tilings corresponding to the 16 reflexive polygons in dimension 2 are related by Seiberg duality (red), specular duality (blue), and birational transformations (yellow). Under Seiberg duality and under birational transformations, the associated dimer integrable systems are equivalent and form equivalence classes, which we call buckets. The labels correspond to the 30 brane tilings classified in [15] with the corresponding 16 reflexive toric diagrams given in Figure 1.

polytopes up to dimension 4.

As illustrated in Figure 1, there are 16 reflexive polygons up to $GL(2, \mathbb{Z})$ equivalence in $\mathbb{Z}^2$. The 30 brane tilings corresponding to these 16 reflexive polytopes have been fully classified in [15]. Under Seiberg duality, multiple brane tilings and the corresponding $4d\ \mathcal{N} = 1$ theories can correspond to the same toric Calabi-Yau 3-fold as summarized in Figure 2. Seiberg duality can be interpreted as a local mutation of the bipartite graph on T^2, which is also referred to as **urban renewal** or **spider move** [4, 43, 44]. The brane tilings and $4d\ \mathcal{N} = 1$ theories corresponding to the same toric Calabi-Yau 3-fold are referred to as **toric phases** [27, 28, 30, 34, 35]. Figure 3(a) illustrates the local mutation on the brane tiling that identifies the two toric phases corresponding to the cone over the zeroth Hirzebruch surface F_0, whose toric diagram is one of the 16 reflexive polygons in $\mathbb{Z}^2$. The two toric phases are referred to as Model 15a and 15b in Figure 1 and Figure 2.

The rich combinatorial structure of brane tilings led to the discovery of a new correspondence in [68] now known as **specular duality**. This new correspondence identifies brane tilings and the associated abelian $4d\ \mathcal{N} = 1$ theories that have the same master space as defined in (2.7). Like Seiberg duality, specular duality can be interpreted as a deformation of the bipartite graph on a 2-torus T^2, where for reflexive toric diagrams the resulting bipartite graph is again on a 2-torus T^2. Specular duality swaps the roles played by zig-zag paths and faces in a brane tiling as illustrated in Figure 3(b).

2.3 Dimer Integrable Systems

In the following section, we review various aspects of integrable systems corresponding to brane tilings and bipartite graphs on T^2 that were introduced by Goncharov and Kenyon in [4, 5]. Every consistent brane tiling on a 2-torus defines such a **dimer integrable system** whose Casimirs and Hamiltonians as well as the spectral curve and the Poisson commutation relations are encoded in the bipartite graph on T^2.

Edge Variables and Perfect Matching Weights. In order to review dimer integrable systems and how they are encoded in a brane tiling, we first recall that every edge in the bipartite graph on T^2 is associated to a bifundamental chiral field X_{ij} of the $4d\ \mathcal{N} = 1$ theory, where the indices i, j label the gauge groups of the $4d\ \mathcal{N} = 1$ theory associated to the faces of the brane tiling.

Equivalently, we can label each edge by an **edge variable** $e_{jk} = (w_j, b_k)$, where now j labels white nodes w_j and k labels black nodes b_k of the brane tiling. As in [13], we also introduce **directed edge variables** e_{jk}^+ and e_{jk}^-, which indicate respectively
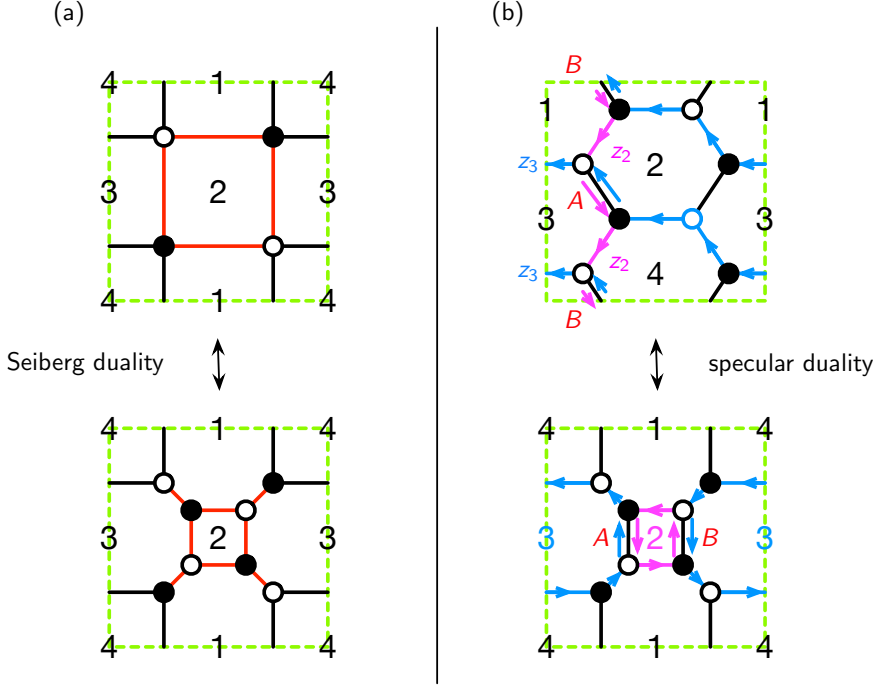
Figure 3: (a) Seiberg duality on brane tilings [27, 28, 30, 34, 35] is a local deformation of the bipartite graph on the 2-torus acting on square faces, which is also known as urban renewal or spider moves [4, 43, 44]. (b) Specular duality on brane tilings [68] swaps directed paths along edges corresponding to zig-zag paths with directed paths around faces and vice versa while preserving intersections between these paths.

whether one moves along an edge from a white node to a black node, or from a black node to a white node,

$$e_{jk}^+ \; : \; w_j \to b_k \; , \; e_{jk}^- \; : \; b_k \to w_j \; . \tag{2.10}$$

Here, we set the convention $e_{jk}^+ \equiv e_{jk}$. As illustrated in [13], directed edge variables $e_{jk}^{\pm}$ allow us to express connected paths along edges in the brane tiling as a sequence of directed edge variables that alternate between white and black nodes. When these connected paths along edges are closed, it is argued in [13, 76, 77] that they form permutations of directed edge variables $e_{jk}^{\pm}$ in the permutation group $S_{2|E|}$, where $|E|$ is the number edges in the brane tiling.

We can also make use of directed edge variables $e_{jk}^{\pm}$ in order to introduce **perfect**
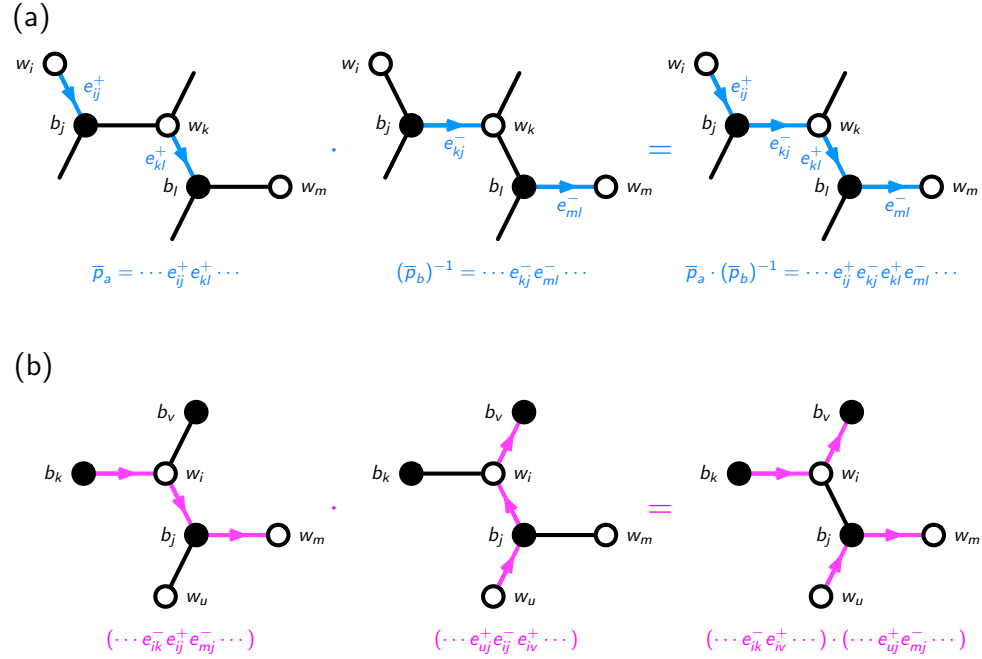
Figure 4: (a) A product of perfect matchings weights $\overline{p}_a$ and $(\overline{p}_b)^{-1}$ in terms of directed edge variables, and (b) a product of closed directed paths given by permutations in $S_{2|E|}$ with a cancellation between a pair of directed edges.

matching weights $\overline{p}_a$ associated to a perfect matching p_a of a brane tiling,

$$\overline{p}_a = \prod_{e_{jk} \in p_a} e_{jk}^+ \ , \ (\overline{p}_a)^{-1} = \prod_{e_{jk} \in p_a} e_{jk}^- \ . \tag{2.11}$$

Defining perfect matching weights $\overline{p}_a$ in terms of directed edge variables allows us to introduce a product of perfect matching weights that can be associated to a directed path along edges of the brane tiling. Taking

$$\overline{p}_a = \cdots e_{ij}^+ e_{kl}^+ \cdots \ , \ (\overline{p}_b)^{-1} = \cdots e_{kj}^- e_{ml}^- \cdots \ , \tag{2.12}$$

we define the following product of perfect matching weights,

$$\overline{p}_a \cdot (\overline{p}_b)^{-1} \equiv \cdots e_{ij}^+ e_{kj}^- e_{kl}^+ e_{ml}^- \cdots \ , \tag{2.13}$$
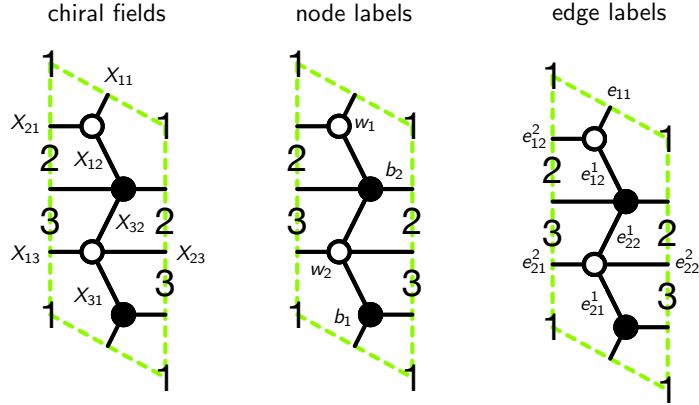
where we see that under the product we obtain a directed connected path along the edges of a brane tiling alternating between white and black nodes as illustrated in Figure 4.

The convention used in [13] is that all directed paths along edges in a brane tiling alternate between white and black nodes and can be therefore expressed as an alternating sequence of directed edge variables e_{jk}^+ and e_{lk}^-. Moreover, when the connected paths are closed, then the directed edge variables $e_{jk}^\pm$ form permutation tuples of the permutation group $S_{2|E|}$. Taking two permutation tuples in $S_{2|E|}$ in terms of $e_{jk}^\pm$, we identify the product between the permutation tuples to be as follows,

$$(\cdots e_{ik}^- \ e_{ij}^+ \ e_{mj}^- \ \cdots) \cdot (\cdots e_{uj}^+ \ e_{ij}^- \ e_{iv}^+ \ \cdots) = (\cdots e_{ik}^- \ e_{iv}^+ \ \cdots) \cdot (\cdots e_{uj}^+ \ e_{mj}^- \ \cdots) \,, \tag{2.14}$$

giving a new pair of closed paths with certain edge variables cancelling each other under the following identities,

$$(e_{jk}^\pm)^{-1} = e_{jk}^\mp \,, \quad e_{jk}^+ \cdot e_{jk}^- = 1 \,. \tag{2.15}$$

$$W = X_{11}X_{12}X_{21} + X_{13}X_{32}X_{23}X_{31} - X_{11}X_{13}X_{31} - X_{12}X_{23}X_{32}X_{21}$$

$$\sigma_W^{-1} = (e_{11} \ e_{12}^1 \ e_{12}^2)(e_{22}^2 \ e_{21}^1 \ e_{21}^2 \ e_{22}^1)$$

$$\sigma_B = (e_{11} \ e_{21}^2 \ e_{21}^1)(e_{12}^1 \ e_{22}^2 \ e_{22}^1 \ e_{12}^2)$$

Figure 5: The brane tiling for the suspended pinch point (SPP) with chiral fields X_{ij}, node labels w_j and b_k, and edge labels e_{jk}. The superpotential W and the corresponding permutation tuples σ_W^{-1} and σ_B in terms of edge labels are also shown.

Examples of closed directed paths in a brane tiling are **zig-zag paths** and **face paths** that go around the boundary edges of a face in the brane tiling. By first using edge variables e_{jk} instead of chiral fields X_{ij}, we are able to rewrite the superpotential W of the brane tiling as a pair of permutation tuples $\sigma_B, \sigma_W \in S_{|E|}$ [76, 77], where σ_B

contains a cycle for every black node in the brane tiling associated to a negative term in W, while σ_W^{-1} has a cycle for every white node in the brane tiling associated to a positive term in W as reviewed in section §2.1. These cycles in σ_B and σ_W^{-1} follow the clockwise and anti-clockwise orientation around white and black nodes in the brane tilings, respectively. Let us illustrate this for the brane tiling for the suspended pinch point (SPP) shown in Figure 5, whose superpotential W is as follows,

$$W = X_{11}X_{12}X_{21} + X_{13}X_{32}X_{23}X_{31} - X_{11}X_{13}X_{31} - X_{12}X_{23}X_{32}X_{21} \ . \qquad (2.16)$$

The corresponding permutation tuples in terms of edge variables e_{jk} are given by,

$$\sigma_W^{-1} = (e_{11}\ e_{12}^1\ e_{12}^2)(e_{22}^2\ e_{21}^1\ e_{21}^2\ e_{22}^1)\ ,\ \ \sigma_B = (e_{11}\ e_{21}^2\ e_{21}^1)(e_{12}^1\ e_{22}^2\ e_{22}^1\ e_{12}^2)\ . \qquad (2.17)$$

In terms of the permutation tuples $\sigma_W, \sigma_B \in S_{|E|}$, we can define the following permutations in $S_{2|E|}$ in terms of directed edge variables $e_{jk}^\pm$,

$$\Sigma_z = (\sigma_W^{-1})^+ \cdot (\sigma_B)^-\ ,\ \ \Sigma_f = (\sigma_W^{-1})^+ \cdot (\sigma_B^{-1})^-\ ,\ \ \Sigma_e = \prod_{e_{jk}}(e_{jk}^+\ e_{jk}^-)\ , \qquad (2.18)$$

where here in $(\sigma)^+$ all edge variables e_{jk} become directed edge variables e_{jk}^+, while in $(\sigma)^-$ all edge variables e_{jk} become directed edge variables e_{jk}^-. Using these permutations in $S_{2|E|}$, we can write permutations that encode the zig-zag paths in the brane tiling [76, 77] as follows,

$$\Sigma_e \cdot \Sigma_z = \prod_{e_{jk}}(e_{jk}^+\ e_{jk}^-) \cdot (\sigma_W^{-1})^+ \cdot (\sigma_B)^-\ , \qquad (2.19)$$

while the permutations that encode the directed paths around boundary edges of faces in the brane tiling are given by,

$$\Sigma_e \cdot \Sigma_f = \prod_{e_{jk}}(e_{jk}^+\ e_{jk}^-) \cdot (\sigma_W^{-1})^+ \cdot (\sigma_B^{-1})^-\ . \qquad (2.20)$$
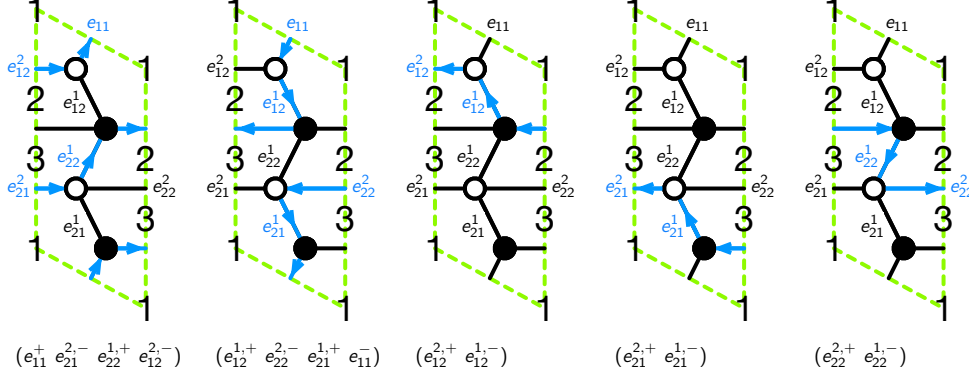
For the SPP example with σ_W^{-1} and σ_B given in (2.17), all distinct zig-zag paths are given by,

$$\Sigma_e \cdot \Sigma_z = (e_{11}^+\ e_{21}^{2,-}\ e_{22}^{1,+}\ e_{12}^{2,-})(e_{12}^{1,+}\ e_{22}^{2,-}\ e_{21}^{1,+}\ e_{11}^-)(e_{12}^{2,+}\ e_{12}^{1,-})(e_{21}^{2,+}\ e_{21}^{1,-})(e_{22}^{2,+}\ e_{22}^{1,-})\ , \tag{2.21}$$

where every cycle corresponds to a closed zig-zag path in the brane tiling. Similarly, the directed paths around the 3 faces of the SPP brane tiling are given by,

$$\Sigma_e \cdot \Sigma_f = (e_{11}^+\ e_{21}^{1,-}\ e_{21}^{2,+}\ e_{11}^-\ e_{12}^{1,+}\ e_{12}^{2,-})(e_{12}^{2,+}\ e_{22}^{1,-}\ e_{22}^{2,+}\ e_{12}^{1,-})(e_{21}^{1,+}\ e_{21}^{2,-}\ e_{22}^{1,+}\ e_{22}^{2,-})\ , \tag{2.22}$$

zig-zag paths $\mathcal{Z}(\sigma_W, \sigma_B^{-1})$

$(e_{11}^+ \; e_{21}^{2,-} \; e_{22}^{1,+} \; e_{12}^{2,-})$ $(e_{12}^{1,+} \; e_{22}^{2,-} \; e_{21}^{1,+} \; e_{11}^-)$ $(e_{12}^{2,+} \; e_{12}^{1,-})$ $(e_{21}^{2,+} \; e_{21}^{1,-})$ $(e_{22}^{2,+} \; e_{22}^{1,-})$

face paths $\mathcal{Z}(\sigma_W^{-1}, \sigma_B^{-1})$

$(e_{11}^+ \; e_{21}^{1,-} \; e_{21}^{2,+} \; e_{11}^- \; e_{12}^{1,+} \; e_{12}^{2,-})$ $(e_{12}^{2,+} \; e_{22}^{1,-} \; e_{22}^{2,+} \; e_{12}^{1,-})$ $(e_{21}^{1,+} \; e_{21}^{2,-} \; e_{22}^{1,+} \; e_{22}^{2,-})$
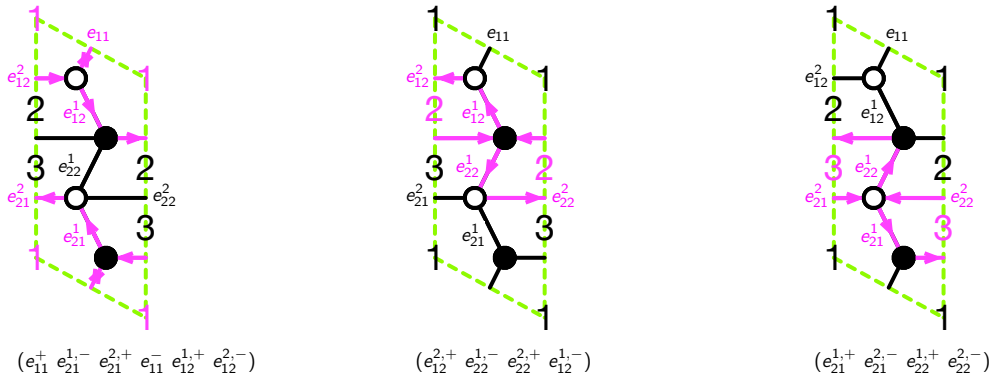
Figure 6: The brane tiling for the suspended pinch point (SPP) with zig-zag paths given by $\Sigma_e \cdot (\sigma_W^{-1})^+ \cdot (\sigma_B)^-$ and face paths given by $\Sigma_e \cdot (\sigma_W^{-1})^+ \cdot (\sigma_B^{-1})^-$.

where we can see that directed paths go anti-clockwise around each of the faces as illustrated in Figure 6.

Casimirs, 1-loops and the Spectral Curve. The Kasteleyn matrix defined in (2.3) is written in terms of edge variables e_{jk}. By taking all the edge variables to be positively oriented such that,

$$K_{w_j,b_k}^+(x,y) = \sum_{e_{jk}=(w_j,b_k)} e_{jk}^+ \, x^{h_1(e_{jk})} y^{h_2(e_{jk})} \,, \tag{2.23}$$

the characteristic polynomial from the permanent then takes the form,

$$P^+(x,y) = \text{perm } K^+_{w_j,b_k}(x,y) = \sum_{\substack{p_{(n_x,n_y)} \\ (n_x,n_y)\in\Delta}} \overline{p}_{(n_x,n_y)} \; x^{n_x} y^{n_y} \; , \qquad (2.24)$$

where $\overline{p}_{(n_x,n_y)}$ is the perfect matching weight defined in (2.11) corresponding to perfect matching $p_{(n_x,n_y)}$ in the brane tiling associated to vertex (n_x, n_y) in the toric diagram Δ. Here, we note that multiple perfect matchings can correspond to the same vertex in the toric diagram and the sum in (2.24) goes over all of them.

By choosing a **reference perfect matching** p_0, we can factor out its corresponding weight from the characteristic polynomial in (2.24) to obtain,

$$P^+(x,y) = \overline{p}_0 \cdot \sum_{\substack{p_{(n_x,n_y)} \\ (n_x,n_y)\in\Delta}} \delta_{(n_x,n_y)} \; x^{n_x} y^{n_y} \; , \qquad (2.25)$$

where

$$\delta_{(n_x,n_y)} = (\overline{p}_0)^{-1} \cdot \overline{p}_{(n_x,n_y)} \; , \qquad (2.26)$$

are identified as **Casimirs** of the associated dimer integrable system given by the brane tiling. For the origin $(0,0) \in \Delta$, which can be chosen by an overall shift of the toric diagram such that it becomes the unique internal vertex for reflexive polygons, we have multiple associated perfect matchings. The corresponding perfect matching weights give the **Hamiltonian** of the dimer integrable system. The expression for the Hamiltonian is as follows,

$$\delta_{(0,0)} \equiv H = \sum_{p^u_{(0,0)}} \gamma_u \; , \qquad (2.27)$$

where

$$\gamma_u = (\overline{p}_0)^{-1} \cdot \overline{p}^u_{(0,0)} \; , \qquad (2.28)$$

are the **1-loops** of the dimer integrable system. Here, the sum in (2.27) is over all perfect matchings associated to the interior point $(0,0)$ of the reflexive toric diagram, where $u = 1, \ldots, m$ labels the perfect matchings with m being the multiplicity of the interior vertex. $\overline{p}^u_{(0,0)}$ is the weight of the u-th perfect matching associated to the interior vertex $(0,0)$. By factorizing out the reference perfect matching weight $\overline{p}_0$, these perfect matching weights are then identified with the 1-loops γ_u in (2.28), with the sum over all 1-loops associated to the unique interior point of the toric diagram corresponding

to the Hamiltonian H of the dimer integrable system. In the case of brane tilings corresponding to non-reflexive toric diagrams with N_i internal vertices, there would be N_i Hamiltonians of the form $H_1, \ldots, H_{N_i}$ where the n-th Hamiltonian is given by the sum over n-loops.

Accordingly, for brane tilings associated with toric Calabi-Yau 3-folds with reflexive toric diagrams, we can write down the general form of the **spectral curve** Σ of the dimer integrable system following the factorized form of the characteristic polynomial in (2.25),

$$\Sigma \ : \ H + \sum_{\substack{(n_x, n_y) \in \Delta \\ (n_x, n_y) \neq (0,0)}} \delta_{(n_x, n_y)} \, x^{n_x} y^{n_y} = 0 \ , \tag{2.29}$$

where the single Hamiltonian H takes the form given in (2.27). In terms of the Newton polynomial $P^+(x, y)$ defined in (2.25), we can express the spectral curve of the dimer integrable system as follows,

$$\Sigma \ : \ (\bar{p}_0)^{-1} \cdot P^+(x, y) = 0 \ . \tag{2.30}$$

Poisson Commutation Relations. We can define Poisson commutation relations between directed closed paths, also referred to as loops, in the dimer integrable systems. For oriented face paths f_i, the Poisson commutation relations are given by,

$$\{f_i, f_j\} = I_{i,j} \ f_i f_j \ , \tag{2.31}$$

where $I_{i,j}$ is the number of arrows from node i to j minus the number of arrows from node j to i in the quiver diagram of the corresponding brane tiling.

We note here that since brane tilings are embedded on a 2-torus T^2 and the fact that brane tilings are bipartite making every face even-sided, the face paths satisfy the following overall constraint relation,

$$\prod_{i=1}^{G} f_i = \text{constant} \ , \tag{2.32}$$

where G is the number of faces corresponding to the number of gauge groups in the brane tiling. Moreover, the face paths f_i form with the the zig-zag paths z_r non-trivial relations. Since in this work, we only consider reflexive polygons as toric diagrams, the dimer integrable systems only have a single Hamiltonian with **canonical variables**
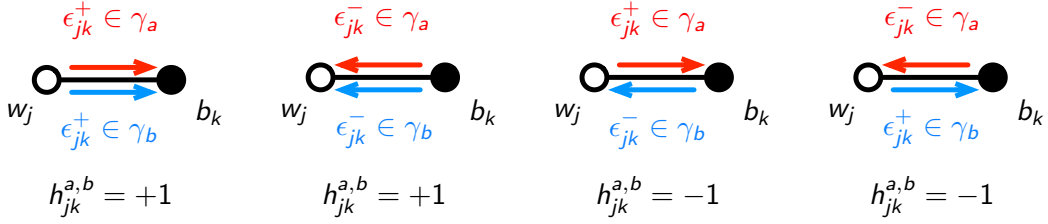
Figure 7: The possible directed intersections between directed paths γ_a and γ_b at edge e_{jk} with the corresponding directed intersection number $h_{jk}^{a,b}$.

e^P and e^Q. The face paths f_i of the corresponding dimer integrable system can be expressed in terms of these canonical variables. We also note that the face paths f_i correspond to cluster variables of the quiver in the corresponding brane tiling [4, 78, 79].

The associated oriented 1-loops γ_u of the single Hamiltonian H can be written in terms of face paths and zig-zag paths, as well as the canonical variables e^P and e^Q. In general, they satisfy the following Poisson commutation relations of the form,

$$\{\gamma_u, \gamma_{u'}\} = \frac{\partial \gamma_u}{\partial P} \cdot \frac{\partial \gamma_{u'}}{\partial Q} - \frac{\partial \gamma_u}{\partial Q} \cdot \frac{\partial \gamma_{u'}}{\partial P} \ . \tag{2.33}$$

These Poisson commutation relations can be rewritten in terms of the original 1-loops γ_u and $\gamma_{u'}$ as follows,

$$\{\gamma_u, \gamma_{u'}\} = \epsilon_{u,u'} \ \gamma_u \gamma_{u'} \ , \tag{2.34}$$

where

$$\epsilon_{u,u'} = \sum_{e_{jk} \in \gamma_u, \gamma_u'} h_{jk}^{u,u'} \tag{2.35}$$

is the ordered intersection number between 1-loops γ_u and $\gamma_{u'}$. The sum in (2.35) is over all common edges e_{jk} between γ_u and $\gamma_{u'}$, and $h_{jk}^{u,u'}$ is the directed intersection number at edge e_{jk} where γ_u and $\gamma_{u'}$ intersect. The different values that $h_{jk}^{u,u'}$ can have at a particular intersection at edge e_{jk} are given in Figure 7 with the corresponding illustrations of the directed intersections.

The Poisson commutation relations between 1-loops can also be written in terms of a **commutation matrix** C as follows,

$$\{\gamma_u, \gamma_{u'}\} = C_{u,u'} \ \gamma_u \gamma_{u'} \ , \tag{2.36}$$

where $C_{u,u'} \in \mathbb{Z}$ are elements of the commutation matrix. The commutation matrices are presented in the following classification for all 30 dimer integrable systems corresponding to reflexive polygons in $\mathbb{Z}^2$.

2.4 Birational Transformations on the Dimer Integrable Systems

Birational transformations have been studied extensively in [38–40] in order to identify birationally equivalent toric Fano 3-folds. In [41, 42], this equivalence has been interpreted as a correspondence between $2d$ $(0, 2)$ supersymmetric gauge theories associated with toric Fano 3-folds and more generally toric Calabi-Yau 4-folds realized by brane brick models [45–50].

In this work, we focus on birational transformations that relate toric Calabi-Yau 3-folds whose toric diagrams are given by the 16 reflexive polygons as summarized in section §2.2. As observed in [13], when two of these toric Calabi-Yau 3-folds are related by a birational transformation, they are associated to a pair of brane tilings on the 2-torus that define dimer integrable systems which are birationally equivalent. Under this equivalence, it is shown in [13] that the Casimirs and Hamiltonians as well as the Poisson commutation relations of the integrable systems are identified to each other by the birational transformation. The spectral curves as defined in (2.29) are also mapped to each other by the birational transformation, making the transformation a true equivalence between two distinct dimer integrable systems.

Given the Newton polynomial $P(x, y)$ as defined in (2.2) for the toric diagram Δ of a toric Calabi-Yau 3-fold, we can expand it in the following form,

$$P(x, y) = \sum_{m=a}^{b} C_m(y) x^m \ , \tag{2.37}$$

where $a < 0$ and $b > 0$ and $C_m(y)$ are sub-polynomials of $P(x, y)$ for $a \leq m \leq b$. Using this expanded form of the Newton polynomial, we can define a **birational transformation** φ_A [36–40] that acts on the coordinates $x, y \in \mathbb{C}^*$ of $P(x, y)$ as follows,

$$\varphi_A \ : \ (x, y) \mapsto (A(y)x, y) \ , \tag{2.38}$$

where $A(y)$ is a polynomial chosen such that $A(y)^{-m}$ is a polynomial divisor of $C_m(y)$ in the expansion in (2.37) for $a \leq m \leq -1$. By calling the new Newton polynomial $P^\vee(x, y)$ with toric diagram $\Delta^\vee$, the toric varieties associated to the original toric diagram Δ and the new toric diagram $\Delta^\vee$ are known to be birationally equivalent to each other [36–40]. This birational equivalence exists if the birational map in (2.38) applies to at least one chosen $GL(2, \mathbb{Z})$ frame or choice of origin in the $\mathbb{Z}^2$ lattice for the toric diagrams Δ and $\Delta^\vee$. Given that the birational transformation φ_A only exists for certain $GL(2, \mathbb{Z})$ frames of a given toric diagram, we can generalize the expression of the birational transformation in (2.38) to,

$$\varphi_{A;M;N} = M \circ \varphi_A \circ N \ , \tag{2.39}$$

in order to include the $GL(2, \mathbb{Z})$ transformations M and N on the coordinates x, y in $P(x, y)$.

Under such birational transformations, dimer integrable systems associated to brane tilings corresponding to Δ and $\Delta^\vee$ are **birationally equivalent** to each other, as observed in [13]. This means that the birational map $\varphi_{A;M;N}$ acts on the spectral curve of the dimer integrable system as follows,

$$\varphi_{A;M;N} \Sigma = \Sigma^\vee \ . \tag{2.40}$$

In other words, the spectral curves are mapped to each other by the birational transformation from Δ to $\Delta^\vee$. As a result of this, the Hamiltonian H and the 1-loops γ_u are identified to each other between the two birationally equivalent dimer integrable systems. This in turn leads to identifications between the Poisson commutation relations as well as relations between zig-zag paths and face paths of the birationally equivalent dimer integrable systems. These relations form a canonical transformation between the birationally equivalent dimer integrable systems.

In the following work, we classify all birational equivalences between dimer integrable systems that correspond to the 30 brane tilings associated to toric Calabi-Yau 3-folds whose toric diagrams are one of the 16 reflexive polygons. Figure 2 summarizes the classification of all birational equivalences between the 30 dimer integrable systems corresponding to the 16 reflexive polygons. While presenting the explicit birational maps that define these equivalences, we also present the relations between zig-zag paths and face paths as well as the associated canonical variables that lead to the identifications of the Hamiltonians, spectral curves and 1-loops between the equivalent dimer integrable systems.

3 Model 1: $\mathbb{C}^3/\mathbb{Z}_3 \times \mathbb{Z}_3$ $(1,0,2)(0,1,2)$
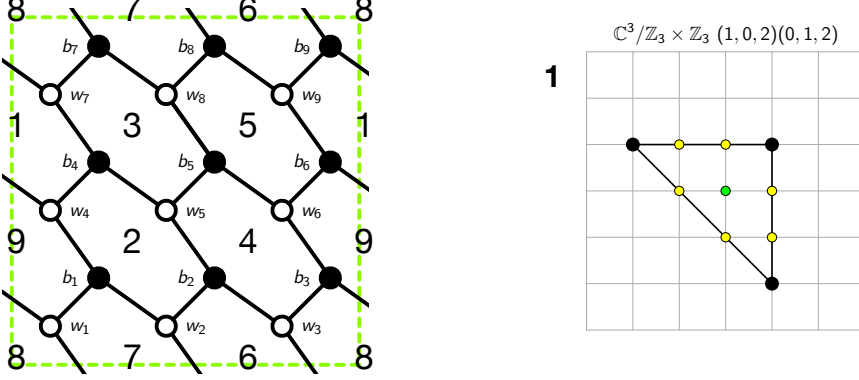

Figure 8: The brane tiling and toric diagram of Model 1.

The brane tiling for Model 1 can be expressed in terms of the following pair of permutation tuples

$$
\begin{aligned}
\sigma_B ={}& (e_{11}\ e_{21}\ e_{41})\ (e_{22}\ e_{32}\ e_{52})\ (e_{13}\ e_{63}\ e_{33})\ (e_{44}\ e_{54}\ e_{74})\ (e_{55}\ e_{65}\ e_{85}) \\
& (e_{46}\ e_{96}\ e_{66})\ (e_{17}\ e_{77}\ e_{87})\ (e_{28}\ e_{88}\ e_{98})\ (e_{39}\ e_{99}\ e_{79})\ , \\
\sigma_W^{-1} ={}& (e_{11}\ e_{17}\ e_{13})\ (e_{21}\ e_{22}\ e_{28})\ (e_{32}\ e_{33}\ e_{39})\ (e_{41}\ e_{46}\ e_{44})\ (e_{52}\ e_{54}\ e_{55}) \\
& (e_{63}\ e_{65}\ e_{66})\ (e_{74}\ e_{79}\ e_{77})\ (e_{85}\ e_{87}\ e_{88})\ (e_{96}\ e_{98}\ e_{99})\ ,
\end{aligned}
\tag{3.1}
$$

which correspond to black and white nodes of the brane tiling, respectively.

The brane tiling for Model 1 has 9 zig-zag paths given by,

$$
\begin{aligned}
z_1 &= (e_{74}^+\ e_{44}^-\ e_{41}^+\ e_{11}^-\ e_{17}^+\ e_{77}^-)\ , \quad z_2 = (e_{46}^+\ e_{96}^-\ e_{98}^+\ e_{28}^-\ e_{21}^+\ e_{41}^-)\ , \\
z_3 &= (e_{99}^+\ e_{79}^-\ e_{77}^+\ e_{87}^-\ e_{88}^+\ e_{98}^-)\ , \quad z_4 = (e_{44}^+\ e_{54}^-\ e_{55}^+\ e_{65}^-\ e_{66}^+\ e_{46}^-)\ , \\
z_5 &= (e_{52}^+\ e_{22}^-\ e_{28}^+\ e_{88}^-\ e_{85}^+\ e_{55}^-)\ , \quad z_6 = (e_{79}^+\ e_{39}^-\ e_{32}^+\ e_{52}^-\ e_{54}^+\ e_{74}^-)\ , \\
z_7 &= (e_{96}^+\ e_{66}^-\ e_{63}^+\ e_{33}^-\ e_{39}^+\ e_{99}^-)\ , \quad z_8 = (e_{87}^+\ e_{17}^-\ e_{13}^+\ e_{63}^-\ e_{65}^+\ e_{85}^-)\ , \\
& \qquad\qquad z_9 = (e_{22}^+\ e_{32}^-\ e_{33}^+\ e_{13}^-\ e_{11}^+\ e_{21}^-)\ ,
\end{aligned}
\tag{3.2}
$$

and 9 face paths given by,

$$f_1 = (e_{44}^+ \ e_{74}^- \ e_{79}^+ \ e_{99}^- \ e_{96}^+ \ e_{46}^-) \ , \quad f_2 = (e_{54}^+ \ e_{44}^- \ e_{41}^+ \ e_{21}^- \ e_{22}^+ \ e_{52}^-) \ ,$$
$$f_3 = (e_{74}^+ \ e_{54}^- \ e_{55}^+ \ e_{85}^- \ e_{87}^+ \ e_{77}^-) \ , \quad f_4 = (e_{52}^+ \ e_{32}^- \ e_{33}^+ \ e_{63}^- \ e_{65}^+ \ e_{55}^-) \ ,$$
$$f_5 = (e_{85}^+ \ e_{65}^- \ e_{66}^+ \ e_{96}^- \ e_{98}^+ \ e_{88}^-) \ , \quad f_6 = (e_{99}^+ \ e_{39}^- \ e_{32}^+ \ e_{22}^- \ e_{28}^+ \ e_{98}^-) \ ,$$
$$f_7 = (e_{21}^+ \ e_{11}^- \ e_{17}^+ \ e_{87}^- \ e_{88}^+ \ e_{28}^-) \ , \quad f_8 = (e_{77}^+ \ e_{17}^- \ e_{13}^+ \ e_{33}^- \ e_{39}^+ \ e_{79}^-) \ ,$$
$$f_9 = (e_{46}^+ \ e_{66}^- \ e_{63}^+ \ e_{13}^- \ e_{11}^+ \ e_{41}^-) \ , \tag{3.3}$$

which satisfy the following constraints,

$$f_1^{-1} f_7 = z_1 z_2 z_3 \ , \quad f_2 f_8^{-1} = z_1 z_6 z_9 \ , \quad f_3 f_9^{-1} = z_1 z_4 z_8 \ ,$$
$$f_4 f_7^{-1} = z_5 z_8 z_9 \ , \quad f_5^{-1} f_8 = z_3 z_7 z_8 \ , \quad f_6^{-1} f_9 = z_2 z_7 z_9 \ ,$$
$$f_7 f_8 f_9 = z_2 z_3 z_7 \ , \quad f_1 f_2 f_3 f_4 f_5 f_6 f_7 f_8 f_9 = 1 \ . \tag{3.4}$$

The face paths can be written in terms of the canonical variables as follows,

$$f_1 = e^{-Q-P} z_1^{-1} z_7 \ , \quad f_2 = e^Q z_1 z_6 z_9 \ , \quad f_3 = e^P z_1 z_4 z_8 \ ,$$
$$f_4 = e^{-Q-P} z_1^{-1} z_4^{-1} z_6^{-1} \ , \quad f_5 = e^Q z_3^{-1} z_7^{-1} z_8^{-1} \ , \quad f_6 = e^P z_2^{-1} z_7^{-1} z_9^{-1} \ ,$$
$$f_7 = e^{-Q-P} z_2 z_3 z_7 \ , \quad f_8 = e^Q \ , \quad f_9 = e^P \ . \tag{3.5}$$

The Kasteleyn matrix of the brane tiling for Model 1 in Figure 8 is given by,

$$K = \begin{pmatrix}
 & b_1 & b_2 & b_3 & b_4 & b_5 & b_6 & b_7 & b_8 & b_9 \\
\hline
w_1 & e_{11} & 0 & e_{13}x^{-1} & 0 & 0 & 0 & e_{17}y^{-1} & 0 & 0 \\
w_2 & e_{21} & e_{22} & 0 & 0 & 0 & 0 & 0 & e_{28}y^{-1} & 0 \\
w_3 & 0 & e_{32} & e_{33} & 0 & 0 & 0 & 0 & 0 & e_{39}y^{-1} \\
w_4 & e_{41} & 0 & 0 & e_{44} & 0 & e_{46}x^{-1} & 0 & 0 & 0 \\
w_5 & 0 & e_{52} & 0 & e_{54} & e_{55} & 0 & 0 & 0 & 0 \\
w_6 & 0 & 0 & e_{63} & 0 & e_{65} & e_{66} & 0 & 0 & 0 \\
w_7 & 0 & 0 & 0 & e_{74} & 0 & 0 & e_{77} & 0 & e_{79}x^{-1} \\
w_8 & 0 & 0 & 0 & 0 & e_{85} & 0 & e_{87} & e_{88} & 0 \\
w_9 & 0 & 0 & 0 & 0 & 0 & e_{96} & 0 & e_{98} & e_{99}
\end{pmatrix} \ . \tag{3.6}$$

By taking the permanent of the Kasteleyn matrix, we obtain the spectral curve of the dimer integrable system for Model 1 as follows,

$$0 = \text{perm } K = \bar{p}_0 \cdot x^{-1} y^{-1} \cdot \left[\delta_{(-2,1)} x^{-2} y + \delta_{(-1,0)} x^{-1} + \delta_{(-1,1)} x^{-1} y \right.$$
$$\left. + \delta_{(0,-1)} y^{-1} + \delta_{(0,1)} y + \delta_{(1,-2)} xy^{-2} + \delta_{(1,-1)} xy^{-1} + \delta_{(1,0)} x + \delta_{(1,1)} xy + H \right] \ , \tag{3.7}$$

where $\bar{p}_0 = e^+_{13}e^+_{21}e^+_{32}e^+_{46}e^+_{54}e^+_{65}e^+_{79}e^+_{87}e^+_{98}$. The Casimirs $\delta_{(m,n)}$ in (3.7) can be expressed in terms of the zig-zag paths in (3.2) as follows,

$$\delta_{(-2,1)} = 1 \ , \ \delta_{(-1,0)} = z_2^{-1} + z_6^{-1} + z_8^{-1} \ , \ \delta_{(-1,1)} = z_3 + z_4 + z_9 \ ,$$
$$\delta_{(0,-1)} = z_2^{-1}z_6^{-1} + z_2^{-1}z_8^{-1} + z_6^{-1}z_8^{-1} \ , \ \delta_{(0,1)} = z_3z_4 + z_3z_9 + z_4z_9 \ ,$$
$$\delta_{(1,-2)} = z_1z_3z_4z_5z_7z_9 \ , \ \delta_{(1,-1)} = z_3z_4z_9(z_1z_5 + z_1z_7 + z_5z_7) \ ,$$
$$\delta_{(1,0)} = z_3z_4z_9(z_1 + z_5 + z_7) \ , \ \delta_{(1,1)} = z_3z_4z_9 \ . \tag{3.8}$$

This leads to the following form of the spectral curve for Model 1,

$$\Sigma \ : \ \frac{y}{x^2} + \left[\frac{1}{z_2} + \frac{1}{z_6} + \frac{1}{z_8} + (z_3 + z_4 + z_9)y\right]\frac{1}{x} + \left(\frac{1}{z_2z_6} + \frac{1}{z_2z_8} + \frac{1}{z_6z_8}\right)\frac{1}{y}$$
$$+ (z_3z_4 + z_3z_9 + z_4z_9)y + z_3z_4z_9\left[z_1z_5z_7\frac{1}{y^2} + (z_1z_5 + z_1z_7 + z_5z_7)\frac{1}{y}\right]$$
$$+ (z_1 + z_5 + z_7) + y\Big]x + H = 0 \ . \tag{3.9}$$

The Hamiltonian is a sum over all 21 1-loops γ_i,

$$H = \sum_{i=1}^{21} \gamma_i \ , \tag{3.10}$$

where the 1-loops γ_i can be expressed in terms of zig-zag paths and face paths as follows,

$$\gamma_1 = z_1z_4z_9f_8f_9 \ , \ \gamma_2 = z_1z_4z_9f_8 \ , \ \gamma_3 = z_8^{-1}z_9f_9^{-1} \ , \ \gamma_4 = z_1^{-1}z_6^{-1}z_8^{-1}f_8^{-1}f_9^{-1} \ ,$$
$$\gamma_5 = z_8^{-1}z_9f_8 \ , \ \gamma_6 = z_8^{-1}z_9f_8f_9^{-1} \ , \ \gamma_7 = z_1^{-1}z_6^{-1}z_8^{-1}f_9^{-1} \ , \ \gamma_8 = z_1^{-1}z_2^{-1}z_6^{-1}f_8^{-1} \ ,$$
$$\gamma_9 = z_2^{-1}z_4f_9 \ , \ \gamma_{10} = z_3z_7z_9f_8^{-1}f_9^{-1} \ , \ \gamma_{11} = z_1z_3z_4f_1f_4f_9 \ , \ \gamma_{12} = z_1z_3z_4f_1f_9 \ ,$$
$$\gamma_{13} = z_1z_3z_9f_1f_8 \ , \ \gamma_{14} = z_3z_6^{-1}f_1 \ , \ \gamma_{15} = z_2^{-1}z_6^{-1}z_7^{-1}f_9 \ , \ \gamma_{16} = z_4z_6^{-1}f_2f_6f_9 \ ,$$
$$\gamma_{17} = z_4z_6^{-1}f_2f_6 \ , \ \gamma_{18} = z_1^{-1}z_6^{-1}z_8^{-1}f_2f_6 \ , \ \gamma_{19} = z_1^{-1}z_6^{-1}z_8^{-1}f_2f_6f_9^{-1} \ ,$$
$$\gamma_{20} = z_2^{-1}z_6^{-1}z_7^{-1}f_7f_9 \ , \ \gamma_{21} = z_1z_3z_4f_9 \ . \tag{3.11}$$

The commutation matrix C for Model 1 takes the following form,

$$C = \begin{array}{c|ccccccccccccccccccccc}
 & \gamma_1 & \gamma_2 & \gamma_3 & \gamma_4 & \gamma_5 & \gamma_6 & \gamma_7 & \gamma_8 & \gamma_9 & \gamma_{10} & \gamma_{11} & \gamma_{12} & \gamma_{13} & \gamma_{14} & \gamma_{15} & \gamma_{16} & \gamma_{17} & \gamma_{18} & \gamma_{19} & \gamma_{20} & \gamma_{21} \\ \hline
\gamma_1 & 0 & -1 & -1 & 0 & -1 & -2 & -1 & 1 & 1 & 0 & 1 & 1 & -1 & 0 & 1 & 1 & 0 & 0 & -1 & 1 & 1 \\
\gamma_2 & 1 & 0 & -1 & -1 & 0 & -1 & -1 & 0 & 1 & -1 & -1 & 0 & -1 & -1 & 1 & 2 & 1 & 1 & 0 & 0 & 1 \\
\gamma_3 & 1 & 1 & 0 & -1 & 1 & 1 & 0 & -1 & 0 & -1 & -2 & -1 & 0 & -1 & 0 & 1 & 1 & 1 & 1 & -1 & 0 \\
\gamma_4 & 0 & 1 & 1 & 0 & 1 & 2 & 1 & -1 & -1 & 0 & -1 & -1 & 1 & 0 & -1 & -1 & 0 & 0 & 1 & -1 & -1 \\
\gamma_5 & 1 & 0 & -1 & -1 & 0 & -1 & -1 & 0 & 1 & -1 & -1 & 0 & -1 & -1 & 1 & 2 & 1 & 1 & 0 & 0 & 1 \\
\gamma_6 & 2 & 1 & -1 & -2 & 1 & 0 & -1 & -1 & 1 & -2 & -3 & -1 & -1 & -2 & 1 & 3 & 2 & 2 & 1 & -1 & 1 \\
\gamma_7 & 1 & 1 & 0 & -1 & 1 & 1 & 0 & -1 & 0 & -1 & -2 & -1 & 0 & -1 & 0 & 1 & 1 & 1 & 1 & -1 & 0 \\
\gamma_8 & -1 & 0 & 1 & 1 & 0 & 1 & 1 & 0 & -1 & 1 & 1 & 0 & 1 & 1 & -1 & -2 & -1 & -1 & 0 & 0 & -1 \\
\gamma_9 & -1 & -1 & 0 & 1 & -1 & -1 & 0 & 1 & 0 & 1 & 2 & 1 & 0 & 1 & 0 & -1 & -1 & -1 & -1 & 1 & 0 \\
\gamma_{10} & 0 & 1 & 1 & 0 & 1 & 2 & 1 & -1 & -1 & 0 & -1 & -1 & 1 & 0 & -1 & -1 & 0 & 0 & 1 & -1 & -1 \\
\gamma_{11} & -1 & 1 & 2 & 1 & 1 & 3 & 2 & -1 & -2 & 1 & 0 & -1 & 2 & 1 & -2 & -3 & -1 & -1 & 1 & -1 & -2 \\
\gamma_{12} & -1 & 0 & 1 & 1 & 0 & 1 & 1 & 0 & -1 & 1 & 1 & 0 & 1 & 1 & -1 & -2 & -1 & -1 & 0 & 0 & -1 \\
\gamma_{13} & 1 & 1 & 0 & -1 & 1 & 1 & 0 & -1 & 0 & -1 & -2 & -1 & 0 & -1 & 0 & 1 & 1 & 1 & 1 & -1 & 0 \\
\gamma_{14} & 0 & 1 & 1 & 0 & 1 & 2 & 1 & -1 & -1 & 0 & -1 & -1 & 1 & 0 & -1 & -1 & 0 & 0 & 1 & -1 & -1 \\
\gamma_{15} & -1 & -1 & 0 & 1 & -1 & -1 & 0 & 1 & 0 & 1 & 2 & 1 & 0 & 1 & 0 & -1 & -1 & -1 & -1 & 1 & 0 \\
\gamma_{16} & -1 & -2 & -1 & 1 & -2 & -3 & -1 & 2 & 1 & 1 & 3 & 2 & -1 & 1 & 1 & 0 & -1 & -1 & -2 & 2 & 1 \\
\gamma_{17} & 0 & -1 & -1 & 0 & -1 & -2 & -1 & 1 & 1 & 0 & 1 & 1 & -1 & 0 & 1 & 1 & 0 & 0 & -1 & 1 & 1 \\
\gamma_{18} & 0 & -1 & -1 & 0 & -1 & -2 & -1 & 1 & 1 & 0 & 1 & 1 & -1 & 0 & 1 & 1 & 0 & 0 & -1 & 1 & 1 \\
\gamma_{19} & 1 & 0 & -1 & -1 & 0 & -1 & -1 & 0 & 1 & -1 & -1 & 0 & -1 & -1 & 1 & 2 & 1 & 1 & 0 & 0 & 1 \\
\gamma_{20} & -1 & 0 & 1 & 1 & 0 & 1 & 1 & 0 & -1 & 1 & 1 & 0 & 1 & 1 & -1 & -2 & -1 & -1 & 0 & 0 & -1 \\
\gamma_{21} & -1 & -1 & 0 & 1 & -1 & -1 & 0 & 1 & 0 & 1 & 2 & 1 & 0 & 1 & 0 & -1 & -1 & -1 & -1 & 1 & 0 \\
\end{array} \qquad (3.12)$$

Satisfying the commutation relations given by the commutation matrix above, the 1-loops can be written in terms of the canonical variables as follows,

$$\gamma_1 = e^{Q+P} z_1 z_4 z_9 \ , \quad \gamma_2 = e^{Q} z_1 z_4 z_9 \ , \quad \gamma_3 = e^{-P} z_8^{-1} z_9 \ ,$$

$$\gamma_4 = e^{-Q-P} z_1^{-1} z_6^{-1} z_8^{-1} \ , \quad \gamma_5 = e^{Q} z_8^{-1} z_9 \ , \quad \gamma_6 = e^{Q-P} z_8^{-1} z_9 \ ,$$

$$\gamma_7 = e^{-P} z_1^{-1} z_6^{-1} z_8^{-1} \ , \quad \gamma_8 = e^{-Q} z_1^{-1} z_2^{-1} z_6^{-1} \ , \quad \gamma_9 = e^{P} z_2^{-1} z_4 \ ,$$

$$\gamma_{10} = e^{-Q-P} z_3 z_7 z_9 \ , \quad \gamma_{11} = e^{-2Q-P} z_1^{-1} z_3 z_6^{-1} z_7 \ , \quad \gamma_{12} = e^{-Q} z_3 z_4 z_7 \ ,$$

$$\gamma_{13} = e^{-P} z_3 z_7 z_9 \ , \quad \gamma_{14} = e^{-Q-P} z_1^{-1} z_3 z_6^{-1} z_7 \ , \quad \gamma_{15} = e^{P} z_2^{-1} z_6^{-1} z_7^{-1} \ ,$$

$$\gamma_{16} = e^{Q+2P} z_1 z_2^{-1} z_4 z_7^{-1} \ , \quad \gamma_{17} = e^{Q+P} z_1 z_2^{-1} z_4 z_7^{-1} \ , \quad \gamma_{18} = e^{Q+P} z_2^{-1} z_7^{-1} z_8^{-1} \ ,$$

$$\gamma_{19} = e^{Q} z_2^{-1} z_7^{-1} z_8^{-1} \ , \quad \gamma_{20} = e^{-Q} z_3 z_6^{-1} \ , \quad \gamma_{21} = e^{P} z_1 z_3 z_4 \ . \qquad (3.13)$$

4 Model 2: $\mathbb{C}^3/\mathbb{Z}_4 \times \mathbb{Z}_2$ $(1, 0, 3)(0, 1, 1)$
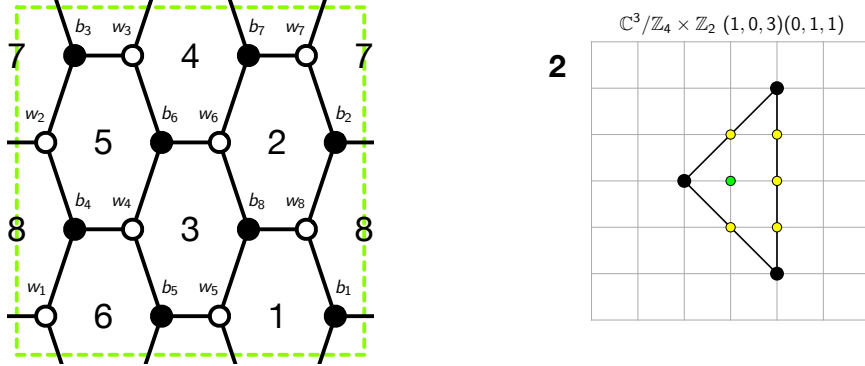

Figure 9: The brane tiling and toric diagram of Model 2.

The brane tiling for Model 2 can be expressed in terms of the following pair of permutation tuples

$$
\begin{aligned}
\sigma_B =\ & (e_{11}\ e_{81}\ e_{71})\ (e_{22}\ e_{72}\ e_{82})\ (e_{13}\ e_{23}\ e_{33})\ (e_{14}\ e_{44}\ e_{24})\ (e_{35}\ e_{55}\ e_{45}) \\
& (e_{36}\ e_{46}\ e_{66})\ (e_{57}\ e_{67}\ e_{77})\ (e_{58}\ e_{88}\ e_{68})\ , \\
\sigma_W^{-1} =\ & (e_{11}\ e_{14}\ e_{13})\ (e_{22}\ e_{23}\ e_{24})\ (e_{33}\ e_{35}\ e_{36})\ (e_{44}\ e_{46}\ e_{45})\ (e_{55}\ e_{58}\ e_{57}) \\
& (e_{66}\ e_{67}\ e_{68})\ (e_{71}\ e_{72}\ e_{77})\ (e_{81}\ e_{88}\ e_{82})\ ,
\end{aligned}
\tag{4.1}
$$

which correspond to black and white nodes of the brane tiling, respectively.

The brane tiling for Model 2 has 8 zig-zag paths given by,

$$
\begin{aligned}
z_1 &= (e_{14}^+\ e_{44}^-\ e_{46}^+\ e_{66}^-\ e_{67}^+\ e_{77}^-\ e_{71}^+\ e_{11}^-)\ , \\
z_2 &= (e_{23}^+\ e_{33}^-\ e_{35}^+\ e_{55}^-\ e_{58}^+\ e_{88}^-\ e_{82}^+\ e_{22}^-)\ , \\
z_3 &= (e_{11}^+\ e_{81}^-\ e_{88}^+\ e_{68}^-\ e_{66}^+\ e_{36}^-\ e_{33}^+\ e_{13}^-)\ , \\
z_4 &= (e_{22}^+\ e_{72}^-\ e_{77}^+\ e_{57}^-\ e_{55}^+\ e_{45}^-\ e_{44}^+\ e_{24}^-)\ , \\
z_5 &= (e_{13}^+\ e_{23}^-\ e_{24}^+\ e_{14}^-)\ ,\ \ z_6 = (e_{36}^+\ e_{46}^-\ e_{45}^+\ e_{35}^-)\ , \\
z_7 &= (e_{57}^+\ e_{67}^-\ e_{68}^+\ e_{58}^-)\ ,\ \ z_8 = (e_{72}^+\ e_{82}^-\ e_{81}^+\ e_{71}^-)\ ,
\end{aligned}
\tag{4.2}
$$

and face paths given by,

$$f_1 = (e_{57}^+ \, e_{77}^- \, e_{71}^+ \, e_{81}^- \, e_{88}^+ \, e_{58}^-) \; , \;\; f_2 = (e_{68}^+ \, e_{88}^- \, e_{82}^+ \, e_{72}^- \, e_{77}^+ \, e_{67}^-) \; ,$$
$$f_3 = (e_{45}^+ \, e_{55}^- \, e_{58}^+ \, e_{68}^- \, e_{66}^+ \, e_{46}^-) \; , \;\; f_4 = (e_{36}^+ \, e_{66}^- \, e_{67}^+ \, e_{57}^- \, e_{55}^+ \, e_{35}^-) \; ,$$
$$f_5 = (e_{24}^+ \, e_{44}^- \, e_{46}^+ \, e_{36}^- \, e_{33}^+ \, e_{23}^-) \; , \;\; f_6 = (e_{13}^+ \, e_{33}^- \, e_{35}^+ \, e_{45}^- \, e_{44}^+ \, e_{14}^-) \; ,$$
$$f_7 = (e_{11}^+ \, e_{71}^- \, e_{72}^+ \, e_{22}^- \, e_{23}^+ \, e_{13}^-) \; , \;\; f_8 = (e_{22}^+ \, e_{82}^- \, e_{81}^+ \, e_{11}^- \, e_{14}^+ \, e_{24}^-) \; , \tag{4.3}$$

which satisfy the following constraints,

$$f_1 f_6^{-1} = z_1 z_3 z_6 z_7, \;\; f_2 f_5^{-1} = z_2 z_4 z_6 z_7 \; , \;\; f_3 f_8^{-1} = z_2 z_3 z_5 z_6 \; ,$$
$$f_4 f_7^{-1} = z_1 z_4 z_5 z_6 \; , \;\; f_5 f_6 = z_5 z_6^{-1} \; , \;\; f_7 f_8 = z_5^{-1} z_8 \; , \;\; f_1 f_2 f_3 f_4 f_5 f_6 f_7 f_8 = 1 \; . \tag{4.4}$$

The face paths can be written in terms of the canonical variables as follows,

$$f_1 = e^{-P} z_1 z_3 z_5 z_7 \; , \;\; f_2 = e^{P} z_2 z_4 z_6 z_7 \; , \;\; f_3 = e^{-Q} z_2 z_3 z_6 z_8 \; ,$$
$$f_4 = e^{Q} z_1 z_4 z_5 z_6 \; , \;\; f_5 = e^{P} \; , \;\; f_6 = e^{-P} z_5 z_6^{-1} \; , \;\; f_7 = e^{Q} \; , \;\; f_8 = e^{-Q} z_5^{-1} z_8 \; . \tag{4.5}$$

The Kasteleyn matrix of the brane tiling for Model 2 in Figure 9 is given by,

$$K = \begin{pmatrix} & b_1 & b_2 & b_3 & b_4 & b_5 & b_6 & b_7 & b_8 \\ \hline w_1 & e_{11}x^{-1} & 0 & e_{13}y^{-1} & e_{14} & 0 & 0 & 0 & 0 \\ w_2. & 0 & e_{22}x^{-1} & e_{23} & e_{24} & 0 & 0 & 0 & 0 \\ w_3 & 0 & 0 & e_{33} & 0 & e_{35}y & e_{36} & 0 & 0 \\ w_4 & 0 & 0 & 0 & e_{44} & e_{45} & e_{46} & 0 & 0 \\ w_5 & 0 & 0 & 0 & 0 & e_{55} & 0 & e_{57}y^{-1} & e_{58} \\ w_6 & 0 & 0 & 0 & 0 & 0 & e_{66} & e_{67} & e_{68} \\ w_7 & e_{71}y & e_{72} & 0 & 0 & 0 & 0 & e_{77} & 0 \\ w_8 & e_{81} & e_{82} & 0 & 0 & 0 & 0 & 0 & e_{88} \end{pmatrix} . \tag{4.6}$$

The permanent of the Kasteleyn matrix gives the spectral curve of the dimer integrable system for Model 2, given by

$$0 = \text{perm} \, K = \bar{p}_0 \cdot x^{-1} \cdot \left[\delta_{(-1,0)} \frac{1}{x} + \delta_{(0,-1)} \frac{1}{y} + \delta_{(0,1)} y + \delta_{(1,-2)} \frac{x}{y^2} \right.$$
$$\left. + \delta_{(1,-1)} \frac{x}{y} + \delta_{(1,0)} x + \delta_{(1,1)} xy + \delta_{(1,2)} xy^2 + H \right] \tag{4.7}$$

where $\bar{p}_0 = e_{11}^+ e_{22}^+ e_{33}^+ e_{44}^+ e_{55}^+ e_{66}^+ e_{77}^+ e_{88}^+$. The Casimirs $\delta_{(m,n)}$ in (4.7) can be expressed in terms of the zig-zag paths in (4.2) as follows,

$$\delta_{(-1,0)} = 1 \; , \;\; \delta_{(0,-1)} = z_3^{-1} + z_4^{-1} \; , \;\; \delta_{(0,1)} = z_1 + z_2 \; .$$
$$\delta_{(1,-2)} = z_3^{-1} z_4^{-1} \; , \;\; \delta_{(1,-1)} = z_3^{-1} z_4^{-1} (z_5^{-1} + z_6^{-1} + z_7^{-1} + z_8^{-1}) \; ,$$
$$\delta_{(1,0)} = z_1 z_2 (z_5 z_6 + z_5 z_7 + z_5 z_8 + z_6 z_7 + z_6 z_8 + z_7 z_8) \; ,$$
$$\delta_{(1,1)} = z_1 z_2 (z_5 + z_6 + z_7 + z_8) \; , \;\; \delta_{(1,2)} = z_1 z_2 \; . \tag{4.8}$$

This allows us to express the spectral curve for Model 2 as follows,

$$\Sigma \; : \; \left(\frac{z_5}{y}+1\right)\left(\frac{z_6}{y}+1\right)\left(\frac{z_7}{y}+1\right)\left(\frac{z_8}{y}+1\right)z_1 z_2 x y^2 + \left(\frac{1}{z_3}+\frac{1}{z_4}\right)\frac{1}{y}$$

$$+(z_1+z_2)y+\frac{1}{x}+H=0 \;. \tag{4.9}$$

The Hamiltonian is given by the sum over all 12 1-loops γ_i,

$$H=\sum_{i=1}^{12}\gamma_i \;, \tag{4.10}$$

where the 1-loops γ_i can be expressed in terms a combination of zig-zag paths and face paths as shown below,

$$\gamma_1 = z_1 z_8 f_2 \;, \quad \gamma_2 = z_1 z_8 f_2 f_3 \;, \quad \gamma_3 = z_1 z_8 f_1 f_2 f_3 \;, \quad \gamma_4 = z_1 z_8 f_2 f_3 f_6 \;,$$

$$\gamma_5 = z_1 z_8 f_1 f_2 f_3 f_6 \;, \quad \gamma_6 = z_1 z_8 f_5^{-1} f_7^{-1} f_8^{-1} \;, \quad \gamma_7 = z_1 z_8 f_4^{-1} f_5^{-1} f_8^{-1} \;,$$

$$\gamma_8 = z_1 z_8 f_5^{-1} f_8^{-1} \;, \quad \gamma_9 = z_1 z_8 f_2 f_5^{-1} f_8^{-1} \;, \quad \gamma_{10} = z_1 z_8 f_8^{-1} \;,$$

$$\gamma_{11} = z_1 z_8 f_2 f_8^{-1} \;, \quad \gamma_{12} = z_1 z_8 f_2 f_3 f_8^{-1} \;. \tag{4.11}$$

The commutation matrix C for Model 2 is given by,

$$C = \begin{pmatrix}
 & \gamma_1 & \gamma_2 & \gamma_3 & \gamma_4 & \gamma_5 & \gamma_6 & \gamma_7 & \gamma_8 & \gamma_9 & \gamma_{10} & \gamma_{11} & \gamma_{12} \\
\hline
\gamma_1 & 0 & 1 & 1 & 1 & 1 & 0 & 0 & -1 & -1 & -1 & -1 & 0 \\
\gamma_2 & -1 & 0 & 1 & 1 & 2 & 1 & 1 & 0 & -1 & -1 & -2 & -1 \\
\gamma_3 & -1 & -1 & 0 & 0 & 1 & 1 & 1 & 1 & 0 & 0 & -1 & -1 \\
\gamma_4 & -1 & -1 & 0 & 0 & 1 & 1 & 1 & 1 & 0 & 0 & -1 & -1 \\
\gamma_5 & -1 & -2 & -1 & -1 & 0 & 1 & 1 & 2 & 1 & 1 & 0 & -1 \\
\gamma_6 & 0 & -1 & -1 & -1 & -1 & 0 & 0 & 1 & 1 & 1 & 1 & 0 \\
\gamma_7 & 0 & -1 & -1 & -1 & -1 & 0 & 0 & 1 & 1 & 1 & 1 & 0 \\
\gamma_8 & 1 & 0 & -1 & -1 & -2 & -1 & -1 & 0 & 1 & 1 & 2 & 1 \\
\gamma_9 & 1 & 1 & 0 & 0 & -1 & -1 & -1 & -1 & 0 & 0 & 1 & 1 \\
\gamma_{10} & 1 & 1 & 0 & 0 & -1 & -1 & -1 & -1 & 0 & 0 & 1 & 1 \\
\gamma_{11} & 1 & 2 & 1 & 1 & 0 & -1 & -1 & -2 & -1 & -1 & 0 & 1 \\
\gamma_{12} & 0 & 1 & 1 & 1 & 1 & 0 & 0 & -1 & -1 & -1 & -1 & 0
\end{pmatrix} . \tag{4.12}$$

The commutation relations are in terms of the 1 -loops, which can be written in terms of the canonical variables as follows,

$$\gamma_1 = e^P z_3^{-1} z_5^{-1} \;, \quad \gamma_2 = e^{-Q+P} z_2 z_5^{-1} z_6 z_8 \;, \quad \gamma_3 = e^{-Q} z_4^{-1} z_5^{-1} \;, \quad \gamma_4 = e^{-Q} z_2 z_8 \;,$$

$$\gamma_5 = e^{-Q-P} z_4^{-1} z_6^{-1} \;, \quad \gamma_6 = e^{-P} z_1 z_5 \;, \quad \gamma_7 = e^{-P} z_4^{-1} z_6^{-1} \;, \quad \gamma_8 = e^{Q-P} z_1 z_5 \;,$$

$$\gamma_9 = e^Q z_3^{-1} z_8^{-1} \;, \quad \gamma_{10} = e^Q z_1 z_5 \;, \quad \gamma_{11} = e^{Q+P} z_3^{-1} z_8^{-1} \;, \quad \gamma_{12} = e^P z_2 z_6 \;. \tag{4.13}$$

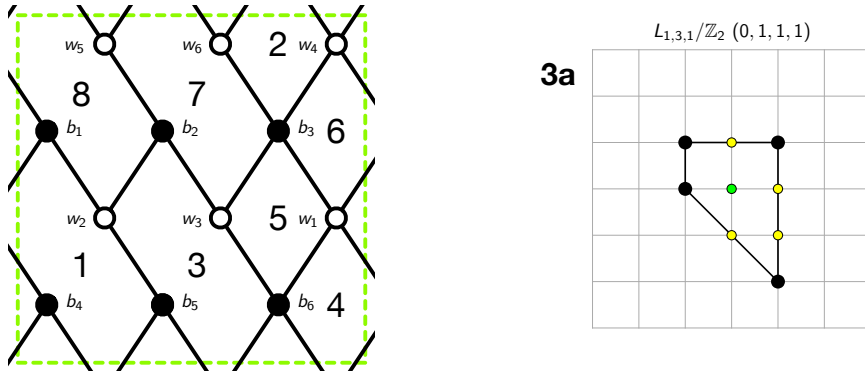# 5   Model 3: $L_{1,3,1}/\mathbb{Z}_2$ $(0,1,1,1)$

5.1   Model 3a

Figure 10: The brane tiling and toric diagram of Model 3a.

The brane tiling for Model 3a can be expressed in terms of the following pair of permutation tuples

$$
\begin{aligned}
\sigma_B &= (e_{11}\ e_{21}\ e_{41})\ (e_{22}\ e_{32}\ e_{52})\ (e_{13}\ e_{43}\ e_{63}\ e_{33})\ (e_{14}\ e_{44}\ e_{54}) \\
&\quad (e_{25}\ e_{55}\ e_{65})\ (e_{16}\ e_{36}\ e_{66}\ e_{46})\ , \\
\sigma_W^{-1} &= (e_{11}\ e_{14}\ e_{16}\ e_{13})\ (e_{21}\ e_{22}\ e_{25})\ (e_{32}\ e_{33}\ e_{36})\ (e_{41}\ e_{43}\ e_{46}\ e_{44}) \\
&\quad (e_{52}\ e_{54}\ e_{55})\ (e_{63}\ e_{65}\ e_{66})\ ,
\end{aligned}
\tag{5.1}
$$

which are associated with black and white nodes in the brane tiling, respectively.

The brane tiling for Model 3a has 8 zig-zag paths given by,

$$
\begin{aligned}
z_1 &= (e_{54}^+\ e_{14}^-\ e_{16}^+\ e_{36}^-\ e_{32}^+\ e_{52}^-)\ ,\ z_2 = (e_{25}^+\ e_{55}^-\ e_{52}^+\ e_{22}^-)\ , \\
z_3 &= (e_{11}^+\ e_{21}^-\ e_{22}^+\ e_{32}^-\ e_{33}^+\ e_{13}^-)\ ,\ z_4 = (e_{55}^+\ e_{65}^-\ e_{66}^+\ e_{46}^-\ e_{44}^+\ e_{54}^-)\ , \\
z_5 &= (e_{21}^+\ e_{41}^-\ e_{43}^+\ e_{63}^-\ e_{65}^+\ e_{25}^-)\ ,\ z_6 = (e_{63}^+\ e_{33}^-\ e_{36}^+\ e_{66}^-)\ , \\
z_7 &= (e_{46}^+\ e_{16}^-\ e_{13}^+\ e_{43}^-)\ ,\ z_8 = (e_{14}^+\ e_{44}^-\ e_{41}^+\ e_{11}^-)\ ,
\end{aligned}
\tag{5.2}
$$

and 8 face paths given by,

$$f_1 = (e_{14}^+ \; e_{54}^- \; e_{55}^+ \; e_{25}^- \; e_{21}^+ \; e_{11}^-) \; , \;\; f_2 = (e_{46}^+ \; e_{66}^- \; e_{63}^+ \; e_{43}^-) \; ,$$
$$f_3 = (e_{25}^+ \; e_{65}^- \; e_{66}^+ \; e_{36}^- \; e_{32}^+ \; e_{22}^-) \; , \;\; f_4 = (e_{16}^+ \; e_{46}^- \; e_{44}^+ \; e_{14}^-) \; ,$$
$$f_5 = (e_{36}^+ \; e_{16}^- \; e_{13}^+ \; e_{33}^-) \; , \;\; f_6 = (e_{11}^+ \; e_{41}^- \; e_{43}^+ \; e_{13}^-) \; ,$$
$$f_7 = (e_{65}^+ \; e_{55}^- \; e_{52}^+ \; e_{32}^- \; e_{33}^+ \; e_{63}^-) \; , \;\; f_8 = (e_{54}^+ \; e_{44}^- \; e_{41}^+ \; e_{21}^- \; e_{22}^+ \; e_{52}^-) \; , \tag{5.3}$$

which satisfy the following constraints,

$$f_1 f_2^{-1} = z_4 z_5 z_8 \; , \;\; f_2 f_8 = z_2^{-1} z_4^{-1} z_5^{-1} \; , \;\; f_3 f_6^{-1} = z_3^{-1} z_5^{-1} z_6^{-1} \; ,$$
$$f_4 f_7^{-1} = z_1 z_4 z_6 \; , f_5 f_8^{-1} = z_1^{-1} z_3^{-1} z_8^{-1} \; , \;\; f_6 f_7 = z_2 z_3 z_5 \; , \;\; f_1 f_2 f_3 f_4 f_5 f_6 f_7 f_8 = 1 \; . \tag{5.4}$$

The face paths can be written in terms of the canonical variables as shown below,

$$f_1 = e^Q z_4 z_5 z_8 \; , \;\; f_2 = e^Q \; , \;\; f_3 = e^{-P} z_2 z_6^{-1} \; , \;\; f_4 = e^P z_1 z_4 z_6 \; ,$$
$$f_5 = e^{-Q} z_6 z_7 \; , \;\; f_6 = e^{-P} z_2 z_3 z_5 \; , \;\; f_7 = e^P \; , \;\; f_8 = e^{-Q} z_2^{-1} z_4^{-1} z_5^{-1} \; . \tag{5.5}$$

The Kasteleyn matrix of the brane tiling for Model 3a in Figure 10 is given by,

$$K = \begin{pmatrix}
 & b_1 & b_2 & b_3 & b_4 & b_5 & b_6 \\
\hline
w_1 & e_{11}x & 0 & e_{13} & e_{14}x & 0 & e_{16} \\
w_2 & e_{21} & e_{22} & 0 & 0 & e_{25} & 0 \\
w_3 & 0 & e_{32} & e_{33} & 0 & 0 & e_{36} \\
w_4 & e_{41}x & 0 & e_{43} & e_{44}xy & 0 & e_{46}y \\
w_5 & 0 & e_{52} & 0 & e_{54}y & e_{55}y & 0 \\
w_6 & 0 & 0 & e_{63} & 0 & e_{65}y & e_{66}y
\end{pmatrix} \; . \tag{5.6}$$

The permanent of the Kasteleyn matrix gives the spectral curve of the dimer integrable system for Model 3a as shown below,

$$0 = \mathrm{perm}\, K = \overline{p}_0 \cdot xy^2 \cdot \left[\delta_{(-1,0)} \frac{1}{x} + \delta_{(-1,1)} \frac{y}{x} + \delta_{(0,-1)} \frac{1}{y} + \delta_{(0,1)} y \right.$$
$$\left. + \delta_{(1,-2)} \frac{x}{y^2} + \delta_{(1,-1)} \frac{x}{y} + \delta_{(1,0)} x + \delta_{(1,1)} xy + H \right] \; , \tag{5.7}$$

where $\overline{p}_0 = e_{11}^+ e_{22}^+ e_{33}^+ e_{44}^+ e_{55}^+ e_{66}^+$. The Casimirs $\delta_{(m,n)}$ in (5.7) can be expressed in terms of zig-zag paths in (5.2) as follows,

$$\delta_{(-1,0)} = z_3^{-1} z_4^{-1} z_7^{-1} \; , \;\; \delta_{(-1,1)} = z_3^{-1} z_4^{-1} \; , \;\; \delta_{(0,-1)} = z_2 z_6 z_8 (z_1 + z_5) \; .$$
$$\delta_{(0,1)} = z_3^{-1} + z_4^{-1} \; , \;\; \delta_{(1,-2)} = z_2 z_6 z_8 \; , \;\; \delta_{(1,-1)} = z_2 z_6 + z_2 z_8 + z_6 z_8 \; ,$$
$$\delta_{(1,0)} = z_2 + z_6 + z_8 \; , \;\; \delta_{(1,1)} = 1 \; . \tag{5.8}$$

Accordingly, we can express the spectral curve for Model 3a as follows,

$$\Sigma \; : \; \left(\frac{1}{z_3} + \frac{1}{z_4}\right)y + \frac{(1 + z_7 y)}{z_3 z_4 z_7}\frac{1}{x} + (z_1 + z_5)z_2 z_6 z_8 \frac{1}{y}$$
$$+ \left(1 + \frac{z_2}{y}\right)\left(1 + \frac{z_6}{y}\right)\left(1 + \frac{z_8}{y}\right)xy + H = 0 \; . \tag{5.9}$$

The Hamiltonian is a sum over all 12 1-loops γ_i given by,

$$H = \sum_{i=1}^{12} \gamma_i \; , \tag{5.10}$$

where the 1-loops γ_i can be expressed in terms of zig-zag paths and face paths as follows,

$$\gamma_1 = z_3^{-1} z_8 f_6 \; , \;\; \gamma_2 = z_2 z_4^{-1} f_1 f_7^{-1} \; , \;\; \gamma_3 = z_1 z_2 z_6 f_1 \; ,$$
$$\gamma_4 = z_2 z_4^{-1} f_1 \; , \;\; \gamma_5 = z_2 z_4^{-1} f_1 f_4 \; , \;\; \gamma_6 = z_1^{-1} z_2 z_3^{-1} z_4^{-1} z_8^{-1} f_1 f_4 f_8 \; ,$$
$$\gamma_7 = z_1 z_2 z_6 f_1 f_7 f_8 \; , \;\; \gamma_8 = z_4^{-1} z_8 f_4 f_5 \; , \;\; \gamma_9 = z_2 z_3 z_4^{-1} z_5 z_8 f_4 f_5 f_7^{-1} \; ,$$
$$\gamma_{10} = z_1 z_2 z_8 f_5 \; , \;\; \gamma_{11} = z_2 z_4^{-1} z_6^{-1} z_7^{-1} f_5 f_7^{-1} \; , \;\; \gamma_{12} = z_4^{-1} z_6 f_3 \; . \tag{5.11}$$

The commutation matrix C for Model 3a takes the following form,

$$C = \begin{array}{c|cccccccccccc}
 & \gamma_1 & \gamma_2 & \gamma_3 & \gamma_4 & \gamma_5 & \gamma_6 & \gamma_7 & \gamma_8 & \gamma_9 & \gamma_{10} & \gamma_{11} & \gamma_{12} \\
\hline
\gamma_1 & 0 & 1 & 1 & 1 & 1 & 0 & 0 & -1 & -1 & -1 & -1 & 0 \\
\gamma_2 & -1 & 0 & 1 & 1 & 2 & 1 & 1 & 0 & -1 & -1 & -2 & -1 \\
\gamma_3 & -1 & -1 & 0 & 0 & 1 & 1 & 1 & 1 & 0 & 0 & -1 & -1 \\
\gamma_4 & -1 & -1 & 0 & 0 & 1 & 1 & 1 & 1 & 0 & 0 & -1 & -1 \\
\gamma_5 & -1 & -2 & -1 & -1 & 0 & 1 & 1 & 2 & 1 & 1 & 0 & -1 \\
\gamma_6 & 0 & -1 & -1 & -1 & -1 & 0 & 0 & 1 & 1 & 1 & 1 & 0 \\
\gamma_7 & 0 & -1 & -1 & -1 & -1 & 0 & 0 & 1 & 1 & 1 & 1 & 0 \\
\gamma_8 & 1 & 0 & -1 & -1 & -2 & -1 & -1 & 0 & 1 & 1 & 2 & 1 \\
\gamma_9 & 1 & 1 & 0 & 0 & -1 & -1 & -1 & -1 & 0 & 0 & 1 & 1 \\
\gamma_{10} & 1 & 1 & 0 & 0 & -1 & -1 & -1 & -1 & 0 & 0 & 1 & 1 \\
\gamma_{11} & 1 & 2 & 1 & 1 & 0 & -1 & -1 & -2 & -1 & -1 & 0 & 1 \\
\gamma_{12} & 0 & 1 & 1 & 1 & 1 & 0 & 0 & -1 & -1 & -1 & -1 & 0 \\
\end{array} \; . \tag{5.12}$$

The 1-loops, which satisfy the commutation relations given by the above commutation matrix, can be written in terms of the canonical variables as follows,

$$\gamma_1 = e^{-P} z_2 z_5 z_8 \; , \;\; \gamma_2 = e^{Q-P} z_2 z_5 z_8 \; , \;\; \gamma_3 = e^Q z_3^{-1} z_7^{-1} \; ,$$
$$\gamma_4 = e^Q z_2 z_5 z_8 \; , \;\; \gamma_5 = e^{Q+P} z_3^{-1} z_7^{-1} \; , \;\; \gamma_6 = e^P z_3^{-1} z_6 \; ,$$
$$\gamma_7 = e^P z_1 z_6 z_8 \; , \;\; \gamma_8 = e^{-Q+P} z_1 z_6^2 z_7 z_8 \; , \;\; \gamma_9 = e^{-Q} z_4^{-1} z_6 \; ,$$
$$\gamma_{10} = e^{-Q} z_3^{-1} z_4^{-1} z_5^{-1} \; , \;\; \gamma_{11} = e^{-Q-P} z_2 z_4^{-1} \; , \;\; \gamma_{12} = e^{-P} z_2 z_4^{-1} \; . \tag{5.13}$$
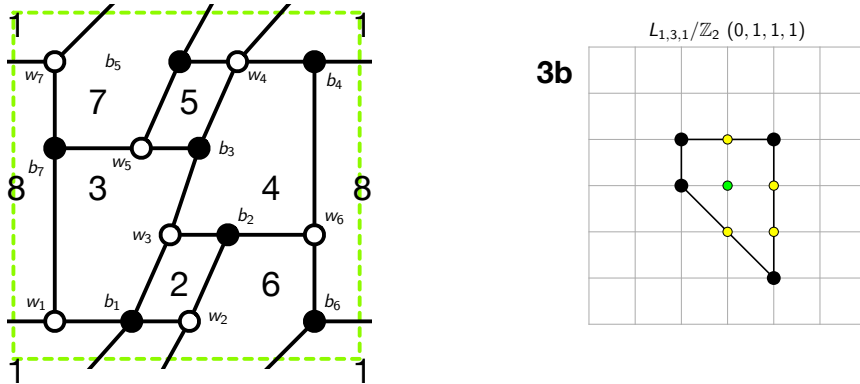
5.2 Model 3b

Figure 11: The brane tiling and toric diagram of Model 3b.

The brane tiling for Model 3b can be expressed in terms of the following pair of permutation tuples

$$
\begin{aligned}
\sigma_B &= (e_{11}\ e_{71}\ e_{21}\ e_{31})\ (e_{22}\ e_{62}\ e_{32})\ (e_{33}\ e_{43}\ e_{53})\ (e_{44}\ e_{64}\ e_{74}) \\
&\quad (e_{25}\ e_{55}\ e_{45})\ (e_{16}\ e_{66}\ e_{46})\ (e_{17}\ e_{57}\ e_{77})\ , \\
\sigma_W^{-1} &= (e_{11}\ e_{16}\ e_{17})\ (e_{21}\ e_{22}\ e_{25})\ (e_{31}\ e_{33}\ e_{32})\ (e_{43}\ e_{45}\ e_{46}\ e_{44}) \\
&\quad (e_{53}\ e_{57}\ e_{55})\ (e_{62}\ e_{64}\ e_{66})\ (e_{71}\ e_{77}\ e_{74})\ ,
\end{aligned}
\tag{5.14}
$$

which are associated with black and white nodes in the brane tiling, respectively.

The brane tiling for Model 3b has 8 zig-zag paths given by,

$$
\begin{aligned}
z_1 &= (e_{74}^+\ e_{44}^-\ e_{43}^+\ e_{53}^-\ e_{57}^+\ e_{77}^-)\ ,\quad z_2 = (e_{11}^+\ e_{71}^-\ e_{77}^+\ e_{17}^-)\ , \\
z_3 &= (e_{46}^+\ e_{16}^-\ e_{17}^+\ e_{57}^-\ e_{55}^+\ e_{45}^-)\ ,\quad z_4 = (e_{21}^+\ e_{31}^-\ e_{33}^+\ e_{43}^-\ e_{45}^+\ e_{25}^-)\ , \\
z_5 &= (e_{32}^+\ e_{22}^-\ e_{25}^+\ e_{55}^-\ e_{53}^+\ e_{33}^-)\ ,\quad z_6 = (e_{16}^+\ e_{66}^-\ e_{62}^+\ e_{32}^-\ e_{31}^+\ e_{11}^-)\ , \\
z_7 &= (e_{44}^+\ e_{64}^-\ e_{66}^+\ e_{46}^-)\ ,\quad z_8 = (e_{71}^+\ e_{21}^-\ e_{22}^+\ e_{62}^-\ e_{64}^+\ e_{74}^-)\ ,
\end{aligned}
\tag{5.15}
$$

and 9 face paths given by,

$$f_1 = (e_{44}^+ \ e_{74}^- \ e_{71}^+ \ e_{11}^- \ e_{16}^+ \ e_{46}^-) \ , \ \ f_2 = (e_{31}^+ \ e_{21}^- \ e_{22}^+ \ e_{32}^-) \ ,$$
$$f_3 = (e_{11}^+ \ e_{31}^- \ e_{33}^+ \ e_{53}^- \ e_{57}^+ \ e_{17}^-) \ , \ \ f_4 = (e_{32}^+ \ e_{62}^- \ e_{64}^+ \ e_{44}^- \ e_{43}^+ \ e_{33}^-) \ ,$$
$$f_5 = (e_{53}^+ \ e_{43}^- \ e_{45}^+ \ e_{55}^-) \ , \ \ f_6 = (e_{46}^+ \ e_{66}^- \ e_{62}^+ \ e_{22}^- \ e_{25}^+ \ e_{45}^-) \ ,$$
$$f_7 = (e_{21}^+ \ e_{71}^- \ e_{77}^+ \ e_{57}^- \ e_{55}^+ \ e_{25}^-) \ , \ \ f_8 = (e_{74}^+ \ e_{64}^- \ e_{66}^+ \ e_{16}^- \ e_{17}^+ \ e_{77}^-) \ , \tag{5.16}$$

which are under the following constraints,

$$f_2 f_8^{-1} = z_2 z_6 z_8 \ , \ \ f_3^{-1} f_6 = z_3 z_5 z_6 \ , \ \ f_4 f_7^{-1} = z_1 z_5 z_8 \ , \ \ f_5^{-1} f_8 = z_1 z_3 z_7 \ ,$$
$$f_6 f_7 f_8 = z_3 z_8^{-1} \ , \ \ f_1^{-1} f_6 f_7 = z_2 z_3 z_7^{-1} z_8^{-1} \ , \ \ f_1 f_2 f_3 f_4 f_5 f_6 f_7 f_8 = 1 \ . \tag{5.17}$$

The face paths can be written in terms of the canonical variables as follows,

$$f_1 = e^{-P} z_2^{-1} z_7 \ , \ \ f_2 = e^P z_2 z_6 z_8 \ , \ \ f_3 = e^{-Q-P} z_5^{-1} z_6^{-1} z_8^{-1} \ , \ \ f_4 = e^Q z_1 z_5 z_8 \ ,$$
$$f_5 = e^P z_1^{-1} z_3^{-1} z_7^{-1} \ , \ \ f_6 = e^{-Q-P} z_3 z_8^{-1} \ , \ \ f_7 = e^Q \ , \ \ f_8 = e^P \ . \tag{5.18}$$

The Kasteleyn matrix of the brane tiling for Model 3b in Figure 11 takes the following form,

$$K = \begin{pmatrix}
\begin{array}{c|ccccccc}
 & b_1 & b_2 & b_3 & b_4 & b_5 & b_6 & b_7 \\
\hline
w_1 & e_{11} & 0 & 0 & 0 & 0 & e_{16}x^{-1} & e_{17} \\
w_2 & e_{21} & e_{22} & 0 & 0 & e_{25}y^{-1} & 0 & 0 \\
w_3 & e_{31} & e_{32} & e_{33} & 0 & 0 & 0 & 0 \\
w_4 & 0 & 0 & e_{43} & e_{44} & e_{45} & e_{46}y & 0 \\
w_5 & 0 & 0 & e_{53} & 0 & e_{55} & 0 & e_{57} \\
w_6 & 0 & e_{62} & 0 & e_{64} & 0 & e_{66} & 0 \\
w_7 & e_{71}y & 0 & 0 & e_{74}x^{-1} & 0 & 0 & e_{77}
\end{array}
\end{pmatrix} \ . \tag{5.19}$$

By taking the permanent of the Kasteleyn matrix in (5.19) with a $GL(2, \mathbb{Z})$ transformation $M : (x, y) \mapsto (x, \frac{1}{y})$, we obtain the following spectral curve of the dimer integrable system for Model 3b,

$$0 = \bar{p}_0 \cdot x^{-1} \cdot \left[\delta_{(-1,1)} \frac{y}{x} + \delta_{(-1,0)} \frac{1}{x} + \delta_{(0,-1)} \frac{1}{y} + \delta_{(0,1)} y \right.$$
$$\left. + \delta_{(1,-2)} \frac{x}{y^2} + \delta_{(1,-1)} \frac{x}{y} + \delta_{(1,0)} x + \delta_{(1,1)} xy + H \right] \ , \tag{5.20}$$

where $\bar{p}_0 = e_{17}^+ e_{22}^+ e_{33}^+ e_{46}^+ e_{55}^+ e_{64}^+ e_{71}^+$. The Casimirs $\delta_{(m,n)}$ in (5.20) can be expressed in terms of the zig-zag paths in (5.15) as follows,

$$\delta_{(-1,1)} = z_3^{-1} z_4^{-1} z_8^{-1} \ , \ \ \delta_{(-1,0)} = z_3^{-1} z_8^{-1} \ , \ \ \delta_{(0,-1)} = z_3^{-1} + z_8^{-1} \ .$$
$$\delta_{(0,1)} = z_2 z_5 z_7 (z_1 + z_6) \ , \ \ \delta_{(1,-2)} = 1 \ , \ \ \delta_{(1,-1)} = z_2 + z_5 + z_7 \ ,$$
$$\delta_{(1,0)} = z_2 z_5 + z_2 z_7 + z_5 z_7 \ , \ \ \delta_{(1,1)} = z_2 z_5 z_7 \ . \tag{5.21}$$

This leads to the following form of the spectral curve for Model 3b,

$$\Sigma \; : \; \left(\frac{1}{y} + z_2\right)\left(\frac{1}{y} + z_5\right)\left(\frac{1}{y} + z_7\right)xy + \left(\frac{1}{z_1 z_4} + \frac{1}{z_4 z_6} + \frac{1}{z_4 x}\right)\frac{y}{z_3 z_8}$$
$$+ \frac{1}{z_3 y} + \left(\frac{1}{z_3} + \frac{x}{y}\right)\frac{1}{z_8 x} + H = 0 \; . \tag{5.22}$$

The Hamiltonian is a sum over all 14 1-loops γ_i given by,

$$H = \sum_{i=1}^{14} \gamma_i \; , \tag{5.23}$$

where the 1-loops γ_i can be expressed in terms of zig-zag paths and face paths as follows,

$$\gamma_1 = z_5 z_6 z_7 f_3 \; , \;\; \gamma_2 = z_2 z_8^{-1} f_1 \; , \;\; \gamma_3 = z_7 z_8^{-1} f_2 f_4 f_8^{-1} \; , \;\; \gamma_4 = z_2 z_8^{-1} f_1 f_4 \; ,$$
$$\gamma_5 = z_3^{-1} z_7 f_4 f_6 \; , \;\; \gamma_6 = z_1^{-1} z_3^{-1} z_8^{-1} f_4 \; , \;\; \gamma_7 = z_1^{-1} z_2 z_3^{-1} z_6 f_4 f_8 \; , \;\; \gamma_8 = z_7 z_8^{-1} f_4 \; ,$$
$$\gamma_9 = z_4 z_5 z_7 z_8^{-1} f_2 f_4 \; , \;\; \gamma_{10} = z_7 z_8^{-1} f_2 f_4 \; , \;\; \gamma_{11} = z_2 z_4 z_7 z_8^{-1} f_2 f_4 f_7^{-1} \; , \;\; \gamma_{12} = z_4^{-1} z_8^{-1} f_3 f_5 \; ,$$
$$\gamma_{13} = z_1^{-1} z_3^{-1} z_8^{-1} f_2 f_4 f_8 \; , \;\; \gamma_{14} = z_5 z_8^{-1} f_2 \; . \tag{5.24}$$

The commutation matrix C for Model 3b has the following form,

$$C = \left(\begin{array}{c|cccccccccccccc}
 & \gamma_1 & \gamma_2 & \gamma_3 & \gamma_4 & \gamma_5 & \gamma_6 & \gamma_7 & \gamma_8 & \gamma_9 & \gamma_{10} & \gamma_{11} & \gamma_{12} & \gamma_{13} & \gamma_{14} \\
\hline
\gamma_1 & 0 & 1 & 1 & 2 & 1 & 1 & 0 & 1 & 0 & 0 & -1 & -1 & -1 & -1 \\
\gamma_2 & -1 & 0 & 1 & 1 & 0 & 1 & 1 & 1 & 1 & 1 & 0 & -1 & 1 & 0 \\
\gamma_3 & -1 & -1 & 0 & -1 & -1 & 0 & 1 & 0 & 1 & 1 & 1 & 0 & 2 & 1 \\
\gamma_4 & -2 & -1 & 1 & 0 & -1 & 1 & 2 & 1 & 2 & 2 & 1 & -1 & 3 & 1 \\
\gamma_5 & -1 & 0 & 1 & 1 & 0 & 1 & 1 & 1 & 1 & 1 & 0 & -1 & 1 & 0 \\
\gamma_6 & -1 & -1 & 0 & -1 & -1 & 0 & 1 & 0 & 1 & 1 & 1 & 0 & 2 & 1 \\
\gamma_7 & 0 & -1 & -1 & -2 & -1 & -1 & 0 & -1 & 0 & 0 & 1 & 1 & 1 & 1 \\
\gamma_8 & -1 & -1 & 0 & -1 & -1 & 0 & 1 & 0 & 1 & 1 & 1 & 0 & 2 & 1 \\
\gamma_9 & 0 & -1 & -1 & -2 & -1 & -1 & 0 & -1 & 0 & 0 & 1 & 1 & 1 & 1 \\
\gamma_{10} & 0 & -1 & -1 & -2 & -1 & -1 & 0 & -1 & 0 & 0 & 1 & 1 & 1 & 1 \\
\gamma_{11} & 1 & 0 & -1 & -1 & 0 & -1 & -1 & -1 & -1 & -1 & 0 & 1 & -1 & 0 \\
\gamma_{12} & 1 & 1 & 0 & 1 & 1 & 0 & -1 & 0 & -1 & -1 & -1 & 0 & -2 & -1 \\
\gamma_{13} & 1 & -1 & -2 & -3 & -1 & -2 & -1 & -2 & -1 & -1 & 1 & 2 & 0 & 1 \\
\gamma_{14} & 1 & 0 & -1 & -1 & 0 & -1 & -1 & -1 & -1 & -1 & 0 & 1 & -1 & 0 \\
\end{array}\right) . \tag{5.25}$$

The 1-loops forming the commutation relations can be written in terms of the canonical variables as follows,

$$\gamma_1 = e^{-Q-P} z_7 z_8^{-1} \ , \ \ \gamma_2 = e^{-P} z_7 z_8^{-1} \ , \ \ \gamma_3 = e^{Q} z_3^{-1} z_4^{-1} \ , \ \ \gamma_4 = e^{Q-P} z_1 z_5 z_7 \ ,$$
$$\gamma_5 = e^{-P} z_1 z_5 z_7 \ , \ \ \gamma_6 = e^{Q} z_3^{-1} z_5 \ , \ \ \gamma_7 = e^{Q+P} z_2 z_3^{-1} z_5 z_6 z_8 \ , \ \ \gamma_8 = e^{Q} z_1 z_5 z_7 \ ,$$
$$\gamma_9 = e^{Q+P} z_3^{-1} z_5 \ , \ \ \gamma_{10} = e^{Q+P} z_3^{-1} z_4^{-1} \ , \ \ \gamma_{11} = e^{P} z_2 z_3^{-1} \ , \ \ \gamma_{12} = e^{-Q} z_2 z_8^{-1} \ ,$$
$$\gamma_{13} = e^{Q+2P} z_2 z_3^{-1} z_5 z_6 z_8 \ , \ \ \gamma_{14} = e^{P} z_2 z_5 z_6 \ . \tag{5.26}$$

6   Model 4: $\mathcal{C}/\mathbb{Z}_2 \times \mathbb{Z}_2 \ (1,0,0,1)(0,1,1,0)$, $\mathbf{PdP}_5$
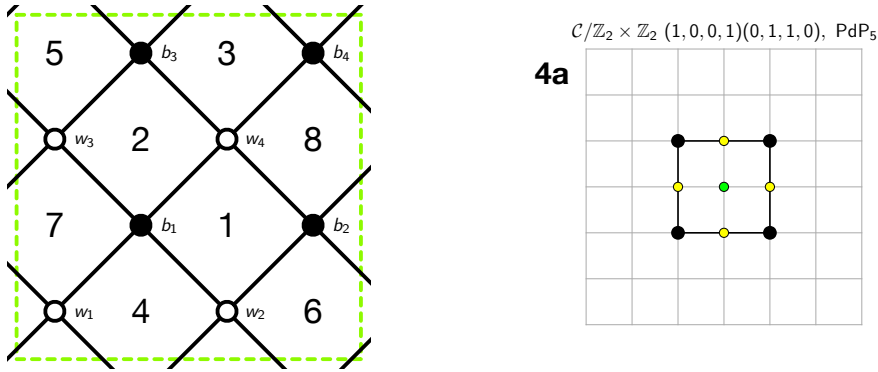
6.1   Model 4a

Figure 12: The brane tiling and toric diagram of Model 4a.

The brane tiling for Model 4a can be expressed in terms of the following pair of permutation tuples

$$\sigma_B = (e_{11} \ e_{21} \ e_{41} \ e_{31}) \ (e_{12} \ e_{32} \ e_{42} \ e_{22}) \ (e_{13} \ e_{33} \ e_{43} \ e_{23}) \ (e_{14} \ e_{24} \ e_{44} \ e_{34}) \ ,$$
$$\sigma_W^{-1} = (e_{11} \ e_{13} \ e_{14} \ e_{12}) \ (e_{21} \ e_{22} \ e_{24} \ e_{23}) \ (e_{31} \ e_{32} \ e_{34} \ e_{33}) \ (e_{41} \ e_{43} \ e_{44} \ e_{42}) \ , \tag{6.1}$$

which correspond to the black and white nodes in the brane tiling, respectively.

The brane tiling for Model 4a has 8 zig-zag paths given by,

$$z_1 = (e_{11}^+ \; e_{21}^- \; e_{22}^+ \; e_{12}^-) \;, \;\; z_2 = (e_{32}^+ \; e_{42}^- \; e_{41}^+ \; e_{31}^-) \;,$$
$$z_3 = (e_{33}^+ \; e_{43}^- \; e_{44}^+ \; e_{34}^-) \;, \;\; z_4 = (e_{14}^+ \; e_{24}^- \; e_{23}^+ \; e_{13}^-) \;,$$
$$z_5 = (e_{13}^+ \; e_{33}^- \; e_{31}^+ \; e_{11}^-) \;, \;\; z_6 = (e_{21}^+ \; e_{41}^- \; e_{43}^+ \; e_{23}^-) \;,$$
$$z_7 = (e_{24}^+ \; e_{44}^- \; e_{42}^+ \; e_{22}^-) \;, \;\; z_8 = (e_{12}^+ \; e_{32}^- \; e_{34}^+ \; e_{14}^-) \;, \tag{6.2}$$

and 8 face paths given by,

$$f_1 = (e_{22}^+ \; e_{42}^- \; e_{41}^+ \; e_{21}^-) \;, \;\; f_2 = (e_{43}^+ \; e_{33}^- \; e_{31}^+ \; e_{41}^-) \;,$$
$$f_3 = (e_{44}^+ \; e_{24}^- \; e_{23}^+ \; e_{43}^-) \;, \;\; f_4 = (e_{21}^+ \; e_{11}^- \; e_{13}^+ \; e_{23}^-) \;,$$
$$f_5 = (e_{33}^+ \; e_{13}^- \; e_{14}^+ \; e_{34}^-) \;, \;\; f_6 = (e_{12}^+ \; e_{22}^- \; e_{24}^+ \; e_{14}^-) \;,$$
$$f_7 = (e_{11}^+ \; e_{31}^- \; e_{32}^+ \; e_{12}^-) \;, \;\; f_8 = (e_{34}^+ \; e_{44}^- \; e_{42}^+ \; e_{32}^-) \;, \tag{6.3}$$

which satisfy the following constraints,

$$f_6 f_8 = z_7 z_8 \;, \;\; f_5 f_7 = z_5^{-1} z_8^{-1} \;, \;\; f_4 f_8^{-1} = z_2 z_3 z_5 z_6 \;, \;\; f_3 f_7^{-1} = z_3 z_4 z_5 z_8 \;,$$
$$f_2 f_6^{-1} = z_1 z_4 z_5 z_6 \;, \;\; f_1 f_5^{-1} = z_1 z_2 z_5 z_8 \;, \;\; f_1 f_2 f_3 f_4 f_5 f_6 f_7 f_8 = 1 \;. \tag{6.4}$$

The face paths can be written in terms of the canonical variables as follows,

$$f_1 = e^Q \;, \;\; f_2 = e^P \;, \;\; f_3 = e^{-Q} z_6^{-1} z_7^{-1} \;, \;\; f_4 = e^{-P} z_5 z_6 \;,$$
$$f_5 = e^Q z_3 z_4 z_6 z_7 \;, \;\; f_6 = e^P z_2 z_3 z_7 z_8 \;, \;\; f_7 = e^{-Q} z_1 z_2 \;, \;\; f_8 = e^{-P} z_2^{-1} z_3^{-1} \;. \tag{6.5}$$

The Kasteleyn matrix of the brane tiling for Model 4a in Figure 12 is given by,

$$K = \begin{pmatrix} \begin{array}{c|cccc} & b_1 & b_2 & b_3 & b_4 \\ \hline w_1 & e_{11} & e_{12}x^{-1} & e_{13}y^{-1} & e_{14}x^{-1}y^{-1} \\ w_2 & e_{21} & e_{22} & e_{23}y^{-1} & e_{24}y^{-1} \\ w_3 & e_{31} & e_{32}x^{-1} & e_{33} & e_{34}x^{-1} \\ w_4 & e_{41} & e_{42} & e_{43} & e_{44} \end{array} \end{pmatrix} \;. \tag{6.6}$$

The permanent of the Kasteleyn matrix in (6.6) gives us the spectral curve of the dimer integrable system for Model 4a as follows,

$$0 = \text{perm } K = \bar{p}_0 \cdot x^{-1} y^{-1} \cdot \Big[\delta_{(-1,-1)} \frac{1}{xy} + \delta_{(-1,1)} \frac{y}{x} + \delta_{(1,-1)} \frac{x}{y} + \delta_{(1,1)} xy$$
$$+ \delta_{(-1,0)} \frac{1}{x} + \delta_{(0,-1)} \frac{1}{y} + \delta_{(1,0)} x + \delta_{(0,1)} y + H \Big] \;, \tag{6.7}$$

where $\bar{p}_0 = e_{14}^+ e_{21}^+ e_{32}^+ e_{43}^+$. The Casimirs $\delta_{(m,n)}$ in (6.7) can be expressed in terms of the zig-zag paths in (6.2) as follows,

$$\delta_{(-1,-1)} = z_6^{-1} \; , \;\; \delta_{(-1,1)} = z_8 \; , \;\; \delta_{(1,-1)} = z_2^{-1} z_4^{-1} z_6^{-1} \; , \;\; \delta_{(1,1)} = z_1 z_3 z_8 \; ,$$

$$\delta_{(-1,0)} = 1 + z_6^{-1} z_8 \; , \;\; \delta_{(0,-1)} = z_2^{-1} z_6^{-1} + z_4^{-1} z_6^{-1} \; ,$$

$$\delta_{(1,0)} = z_1 z_3 z_7 z_8 + z_1 z_3 z_5 z_8 \; , \;\; \delta_{(0,1)} = z_1 z_8 + z_3 z_8 \; . \tag{6.8}$$

This leads to the following form for the spectral curve of Model 4a,

$$\Sigma \;:\; \left(\frac{1}{y} + z_6\right)\left(\frac{1}{y} + z_8\right)\frac{y}{z_6 x} + \left(\frac{1}{z_2} + \frac{1}{z_4}\right)\frac{1}{z_6 y}$$

$$+ \left(\frac{1}{y} + \frac{1}{z_5}\right)\left(\frac{1}{y} + \frac{1}{z_7}\right)\frac{xy}{z_2 z_4 z_6} + (z_1 + z_3) z_8 y + H = 0 \; . \tag{6.9}$$

The Hamiltonian is a sum over all 12 1-loops γ_i,

$$H = \sum_{i=1}^{12} \gamma_i \; , \tag{6.10}$$

where the 1-loops γ_i can be expressed in terms of zig-zag paths and face paths as follows,

$$\gamma_1 = z_1 f_6 \; , \;\; \gamma_2 = z_1 f_3 f_6 \; , \;\; \gamma_3 = z_1 f_3 f_6 f_8 \; , \;\; \gamma_4 = z_1 f_3 f_4 f_6 \; ,$$

$$\gamma_5 = z_1 f_3 f_4 f_6 f_8 \; , \;\; \gamma_6 = z_1 f_1 f_3 f_4 f_6 f_8 \; , \;\; \gamma_7 = z_1 f_3 f_4 f_5 f_6 f_8 \; ,$$

$$\gamma_8 = z_1 f_1 f_3 f_4 f_5 f_6 f_8 \; , \;\; \gamma_9 = z_1 f_1 f_3 f_4 f_5 f_6^2 f_8 \; , \;\; \gamma_{10} = z_1 f_1 f_2 f_3 f_4 f_5 f_6 f_8 \; ,$$

$$\gamma_{11} = z_1 f_1 f_2 f_3 f_4 f_5 f_6^2 f_8 \; , \;\; \gamma_{12} = z_1 f_1 f_2 f_3^2 f_4 f_5 f_6^2 f_8 \; . \tag{6.11}$$

The commutation matrix C for Model 4a takes the following form,

$$C = \begin{pmatrix} & \gamma_1 & \gamma_2 & \gamma_3 & \gamma_4 & \gamma_5 & \gamma_6 & \gamma_7 & \gamma_8 & \gamma_9 & \gamma_{10} & \gamma_{11} & \gamma_{12} \\ \hline \gamma_1 & 0 & 1 & 1 & 1 & 1 & 0 & 0 & -1 & -1 & -1 & -1 & 0 \\ \gamma_2 & -1 & 0 & 1 & 1 & 2 & 1 & 1 & 0 & -1 & -1 & -2 & -1 \\ \gamma_3 & -1 & -1 & 0 & 0 & 1 & 1 & 1 & 1 & 0 & 0 & -1 & -1 \\ \gamma_4 & -1 & -1 & 0 & 0 & 1 & 1 & 1 & 1 & 0 & 0 & -1 & -1 \\ \gamma_5 & -1 & -2 & -1 & -1 & 0 & 1 & 1 & 2 & 1 & 1 & 0 & -1 \\ \gamma_6 & 0 & -1 & -1 & -1 & -1 & 0 & 0 & 1 & 1 & 1 & 1 & 0 \\ \gamma_7 & 0 & -1 & -1 & -1 & -1 & 0 & 0 & 1 & 1 & 1 & 1 & 0 \\ \gamma_8 & 1 & 0 & -1 & -1 & -2 & -1 & -1 & 0 & 1 & 1 & 2 & 1 \\ \gamma_9 & 1 & 1 & 0 & 0 & -1 & -1 & -1 & -1 & 0 & 0 & 1 & 1 \\ \gamma_{10} & 1 & 1 & 0 & 0 & -1 & -1 & -1 & -1 & 0 & 0 & 1 & 1 \\ \gamma_{11} & 1 & 2 & 1 & 1 & 0 & -1 & -1 & -2 & -1 & -1 & 0 & 1 \\ \gamma_{12} & 0 & 1 & 1 & 1 & 1 & 0 & 0 & -1 & -1 & -1 & -1 & 0 \end{pmatrix} \; , \tag{6.12}$$

where the 1-loops satisfying the commutation relations can be written in terms of the canonical variables as follows,

$$\gamma_1 = e^P z_4^{-1} z_5^{-1} z_6^{-1} \ , \ \ \gamma_2 = e^{-Q+P} z_1 z_2 z_3 z_6^{-1} z_8 \ , \ \ \gamma_3 = e^{-Q} z_1 z_6^{-1} z_8 \ ,$$
$$\gamma_4 = e^{-Q} z_4^{-1} z_6^{-1} z_7^{-1} \ , \ \ \gamma_5 = e^{-Q-P} z_1 z_5 z_8 \ , \ \ \gamma_6 = e^{-P} z_1 z_5 z_8 \ ,$$
$$\gamma_7 = e^{-P} z_2^{-1} \ , \ \ \gamma_8 = e^{Q-P} z_2^{-1} \ , \ \ \gamma_9 = e^Q z_3 z_7 z_8 \ ,$$
$$\gamma_{10} = e^Q z_2^{-1} \ , \ \ \gamma_{11} = e^{Q+P} z_3 z_7 z_8 \ , \ \ \gamma_{12} = e^P z_3 z_6^{-1} z_8 \ . \tag{6.13}$$
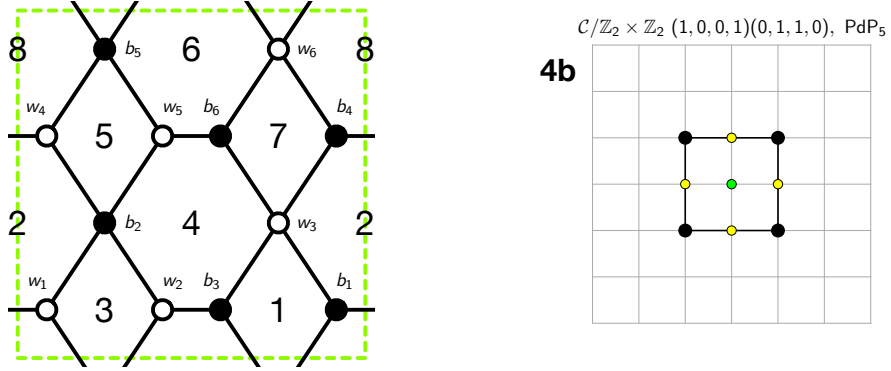
6.2 Model 4b

Figure 13: The brane tiling and toric diagram of Model 4b.

The brane tiling for Model 4b can be expressed in terms of the following pair of permutation tuples

$$\sigma_B = (e_{11} \ e_{31} \ e_{61}) \ (e_{12} \ e_{22} \ e_{52} \ e_{42}) \ (e_{23} \ e_{63} \ e_{33}) \ (e_{34} \ e_{44} \ e_{64})$$
$$(e_{15} \ e_{45} \ e_{55} \ e_{25}) \ (e_{36} \ e_{66} \ e_{56}) \ ,$$
$$\sigma_W^{-1} = (e_{12} \ e_{15} \ e_{11}) \ (e_{22} \ e_{23} \ e_{25}) \ (e_{31} \ e_{33} \ e_{36} \ e_{34}) \ (e_{42} \ e_{44} \ e_{45})$$
$$(e_{52} \ e_{55} \ e_{56}) \ (e_{61} \ e_{64} \ e_{66} \ e_{63}) \ . \tag{6.14}$$

The above permutation tuples correspond to black and white nodes in the brane tiling, respectively.

The brane tiling for Model 4b has 8 zig-zag paths given by,

$$z_1 = (e_{63}^+ \; e_{33}^- \; e_{36}^+ \; e_{66}^-) \;, \quad z_2 = (e_{31}^+ \; e_{61}^- \; e_{64}^+ \; e_{34}^-) \;,$$
$$z_3 = (e_{33}^+ \; e_{23}^- \; e_{25}^+ \; e_{15}^- \; e_{11}^+ \; e_{31}^-) \;, \quad z_4 = (e_{42}^+ \; e_{12}^- \; e_{15}^+ \; e_{45}^-) \;,$$
$$z_5 = (e_{34}^+ \; e_{44}^- \; e_{45}^+ \; e_{55}^- \; e_{56}^+ \; e_{36}^-) \;, \quad z_6 = (e_{61}^+ \; e_{11}^- \; e_{12}^+ \; e_{22}^- \; e_{23}^+ \; e_{63}^-) \;,$$
$$z_7 = (e_{22}^+ \; e_{52}^- \; e_{55}^+ \; e_{25}^-) \;, \quad z_8 = (e_{44}^+ \; e_{64}^- \; e_{66}^+ \; e_{56}^- \; e_{52}^+ \; e_{42}^-) \;, \tag{6.15}$$

and 8 face paths given by,

$$f_1 = (e_{33}^+ \; e_{63}^- \; e_{61}^+ \; e_{31}^-) \;, \quad f_2 = (e_{31}^+ \; e_{11}^- \; e_{12}^+ \; e_{42}^- \; e_{44}^+ \; e_{34}^-) \;,$$
$$f_3 = (e_{22}^+ \; e_{12}^- \; e_{15}^+ \; e_{25}^-) \;, \quad f_4 = (e_{52}^+ \; e_{22}^- \; e_{23}^+ \; e_{33}^- \; e_{36}^+ \; e_{56}^-) \;,$$
$$f_5 = (e_{42}^+ \; e_{52}^- \; e_{55}^+ \; e_{45}^-) \;, \quad f_6 = (e_{63}^+ \; e_{23}^- \; e_{25}^+ \; e_{55}^- \; e_{56}^+ \; e_{66}^-) \;,$$
$$f_7 = (e_{34}^+ \; e_{64}^- \; e_{66}^+ \; e_{36}^-) \;, \quad f_8 = (e_{11}^+ \; e_{61}^- \; e_{64}^+ \; e_{44}^- \; e_{45}^+ \; e_{15}^-) \;, \tag{6.16}$$

which satisfy the following constraints,

$$f_1 f_3^{-1} = z_3 z_6 \;, \quad f_2 f_6^{-1} = z_2 z_6 z_7 z_8 \;, \quad f_3 f_7 = z_4 z_5 z_7 z_8 \;, \quad f_4 f_8^{-1} = z_1 z_4 z_6 z_8 \;,$$
$$f_5^{-1} f_7 = z_5 z_8 \;, \quad f_6 f_8 = z_1 z_2 z_3 z_5 \;, \quad f_1 f_2 f_3 f_4 f_5 f_6 f_7 f_8 = 1 \;. \tag{6.17}$$

The face paths can be written in terms of the canonical variables as follows,

$$f_1 = e^P z_3 z_6 \;, \quad f_2 = e^Q z_2 z_6 z_7 z_8 \;, \quad f_3 = e^P \;, \quad f_4 = e^{-Q} z_1 z_7^{-1} \;,$$
$$f_5 = e^{-P} z_4 z_7 \;, \quad f_6 = e^Q \;, \quad f_7 = e^{-P} z_4 z_5 z_7 z_8 \;, \quad f_8 = e^{-Q} z_1 z_2 z_3 z_5 \;. \tag{6.18}$$

The Kasteleyn matrix of the brane tiling for Model 4b in Figure 13 takes the following form,

$$K = \begin{pmatrix}
 & b_1 & b_2 & b_3 & b_4 & b_5 & b_6 \\
\hline
w_1 & e_{11}x^{-1} & e_{12} & 0 & 0 & e_{15}y^{-1} & 0 \\
w_2 & 0 & e_{22} & e_{23} & 0 & e_{25}y^{-1} & 0 \\
w_3 & e_{31} & 0 & e_{33} & e_{34} & 0 & e_{36} \\
w_4 & 0 & e_{42} & 0 & e_{44}x^{-1} & e_{45} & 0 \\
w_5 & 0 & e_{52} & 0 & 0 & e_{55} & e_{56} \\
w_6 & e_{61}y & 0 & e_{63}y & e_{64} & 0 & e_{66}
\end{pmatrix} \;. \tag{6.19}$$

By taking the permanent of the Kasteleyn matrix, we obtain the spectral curve of the dimer integrable system for Model 4b as follows,

$$0 = \mathrm{perm}\, K = \bar{p}_0 \cdot x^{-1} \cdot \left[\delta_{(-1,-1)} \frac{1}{xy} + \delta_{(-1,1)} \frac{y}{x} + \delta_{(1,-1)} \frac{x}{y} \right.$$
$$\left. + \delta_{(1,1)} xy + \delta_{(-1,0)} \frac{1}{x} + \delta_{(0,-1)} \frac{1}{y} + \delta_{(1,0)} x + \delta_{(0,1)} y + H \right] \;, \tag{6.20}$$

where $\bar{p}_0 = e_{12}^+ e_{23}^+ e_{34}^+ e_{45}^+ e_{56}^+ e_{61}^+$. The Casimirs $\delta_{(m,n)}$ in (6.20) can be expressed in terms of the zig-zag paths in (6.15) as follows,

$$\delta_{(-1,-1)} = z_2 z_3 z_4 z_8 \ , \ \ \delta_{(-1,0)} = z_5^{-1} z_6^{-1} z_7^{-1} + z_1^{-1} z_5^{-1} z_6^{-1} \ , \ \ \delta_{(-1,1)} = z_5^{-1} z_6^{-1} \ ,$$

$$\delta_{(0,-1)} = z_2 z_3 z_4 + z_2 z_4 z_8 \ , \ \ \delta_{(0,1)} = z_5^{-1} + z_6^{-1} \ , \ \ \delta_{(1,-1)} = z_2 z_4 \ ,$$

$$\delta_{(1,0)} = z_2 + z_4 \ , \ \ \delta_{(1,1)} = 1 \ . \tag{6.21}$$

This leads to the following form of the spectral curve for Model 4b,

$$\Sigma \ : \ (z_2 + z_4)x + z_2 z_4 \frac{x}{y} + \left(\frac{1}{z_5} + \frac{1}{z_6} \right) y + (z_2 z_3 z_4 + z_2 z_4 z_8) \frac{1}{y}$$

$$+ \frac{1}{z_5 z_6} \frac{y}{x} + \left(\frac{1}{z_5 z_6 z_7} + \frac{1}{z_1 z_5 z_6} \right) \frac{1}{x} + z_2 z_3 z_4 z_8 \frac{1}{xy} + xy + H = 0 \ . \tag{6.22}$$

The Hamiltonian is a sum over all 12 1-loops γ_i,

$$H = \sum_{i=1}^{12} \gamma_i \ , \tag{6.23}$$

where the 1-loops γ_i's can be expressed in terms of zig-zag paths and face paths as follows,

$$\gamma_1 = z_1 z_2 z_4 z_8 f_1 \ , \ \ \gamma_2 = z_3^{-1} z_5^{-1} z_6^{-1} z_7^{-1} f_1 f_8 \ , \ \ \gamma_3 = z_1 z_2 z_4 z_8 f_1 f_7 f_8 \ ,$$

$$\gamma_4 = z_1 z_2 z_4 z_5^{-1} f_1 f_7 f_8 \ , \ \ \gamma_5 = z_4 z_8 f_5 f_8 \ , \ \ \gamma_6 = z_2 z_8 f_5 \ ,$$

$$\gamma_7 = z_6^{-1} z_7^{-1} f_5 \ , \ \ \gamma_8 = z_2 z_4^{-1} z_6^{-1} z_7^{-1} f_5 f_8^{-1} \ , \ \ \gamma_9 = z_3 z_4 f_2 \ ,$$

$$\gamma_{10} = z_2 z_5 z_6^{-1} z_8 f_5 f_7^{-1} f_8^{-1} \ , \ \ \gamma_{11} = z_2 z_6^{-1} f_1 f_8^{-1} \ , \ \ \gamma_{12} = z_2 z_6^{-1} f_1 \ , \tag{6.24}$$

The commutation matrix C for Model 4b takes the following form,

$$C = \begin{array}{c|cccccccccccc}
 & \gamma_1 & \gamma_2 & \gamma_3 & \gamma_4 & \gamma_5 & \gamma_6 & \gamma_7 & \gamma_8 & \gamma_9 & \gamma_{10} & \gamma_{11} & \gamma_{12} \\
\hline
\gamma_1 & 0 & 1 & 1 & 1 & 1 & 0 & 0 & -1 & -1 & -1 & -1 & 0 \\
\gamma_2 & -1 & 0 & 1 & 1 & 2 & 1 & 1 & 0 & -1 & -1 & -2 & -1 \\
\gamma_3 & -1 & -1 & 0 & 0 & 1 & 1 & 1 & 1 & 0 & 0 & -1 & -1 \\
\gamma_4 & -1 & -1 & 0 & 0 & 1 & 1 & 1 & 1 & 0 & 0 & -1 & -1 \\
\gamma_5 & -1 & -2 & -1 & -1 & 0 & 1 & 1 & 2 & 1 & 1 & 0 & -1 \\
\gamma_6 & 0 & -1 & -1 & -1 & -1 & 0 & 0 & 1 & 1 & 1 & 1 & 0 \\
\gamma_7 & 0 & -1 & -1 & -1 & -1 & 0 & 0 & 1 & 1 & 1 & 1 & 0 \\
\gamma_8 & 1 & 0 & -1 & -1 & -2 & -1 & -1 & 0 & 1 & 1 & 2 & 1 \\
\gamma_9 & 1 & 1 & 0 & 0 & -1 & -1 & -1 & -1 & 0 & 0 & 1 & 1 \\
\gamma_{10} & 1 & 1 & 0 & 0 & -1 & -1 & -1 & -1 & 0 & 0 & 1 & 1 \\
\gamma_{11} & 1 & 2 & 1 & 1 & 0 & -1 & -1 & -2 & -1 & -1 & 0 & 1 \\
\gamma_{12} & 0 & 1 & 1 & 1 & 1 & 0 & 0 & -1 & -1 & -1 & -1 & 0 \\
\end{array} \ . \tag{6.25}$$

The 1-loops satisfying the commutation relations can be written in terms of the canonical canonical variables as follows,

$$\gamma_1 = e^P z_5^{-1} z_7^{-1} \ , \ \ \gamma_2 = e^{-Q+P} z_1 z_2 z_3 z_7^{-1} \ , \ \ \gamma_3 = e^{-Q} z_6^{-1} z_7^{-1} \ ,$$

$$\gamma_4 = e^{-Q} z_1 z_2 z_3 z_4 \ , \ \ \gamma_5 = e^{-Q-P} z_4 z_6^{-1} \ , \ \ \gamma_6 = e^{-P} z_2 z_4 z_7 z_8 \ ,$$

$$\gamma_7 = e^{-P} z_4 z_6^{-1} \ , \ \ \gamma_8 = e^{Q-P} z_2 z_4 z_7 z_8 \ , \ \ \gamma_9 = e^{Q} z_1^{-1} z_5^{-1} \ ,$$

$$\gamma_{10} = e^{Q} z_2 z_4 z_7 z_8 \ , \ \ \gamma_{11} = e^{Q+P} z_1^{-1} z_5^{-1} \ , \ \ \gamma_{12} = e^{P} z_2 z_3 \ . \tag{6.26}$$
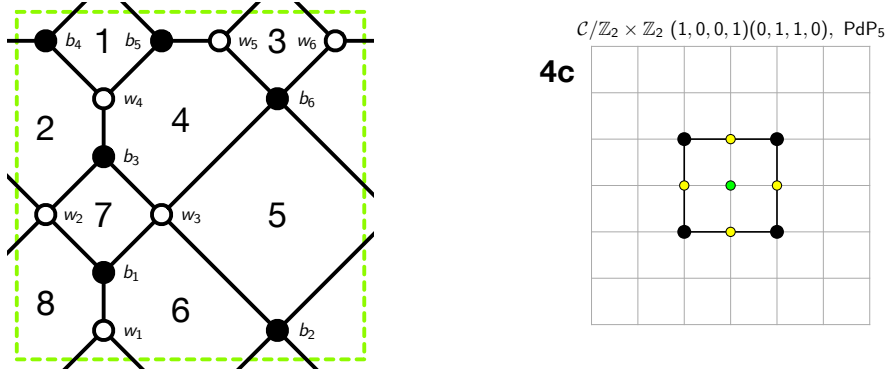
6.3 Model 4c

Figure 14: The brane tiling and toric diagram of Model 4c.

The brane tiling for Model 4c can be expressed in terms of the following pair of permutation tuples

$$\sigma_B = (e_{11} \ e_{31} \ e_{21}) \ (e_{22} \ e_{32} \ e_{52} \ e_{62}) \ (e_{23} \ e_{33} \ e_{43}) \ (e_{14} \ e_{64} \ e_{44})$$
$$(e_{15} \ e_{45} \ e_{55}) \ (e_{26} \ e_{66} \ e_{56} \ e_{36}) \ ,$$
$$\sigma_W^{-1} = (e_{11} \ e_{15} \ e_{14}) \ (e_{21} \ e_{22} \ e_{26} \ e_{23}) \ (e_{31} \ e_{33} \ e_{36} \ e_{32}) \ (e_{43} \ e_{44} \ e_{45})$$
$$(e_{52} \ e_{56} \ e_{55}) \ (e_{62} \ e_{64} \ e_{66}) \ , \tag{6.27}$$

which correspond to the black and white nodes in the brane tiling, respectively.

The brane tiling for Model 4c has 8 zig-zag paths given by,

$$z_1 = (e_{15}^+ \ e_{45}^- \ e_{43}^+ \ e_{23}^- \ e_{21}^+ \ e_{11}^-) \ , \ z_2 = (e_{44}^+ \ e_{14}^- \ e_{11}^+ \ e_{31}^- \ e_{33}^+ \ e_{43}^-) \ ,$$
$$z_3 = (e_{45}^+ \ e_{55}^- \ e_{52}^+ \ e_{62}^- \ e_{64}^+ \ e_{44}^-) \ , \ z_4 = (e_{26}^+ \ e_{66}^- \ e_{62}^+ \ e_{22}^-) \ ,$$
$$z_5 = (e_{14}^+ \ e_{64}^- \ e_{66}^+ \ e_{56}^- \ e_{55}^+ \ e_{15}^-) \ , \ z_6 = (e_{56}^+ \ e_{36}^- \ e_{32}^+ \ e_{52}^-) \ ,$$
$$z_7 = (e_{23}^+ \ e_{33}^- \ e_{36}^+ \ e_{26}^-) \ , \ z_8 = (e_{22}^+ \ e_{32}^- \ e_{31}^+ \ e_{21}^-) \ , \tag{6.28}$$

and 8 face paths given by,

$$f_1 = (e_{45}^+ \ e_{15}^- \ e_{14}^+ \ e_{44}^-) \ , \ f_2 = (e_{44}^+ \ e_{64}^- \ e_{66}^+ \ e_{26}^- \ e_{23}^+ \ e_{43}^-) \ ,$$
$$f_3 = (e_{56}^+ \ e_{66}^- \ e_{62}^+ \ e_{52}^-) \ , \ f_4 = (e_{43}^+ \ e_{33}^- \ e_{36}^+ \ e_{56}^- \ e_{55}^+ \ e_{45}^-) \ ,$$
$$f_5 = (e_{26}^+ \ e_{36}^- \ e_{32}^+ \ e_{22}^-) \ , \ f_6 = (e_{15}^+ \ e_{55}^- \ e_{52}^+ \ e_{32}^- \ e_{31}^+ \ e_{11}^-) \ ,$$
$$f_7 = (e_{33}^+ \ e_{23}^- \ e_{21}^+ \ e_{31}^-) \ , \ f_8 = (e_{64}^+ \ e_{14}^- \ e_{11}^+ \ e_{21}^- \ e_{22}^+ \ e_{62}^-) \ , \tag{6.29}$$

satisfying the following constraints,

$$f_6 f_7 f_8 = z_1 z_2 z_3 z_8 \ , \ f_5 f_6^{-1} f_8^{-1} = z_4 z_5 z_6 z_8^{-1} \ , \ f_4 f_8^{-1} = z_1 z_4 z_5 z_7 \ ,$$
$$f_3 f_7^{-1} = z_4 z_6 z_7 z_8 \ , \ f_2 f_6^{-1} = z_2 z_5 z_6 z_7 \ , \ f_1 f_7^{-1} = z_1^{-1} z_2^{-1} \ ,$$
$$f_1 f_2 f_3 f_4 f_5 f_6 f_7 f_8 = 1 \ . \tag{6.30}$$

The face paths can be written in terms of the canonical variables as follows,

$$f_1 = e^P z_1^{-1} z_2^{-1} \ , \ f_2 = e^Q z_2 z_5 z_6 z_7 \ , \ f_3 = e^P z_4 z_6 z_7 z_8 \ , \ f_4 = e^{-Q-P} z_1 z_6^{-1} \ ,$$
$$f_5 = e^{-P} z_7^{-1} z_8^{-1} \ , \ f_6 = e^Q \ , \ f_7 = e^P \ , \ f_8 = e^{-Q-P} z_1 z_2 z_3 z_8 \ . \tag{6.31}$$

The Kasteleyn matrix of the brane tiling for Model 4c in Figure 14 takes the following form,

$$K = \begin{pmatrix} & b_1 & b_2 & b_3 & b_4 & b_5 & b_6 \\ \hline w_1 & e_{11} & 0 & 0 & e_{14}y^{-1} & e_{15}y^{-1} & 0 \\ w_2 & e_{21} & e_{22}x^{-1} & e_{23} & 0 & 0 & e_{26}x^{-1} \\ w_3 & e_{31} & e_{32} & e_{33} & 0 & 0 & e_{36} \\ w_4 & 0 & 0 & e_{43} & e_{44} & e_{45} & 0 \\ w_5 & 0 & e_{52}y & 0 & 0 & e_{55} & e_{56} \\ w_6 & 0 & e_{62}y & 0 & e_{64}x & 0 & e_{66} \end{pmatrix} \ . \tag{6.32}$$

By taking a permanent of the Kasteleyn matrix, we obtain the spectral curve of the dimer integrable system for Model 4c as follows,

$$0 = \text{perm} \ K = \bar{p}_0 \cdot \left[\delta_{(-1,-1)} \frac{1}{xy} + \delta_{(-1,1)} \frac{y}{x} + \delta_{(1,-1)} \frac{x}{y} + \delta_{(1,1)} xy \right.$$
$$\left. + \delta_{(-1,0)} \frac{1}{x} + \delta_{(0,-1)} \frac{1}{y} + \delta_{(1,0)} x + \delta_{(0,1)} y + H \right] \ , \tag{6.33}$$

where $\bar{p}_0 = e_{11}^+ e_{23}^+ e_{36}^+ e_{45}^+ e_{52}^+ e_{64}^+$. The Casimirs $\delta_{(m,n)}$ in (6.33) can be expressed in terms of the zig-zag paths in (6.28) as follows,

$$
\delta_{(-1,-1)} = z_1 z_5 z_6 z_8 \ , \ \ \delta_{(-1,0)} = z_2^{-1} z_3^{-1} z_7^{-1} + z_3^{-1} z_4^{-1} z_7^{-1} \ ,
$$
$$
\delta_{(-1,1)} = z_3^{-1} z_7^{-1} \ , \ \ \delta_{(0,-1)} = z_1 z_6 z_8 + z_1 z_5 z_6 \ , \ \ \delta_{(0,1)} = z_3^{-1} + z_7^{-1} \ ,
$$
$$
\delta_{(1,-1)} = z_1 z_6 \ , \ \ \delta_{(1,0)} = z_1 + z_6 \ , \ \ \delta_{(1,1)} = 1 \ . \tag{6.34}
$$

This leads to the following form of the spectral curve for Model 4c,

$$
\Sigma \ : \ z_1 z_5 z_6 z_8 \frac{1}{xy} + \Big(\frac{1}{z_2 z_3 z_7} + \frac{1}{z_3 z_4 z_7} \Big) \frac{1}{x} + \frac{1}{z_3 z_7} \frac{y}{x} + (z_1 z_6 z_8 + z_1 z_5 z_6) \frac{1}{y}
$$
$$
+ \Big(\frac{1}{z_3} + \frac{1}{z_7} \Big) y + (z_1 + z_6) x + z_1 z_6 \frac{x}{y} + xy + H = 0 \ . \tag{6.35}
$$

The Hamiltonian is a sum over all 14 1-loops γ_i,

$$
H = \sum_{i=1}^{14} \gamma_i \ , \tag{6.36}
$$

where the 1-loops γ_i can be expressed in terms of zig-zag paths and face paths as follows,

$$
\gamma_1 = z_1 z_3^{-1} z_7^{-1} z_8^{-1} f_1 f_7^{-1} f_8 \ , \ \ \gamma_2 = z_1 z_4 z_5 z_6 f_2 f_8 \ , \ \ \gamma_3 = z_2^{-1} z_7^{-1} f_2 \ ,
$$
$$
\gamma_4 = z_1 z_7^{-1} f_2 f_7^{-1} \ , \ \ \gamma_5 = z_1 z_8 f_5 \ , \ \ \gamma_6 = z_1 z_7^{-1} f_2 \ ,
$$
$$
\gamma_7 = z_2^{-1} z_7^{-1} f_2 f_7 \ , \ \ \gamma_8 = z_1 z_4 z_6 z_8 f_2 \ , \ \ \gamma_9 = z_1 z_4 z_6 z_8 f_2 f_7 \ ,
$$
$$
\gamma_{10} = z_1 z_2 z_6 z_8 f_1 f_7^{-1} f_8^{-1} \ , \ \ \gamma_{11} = z_1 z_2 z_6 z_8 f_1 \ , \ \ \gamma_{12} = z_1 z_3^{-1} f_1 f_8 \ ,
$$
$$
\gamma_{13} = z_1 z_2 z_6 z_8 f_1 f_8^{-1} \ , \ \ \gamma_{14} = z_1 z_3^{-1} f_1 \ . \tag{6.37}
$$

The commutation matrix C for Model 4c is given by,

$$
C = \begin{pmatrix}
 & \gamma_1 & \gamma_2 & \gamma_3 & \gamma_4 & \gamma_5 & \gamma_6 & \gamma_7 & \gamma_8 & \gamma_9 & \gamma_{10} & \gamma_{11} & \gamma_{12} & \gamma_{13} & \gamma_{14} \\
\hline
\gamma_1 & 0 & 1 & 1 & 2 & 1 & 1 & 0 & 1 & 0 & 0 & -1 & -1 & -1 & -1 \\
\gamma_2 & -1 & 0 & 1 & 1 & 0 & 1 & 1 & 1 & 1 & 1 & 0 & -1 & 1 & 0 \\
\gamma_3 & -1 & -1 & 0 & -1 & -1 & 0 & 1 & 0 & 1 & 1 & 1 & 0 & 2 & 1 \\
\gamma_4 & -2 & -1 & 1 & 0 & -1 & 1 & 2 & 1 & 2 & 2 & 1 & -1 & 3 & 1 \\
\gamma_5 & -1 & 0 & 1 & 1 & 0 & 1 & 1 & 1 & 1 & 1 & 0 & -1 & 1 & 0 \\
\gamma_6 & -1 & -1 & 0 & -1 & -1 & 0 & 1 & 0 & 1 & 1 & 1 & 0 & 2 & 1 \\
\gamma_7 & 0 & -1 & -1 & -2 & -1 & -1 & 0 & -1 & 0 & 0 & 1 & 1 & 1 & 1 \\
\gamma_8 & -1 & -1 & 0 & -1 & -1 & 0 & 1 & 0 & 1 & 1 & 1 & 0 & 2 & 1 \\
\gamma_9 & 0 & -1 & -1 & -2 & -1 & -1 & 0 & -1 & 0 & 0 & 1 & 1 & 1 & 1 \\
\gamma_{10} & 0 & -1 & -1 & -2 & -1 & -1 & 0 & -1 & 0 & 0 & 1 & 1 & 1 & 1 \\
\gamma_{11} & 1 & 0 & -1 & -1 & 0 & -1 & -1 & -1 & -1 & -1 & 0 & 1 & -1 & 0 \\
\gamma_{12} & 1 & 1 & 0 & 1 & 1 & 0 & -1 & 0 & -1 & -1 & -1 & 0 & -2 & -1 \\
\gamma_{13} & 1 & -1 & -2 & -3 & -1 & -2 & -1 & -2 & -1 & -1 & 1 & 2 & 0 & 1 \\
\gamma_{14} & 1 & 0 & -1 & -1 & 0 & -1 & -1 & -1 & -1 & -1 & 0 & 1 & -1 & 0
\end{pmatrix} , \qquad (6.38)
$$

where the 1-loops satisfying the commutation relations can be written in terms of the canonical variables as follows,

$$
\gamma_1 = e^{-Q-P} z_1 z_7^{-1} \ , \quad \gamma_2 = e^{-P} z_1 z_2 z_5 z_6 \ , \quad \gamma_3 = e^Q z_5 z_6 \ ,
$$
$$
\gamma_4 = e^{Q-P} z_1 z_2 z_5 z_6 \ , \quad \gamma_5 = e^{-P} z_1 z_7^{-1} \ , \quad \gamma_6 = e^Q z_1 z_2 z_5 z_6 \ ,
$$
$$
\gamma_7 = e^{Q+P} z_5 z_6 \ , \quad \gamma_8 = e^Q z_3^{-1} z_6 \ , \quad \gamma_9 = e^{Q+P} z_3^{-1} z_6 \ ,
$$
$$
\gamma_{10} = e^{Q+P} z_1^{-1} z_2^{-1} z_3^{-1} z_6 \ , \quad \gamma_{11} = e^P z_6 z_8 \ , \quad \gamma_{12} = e^{-Q} z_1 z_8 \ ,
$$
$$
\gamma_{13} = e^{Q+2P} z_1^{-1} z_2^{-1} z_3^{-1} z_6 \ , \quad \gamma_{14} = e^P z_2^{-1} z_3^{-1} \ . \qquad (6.39)
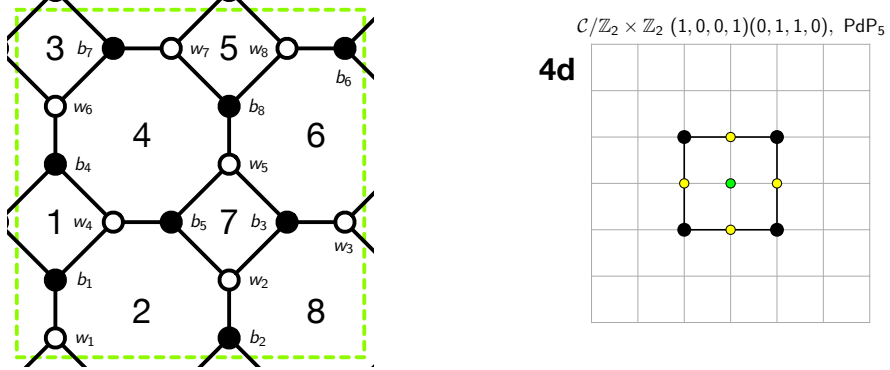$$

6.4 Model 4d

Figure 15: The brane tiling and toric diagram of Model 4d.

The brane tiling for Model 4d can be expressed in terms of the following pair of permutation tuples

$$\sigma_B = (e_{11}\ e_{41}\ e_{31})\ (e_{22}\ e_{72}\ e_{82})\ (e_{23}\ e_{33}\ e_{53})\ (e_{34}\ e_{44}\ e_{64})$$
$$(e_{25}\ e_{55}\ e_{45})\ (e_{16}\ e_{86}\ e_{66})\ (e_{17}\ e_{67}\ e_{77})\ (e_{58}\ e_{88}\ e_{78})\ ,$$
$$\sigma_W^{-1} = (e_{11}\ e_{17}\ e_{16})\ (e_{22}\ e_{25}\ e_{23})\ (e_{31}\ e_{33}\ e_{34})\ (e_{41}\ e_{44}\ e_{45})$$
$$(e_{53}\ e_{55}\ e_{58})\ (e_{64}\ e_{66}\ e_{67})\ (e_{72}\ e_{78}\ e_{77})\ (e_{82}\ e_{86}\ e_{88})\ , \tag{6.40}$$

which correspond to the black and white nodes in the brane tiling, respectively.

The brane tiling for Model 4d has 8 zig-zag paths given by,

$$z_1 = (e_{34}^+\ e_{44}^-\ e_{45}^+\ e_{25}^-\ e_{23}^+\ e_{33}^-)\ ,\quad z_2 = (e_{41}^+\ e_{31}^-\ e_{33}^+\ e_{53}^-\ e_{55}^+\ e_{45}^-)\ ,$$
$$z_3 = (e_{44}^+\ e_{64}^-\ e_{66}^+\ e_{16}^-\ e_{11}^+\ e_{41}^-)\ ,\quad z_4 = (e_{77}^+\ e_{17}^-\ e_{16}^+\ e_{86}^-\ e_{88}^+\ e_{78}^-)\ ,$$
$$z_5 = (e_{22}^+\ e_{72}^-\ e_{78}^+\ e_{58}^-\ e_{53}^+\ e_{23}^-)\ ,\quad z_6 = (e_{31}^+\ e_{11}^-\ e_{17}^+\ e_{67}^-\ e_{64}^+\ e_{34}^-)\ ,$$
$$z_7 = (e_{72}^+\ e_{82}^-\ e_{86}^+\ e_{66}^-\ e_{67}^+\ e_{77}^-)\ ,\quad z_8 = (e_{25}^+\ e_{55}^-\ e_{58}^+\ e_{88}^-\ e_{82}^+\ e_{22}^-)\ , \tag{6.41}$$

and 8 face paths given by,

$$f_1 = (e_{44}^+\ e_{34}^-\ e_{31}^+\ e_{41}^-)\ ,\quad f_2 = (e_{41}^+\ e_{11}^-\ e_{17}^+\ e_{77}^-\ e_{72}^+\ e_{22}^-\ e_{25}^+\ e_{45}^-)\ ,$$
$$f_3 = (e_{67}^+\ e_{17}^-\ e_{16}^+\ e_{66}^-)\ ,\quad f_4 = (e_{45}^+\ e_{55}^-\ e_{58}^+\ e_{78}^-\ e_{77}^+\ e_{67}^-\ e_{64}^+\ e_{44}^-)\ ,$$
$$f_5 = (e_{78}^+\ e_{88}^-\ e_{82}^+\ e_{72}^-)\ ,\quad f_6 = (e_{34}^+\ e_{64}^-\ e_{66}^+\ e_{86}^-\ e_{88}^+\ e_{58}^-\ e_{53}^+\ e_{33}^-)\ ,$$
$$f_7 = (e_{55}^+\ e_{25}^-\ e_{23}^+\ e_{53}^-)\ ,\quad f_8 = (e_{11}^+\ e_{31}^-\ e_{33}^+\ e_{23}^-\ e_{22}^+\ e_{82}^-\ e_{86}^+\ e_{16}^-)\ , \tag{6.42}$$

which satisfy the following constraints,

$$f_6 f_7^2 f_8 = z_1 z_2 z_3 z_8^{-1} \ , \quad f_5 f_7^{-1} = z_5 z_8 \ , \quad f_4 f_8^{-1} = z_1 z_4 z_6 z_8 \ , \quad f_3 f_7^{-1} = z_4 z_5 z_7 z_8 \ ,$$

$$f_2 f_6^{-1} = z_2 z_6 z_7 z_8 \ , \quad f_1 f_7^{-1} = z_1^{-1} z_2^{-1} \ , \quad f_1 f_2 f_3 f_4 f_5 f_6 f_7 f_8 = 1 \ . \tag{6.43}$$

The face paths can be written in terms of the canonical variables as follows,

$$f_1 = e^P z_1^{-1} z_2^{-1} \ , \quad f_2 = e^Q z_2 z_6 z_7 z_8 \ , \quad f_3 = e^P z_4 z_5 z_7 z_8 \ ,$$

$$f_4 = e^{-Q-2P} z_1 z_5^{-1} z_7^{-1} z_8^{-1} \ , \quad f_5 = e^P z_5 z_8 \ , \quad f_6 = e^Q \ , \quad f_7 = e^P \ ,$$

$$f_8 = e^{-Q-2P} z_1 z_2 z_3 z_8^{-1} \ . \tag{6.44}$$

The Kasteleyn matrix of the brane tiling for Model 4d in Figure 15 is given by,

$$K = \begin{pmatrix}
 & b_1 & b_2 & b_3 & b_4 & b_5 & b_6 & b_7 & b_8 \\
\hline
w_1 & e_{11} & 0 & 0 & 0 & 0 & e_{16}x^{-1}y^{-1} & e_{17}y^{-1} & 0 \\
w_2 & 0 & e_{22} & e_{23} & 0 & e_{25} & 0 & 0 & 0 \\
w_3 & e_{31}x & 0 & e_{33} & e_{34}x & 0 & 0 & 0 & 0 \\
w_4 & e_{41} & 0 & 0 & e_{44} & e_{45} & 0 & 0 & 0 \\
w_5 & 0 & 0 & e_{53} & 0 & e_{55} & 0 & 0 & e_{58} \\
w_6 & 0 & 0 & 0 & e_{64} & 0 & e_{66}x^{-1} & e_{67} & 0 \\
w_7 & 0 & e_{72}y & 0 & 0 & 0 & 0 & e_{77} & e_{78} \\
w_8 & 0 & e_{82}y & 0 & 0 & 0 & e_{86} & 0 & e_{88}
\end{pmatrix} . \tag{6.45}$$

The permanent of the Kasteleyn matrix in (6.45) gives the spectral curve of the dimer integrable system for Model 4d as follows,

$$0 = \mathrm{perm}\ K = \bar{p}_0 \cdot \left[\delta_{(-1,-1)} \frac{1}{xy} + \delta_{(-1,1)} \frac{y}{x} + \delta_{(1,-1)} \frac{x}{y} + \delta_{(1,1)} xy \right.$$

$$\left. + \delta_{(-1,0)} \frac{1}{x} + \delta_{(0,-1)} \frac{1}{y} + \delta_{(1,0)} x + \delta_{(0,1)} y + H \right] \ , \tag{6.46}$$

where $\bar{p}_0 = e_{11}^+ e_{23}^+ e_{34}^+ e_{45}^+ e_{58}^+ e_{67}^+ e_{72}^+ e_{86}^+$. The Casimirs $\delta_{(m,n)}$ in (6.46) can be expressed in terms of the zig-zag paths in (6.41) as follows,

$$\delta_{(-1,-1)} = z_2 z_4 z_5 z_6 \ , \quad \delta_{(-1,0)} = z_1^{-1} z_3^{-1} z_7^{-1} + z_1^{-1} z_7^{-1} z_8^{-1} \ ,$$

$$\delta_{(-1,1)} = z_1^{-1} z_7^{-1} \ , \quad \delta_{(0,-1)} = z_2 z_5 z_6 + z_4 z_5 z_6 \ , \quad \delta_{(0,1)} = z_1^{-1} + z_7^{-1} \ ,$$

$$\delta_{(1,-1)} = z_5 z_6 \ , \quad \delta_{(1,0)} = z_5 + z_6 \ , \quad \delta_{(1,1)} = 1 \ . \tag{6.47}$$

Accordingly, we can express the spectral curve for Model 4d as follows,

$$\Sigma \ : \ z_2 z_4 z_5 z_6 \frac{1}{xy} + \left(\frac{1}{z_1 z_3 z_7} + \frac{1}{z_1 z_7 z_8} \right) \frac{1}{x} + \frac{1}{z_1 z_7} \frac{y}{x} + (z_2 z_5 z_6 + z_4 z_5 z_6) \frac{1}{y}$$

$$+ \left(\frac{1}{z_1} + \frac{1}{z_7} \right) y + (z_5 + z_6) x + z_5 z_6 \frac{x}{y} + xy + H = 0 \ . \tag{6.48}$$

The Hamiltonian is a sum over all 21 1-loops γ_i,

$$H = \sum_{i=1}^{21} \gamma_i \ , \tag{6.49}$$

where the 1-loops γ_i can be expressed in terms of zig-zag paths and face paths as shown below,

$$\gamma_1 = z_3^{-1} z_7^{-1} f_1 f_2 f_8 \ , \ \ \gamma_2 = z_2 z_5 f_1 f_4 \ , \ \ \gamma_3 = z_2 z_5 f_1 \ , \ \ \gamma_4 = z_3^{-1} z_7^{-1} f_1 \ ,$$
$$\gamma_5 = z_5 z_7^{-1} f_2 f_3 \ , \ \ \gamma_6 = z_1^{-1} z_5 f_8^{-1} \ , \ \ \gamma_7 = z_2 z_5 f_8^{-1} \ , \ \ \gamma_8 = z_1^{-1} z_5 f_7 f_8^{-1} \ ,$$
$$\gamma_9 = z_2 z_3 z_5 z_6 f_1^{-1} f_7^{-1} f_8^{-1} \ , \ \ \gamma_{10} = z_1^{-1} z_3 z_5 z_6 f_1^{-1} f_8^{-1} \ , \ \ \gamma_{11} = z_2 z_3 z_5 z_6 f_1^{-1} f_8^{-1} \ ,$$
$$\gamma_{12} = z_1^{-1} z_3 z_5 z_6 f_1^{-1} f_7 f_8^{-1} \ , \ \ \gamma_{13} = z_1^{-1} z_8^{-1} f_1^{-1} f_7^{-1} f_8^{-1} \ , \ \ \gamma_{14} = z_1^{-2} z_2^{-1} z_8^{-1} f_1^{-1} f_8^{-1} \ ,$$
$$\gamma_{15} = z_1^{-1} z_8^{-1} f_1^{-1} f_8^{-1} \ , \ \ \gamma_{16} = z_1^{-2} z_2^{-1} z_8^{-1} f_1^{-1} f_7 f_8^{-1} \ , \ \ \gamma_{17} = z_1^{-1} z_5 f_2 f_4 f_6 f_7 \ ,$$
$$\gamma_{18} = z_1^{-1} z_2^{-1} z_7^{-1} z_8^{-1} f_2 \ , \ \ \gamma_{19} = z_7^{-1} z_8^{-1} f_2 \ , \ \ \gamma_{20} = z_3 z_4 z_5 z_6 f_2 f_7 \ ,$$
$$\gamma_{21} = z_2^{-1} z_4 z_5 z_7^{-1} f_2 f_7 f_8 \ . \tag{6.50}$$

The commutation matrix C for Model 4d is given by,

$$C = \begin{pmatrix}
 & \gamma_1 & \gamma_2 & \gamma_3 & \gamma_4 & \gamma_5 & \gamma_6 & \gamma_7 & \gamma_8 & \gamma_9 & \gamma_{10} & \gamma_{11} & \gamma_{12} & \gamma_{13} & \gamma_{14} & \gamma_{15} & \gamma_{16} & \gamma_{17} & \gamma_{18} & \gamma_{19} & \gamma_{20} & \gamma_{21} \\
\hline
\gamma_1 & 0 & -1 & 0 & 0 & 1 & 1 & 1 & 1 & 1 & 1 & 1 & 1 & 1 & 1 & 1 & 1 & 1 & 1 & 1 & 1 & 0 \\
\gamma_2 & 1 & 0 & -1 & -1 & 0 & -1 & -1 & -2 & 1 & 0 & 0 & -1 & 1 & 0 & 0 & -1 & 2 & 1 & 1 & 0 & 1 \\
\gamma_3 & 0 & 1 & 0 & 0 & -1 & -1 & -1 & -1 & -1 & -1 & -1 & -1 & -1 & -1 & -1 & -1 & -1 & -1 & -1 & -1 & 0 \\
\gamma_4 & 0 & 1 & 0 & 0 & -1 & -1 & -1 & -1 & -1 & -1 & -1 & -1 & -1 & -1 & -1 & -1 & -1 & -1 & -1 & -1 & 0 \\
\gamma_5 & -1 & 0 & 1 & 1 & 0 & 1 & 1 & 2 & -1 & 0 & 0 & 1 & -1 & 0 & 0 & 1 & -2 & -1 & -1 & 0 & -1 \\
\gamma_6 & -1 & 1 & 1 & 1 & -1 & 0 & 0 & 1 & -2 & -1 & -1 & 0 & -2 & -1 & -1 & 0 & -3 & -2 & -2 & -1 & -1 \\
\gamma_7 & -1 & 1 & 1 & 1 & -1 & 0 & 0 & 1 & -2 & -1 & -1 & 0 & -2 & -1 & -1 & 0 & -3 & -2 & -2 & -1 & -1 \\
\gamma_8 & -1 & 2 & 1 & 1 & -2 & -1 & -1 & 0 & -3 & -2 & -2 & -1 & -3 & -2 & -2 & -1 & -4 & -3 & -3 & -2 & -1 \\
\gamma_9 & -1 & -1 & 1 & 1 & 1 & 2 & 2 & 3 & 0 & 1 & 1 & 2 & 0 & 1 & 1 & 2 & -1 & 0 & 0 & 1 & -1 \\
\gamma_{10} & -1 & 0 & 1 & 1 & 0 & 1 & 1 & 2 & -1 & 0 & 0 & 1 & -1 & 0 & 0 & 1 & -2 & -1 & -1 & 0 & -1 \\
\gamma_{11} & -1 & 0 & 1 & 1 & 0 & 1 & 1 & 2 & -1 & 0 & 0 & 1 & -1 & 0 & 0 & 1 & -2 & -1 & -1 & 0 & -1 \\
\gamma_{12} & -1 & 1 & 1 & 1 & -1 & 0 & 0 & 1 & -2 & -1 & -1 & 0 & -2 & -1 & -1 & 0 & -3 & -2 & -2 & -1 & -1 \\
\gamma_{13} & -1 & -1 & 1 & 1 & 1 & 2 & 2 & 3 & 0 & 1 & 1 & 2 & 0 & 1 & 1 & 2 & -1 & 0 & 0 & 1 & -1 \\
\gamma_{14} & -1 & 0 & 1 & 1 & 0 & 1 & 1 & 2 & -1 & 0 & 0 & 1 & -1 & 0 & 0 & 1 & -2 & -1 & -1 & 0 & -1 \\
\gamma_{15} & -1 & 0 & 1 & 1 & 0 & 1 & 1 & 2 & -1 & 0 & 0 & 1 & -1 & 0 & 0 & 1 & -2 & -1 & -1 & 0 & -1 \\
\gamma_{16} & -1 & 1 & 1 & 1 & -1 & 0 & 0 & 1 & -2 & -1 & -1 & 0 & -2 & -1 & -1 & 0 & -3 & -2 & -2 & -1 & -1 \\
\gamma_{17} & -1 & -2 & 1 & 1 & 2 & 3 & 3 & 4 & 1 & 2 & 2 & 3 & 1 & 2 & 2 & 3 & 0 & 1 & 1 & 2 & -1 \\
\gamma_{18} & -1 & -1 & 1 & 1 & 1 & 2 & 2 & 3 & 0 & 1 & 1 & 2 & 0 & 1 & 1 & 2 & -1 & 0 & 0 & 1 & -1 \\
\gamma_{19} & -1 & -1 & 1 & 1 & 1 & 2 & 2 & 3 & 0 & 1 & 1 & 2 & 0 & 1 & 1 & 2 & -1 & 0 & 0 & 1 & -1 \\
\gamma_{20} & -1 & 0 & 1 & 1 & 0 & 1 & 1 & 2 & -1 & 0 & 0 & 1 & -1 & 0 & 0 & 1 & -2 & -1 & -1 & 0 & -1 \\
\gamma_{21} & 0 & -1 & 0 & 0 & 1 & 1 & 1 & 1 & 1 & 1 & 1 & 1 & 1 & 1 & 1 & 1 & 1 & 1 & 1 & 1 & 0 \\
\end{pmatrix} . \tag{6.51}$$

The 1-loops satisfying the commutation relations can be written in terms of the canon-

ical variables as follows,

$$\gamma_1 = e^{-P} z_2 z_6 \ , \ \ \gamma_2 = e^{-Q-P} z_7^{-1} z_8^{-1} \ , \ \ \gamma_3 = e^{P} z_1^{-1} z_5 \ ,$$
$$\gamma_4 = e^{P} z_4 z_5 z_6 z_8 \ , \ \ \gamma_5 = e^{Q+P} z_1^{-1} z_3^{-1} z_5 z_8 \ , \ \ \gamma_6 = e^{Q+2P} z_1^{-2} z_2^{-1} z_3^{-1} z_5 z_8 \ ,$$
$$\gamma_7 = e^{Q+2P} z_1^{-1} z_3^{-1} z_5 z_8 \ , \ \ \gamma_8 = e^{Q+3P} z_1^{-2} z_2^{-1} z_3^{-1} z_5 z_8 \ , \ \ \gamma_9 = e^{Q} z_2 z_5 z_6 z_8 \ ,$$
$$\gamma_{10} = e^{Q+P} z_1^{-1} z_5 z_6 z_8 \ , \ \ \gamma_{11} = e^{Q+P} z_2 z_5 z_6 z_8 \ , \ \ \gamma_{12} = e^{Q+2P} z_1^{-1} z_5 z_6 z_8 \ ,$$
$$\gamma_{13} = e^{Q} z_1^{-1} z_3^{-1} \ , \ \ \gamma_{14} = e^{Q+P} z_1^{-2} z_2^{-1} z_3^{-1} \ , \ \ \gamma_{15} = e^{Q+P} z_1^{-1} z_3^{-1} \ ,$$
$$\gamma_{16} = e^{Q+2P} z_1^{-2} z_2^{-1} z_3^{-1} \ , \ \ \gamma_{17} = e^{Q-P} z_2 z_6 \ , \ \ \gamma_{18} = e^{Q} z_1^{-1} z_6 \ ,$$
$$\gamma_{19} = e^{Q} z_2 z_6 \ , \ \ \gamma_{20} = e^{Q+P} z_1^{-1} z_6 \ , \ \ \gamma_{21} = e^{-P} z_7^{-1} z_8^{-1} \ . \tag{6.52}$$
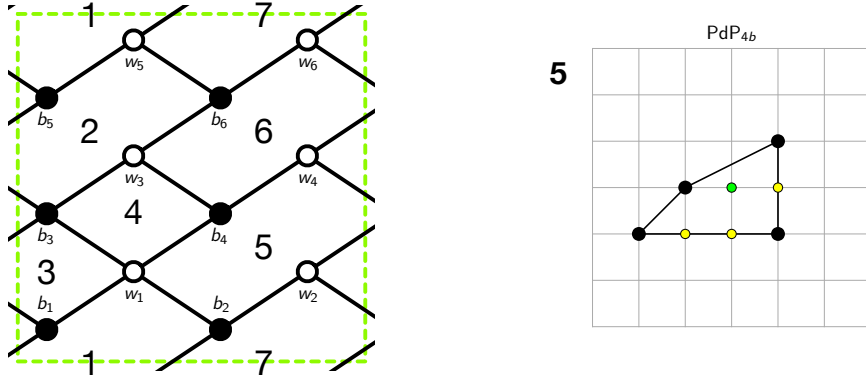
7 Model 5: PdP$_{4b}$

Figure 16: The brane tiling and toric diagram of Model 5.

The brane tiling for Model 5 can be expressed in terms of the following pair of permutation tuples

$$\sigma_B = (e_{11} \ e_{21} \ e_{61}) \ (e_{12} \ e_{52} \ e_{22}) \ (e_{13} \ e_{33} \ e_{42} \ e_{22}) \ (e_{14} \ e_{44} \ e_{34})$$
$$(e_{45} \ e_{55} \ e_{65}) \ (e_{36} \ e_{66} \ e_{56})$$
$$\sigma_W^{-1} = (e_{11} \ e_{13} \ e_{14} \ e_{12}) \ (e_{21} \ e_{22} \ e_{23}) \ (e_{33} \ e_{36} \ e_{34}) \ (e_{43} \ e_{44} \ e_{45})$$
$$(e_{52} \ e_{56} \ e_{55}) \ (e_{61} \ e_{65} \ e_{66}) \tag{7.1}$$

which correspond to the black and white nodes in the brane tiling, respectively.

The brane tiling for Model 5 has 7 zig-zag paths given by,

$$z_1 = (e_{61}^+ \ e_{11}^- \ e_{13}^+ \ e_{33}^- \ e_{36}^+ \ e_{66}^-) \ , \quad z_2 = (e_{55}^+ \ e_{65}^- \ e_{66}^+ \ e_{56}^-) \ ,$$
$$z_3 = (e_{12}^+ \ e_{52}^- \ e_{56}^+ \ e_{36}^- \ e_{34}^+ \ e_{14}^-) \ , \quad z_4 = (e_{52}^+ \ e_{22}^- \ e_{23}^+ \ e_{13}^- \ e_{14}^+ \ e_{44}^- \ e_{45}^+ \ e_{55}^-) \ ,$$
$$z_5 = (e_{33}^+ \ e_{43}^- \ e_{44}^+ \ e_{34}^-) \ , \quad z_6 = (e_{11}^+ \ e_{21}^- \ e_{22}^+ \ e_{12}^-) \ ,$$
$$z_7 = (e_{65}^+ \ e_{45}^- \ e_{43}^+ \ e_{23}^- \ e_{21}^+ \ e_{61}^-) \ , \tag{7.2}$$

and 7 face paths given by,

$$f_1 = (e_{11}^+ \ e_{61}^- \ e_{65}^+ \ e_{55}^- \ e_{52}^+ \ e_{12}^-) \ , \quad f_2 = (e_{55}^+ \ e_{45}^- \ e_{43}^+ \ e_{33}^- \ e_{36}^+ \ e_{56}^-) \ ,$$
$$f_3 = (e_{13}^+ \ e_{23}^- \ e_{21}^+ \ e_{11}^-) \ , \quad f_4 = (e_{33}^+ \ e_{13}^- \ e_{14}^+ \ e_{34}^-) \ ,$$
$$f_5 = (e_{12}^+ \ e_{22}^- \ e_{23}^+ \ e_{43}^- \ e_{44}^+ \ e_{14}^-) \ , \quad f_6 = (e_{45}^+ \ e_{65}^- \ e_{66}^+ \ e_{36}^- \ e_{34}^+ \ e_{44}^-) \ ,$$
$$f_7 = (e_{61}^+ \ e_{21}^- \ e_{22}^+ \ e_{52}^- \ e_{56}^+ \ e_{66}^-) \ , \tag{7.3}$$

which satisfy the following relations,

$$f_5 f_6 f_7 = z_3 z_7^{-1} \ , \quad f_4 f_7^{-1} = z_2 z_4 z_5 z_7 \ , \quad f_3 f_6^{-1} = z_1 z_5 z_7 \ ,$$
$$f_2 f_5^{-1} f_7^{-1} = z_2 z_3^{-1} z_5^{-1} z_7 \ , \quad f_1 f_5^{-1} f_6^{-1} = z_2^{-1} z_3^{-1} z_6 z_7 \ , \quad f_1 f_2 f_3 f_4 f_5 f_6 f_7 = 1 \ . \tag{7.4}$$

The face paths can be written in terms of the canonical variables as follows,

$$f_1 = e^{-P} z_2^{-1} z_6 \ , \quad f_2 = e^{-Q} z_2 z_5^{-1} \ , \quad f_3 = e^{Q} z_1 z_5 z_7 \ , \quad f_4 = e^{P} z_2 z_4 z_5 z_7 \ ,$$
$$f_5 = e^{-Q-P} z_3 z_7^{-1} \ , \quad f_6 = e^{Q} \ , \quad f_7 = e^{P} \ . \tag{7.5}$$

The Kasteleyn matrix of the brane tiling for Model 5 in Figure 16 is given by,

$$K = \begin{pmatrix} & b_1 & b_2 & b_3 & b_4 & b_5 & b_6 \\ \hline w_1 & e_{11} & e_{12} & e_{13} & e_{14} & 0 & 0 \\ w_2 & e_{21}x & e_{22} & e_{23}x & 0 & 0 & 0 \\ w_3 & 0 & 0 & e_{33} & e_{34} & 0 & e_{36} \\ w_4 & 0 & 0 & e_{43}x & e_{44} & e_{45}x & 0 \\ w_5 & 0 & e_{52}y & 0 & 0 & e_{55} & e_{56} \\ w_6 & e_{61}xy & 0 & 0 & 0 & e_{65}x & e_{66} \end{pmatrix} \ . \tag{7.6}$$

By taking the permanent of the Kasteleyn matrix, we obtain the spectral curve of the dimer integrable system for Model 5 as follows,

$$0 = \mathrm{perm}\, K = \bar{p}_0 \cdot x^2 y \cdot \Big[\delta_{(-2,-1)} \frac{1}{x^2 y} + \delta_{(-1,-1)} \frac{1}{xy} + \delta_{(-1,0)} \frac{1}{x} + \delta_{(0,-1)} \frac{1}{y}$$
$$+ \delta_{(1,-1)} \frac{x}{y} + \delta_{(1,0)} x + \delta_{(1,1)} xy + H \Big] \ , \tag{7.7}$$

where $\bar{p}_0 = e_{14}^+ e_{23}^+ e_{36}^+ e_{45}^+ e_{52}^+ e_{61}^+$. The Casimirs $\delta_{(m,n)}$ in (7.7) can be expressed in terms of the zig-zag paths in (7.2) as follows,

$$\delta_{(-2,-1)} = z_2 z_3 z_5 z_6 z_7 \ , \quad \delta_{(-1,-1)} = z_3 z_5 z_6 z_7 + z_2 z_3 z_6 z_7 + z_2 z_3 z_5 z_7 \ ,$$

$$\delta_{(-1,0)} = z_4^{-1} \ , \quad \delta_{(0,-1)} = z_3 z_6 z_7 + z_3 z_5 z_7 + z_2 z_3 z_7 \ , \quad \delta_{(1,-1)} = z_3 z_7 \ ,$$

$$\delta_{(1,0)} = z_3 + z_7 \ , \quad \delta_{(1,1)} = 1 \ , \tag{7.8}$$

such that the spectral curve for Model 5 takes the following form,

$$\Sigma \ : \ z_2 z_3 z_5 z_6 z_7 \frac{1}{x^2 y} + (z_3 z_5 z_6 z_7 + z_2 z_3 z_6 z_7 + z_2 z_3 z_5 z_7) \frac{1}{xy} + \frac{1}{z_4 x}$$

$$+ (z_3 z_6 z_7 + z_3 z_5 z_7 + z_2 z_3 z_7) \frac{1}{y} + z_3 z_7 \frac{x}{y} + (z_3 + z_7) x + xy + H \ . \tag{7.9}$$

The Hamiltonian is a sum over all 9 1-loops γ_i,

$$H = \sum_{i=1}^{9} \gamma_i \ , \tag{7.10}$$

where the 1-loops γ_i can be expressed in terms of zig-zag paths and face paths as follows,

$$\gamma_1 = z_3 z_5 f_2 \ , \quad \gamma_2 = z_2^{-1} z_3 z_5 z_6 f_2 f_7^{-1} \ , \quad \gamma_3 = z_3 z_6 f_7^{-1} \ ,$$

$$\gamma_4 = z_2^{-1} z_4^{-1} f_7^{-1} \ , \quad \gamma_5 = z_3 z_6 f_3 f_7^{-1} \ , \quad \gamma_6 = z_3 z_6 f_3 \ ,$$

$$\gamma_7 = z_1^{-1} f_3 \ , \quad \gamma_8 = z_3 z_6 f_3 f_4 \ , \quad \gamma_9 = z_4^{-1} z_5^{-1} f_4 \ . \tag{7.11}$$

The commutation matrix C for Model 5 takes the following form,

$$C = \begin{pmatrix}
 & \gamma_1 & \gamma_2 & \gamma_3 & \gamma_4 & \gamma_5 & \gamma_6 & \gamma_7 & \gamma_8 & \gamma_9 \\
\hline
\gamma_1 & 0 & 1 & 1 & 1 & 1 & 0 & 0 & -1 & -1 \\
\gamma_2 & -1 & 0 & 1 & 1 & 2 & 1 & 1 & 0 & -1 \\
\gamma_3 & -1 & -1 & 0 & 0 & 1 & 1 & 1 & 1 & 0 \\
\gamma_4 & -1 & -1 & 0 & 0 & 1 & 1 & 1 & 1 & 0 \\
\gamma_5 & -1 & -2 & -1 & -1 & 0 & 1 & 1 & 2 & 1 \\
\gamma_6 & 0 & -1 & -1 & -1 & -1 & 0 & 0 & 1 & 1 \\
\gamma_7 & 0 & -1 & -1 & -1 & -1 & 0 & 0 & 1 & 1 \\
\gamma_8 & 1 & 0 & -1 & -1 & -2 & -1 & -1 & 0 & 1 \\
\gamma_9 & 1 & 1 & 0 & 0 & -1 & -1 & -1 & -1 & 0
\end{pmatrix} \ , \tag{7.12}$$

where the 1-loops satisfying the commutation relations can be written in terms of the canonical variables as follows,

$$\gamma_1 = e^{-Q} z_2 z_3 \ , \quad \gamma_2 = e^{-Q-P} z_3 z_6 \ , \quad \gamma_3 = e^{-P} z_3 z_6 \ ,$$

$$\gamma_4 = e^{-P} z_2^{-1} z_4^{-1} \ , \quad \gamma_5 = e^{Q-P} z_2^{-1} z_4^{-1} \ , \quad \gamma_6 = e^{Q} z_2^{-1} z_4^{-1} \ ,$$

$$\gamma_7 = e^{Q} z_5 z_7 \ , \quad \gamma_8 = e^{Q+P} z_5 z_7 \ , \quad \gamma_9 = e^{P} z_2 z_7 \ . \tag{7.13}$$
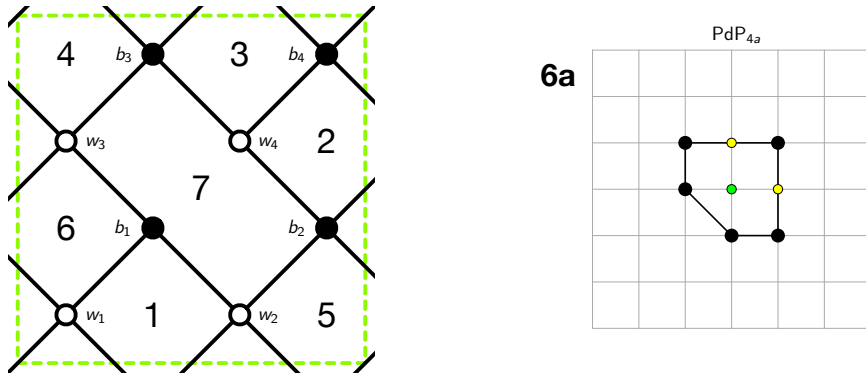
8   Model 6: PdP$_{4a}$

8.1   Model 6a

Figure 17: The brane tiling and toric diagram of Model 6a.

The brane tiling for Model 6a can be expressed in terms of the following pair of permutation tuples

$$\sigma_B = (e_{11}\ e_{21}\ e_{31})\ (e_{12}\ e_{32}\ e_{42}\ e_{22})\ (e_{13}\ e_{33}\ e_{43}\ e_{23})\ (e_{41}\ e_{42}\ e_{44}\ e_{43})$$
$$\sigma_W^{-1} = (e_{11}\ e_{13}\ e_{14}\ e_{12})\ (e_{21}\ e_{22}\ e_{24}\ e_{23})\ (e_{31}\ e_{32}\ e_{34}\ e_{33})\ (e_{42}\ e_{43}\ e_{44}) \quad (8.1)$$

which correspond to black and white nodes in the brane tiling, respectively.

The brane tiling for Model 6a has 7 zig-zag paths given by,

$$z_1 = (e_{23}^+\ e_{13}^-\ e_{14}^+\ e_{24}^-)\ ,\ z_2 = (e_{11}^+\ e_{21}^-\ e_{22}^+\ e_{12}^-)\ ,$$
$$z_3 = (e_{44}^+\ e_{34}^-\ e_{33}^+\ e_{43}^-)\ ,\ z_4 = (e_{21}^+\ e_{31}^-\ e_{32}^+\ e_{42}^-\ e_{43}^+\ e_{23}^-)\ ,$$
$$z_5 = (e_{42}^+\ e_{22}^-\ e_{24}^+\ e_{44}^-)\ ,\ z_6 = (e_{34}^+\ e_{14}^-\ e_{12}^+\ e_{32}^-)\ ,$$
$$z_7 = (e_{13}^+\ e_{33}^-\ e_{31}^+\ e_{11}^-)\ , \quad (8.2)$$

and 7 face paths given by,

$$f_1 = (e_{13}^+ \, e_{23}^- \, e_{21}^+ \, e_{11}^-) \; , \quad f_2 = (e_{34}^+ \, e_{44}^- \, e_{42}^+ \, e_{32}^-) \; ,$$
$$f_3 = (e_{23}^+ \, e_{43}^- \, e_{44}^+ \, e_{24}^-) \; , \quad f_4 = (e_{14}^+ \, e_{34}^- \, e_{33}^+ \, e_{13}^-) \; ,$$
$$f_5 = (e_{24}^+ \, e_{14}^- \, e_{12}^+ \, e_{22}^-) \; , \quad f_6 = (e_{11}^+ \, e_{31}^- \, e_{32}^+ \, e_{12}^-) \; ,$$
$$f_7 = (e_{43}^+ \, e_{33}^- \, e_{31}^+ \, e_{21}^- \, e_{22}^+ \, e_{42}^-) \; , \tag{8.3}$$

which satisfy the following relations,

$$f_4 f_6 = z_6^{-1} z_7^{-1} \; , \quad f_3 f_6^{-1} = z_1 z_3 z_6 z_7 \; , \quad f_1 f_2^{-1} = z_3 z_4 z_7 \; ,$$
$$f_2 f_4^{-1} f_7 = z_2 z_3^{-1} z_6 z_7 \; , \quad f_5 f_6^{-1} f_7^{-1} = z_2^{-1} z_3 z_5 z_6 \; , \quad f_1 f_2 f_3 f_4 f_5 f_6 f_7 = 1 \; . \tag{8.4}$$

The face paths can be written in terms of the canonical variables as follows,

$$f_1 = e^P \; , \quad f_2 = e^P z_1 z_2 z_5 z_6 \; , \quad f_3 = e^Q z_2^{-1} z_4^{-1} z_5^{-1} \; , \quad f_4 = e^{-Q} z_1 z_2 z_3 z_4 z_5 \; ,$$
$$f_5 = e^{-P} z_1^{-1} z_2^{-1} \; , \quad f_6 = e^Q \; , \quad f_7 = e^{-Q-P} z_2 z_4 z_7 \; . \tag{8.5}$$

The Kasteleyn matrix of the brane tiling for Model 6a in Figure 17 is given by,

$$K = \begin{pmatrix}
 & b_1 & b_2 & b_3 & b_4 \\
\hline
w_1 & e_{11} & e_{12}x^{-1} & e_{13}y^{-1} & e_{14}x^{-1}y^{-1} \\
w_2 & e_{21}x & e_{22} & e_{23}y^{-1} & e_{24}y^{-1} \\
w_3 & e_{31} & e_{32}x^{-1} & e_{33} & e_{34}x^{-1} \\
w_4 & 0 & e_{42} & e_{43}x & e_{44}
\end{pmatrix} \; . \tag{8.6}$$

By taking the permanent of the Kasteleyn matrix, we obtain the spectral curve of the dimer integrable system for Model 6a as follows,

$$0 = \operatorname{perm} K = \bar{p}_0 \cdot x^{-1} y^{-1} \cdot \Big[\delta_{(-1,0)} \frac{1}{x} + \delta_{(-1,1)} \frac{y}{x} + \delta_{(0,-1)} \frac{1}{y} + \delta_{(0,1)} y$$
$$+ \delta_{(1,-1)} \frac{x}{y} + \delta_{(1,0)} x + \delta_{(1,1)} xy + H \Big] \; , \tag{8.7}$$

where $\bar{p}_0 = e_{11}^+ e_{22}^+ e_{33}^+ e_{44}^+$. The Casimirs $\delta_{(m,n)}$ in (8.7) can be expressed in terms of the zig-zag paths in (8.2) as follows,

$$\delta_{(-1,0)} = z_1 z_4 z_5 z_7 \; , \quad \delta_{(-1,1)} = z_1 z_4 z_5 z_6 z_7 \; , \quad \delta_{(0,-1)} = z_1 z_5 z_7 \; ,$$
$$\delta_{(0,1)} = z_2^{-1} + z_3^{-1} \; , \quad \delta_{(1,-1)} = z_5 z_7 \; , \quad \delta_{(1,0)} = z_5 + z_7 \; , \quad \delta_{(1,1)} = 1 \; , \tag{8.8}$$

which allows us to express the spectral curve of Model 6a in the following form,

$$\Sigma \; : \; \left(\frac{1}{z_2} + \frac{1}{z_3} \right) y + z_1 z_5 z_7 \frac{1}{y} + (y + z_5)(y + z_7) \frac{x}{y} + (1 + y z_6) \frac{z_1 z_4 z_5 z_7}{x} + H = 0 \; . \tag{8.9}$$

The Hamiltonian is a sum over all 9 1-loops γ_i,

$$H = \sum_{i=1}^{9} \gamma_i \ , \tag{8.10}$$

where the 1-loops γ_i's can be expressed in terms of zig-zag paths and face paths as follows,

$$\gamma_1 = z_3^{-1} z_7 f_4 \ , \ \ \gamma_2 = z_1^{-1} z_2^{-1} z_3^{-1} z_7 f_1^{-1} f_4 \ , \ \ \gamma_3 = z_1 z_7 f_5 \ ,$$
$$\gamma_4 = z_3^{-1} z_6^{-1} f_5 \ , \ \ \gamma_5 = z_4 z_5 z_7 f_1^{-1} f_3 \ , \ \ \gamma_6 = z_4 z_5 z_7 f_3 \ ,$$
$$\gamma_7 = z_3^{-1} z_5 f_3 \ , \ \ \gamma_8 = z_3^{-1} z_5 f_1 f_3 \ , \ \ \gamma_9 = z_1 z_5 f_1 \ . \tag{8.11}$$

The commutation matrix C for Model 6a is given by,

$$C = \left(
\begin{array}{c|ccccccccc}
 & \gamma_1 & \gamma_2 & \gamma_3 & \gamma_4 & \gamma_5 & \gamma_6 & \gamma_7 & \gamma_8 & \gamma_9 \\
\hline
\gamma_1 & 0 & 1 & 1 & 1 & 1 & 0 & 0 & -1 & -1 \\
\gamma_2 & -1 & 0 & 1 & 1 & 2 & 1 & 1 & 0 & -1 \\
\gamma_3 & -1 & -1 & 0 & 0 & 1 & 1 & 1 & 1 & 0 \\
\gamma_4 & -1 & -1 & 0 & 0 & 1 & 1 & 1 & 1 & 0 \\
\gamma_5 & -1 & -2 & -1 & -1 & 0 & 1 & 1 & 2 & 1 \\
\gamma_6 & 0 & -1 & -1 & -1 & -1 & 0 & 0 & 1 & 1 \\
\gamma_7 & 0 & -1 & -1 & -1 & -1 & 0 & 0 & 1 & 1 \\
\gamma_8 & 1 & 0 & -1 & -1 & -2 & -1 & -1 & 0 & 1 \\
\gamma_9 & 1 & 1 & 0 & 0 & -1 & -1 & -1 & -1 & 0 \\
\end{array}
\right) \ , \tag{8.12}$$

where the 1-loops satisfying the commutation relations can be written in terms of the canonical variables as follows,

$$\gamma_1 = e^{-Q} z_1 z_2 z_4 z_5 z_7 \ , \ \ \gamma_2 = e^{-Q-P} z_4 z_5 z_7 \ , \ \ \gamma_3 = e^{-P} z_2^{-1} z_7 \ ,$$
$$\gamma_4 = e^{-P} z_4 z_5 z_7 \ , \ \ \gamma_5 = e^{Q-P} z_2^{-1} z_7 \ , \ \ \gamma_6 = e^{Q} z_2^{-1} z_7 \ ,$$
$$\gamma_7 = e^{Q} z_2^{-1} z_3^{-1} z_4^{-1} \ , \ \ \gamma_8 = e^{Q+P} z_2^{-1} z_3^{-1} z_4^{-1} \ , \ \ \gamma_9 = e^{P} z_1 z_5 \ . \tag{8.13}$$
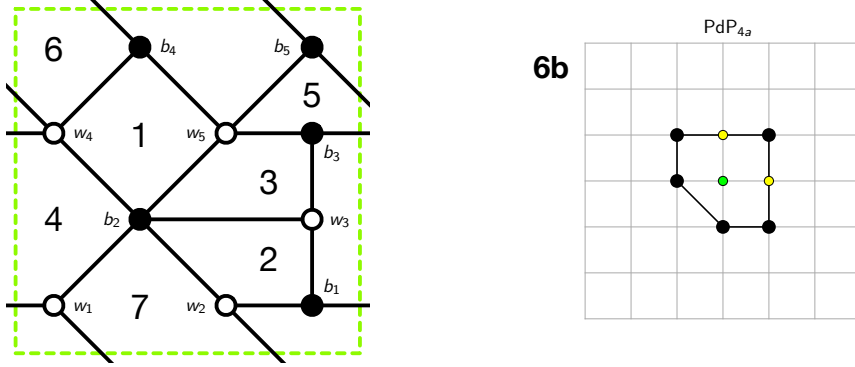
8.2 Model 6b

Figure 18: The brane tiling and toric diagram of Model 6b.

The brane tiling for Model 6b can be expressed in terms of the following pair of permutation tuples

$$
\begin{aligned}
\sigma_B = &\ (e_{11}\ e_{31}\ e_{21})\ (e_{12}\ e_{22}\ e_{32}\ e_{52}\ e_{42})\ (e_{33}\ e_{43}\ e_{53})\ (e_{14}\ e_{44}\ e_{54}) \\
&\ (e_{25}\ e_{55}\ e_{45}) \\
\sigma_W = &\ (e_{11}\ e_{12}\ e_{14})\ (e_{21}\ e_{25}\ e_{22})\ (e_{31}\ e_{32}\ e_{33})\ (e_{42}\ e_{43}\ e_{45}\ e_{44}) \\
&\ (e_{52}\ e_{54}\ e_{55}\ e_{53})
\end{aligned}
\tag{8.14}
$$

which correspond to black and white nodes in the brane tiling, respectively.

The brane tiling for Model 6b has 7 zig-zag paths given by,

$$
z_1 = (e_{52}^+\ e_{42}^-\ e_{43}^+\ e_{53}^-)\ ,\quad z_2 = (e_{44}^+\ e_{54}^-\ e_{55}^+\ e_{45}^-)\ ,\quad z_3 = (e_{22}^+\ e_{32}^-\ e_{33}^+\ e_{43}^-\ e_{45}^+\ e_{25}^-)\ ,
$$
$$
z_4 = (e_{31}^+\ e_{21}^-\ e_{25}^+\ e_{55}^-\ e_{53}^+\ e_{33}^-)\ ,\quad z_5 = (e_{54}^+\ e_{14}^-\ e_{11}^+\ e_{31}^-\ e_{32}^+\ e_{52}^-)\ ,
$$
$$
z_6 = (e_{42}^+\ e_{12}^-\ e_{14}^+\ e_{44}^-)\ ,\quad z_7 = (e_{21}^+\ e_{11}^-\ e_{12}^+\ e_{22}^-)\ .
\tag{8.15}
$$

and 7 face paths given by,

$$
f_1 = (e_{13}^+\ e_{23}^-\ e_{21}^+\ e_{11}^-)\ ,\quad f_2 = (e_{34}^+\ e_{44}^-\ e_{42}^+\ e_{32}^-)\ ,
$$
$$
f_3 = (e_{23}^+\ e_{43}^-\ e_{44}^+\ e_{24}^-)\ ,\quad f_4 = (e_{14}^+\ e_{34}^-\ e_{33}^+\ e_{13}^-)\ ,
$$
$$
f_5 = (e_{24}^+\ e_{14}^-\ e_{12}^+\ e_{22}^-)\ ,\quad f_6 = (e_{11}^+\ e_{31}^-\ e_{32}^+\ e_{12}^-)\ ,
$$
$$
f_7 = (e_{43}^+\ e_{33}^-\ e_{31}^+\ e_{21}^-\ e_{22}^+\ e_{42}^-)\ ,
\tag{8.16}
$$

which satisfy the following relations,

$$f_6 f_7 = z_2 z_7^{-1} \ , \ \ f_4 f_5 f_7^{-1} = z_2^{-1} z_4 z_6^{-1} z_7 \ , \ \ f_3 f_6^{-1} = z_1 z_3 z_6 z_7 \ ,$$

$$f_2 f_5^{-1} = z_3^{-1} z_4^{-1} \ , \ \ f_1 f_4^{-1} f_6^{-1} = z_1^{-1} z_2^{-1} z_4^{-1} z_6 \ , \ \ f_1 f_2 f_3 f_4 f_5 f_6 f_7 = 1 \ . \tag{8.17}$$

The face paths can be written in terms of the canonical variables as follows,

$$f_1 = e^{-Q} z_5 z_6 z_7 \ , \ \ f_2 = e^Q \ , \ \ f_3 = e^P z_1 z_3 z_6 z_7 \ , \ \ f_4 = e^{-Q-P} z_3^{-1} z_6^{-1} \ ,$$

$$f_5 = e^Q z_3 z_4 \ , \ \ f_6 = e^P \ , \ \ f_7 = e^{-P} z_2 z_7^{-1} \ . \tag{8.18}$$

The Kasteleyn matrix of the brane tiling for Model 6b in Figure 18 is given by,

$$K = \left(\begin{array}{c|ccccc} & b_1 & b_2 & b_3 & b_4 & b_5 \\ \hline w_1 & e_{11}x^{-1} & e_{12} & 0 & e_{14}y^{-1} & 0 \\ w_2 & e_{21}x & e_{22} & 0 & 0 & e_{25}y^{-1} \\ w_3 & e_{31} & e_{32} & e_{33} & 0 & 0 \\ w_4 & 0 & e_{42} & e_{43}x^{-1} & e_{44} & e_{45}x^{-1} \\ w_5 & 0 & e_{52} & e_{53}x & e_{54} & e_{55} \end{array} \right) \ . \tag{8.19}$$

The permanent of the Kasteleyn matrix gives the expression for the spectral curve of the dimer integrable system for Model 6b as follows,

$$0 = \text{perm } K = \bar{p}_0 \cdot x^{-1} y^{-1} \cdot \left[\delta_{(-1,0)} \frac{1}{x} + \delta_{(-1,1)} \frac{y}{x} + \delta_{(0,-1)} \frac{1}{y} + \delta_{(0,1)} y \right.$$

$$\left. + \delta_{(1,-1)} \frac{x}{y} + \delta_{(1,0)} x + \delta_{(1,1)} xy + H \right] \ , \tag{8.20}$$

where $\bar{p}_0 = e_{12}^+ e_{21}^+ e_{33}^+ e_{44}^+ e_{55}^+$. The Casimirs $\delta_{(m,n)}$ in (8.20) can be expressed in terms of the zig-zag paths in (8.15) as shown below,

$$\delta_{(-1,0)} = z_1 z_4 z_5 z_6 \ , \ \ \delta_{(-1,1)} = z_1 z_3 z_4 z_5 z_6 \ , \ \ \delta_{(0,-1)} = z_1 z_4 z_6 \ ,$$

$$\delta_{(0,1)} = z_2^{-1} + z_7^{-1} \ , \ \ \delta_{(1,-1)} = z_4 z_6 \ , \ \ \delta_{(1,0)} = z_4 + z_6 \ , \ \ \delta_{(1,1)} = 1 \ , \tag{8.21}$$

such that the spectral curve for Model 6b can be written in the following form,

$$\Sigma \ : \ \left(\frac{1}{z_2} + \frac{1}{z_7} \right) y + z_1 z_4 z_6 \frac{1}{y} + (y + z_4)(y + z_6) \frac{x}{y} + (1 + y z_3) \frac{z_1 z_4 z_5 z_6}{x} + H = 0 \ . \tag{8.22}$$

The Hamiltonian is a sum over all 9 1-loops γ_i,

$$H = \sum_{i=1}^{9} \gamma_i \ , \tag{8.23}$$

where the 1-loops γ_i's can be expressed in terms of zig-zag paths and face paths as follows,

$$\gamma_1 = z_1 z_4 f_1 \ , \ \ \gamma_2 = z_1 z_4 f_1 f_7 \ , \ \ \gamma_3 = z_2^{-1} z_4 f_7 \ ,$$
$$\gamma_4 = z_2^{-1} z_3^{-1} f_7 \ , \ \ \gamma_5 = z_2^{-1} z_4 f_2 f_7 \ , \ \ \gamma_6 = z_4 z_7^{-1} f_2 \ ,$$
$$\gamma_7 = z_1 z_3 z_4 z_6 f_2 \ , \ \ \gamma_8 = z_4 z_7^{-1} f_2 f_3 \ , \ \ \gamma_9 = z_4 z_5 z_6 f_3 \ . \tag{8.24}$$

The commutation matrix C for Model 6b is given by,

$$C = \left(\begin{array}{c|ccccccccc}
 & \gamma_1 & \gamma_2 & \gamma_3 & \gamma_4 & \gamma_5 & \gamma_6 & \gamma_7 & \gamma_8 & \gamma_9 \\
\hline
\gamma_1 & 0 & 1 & 1 & 1 & 1 & 0 & 0 & -1 & -1 \\
\gamma_2 & -1 & 0 & 1 & 1 & 2 & 1 & 1 & 0 & -1 \\
\gamma_3 & -1 & -1 & 0 & 0 & 1 & 1 & 1 & 1 & 0 \\
\gamma_4 & -1 & -1 & 0 & 0 & 1 & 1 & 1 & 1 & 0 \\
\gamma_5 & -1 & -2 & -1 & -1 & 0 & 1 & 1 & 2 & 1 \\
\gamma_6 & 0 & -1 & -1 & -1 & -1 & 0 & 0 & 1 & 1 \\
\gamma_7 & 0 & -1 & -1 & -1 & -1 & 0 & 0 & 1 & 1 \\
\gamma_8 & 1 & 0 & -1 & -1 & -2 & -1 & -1 & 0 & 1 \\
\gamma_9 & 1 & 1 & 0 & 0 & -1 & -1 & -1 & -1 & 0
\end{array} \right) . \tag{8.25}$$

The 1-loops satisfying the commutation relations can be written in terms of the canonical variables as follows,

$$\gamma_1 = e^{-Q} z_2^{-1} z_3^{-1} \ , \ \ \gamma_2 = e^{-Q-P} z_3^{-1} z_7^{-1} \ , \ \ \gamma_3 = e^{-P} z_4 z_7^{-1} \ ,$$
$$\gamma_4 = e^{-P} z_3^{-1} z_7^{-1} \ , \ \ \gamma_5 = e^{Q-P} z_4 z_7^{-1} \ , \ \ \gamma_6 = e^Q z_4 z_7^{-1} \ ,$$
$$\gamma_7 = e^Q z_1 z_3 z_4 z_6 \ , \ \ \gamma_8 = e^{Q+P} z_1 z_3 z_4 z_6 \ , \ \ \gamma_9 = e^P z_2^{-1} z_6 \ . \tag{8.26}$$
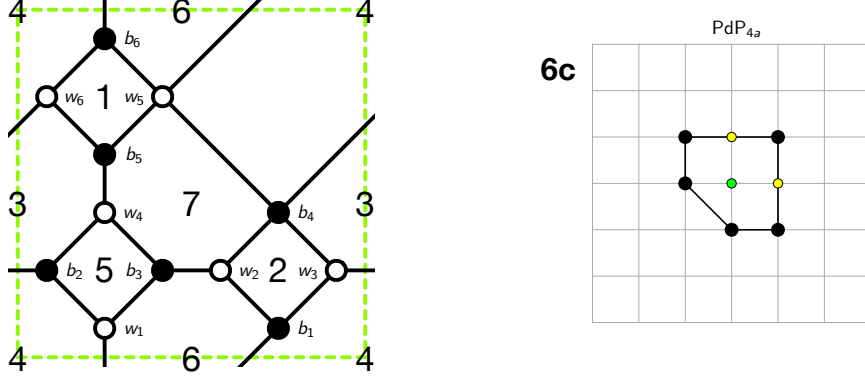
8.3 Model 6c

Figure 19: The brane tiling and toric diagram of Model 6c.

The brane tiling for Model 6c can be expressed in terms of the following pair of permutation tuples

$$\sigma_B = (e_{21}\ e_{51}\ e_{31})\ (e_{12}\ e_{42}\ e_{32})\ (e_{13}\ e_{23}\ e_{43})\ (e_{24}\ e_{34}\ e_{64}\ e_{54})$$
$$(e_{45}\ e_{55}\ e_{65})\ (e_{16}\ e_{66}\ e_{56})$$
$$\sigma_W^{-1} = (e_{12}\ e_{13}\ e_{16})\ (e_{21}\ e_{23}\ e_{24})\ (e_{31}\ e_{34}\ e_{32})\ (e_{42}\ e_{45}\ e_{43})$$
$$(e_{51}\ e_{54}\ e_{55}\ e_{56})\ (e_{64}\ e_{66}\ e_{65}) \tag{8.27}$$

which correspond to black and white nodes in the brane tiling, respectively.

The brane tiling for Model 6c has 7 zig-zag paths given by,

$$z_1 = (e_{55}^+\ e_{65}^-\ e_{64}^+\ e_{54}^-)\ ,\quad z_2 = (e_{66}^+\ e_{56}^-\ e_{51}^+\ e_{31}^-\ e_{34}^+\ e_{64}^-)\ ,$$
$$z_3 = (e_{24}^+\ e_{34}^-\ e_{32}^+\ e_{12}^-\ e_{13}^+\ e_{23}^-)\ ,\quad z_4 = (e_{31}^+\ e_{21}^-\ e_{23}^+\ e_{43}^-\ e_{42}^+\ e_{32}^-)\ ,$$
$$z_5 = (e_{65}^+\ e_{45}^-\ e_{43}^+\ e_{13}^-\ e_{16}^+\ e_{66}^-)\ ,\quad z_6 = (e_{56}^+\ e_{16}^-\ e_{12}^+\ e_{42}^-\ e_{45}^+\ e_{55}^-)\ ,$$
$$z_7 = (e_{21}^+\ e_{51}^-\ e_{54}^+\ e_{24}^-)\ . \tag{8.28}$$

and 7 face paths given by,

$$f_1 = (e_{65}^+\ e_{55}^-\ e_{56}^+\ e_{66}^-)\ ,\quad f_2 = (e_{34}^+\ e_{24}^-\ e_{21}^+\ e_{31}^-)\ ,$$
$$f_3 = (e_{32}^+\ e_{42}^-\ e_{45}^+\ e_{65}^-\ e_{64}^+\ e_{34}^-)\ ,\quad f_4 = (e_{66}^+\ e_{16}^-\ e_{12}^+\ e_{32}^-\ e_{31}^+\ e_{51}^-\ e_{54}^+\ e_{64}^-)\ ,$$
$$f_5 = (e_{42}^+\ e_{12}^-\ e_{13}^+\ e_{43}^-)\ ,\quad f_6 = (e_{51}^+\ e_{21}^-\ e_{23}^+\ e_{13}^-\ e_{16}^+\ e_{56}^-)\ ,$$
$$f_7 = (e_{55}^+\ e_{45}^-\ e_{43}^+\ e_{23}^-\ e_{24}^+\ e_{54}^-)\ , \tag{8.29}$$

satisfying the following relations,

$$f_5 f_6 f_7 = z_6^{-1} z_7^{-1} \ , \ \ f_4 f_6^{-1} f_7^{-2} = z_2 z_3 z_4^2 z_6^2 z_7^3 \ , \ \ f_3 f_6^{-1} = z_1 z_3 z_6 z_7 \ ,$$
$$f_2 f_5^{-1} = z_3^{-1} z_4^{-1} \ , \ \ f_1 f_5^{-1} = z_5 z_6 \ , \ \ f_1 f_2 f_3 f_4 f_5 f_6 f_7 = 1 \ . \tag{8.30}$$

The face paths can be written in terms of the canonical variables as follows,

$$f_1 = e^P z_5 z_6 \ , \ \ f_2 = e^P z_3^{-1} z_4^{-1} \ , \ \ f_3 = e^Q z_2^{-1} z_4^{-1} z_5^{-1} \ , \ \ f_4 = e^{-Q-2P} z_1^{-1} z_4 z_5^{-1} z_6^{-1} \ ,$$
$$f_5 = e^P \ , \ \ f_6 = e^Q \ , \ \ f_7 = e^{-Q-P} z_6^{-1} z_7^{-1} \ . \tag{8.31}$$

The Kasteleyn matrix of the brane tiling for Model 6c in Figure 19 is given by,

$$K = \begin{pmatrix}
 & b_1 & b_2 & b_3 & b_4 & b_5 & b_6 \\
\hline
w_1 & 0 & e_{12} & e_{13} & 0 & 0 & e_{16}y^{-1} \\
w_2 & e_{21} & 0 & e_{23} & e_{24} & 0 & 0 \\
w_3 & e_{31} & e_{32}x & 0 & e_{34} & 0 & 0 \\
w_4 & 0 & e_{42} & e_{43} & 0 & e_{45} & 0 \\
w_5 & e_{51}y & 0 & 0 & e_{54} & e_{55} & e_{56} \\
w_6 & 0 & 0 & 0 & e_{64}x^{-1} & e_{65} & e_{66}
\end{pmatrix} \ . \tag{8.32}$$

By taking the permanent of the Kasteleyn matrix in (8.32) with a $GL(2,\mathbb{Z})$ transformation $M : (x,y) \mapsto (x, \frac{1}{y})$, we obtain the spectral curve of the dimer integrable system for Model 6c as follows,

$$0 = \bar{p}_0 \cdot \left[\delta_{(-1,0)} \frac{1}{x} + \delta_{(-1,1)} \frac{y}{x} + \delta_{(0,-1)} \frac{1}{y} + \delta_{(0,1)} y \right.$$
$$\left. + \delta_{(1,-1)} \frac{x}{y} + \delta_{(1,0)} x + \delta_{(1,1)} xy + H \right] \ , \tag{8.33}$$

where $\bar{p}_0 = e_{13}^+ e_{24}^+ e_{32}^+ e_{45}^+ e_{51}^+ e_{66}^+$. The Casimirs $\delta_{(m,n)}$ in (8.33) can be expressed in terms of the zig-zag paths in (8.28) as shown below,

$$\delta_{(-1,0)} = z_1 z_4 z_5 z_6 z_7 \ , \ \ \delta_{(-1,1)} = z_1 z_4 z_5 z_7 \ , \ \ \delta_{(0,-1)} = z_3^{-1} \ ,$$
$$\delta_{(0,1)} = z_1 z_5 z_7 + z_4 z_5 z_7 \ , \ \ \delta_{(1,-1)} = 1 \ , \ \ \delta_{(1,0)} = z_5 + z_7 \ , \ \ \delta_{(1,1)} = z_5 z_7 \ , \tag{8.34}$$

allowing us to express the spectral curve of Model 6c in the following form,

$$\Sigma \ : \ (z_5 + z_7)x + \frac{1}{z_3 y} + (x + z_1)(x + z_4) \frac{z_5 z_7}{x} y + z_1 z_4 z_5 z_6 z_7 \frac{1}{x} + \frac{x}{y} + H = 0 \ . \tag{8.35}$$

The Hamiltonian is a sum over all 12 1-loops γ_i,

$$H = \sum_{i=1}^{12} \gamma_i \ , \tag{8.36}$$

where the 1-loops γ_i's can be expressed in terms of zig-zag paths and face paths as follows,

$$\gamma_1 = z_3^{-1} z_5 z_6^{-1} z_7^{-1} f_3 f_4 f_6^{-1} f_7^{-1} \ , \ \ \gamma_2 = z_4 z_7 f_7 \ , \ \ \gamma_3 = z_3^{-1} z_6^{-1} f_6^{-1} \ ,$$

$$\gamma_4 = z_1 z_5 f_4 \ , \ \ \gamma_5 = z_3^{-1} z_7 f_7 \ , \ \ \gamma_6 = z_2^{-1} z_3^{-1} z_4^{-1} f_5 f_6 \ ,$$

$$\gamma_7 = z_2^{-1} z_3^{-1} z_4^{-1} f_5 \ , \ \ \gamma_8 = z_3^{-1} z_5 f_5 \ , \ \ \gamma_9 = z_4 z_5 z_6 z_7 f_5 f_7 \ ,$$

$$\gamma_{10} = z_3^{-1} z_5 f_5 f_6^{-1} \ , \ \ \gamma_{11} = z_1^{-1} z_2^{-1} z_3^{-1} f_7 \ , \ \ \gamma_{12} = z_3^{-1} z_5 z_6 z_7 f_5 f_7 \ . \tag{8.37}$$

The commutation matrix C for Model 6c takes the following form,

$$C = \begin{array}{c} \\ \gamma_1 \\ \gamma_2 \\ \gamma_3 \\ \gamma_4 \\ \gamma_5 \\ \gamma_6 \\ \gamma_7 \\ \gamma_8 \\ \gamma_9 \\ \gamma_{10} \\ \gamma_{11} \\ \gamma_{12} \end{array} \left(\begin{array}{c|cccccccccccc} & \gamma_1 & \gamma_2 & \gamma_3 & \gamma_4 & \gamma_5 & \gamma_6 & \gamma_7 & \gamma_8 & \gamma_9 & \gamma_{10} & \gamma_{11} & \gamma_{12} \\ \hline & 0 & -1 & -1 & -1 & -1 & 1 & 0 & 0 & -1 & -1 & -1 & -1 \\ & 1 & 0 & -1 & 1 & 0 & 0 & -1 & -1 & -1 & -2 & 0 & -1 \\ & 1 & 1 & 0 & 2 & 1 & -1 & -1 & -1 & 0 & -1 & 1 & 0 \\ & 1 & -1 & -2 & 0 & -1 & 1 & -1 & -1 & -2 & -3 & -1 & -2 \\ & 1 & 0 & -1 & 1 & 0 & 0 & -1 & -1 & -1 & -2 & 0 & -1 \\ & -1 & 0 & 1 & -1 & 0 & 0 & 1 & 1 & 1 & 2 & 0 & 1 \\ & 0 & 1 & 1 & 1 & 1 & -1 & 0 & 0 & 1 & 1 & 1 & 1 \\ & 0 & 1 & 1 & 1 & 1 & -1 & 0 & 0 & 1 & 1 & 1 & 1 \\ & 1 & 1 & 0 & 2 & 1 & -1 & -1 & -1 & 0 & -1 & 1 & 0 \\ & 1 & 2 & 1 & 3 & 2 & -2 & -1 & -1 & 1 & 0 & 2 & 1 \\ & 1 & 0 & -1 & 1 & 0 & 0 & -1 & -1 & -1 & -2 & 0 & -1 \\ & 1 & 1 & 0 & 2 & 1 & -1 & -1 & -1 & 0 & -1 & 1 & 0 \end{array} \right) . \tag{8.38}$$

The 1-loops satisfying the commutation relations can be written in terms of the canonical variables as follows,

$$\gamma_1 = e^{-P} z_4 z_7 \ , \ \ \gamma_2 = e^{-Q-P} z_4 z_6^{-1} \ , \ \ \gamma_3 = e^{-Q} z_3^{-1} z_6^{-1} \ ,$$

$$\gamma_4 = e^{-Q-2P} z_4 z_6^{-1} \ , \ \ \gamma_5 = e^{-Q-P} z_1 z_2 z_4 z_5 z_7 \ , \ \ \gamma_6 = e^{Q+P} z_2^{-1} z_3^{-1} z_4^{-1} \ ,$$

$$\gamma_7 = e^{P} z_2^{-1} z_3^{-1} z_4^{-1} \ , \ \ \gamma_8 = e^{P} z_3^{-1} z_5 \ , \ \ \gamma_9 = e^{-Q} z_4 z_5 \ ,$$

$$\gamma_{10} = e^{-Q+P} z_3^{-1} z_5 \ , \ \ \gamma_{11} = e^{-Q-P} z_4 z_5 \ , \ \ \gamma_{12} = e^{-Q} z_3^{-1} z_5 \ . \tag{8.39}$$

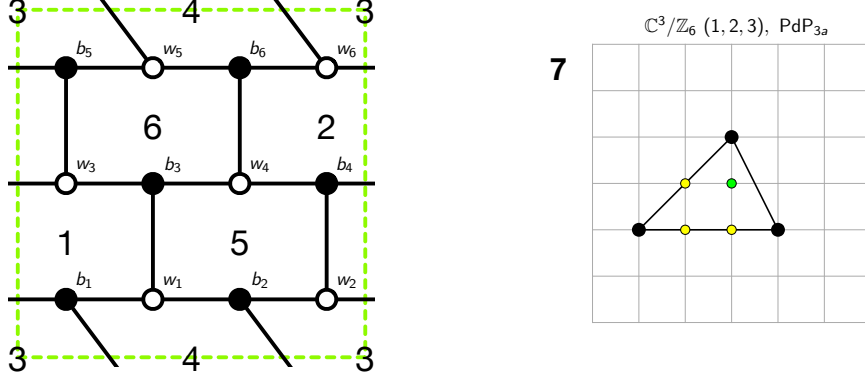# 9 Model 7: $\mathbb{C}^3/\mathbb{Z}_6$ $(1,2,3)$, $\mathbf{PdP}_{3a}$

Figure 20: The brane tiling and toric diagram of Model 7.

The brane tiling for Model 7 can be expressed in terms of the following pair of permutation tuples

$$
\begin{aligned}
\sigma_B &= (e_{11} \; e_{21} \; e_{51}) \, (e_{12} \; e_{62} \; e_{22}) \, (e_{13} \; e_{43} \; e_{33}) \, (e_{23} \; e_{34} \; e_{44}) \\
&\quad (e_{35} \; e_{55} \; e_{65}) \, (e_{46} \; e_{66} \; e_{56}) \\
\sigma_W^{-1} &= (e_{11} \; e_{13} \; e_{12}) \, (e_{21} \; e_{22} \; e_{24}) \, (e_{33} \; e_{34} \; e_{35}) \, (e_{43} \; e_{46} \; e_{44}) \\
&\quad (e_{51} \; e_{56} \; e_{55}) \, (e_{62} \; e_{65} \; e_{66})
\end{aligned}
\tag{9.1}
$$

which correspond to black and white nodes in the brane tiling, respectively.

The brane tiling for Model 7 has 6 zig-zag paths given by,

$$
\begin{aligned}
z_1 &= (e_{24}^+ \; e_{34}^- \; e_{35}^+ \; e_{55}^- \; e_{51}^+ \; e_{11}^- \; e_{13}^+ \; e_{43}^- \; e_{46}^+ \; e_{66}^- \; e_{62}^+ \; e_{22}^-) \;, \quad z_2 = (e_{11}^+ \; e_{21}^- \; e_{22}^+ \; e_{12}^-) \;, \\
z_3 &= (e_{33}^+ \; e_{13}^- \; e_{12}^+ \; e_{62}^- \; e_{65}^+ \; e_{35}^-) \;, \quad z_4 = (e_{34}^+ \; e_{44}^- \; e_{43}^+ \; e_{33}^-) \;, \\
z_5 &= (e_{66}^+ \; e_{56}^- \; e_{55}^+ \; e_{65}^-) \;, \quad z_6 = (e_{21}^+ \; e_{51}^- \; e_{56}^+ \; e_{46}^- \; e_{44}^+ \; e_{24}^-) \;,
\end{aligned}
\tag{9.2}
$$

and 6 face paths given by,

$$
\begin{aligned}
f_1 &= (e_{34}^+ \; e_{24}^- \; e_{21}^+ \; e_{11}^- \; e_{13}^+ \; e_{33}^-) \;, \quad f_2 = (e_{66}^+ \; e_{46}^- \; e_{44}^+ \; e_{34}^- \; e_{35}^+ \; e_{65}^-) \;, \\
f_3 &= (e_{65}^+ \; e_{55}^- \; e_{51}^+ \; e_{21}^- \; e_{22}^+ \; e_{62}^-) \;, \quad f_4 = (e_{11}^+ \; e_{51}^- \; e_{56}^+ \; e_{66}^- \; e_{62}^+ \; e_{12}^-) \;, \\
f_5 &= (e_{24}^+ \; e_{44}^- \; e_{43}^+ \; e_{13}^- \; e_{12}^+ \; e_{22}^-) \;, \quad f_6 = (e_{33}^+ \; e_{43}^- \; e_{46}^+ \; e_{56}^- \; e_{55}^+ \; e_{35}^-) \;,
\end{aligned}
\tag{9.3}
$$

which satisfy the following relations,

$$f_3 f_5 f_6 = z_3 z_6^{-1} z_7^{-1} \ , \ \ f_4 f_5^{-1} f_6^{-1} = z_1 z_2^2 z_4 z_6^2 \ ,$$

$$f_2 f_3^{-1} f_5^{-1} = z_1 z_2 z_5^2 z_6^2 \ , \ \ f_1 f_3^{-1} f_6^{-1} = z_1 z_4^2 z_5 z_6^2 \ , \ \ f_1 f_2 f_3 f_4 f_5 f_6 = 1 \ . \tag{9.4}$$

The face paths can be written in terms of the canonical variables as follows,

$$f_1 = e^Q \ , \ \ f_2 = e^P \ , \ \ f_3 = e^{Q+P} z_2 z_3 z_5^{-1} z_6^{-1} \ ,$$

$$f_4 = e^{-Q-P} z_3^{-1} z_6 \ , \ \ f_5 = e^{-Q} z_2^{-1} z_4 \ , \ \ f_6 = e^{-P} z_4^{-1} z_5 \ . \tag{9.5}$$

The Kasteleyn matrix of the brane tiling for Model 7 in Figure 20 is given by,

$$K = \begin{pmatrix}
 & b_1 & b_2 & b_3 & b_4 & b_5 & b_6 \\
\hline
w_1 & e_{11} & e_{12} & e_{13} & 0 & 0 & 0 \\
w_2 & e_{21}x^{-1} & e_{22} & 0 & e_{24} & 0 & 0 \\
w_3 & 0 & 0 & e_{33} & e_{34}x & e_{35} & 0 \\
w_4 & 0 & 0 & e_{43} & e_{44} & 0 & e_{46} \\
w_5 & e_{51}y & 0 & 0 & 0 & e_{55} & e_{56} \\
w_6 & 0 & e_{62}y & 0 & 0 & e_{65}x^{-1} & e_{66}
\end{pmatrix} \ . \tag{9.6}$$

The permanent of the Kasteleyn matrix gives the expression for the spectral curve of the dimer integrable system for Model 7 as follows,

$$0 = \text{perm } K = \bar{p}_0 \cdot y \cdot \left[\delta_{(-2,-1)} \frac{1}{x^2 y} + \delta_{(-1,-1)} \frac{1}{xy} + \delta_{(-1,0)} \frac{1}{x} \right.$$

$$\left. + \delta_{(0,-1)} \frac{1}{y} + \delta_{(0,1)} y + \delta_{(1,-1)} \frac{x}{y} + H \right] \tag{9.7}$$

where $\bar{p}_0 = e_{13}^+ e_{24}^+ e_{35}^+ e_{46}^+ e_{51}^+ e_{62}^+$. The Casimirs $\delta_{(m,n)}$ in (9.7) can be expressed in terms of the zig-zag paths in (9.2) as follows,

$$\delta_{(-2,-1)} = z_3 z_6 \ , \ \ \delta_{(-1,-1)} = z_2 z_3 z_6 + z_3 z_4 z_6 + z_3 z_5 z_6 \ , \ \ \delta_{(-1,0)} = z_3 + z_6 \ ,$$

$$\delta_{(0,-1)} = z_2 z_3 z_4 z_6 + z_2 z_3 z_5 z_6 + z_3 z_4 z_5 z_6 \ , \ \ \delta_{(0,1)} = 1 \ , \ \ \delta_{(1,-1)} = z_2 z_3 z_4 z_5 z_6 \ , \tag{9.8}$$

such that the spectral curve for Model 7 can be written in the following form,

$$\Sigma \ : \ z_3 z_6 \frac{1}{x^2 y} + z_3 z_6 (z_2 + z_4 + z_5) \frac{1}{xy} + (z_3 + z_6) \frac{1}{x}$$

$$+ z_3 z_6 (z_2 z_4 + z_2 z_5 + z_4 z_5) \frac{1}{y} + y + z_2 z_3 z_4 z_5 z_6 \frac{x}{y} + H = 0 \ . \tag{9.9}$$

The Hamiltonian is a sum over all 6 1-loops γ_i,

$$H = \sum_{i=1}^{6} \gamma_i \ , \tag{9.10}$$

where the 1-loops γ_i can be expressed in terms of zig-zag paths and face paths as follows,

$$\gamma_1 = z_2 z_6 f_5 f_6 \ , \ \ \gamma_2 = z_4 z_6 f_6 \ , \ \ \gamma_3 = z_2 z_3 f_1 \ ,$$
$$\gamma_4 = z_2 z_3 f_1 f_2 \ , \ \ \gamma_5 = z_3 z_4 f_2 \ , \ \ \gamma_6 = z_2 z_6 f_5 \ . \tag{9.11}$$

The commutation matrix C for Model 7 takes the following form,

$$C = \begin{pmatrix}
 & \gamma_1 & \gamma_2 & \gamma_3 & \gamma_4 & \gamma_5 & \gamma_6 \\
\hline
\gamma_1 & 0 & 1 & 1 & 0 & -1 & -1 \\
\gamma_2 & -1 & 0 & 1 & 1 & 0 & -1 \\
\gamma_3 & -1 & -1 & 0 & 1 & 1 & 0 \\
\gamma_4 & 0 & -1 & -1 & 0 & 1 & 1 \\
\gamma_5 & 1 & 0 & -1 & -1 & 0 & 1 \\
\gamma_6 & 1 & 1 & 0 & -1 & -1 & 0
\end{pmatrix} \ , \tag{9.12}$$

where the 1-loops satisfying the commutation relations can be written in terms of the canonical variables as follows,

$$\gamma_1 = e^{-Q-P} z_5 z_6 \ , \ \ \gamma_2 = e^{-P} z_5 z_6 \ , \ \ \gamma_3 = e^{Q} z_2 z_3 \ ,$$
$$\gamma_4 = e^{Q+P} z_2 z_3 \ , \ \ \gamma_5 = e^{P} z_3 z_4 \ , \ \ \gamma_6 = e^{-Q} z_4 z_6 \ . \tag{9.13}$$

10 Model 8: SPP/$\mathbb{Z}_2$ $(0, 1, 1, 1)$, PdP$_{3c}$
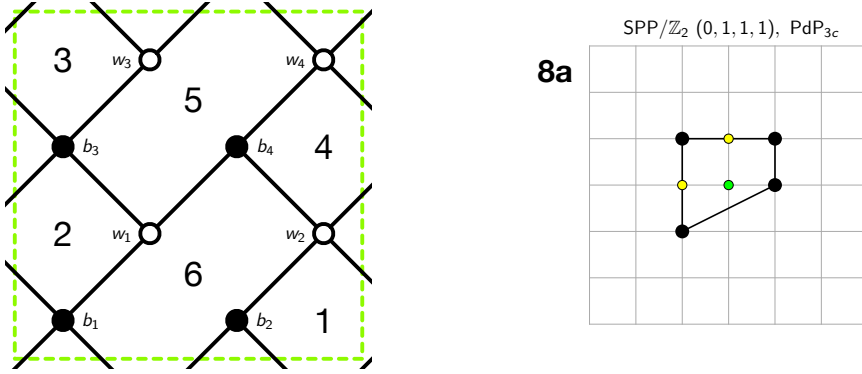
10.1 Model 8a

Figure 21: The brane tiling and toric diagram of Model 8a.

The brane tiling for Model 8a can be expressed in terms of the following pair of permutation tuples

$$\sigma_B = (e_{11} \ e_{21} \ e_{41} \ e_{31}) \ (e_{22} \ e_{32} \ e_{42}) \ (e_{13} \ e_{33} \ e_{43} \ e_{23}) \ (e_{14} \ e_{24} \ e_{44})$$
$$\sigma_W^{-1} = (e_{11} \ e_{13} \ e_{14}) \ (e_{21} \ e_{22} \ e_{24} \ e_{23}) \ (e_{31} \ e_{32} \ e_{33}) \ (e_{41} \ e_{43} \ e_{44} \ e_{42}) \qquad (10.1)$$

which correspond to black and white nodes in the brane tiling, respectively.

The brane tiling for Model 8a has 6 zig-zag paths given by,

$$z_1 = (e_{21}^+ \ e_{41}^- \ e_{43}^+ \ e_{23}^-) \ , \quad z_2 = (e_{42}^+ \ e_{22}^- \ e_{24}^+ \ e_{44}^-) \ ,$$
$$z_3 = (e_{22}^+ \ e_{32}^- \ e_{33}^+ \ e_{43}^- \ e_{44}^+ \ e_{14}^- \ e_{11}^+ \ e_{21}^-) \ , \quad z_4 = (e_{23}^+ \ e_{13}^- \ e_{14}^+ \ e_{24}^-) \ ,$$
$$z_5 = (e_{41}^+ \ e_{31}^- \ e_{32}^+ \ e_{42}^-) \ , \quad z_6 = (e_{13}^+ \ e_{33}^- \ e_{31}^+ \ e_{11}^-) \ , \qquad (10.2)$$

and 6 face paths given by,

$$f_1 = (e_{41}^+ \ e_{21}^- \ e_{22}^+ \ e_{42}^-) \ , \quad f_2 = (e_{21}^+ \ e_{11}^- \ e_{13}^+ \ e_{23}^-) \ ,$$
$$f_3 = (e_{43}^+ \ e_{33}^- \ e_{31}^+ \ e_{41}^-) \ , \quad f_4 = (e_{23}^+ \ e_{43}^- \ e_{44}^+ \ e_{24}^-) \ ,$$
$$f_5 = (e_{42}^+ \ e_{32}^- \ e_{33}^+ \ e_{13}^- \ e_{14}^+ \ e_{44}^-) \ , \quad f_6 = (e_{11}^+ \ e_{31}^- \ e_{32}^+ \ e_{22}^- \ e_{24}^+ \ e_{14}^-) \ , \qquad (10.3)$$

which satisfy the following constraints,

$$f_5 f_6 = z_2 z_6^{-1} \ , \quad f_3 f_4 f_6^{-1} = z_2^{-1} z_4 z_5^{-1} z_6 \ , \quad f_2 f_4^{-1} f_5^{-1} = z_1 z_4^{-1} z_5 z_6 \ ,$$
$$f_1 f_3^{-1} f_5^{-1} = z_3 z_5^2 z_6 \ , \quad f_1 f_2 f_3 f_4 f_5 f_6 = 1 \ . \tag{10.4}$$

The face paths can be written in terms of the canonical variables as follows,

$$f_1 = e^{-P} z_1^{-1} z_2^{-1} \ , \quad f_2 = e^{-Q+P} z_1 z_2 z_4^{-1} z_5 \ , \quad f_3 = e^{Q-P} z_2^{-1} z_4 z_5^{-1} z_6 \ ,$$
$$f_4 = e^{P} \ , \quad f_5 = e^{-Q} z_2 z_6^{-1} \ , \quad f_6 = e^{Q} \ . \tag{10.5}$$

The Kasteleyn matrix of the brane tiling for Model 8a in Figure 21 is given by,

$$K = \begin{pmatrix} & b_1 & b_2 & b_3 & b_4 \\ \hline w_1 & e_{11} & 0 & e_{13} & e_{14} \\ w_2 & e_{21}x & e_{22} & e_{23}x & e_{24} \\ w_3 & e_{31}y & e_{32}y & e_{33} & 0 \\ w_4 & e_{41}xy & e_{42}y & e_{43}x & e_{44} \end{pmatrix} \ . \tag{10.6}$$

By taking the permanent of the Kasteleyn matrix, we obtain the spectral curve of the dimer integrable system for Model 8a as follows,

$$0 = \text{perm } K = \overline{p}_0 \cdot xy \cdot \left[\delta_{(-1,-1)} \frac{1}{xy} + \delta_{(-1,0)} \frac{1}{x} + \delta_{(-1,1)} \frac{y}{x} \right.$$
$$\left. + \delta_{(0,1)} y + \delta_{(1,0)} x + \delta_{(1,1)} xy + H \right] \ , \tag{10.7}$$

where $\overline{p}_0 = e_{14}^+ e_{23}^+ e_{32}^+ e_{41}^+$. The Casimirs $\delta_{(m,n)}$ in (10.7) can be expressed in terms of the zig-zag paths in (10.2) as shown below,

$$\delta_{(-1,-1)} = z_1 z_3 \ , \quad \delta_{(-1,-0)} = z_1 z_2 z_3 + z_1 z_3 z_6 \ , \quad \delta_{(-1,1)} = z_1 z_2 z_3 z_6 \ ,$$
$$\delta_{(0,1)} = z_1 z_2 z_3 z_4 z_6 + z_1 z_2 z_3 z_5 z_6 \ , \quad \delta_{(1,0)} = z_1 \ , \quad \delta_{(1,1)} = 1 \ . \tag{10.8}$$

Accordingly, we can express the spectral curve of Model 8a as follows,

$$\Sigma \ : \ (y + z_1)x + \left(\frac{1}{z_4} + \frac{1}{z_5} \right) y + (1 + z_2 y)(1 + z_6 y) \frac{z_1 z_3}{xy} + H = 0 \ . \tag{10.9}$$

The Hamiltonian is a sum over all 6 1-loops γ_i,

$$H = \sum_{i=1}^{6} \gamma_i \ , \tag{10.10}$$

where the 1-loops γ_i can be expressed in terms of zig-zag paths and face paths as follows,

$$\gamma_1 = z_1 z_4^{-1} f_4 f_5 \ , \ \ \gamma_2 = z_2^{-1} z_4^{-1} f_5 \ , \ \ \gamma_3 = z_1 z_5^{-1} f_1 \ ,$$
$$\gamma_4 = z_1 z_5^{-1} f_1 f_6 \ , \ \ \gamma_5 = z_1 z_5^{-1} f_1 f_4 f_6 \ , \ \ \gamma_6 = z_2^{-1} z_4^{-1} f_1^{-1} \ . \tag{10.11}$$

The commutation matrix C for Model 8a is given by,

$$C = \begin{pmatrix}
 & \gamma_1 & \gamma_2 & \gamma_3 & \gamma_4 & \gamma_5 & \gamma_6 \\
\hline
\gamma_1 & 0 & 1 & 1 & 0 & -1 & -1 \\
\gamma_2 & -1 & 0 & 1 & 1 & 0 & -1 \\
\gamma_3 & -1 & -1 & 0 & 1 & 1 & 0 \\
\gamma_4 & 0 & -1 & -1 & 0 & 1 & 1 \\
\gamma_5 & 1 & 0 & -1 & -1 & 0 & 1 \\
\gamma_6 & 1 & 1 & 0 & -1 & -1 & 0
\end{pmatrix} \ . \tag{10.12}$$

The 1-loops satisfying the commutation relations can be written in terms of the canonical variables as follows,

$$\gamma_1 = e^{-Q+P} z_1 z_2 z_4^{-1} z_6^{-1} \ , \ \ \gamma_2 = e^{-Q} z_4^{-1} z_6^{-1} \ , \ \ \gamma_3 = e^{-P} z_2^{-1} z_5^{-1} \ ,$$
$$\gamma_4 = e^{Q-P} z_2^{-1} z_5^{-1} \ , \ \ \gamma_5 = e^{Q} z_2^{-1} z_5^{-1} \ , \ \ \gamma_6 = e^{P} z_1 z_4^{-1} \ . \tag{10.13}$$
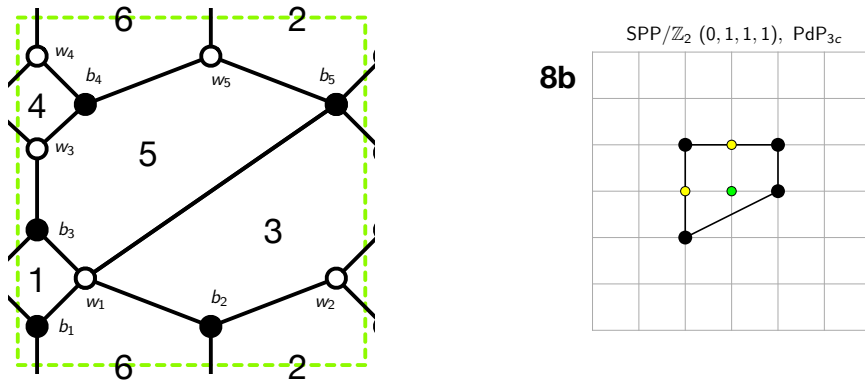
10.2 Model 8b

Figure 22: The brane tiling and toric diagram of Model 8b.

The brane tiling for Model 8b can be expressed in terms of the following pair of permutation tuples

$$\sigma_B = (e_{11}\ e_{21}\ e_{41})\ (e_{12}\ e_{52}\ e_{22})\ (e_{13}\ e_{33}\ e_{23})\ (e_{34}\ e_{54}\ e_{44})\ (e_{15}\ e_{35}\ e_{45}\ e_{55})$$
$$\sigma_W^{-1} = (e_{11}\ e_{13}\ e_{15}\ e_{12})\ (e_{21}\ e_{22}\ e_{23})\ (e_{33}\ e_{35}\ e_{34})\ (e_{41}\ e_{44}\ e_{45})\ (e_{52}\ e_{55}\ e_{54})$$

$$(10.14)$$

which correspond to black and white nodes in the brane tiling, respectively.

The brane tiling for Model 8b has 6 zig-zag paths given by,

$$z_1 = (e_{11}^+\ e_{21}^-\ e_{22}^+\ e_{12}^-)\ ,\quad z_2 = (e_{23}^+\ e_{13}^-\ e_{15}^+\ e_{35}^-\ e_{34}^+\ e_{54}^-\ e_{52}^+\ e_{22}^-)\ ,$$
$$z_3 = (e_{45}^+\ e_{55}^-\ e_{54}^+\ e_{44}^-)\ ,\quad z_4 = (e_{21}^+\ e_{41}^-\ e_{44}^+\ e_{34}^-\ e_{33}^+\ e_{23}^-)\ ,$$
$$z_5 = (e_{13}^+\ e_{33}^-\ e_{35}^+\ e_{45}^-\ e_{41}^+\ e_{11}^-)\ ,\quad z_6 = (e_{55}^+\ e_{15}^-\ e_{12}^+\ e_{52}^-)\ ,$$

$$(10.15)$$

and 6 face paths given by,

$$f_1 = (e_{21}^+\ e_{11}^-\ e_{13}^+\ e_{23}^-)\ ,\quad f_2 = (e_{22}^+\ e_{52}^-\ e_{55}^+\ e_{45}^-\ e_{41}^+\ e_{21}^-)\ ,$$
$$f_3 = (e_{23}^+\ e_{33}^-\ e_{35}^+\ e_{15}^-\ e_{12}^+\ e_{22}^-)\ ,\quad f_4 = (e_{45}^+\ e_{35}^-\ e_{34}^+\ e_{44}^-)\ ,$$
$$f_5 = (e_{15}^+\ e_{55}^-\ e_{54}^+\ e_{34}^-\ e_{33}^+\ e_{13}^-)\ ,\quad f_6 = (e_{11}^+\ e_{41}^-\ e_{44}^+\ e_{54}^-\ e_{52}^+\ e_{12}^-)\ ,$$

$$(10.16)$$

which satisfy the following relations,

$$f_1 f_4^{-1} = z_4 z_5\ ,\quad f_4 f_5 f_6 = z_5^{-1} z_6^{-1}\ ,\quad f_2 f_4^{-1} f_5^{-1} = z_1 z_3^{-1} z_5 z_6\ ,$$
$$f_3 f_5^{-1} f_6^{-2} = z_1^{-1} z_4^{-1} z_3 z_5 z_6^2\ ,\quad f_1 f_2 f_3 f_4 f_5 f_6 = 1\ .$$

$$(10.17)$$

The face paths can be expressed in terms of the canonical variables as follows,

$$f_1 = e^Q z_4 z_5\ ,\quad f_2 = e^{Q+P} z_1 z_3^{-1} z_5 z_6\ ,\quad f_3 = e^{-2Q-P} z_2 z_3^2 z_6\ ,$$
$$f_4 = e^Q\ ,\quad f_5 = e^P\ ,\quad f_6 = e^{-Q-P} z_5^{-1} z_6^{-1}\ .$$

$$(10.18)$$

The Kasteleyn matrix of the brane tiling for Model 8b in Figure 22 takes the following form,

$$K = \left(\begin{array}{c|ccccc} & b_1 & b_2 & b_3 & b_4 & b_5 \\ \hline w_1 & e_{11} & e_{12} & e_{13} & 0 & e_{15} \\ w_2 & e_{21}x & e_{22} & e_{23}x & 0 & 0 \\ w_3 & 0 & 0 & e_{33} & e_{34} & e_{35}x^{-1} \\ w_4 & e_{41}y & 0 & 0 & e_{44} & e_{45}x^{-1} \\ w_5 & 0 & e_{52}y & 0 & e_{54} & e_{55} \end{array}\right)\ . \qquad (10.19)$$

By taking the permanent of the Kasteleyn matrix in (10.19) with a $GL(2, \mathbb{Z})$ transformation $M : (x, y) \mapsto (\frac{1}{x}, \frac{1}{y})$, we obtain the spectral curve of the dimer integrable system for Model 8b as follows,

$$0 = \bar{p}_0 \cdot y^{-1} \cdot \left[\delta_{(-1,-1)} \frac{1}{xy} + \delta_{(-1,0)} \frac{1}{x} + \delta_{(-1,1)} \frac{y}{x} \right.$$
$$\left. + \delta_{(0,1)} y + \delta_{(1,0)} x + \delta_{(1,1)} xy + H \right] , \tag{10.20}$$

where $\bar{p}_0 = e_{11}^+ e_{22}^+ e_{33}^+ e_{45}^+ e_{54}^+$. The Casimirs $\delta_{(m,n)}$ in (10.20) can be written in terms of the zig-zag paths in (10.15) as follows,

$$\delta_{(-1,-1)} = z_2 z_5 , \ \ \delta_{(-1,-0)} = z_2 z_4 z_5 + z_2 z_5 z_6 , \ \ \delta_{(-1,1)} = z_2 z_4 z_5 z_6 ,$$
$$\delta_{(0,1)} = z_1 z_2 z_4 z_5 z_6 + z_2 z_3 z_4 z_5 z_6 , \ \ \delta_{(1,0)} = z_5 , \ \ \delta_{(1,1)} = 1 , \tag{10.21}$$

such that the spectral curve for Model 8b takes the following form,

$$\Sigma \ : \ (y + z_5) x + \left(\frac{1}{z_1} + \frac{1}{z_3} \right) y + (1 + z_4 y)(1 + z_6 y) \frac{z_2 z_5}{xy} + H = 0 . \tag{10.22}$$

The Hamiltonian is a sum over all 7 1-loops γ_i,

$$H = \sum_{i=1}^{7} \gamma_i , \tag{10.23}$$

where the 1-loops γ_i can be expressed in terms zig-zag paths and face paths as follows,

$$\gamma_1 = z_3^{-1} z_4^{-1} f_1 , \ \ \gamma_2 = z_3^{-1} z_4^{-1} f_1 f_5 , \ \ \gamma_3 = z_1^{-1} z_4^{-1} f_4^{-1} ,$$
$$\gamma_4 = z_1^{-1} z_5 f_1^{-1} f_6 , \ \ \gamma_5 = z_1^{-1} z_4^{-1} f_6 , \ \ \gamma_6 = z_1^{-1} z_5 f_6 , \ \ \gamma_7 = f_1 f_2^{-1} z_3^{-1} z_4^{-1} . \tag{10.24}$$

The commutation matrix C for Model 8b is given by,

$$C = \begin{pmatrix} & \gamma_1 & \gamma_2 & \gamma_3 & \gamma_4 & \gamma_5 & \gamma_6 & \gamma_7 \\ \hline \gamma_1 & 0 & 1 & 0 & -1 & -1 & -1 & -1 \\ \gamma_2 & -1 & 0 & 1 & 1 & 0 & 0 & -1 \\ \gamma_3 & 0 & -1 & 0 & 1 & 1 & 1 & 1 \\ \gamma_4 & 1 & -1 & -1 & 0 & 1 & 1 & 2 \\ \gamma_5 & 1 & 0 & -1 & -1 & 0 & 0 & 1 \\ \gamma_6 & 1 & 0 & -1 & -1 & 0 & 0 & 1 \\ \gamma_7 & 1 & 1 & -1 & -2 & -1 & -1 & 0 \end{pmatrix} . \tag{10.25}$$

The 1-loops satisfying the commutation relations can be written in terms of the canonical variables as follows,

$$\gamma_1 = e^Q z_3^{-1} z_5 \ , \ \ \gamma_2 = e^{Q+P} z_3^{-1} z_5 \ , \ \ \gamma_3 = e^{-Q} z_1^{-1} z_4^{-1} \ ,$$
$$\gamma_4 = e^{-2Q-P} z_2 z_3 \ , \ \ \gamma_5 = e^{-Q-P} z_2 z_3 \ , \ \ \gamma_6 = e^{-Q-P} z_1^{-1} z_6^{-1} \ ,$$
$$\gamma_7 = e^{-P} z_1^{-1} z_6^{-1} \ . \tag{10.26}$$

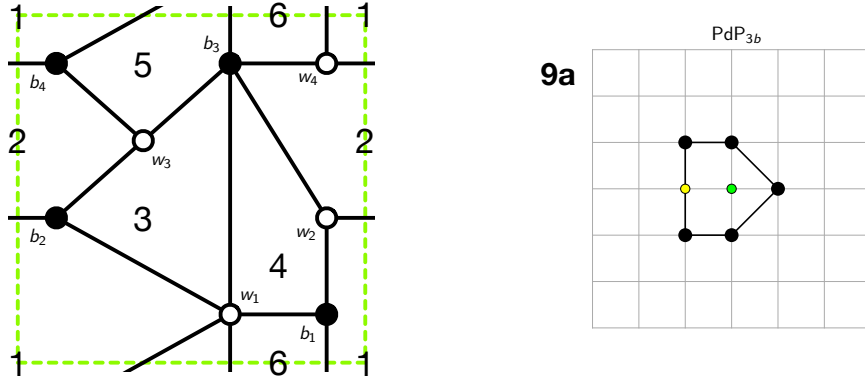# 11 Model 9: PdP$_{3b}$

11.1 Model 9a

Figure 23: The brane tiling and toric diagram of Model 9a.

The brane tiling for Model 9a can be expressed in terms of the following pair of permutation tuples

$$\sigma_B = (e_{11} \ e_{41} \ e_{21}) \ (e_{12} \ e_{32} \ e_{22}) \ (e_{13}^1 \ e_{23} \ e_{43} \ e_{13}^2 \ e_{33}) \ (e_{14} \ e_{44} \ e_{34})$$
$$\sigma_W^{-1} = (e_{11} \ e_{13}^2 \ e_{14} \ e_{12} \ e_{13}^1) \ (e_{21} \ e_{23} \ e_{22}) \ (e_{32} \ e_{34} \ e_{33}) \ (e_{41} \ e_{44} \ e_{43}) \tag{11.1}$$

which correspond to black and white nodes in the brane tiling, respectively.

The brane tiling for Model 9a has 6 zig-zag paths given by,

$$z_1 = (e_{14}^+ \ e_{44}^- \ e_{43}^+ \ e_{13}^{2,-}) \ , \quad z_2 = (e_{22}^+ \ e_{12}^- \ e_{13}^{1,+}, e_{23}^-) \ ,$$
$$z_3 = (e_{41}^+ \ e_{21}^- \ e_{23}^+ \ e_{43}^-) \ , \quad z_4 = (e_{21}^+ \ e_{11}^- \ e_{13}^{2,+}, e_{33}^- \ e_{32}^+ \ e_{22}^-) \ ,$$
$$z_5 = (e_{44}^+ \ e_{34}^- \ e_{33}^+ \ e_{13}^{1,-}, e_{11}^+ \ e_{41}^-) \ , \quad z_6 = (e_{12}^+ \ e_{32}^- \ e_{34}^+ \ e_{14}^-) \ , \tag{11.2}$$

and 6 face paths given by,

$$f_1 = (e_{44}^+ \ e_{14}^- \ e_{12}^+ \ e_{22}^- \ e_{21}^+ \ e_{41}^-) \ , \quad f_2 = (e_{22}^+ \ e_{32}^- \ e_{34}^+ \ e_{44}^- \ e_{43}^+ \ e_{23}^-) \ ,$$
$$f_3 = (e_{32}^+ \ e_{12}^- \ e_{13}^{1,+}, e_{33}^-) \ , \quad f_4 = (e_{23}^+ \ e_{13}^{1,-}, e_{11}^+ \ e_{21}^-) \ ,$$
$$f_5 = (e_{14}^+ \ e_{34}^- \ e_{33}^+ \ e_{13}^{2,-}) \ , \quad f_6 = (e_{41}^+ \ e_{11}^- \ e_{13}^{2,+}, e_{43}^-) \ , \tag{11.3}$$

satisfying the following relations,

$$f_4 f_5 = z_1 z_3 z_5 \ , \quad f_3 f_6 = z_2 z_3 z_4 \ , \quad f_2 f_4^{-1} f_6^{-1} = z_1 z_2 z_3^{-1} z_6 \ ,$$
$$f_1^{-1} f_3 f_5 = z_1 z_2 z_3 z_6^{-1} \ , \quad f_1 f_2 f_3 f_4 f_5 f_6 = 1 \ . \tag{11.4}$$

The face paths can be written in terms of the canonical variables as follows,

$$f_1 = z_2^{-1} z_5 z_6 e^{Q-P} \ , \quad f_2 = z_2 z_3^{-1} z_5^{-1} e^{-Q+P} \ , \quad f_3 = e^Q \ ,$$
$$f_4 = e^P \ , \quad f_5 = e^{-P} z_1 z_3 z_5 \ , \quad f_6 = e^{-Q} z_2 z_3 z_4 \ . \tag{11.5}$$

The Kasteleyn matrix of the brane tiling for Model 9a in Figure 23 is given by,

$$K = \begin{pmatrix} & b_1 & b_2 & b_3 & b_4 \\ \hline w_1 & e_{11} & e_{12} & e_{13}^1 + e_{13}^2 y^{-1} & e_{14} y^{-1} \\ w_2 & e_{21} & e_{22} x & e_{23} & 0 \\ w_3 & 0 & e_{32} & e_{33} & e_{34} \\ w_4 & e_{41} y & 0 & e_{43} & e_{44} x \end{pmatrix} \ . \tag{11.6}$$

By taking a permanent of the Kasteleyn matrix, we obtain the spectral curve of the dimer integrable system for Model 9a as follows,

$$0 = \operatorname{perm} K = \bar{p}_0 \cdot x \cdot \left[\delta_{(-1,-1)} \frac{1}{xy} + \delta_{(-1,0)} \frac{1}{x} + \delta_{(-1,1)} \frac{y}{x} \right.$$
$$\left. + \delta_{(0,-1)} \frac{1}{y} + \delta_{(0,1)} y + \delta_{(1,0)} x + H \right] \ , \tag{11.7}$$

where $\bar{p}_0 = e_{11}^+ e_{22}^+ e_{33}^+ e_{44}^+$. The Casimirs $\delta_{(m,n)}$ in (11.7) can be written in terms of the zig-zag paths in (11.2) as shown below,

$$\delta_{(-1,-1)} = z_1 z_4 \ , \quad \delta_{(-1,-0)} = z_1 z_3 z_4 + z_1 z_4 z_6 \ , \quad \delta_{(-1,1)} = z_1 z_3 z_4 z_6 \ ,$$
$$\delta_{(0,-1)} = z_4 \ , \quad \delta_{(0,1)} = z_5^{-1} \ , \quad \delta_{(1,0)} = 1 \ , \tag{11.8}$$

such that the spectral curve for Model 9a takes the following form,

$$\Sigma \; : \; (1 + z_3 y)(1 + z_6 y)\frac{z_1 z_4}{xy} + \frac{y}{z_5} + \frac{z_4}{y} + x + H = 0 \; . \tag{11.9}$$

The Hamiltonian is a sum over all 6 1-loops γ_i,

$$H = \sum_{i=1}^{6} \gamma_i \; , \tag{11.10}$$

where the 1-loops γ_i can be expressed in terms of zig-zag paths and face paths as follows,

$$\gamma_1 = z_2^{-1} f_2 f_3 \; , \; \gamma_2 = z_3 z_4 f_2 \; , \; \gamma_3 = z_1 z_2 z_3 z_4 f_3^{-1} \; ,$$
$$\gamma_4 = z_1 z_2 z_3 z_4 f_1 f_3^{-1} \; , \; \gamma_5 = z_1 z_2 z_3 z_4 f_1 \; , \; \gamma_6 = z_2^{-1} f_3 \; . \tag{11.11}$$

The commutation matrix C for Model 9a takes the following form,

$$C = \begin{pmatrix}
 & \gamma_1 & \gamma_2 & \gamma_3 & \gamma_4 & \gamma_5 & \gamma_6 \\
\hline
\gamma_1 & 0 & 1 & 1 & 0 & -1 & -1 \\
\gamma_2 & -1 & 0 & 1 & 1 & 0 & -1 \\
\gamma_3 & -1 & -1 & 0 & 1 & 1 & 0 \\
\gamma_4 & 0 & -1 & -1 & 0 & 1 & 1 \\
\gamma_5 & 1 & 0 & -1 & -1 & 0 & 1 \\
\gamma_6 & 1 & 1 & 0 & -1 & -1 & 0
\end{pmatrix} \; . \tag{11.12}$$

The 1-loops satisfying the commutation relations can be written in terms of the canonical variables as follows,

$$\gamma_1 = e^{P} z_3^{-1} z_5^{-1} \; , \; \gamma_2 = e^{-Q+P} z_2 z_4 z_5^{-1} \; , \; \gamma_3 = e^{-Q} z_5^{-1} z_6^{-1} \; ,$$
$$\gamma_4 = e^{-P} z_2^{-1} \; , \; \gamma_5 = e^{Q-P} z_2^{-1} \; , \; \gamma_6 = e^{Q} z_2^{-1} \; . \tag{11.13}$$
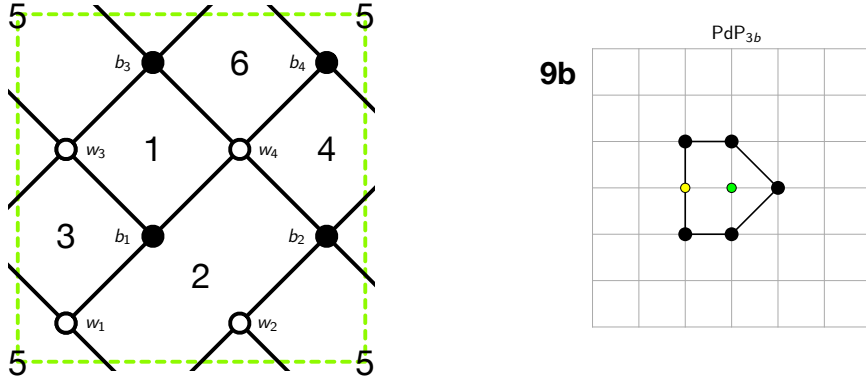
11.2   Model 9b

Figure 24: The brane tiling and toric diagram of Model 9b.

The brane tiling for Model 9b can be expressed in terms of the following pair of permutation tuples

$$\sigma_B = (e_{11}\ e_{41}\ e_{31})\ (e_{12}\ e_{32}\ e_{42}\ e_{32})\ (e_{13}\ e_{33}\ e_{43}\ e_{23})\ (e_{24}\ e_{44}\ e_{34})$$
$$\sigma_W^{-1} = (e_{11}\ e_{13}\ e_{12})\ (e_{22}\ e_{24}\ e_{23})\ (e_{31}\ e_{32}\ e_{34}\ e_{33})\ (e_{41}\ e_{43}\ e_{44}\ e_{42}) \qquad (11.14)$$

which correspond to black and white nodes in the brane tiling, respectively.

The brane tiling for Model 9b has 6 zig-zag paths given by,

$$z_1 = (e_{41}^+\ e_{31}^-\ e_{32}^+\ e_{42}^-)\ ,\ z_2 = (e_{33}^+\ e_{43}^-\ e_{44}^+\ e_{34}^-)\ ,$$
$$z_3 = (e_{43}^+\ e_{23}^-\ e_{22}^+\ e_{12}^-\ e_{11}^+\ e_{41}^-)\ ,\ z_4 = (e_{42}^+\ e_{22}^-\ e_{24}^+\ e_{44}^-)\ ,$$
$$z_5 = (e_{31}^+\ e_{11}^-\ e_{13}^+\ e_{33}^-)\ ,\ z_6 = (e_{12}^+\ e_{32}^-\ e_{34}^+\ e_{24}^-\ e_{23}^+\ e_{13}^-)\ , \qquad (11.15)$$

and 6 face paths given by,

$$f_1 = (e_{31}^+\ e_{41}^-\ e_{43}^+\ e_{33}^-)\ ,\ f_2 = (e_{41}^+\ e_{11}^-\ e_{13}^+\ e_{23}^-\ e_{22}^+\ e_{42}^-)\ ,$$
$$f_3 = (e_{11}^+\ e_{31}^-\ e_{32}^+\ e_{12}^-)\ ,\ f_4 = (e_{42}^+\ e_{32}^-\ e_{34}^+\ e_{44}^-)\ ,$$
$$f_5 = (e_{33}^+\ e_{13}^-\ e_{12}^+\ e_{22}^-\ e_{24}^+\ e_{34}^-)\ ,\ f_6 = (e_{23}^+\ e_{43}^-\ e_{44}^+\ e_{24}^-)\ , \qquad (11.16)$$

which satisfy the following relations,

$$f_4 f_5 f_6 = z_2 z_4 z_6\ ,\ f_3 f_6^{-1} = z_1 z_3 z_4\ ,\ f_2 f_4^{-2} f_5^{-1} = z_1^3 z_2^2 z_3^2 z_5^3 z_6\ ,$$
$$f_1 f_5^{-1} f_6^{-1} = z_1 z_3^2 z_4 z_5^2 z_6\ ,\ f_1 f_2 f_3 f_4 f_5 f_6 = 1\ . \qquad (11.17)$$

The face paths can be written in terms of the canonical variables as follows,

$$f_1 = e^P \ , \ \ f_2 = e^Q \ , \ \ f_3 = e^{-Q-P} z_1 z_3 z_5 \ ,$$

$$f_4 = e^{-P} z_1^{-1} z_2^{-1} \ , \ \ f_5 = e^{Q+2P} z_2 z_3^{-1} z_4 z_5^{-2} \ , \ \ f_6 = e^{-Q-P} z_4^{-1} z_5 \ . \qquad (11.18)$$

The Kasteleyn matrix of the brane tiling for Model 9b in Figure 24 is given by,

$$K = \begin{pmatrix}
 & b_1 & b_2 & b_3 & b_4 \\
\hline
w_1 & e_{11} & e_{12}x^{-1} & e_{13}y^{-1} & 0 \\
w_2 & 0 & e_{22}x & e_{23}y^{-1} & e_{24}y^{-1} \\
w_3 & e_{31} & e_{32}x^{-1} & e_{33} & e_{34}x^{-1} \\
w_4 & e_{41} & e_{42} & e_{43} & e_{44}
\end{pmatrix} \ . \qquad (11.19)$$

By taking the permanent of the Kasteleyn matrix in (11.19) with a $GL(2,\mathbb{Z})$ transformation $M : (x,y) \mapsto (\frac{1}{x}, y)$, we obtain the spectral curve of the dimer integrable system for Model 9b as follows,

$$0 = \overline{p}_0 \cdot xy^{-1} \cdot \left[\delta_{(-1,-1)} \frac{1}{xy} + \delta_{(-1,0)} \frac{1}{x} + \delta_{(-1,1)} \frac{y}{x} \right.$$

$$\left. + \delta_{(0,-1)} \frac{1}{y} + \delta_{(0,1)} y + \delta_{(1,0)} x + H \right] \ , \qquad (11.20)$$

where $\overline{p}_0 = e_{12}^+ e_{23}^+ e_{34}^+ e_{41}^+$. The Casimirs $\delta_{(m,n)}$ in (11.20) can be written in terms of the zig-zag paths in (11.15) as follows,

$$\delta_{(-1,-1)} = z_1^{-1} z_6^{-1} \ , \ \ \delta_{(-1,-0)} = z_2 z_3 z_4 + z_2 z_3 z_5 \ , \ \ \delta_{(-1,1)} = z_2 z_3 \ ,$$

$$\delta_{(0,-1)} = z_6^{-1} \ , \ \ \delta_{(0,1)} = z_3 \ , \ \ \delta_{(1,0)} = 1 \ , \qquad (11.21)$$

such that the spectral curve for Model 9b takes the following form,

$$\Sigma \ : \ (z_2 z_3 z_4 + z_2 z_3 z_5) \frac{1}{x} + \frac{1}{z_6 y} + \frac{1}{z_1 z_6 xy} + z_2 z_3 \frac{y}{x} + z_3 y + x + H = 0 \ . \qquad (11.22)$$

The Hamiltonian is a sum over all 7 1-loops γ_i,

$$H = \sum_{i=1}^{7} \gamma_i \ , \qquad (11.23)$$

where the 1-loops γ_i can be expressed in terms of zig-zag paths and face paths as follows,

$$\gamma_1 = z_2 z_4 z_5^{-1} f_1 f_5^{-1} \ , \ \ \gamma_2 = z_1^{-1} f_2 f_3 \ , \ \ \gamma_3 = z_5^{-1} z_6^{-1} f_3^{-1} \ ,$$

$$\gamma_4 = z_5^{-1} z_6^{-1} f_1 f_3^{-1} \ , \ \ \gamma_5 = z_5^{-1} z_6^{-1} f_1 \ , \ \ \gamma_6 = z_2 f_1 \ , \ \ \gamma_7 = z_2 f_1 f_3 \ . \qquad (11.24)$$

The commutation matrix C for Model 9b is given by,

$$C = \begin{pmatrix} & \gamma_1 & \gamma_2 & \gamma_3 & \gamma_4 & \gamma_5 & \gamma_6 & \gamma_7 \\ \hline \gamma_1 & 0 & 1 & 0 & -1 & -1 & -1 & -1 \\ \gamma_2 & -1 & 0 & 1 & 1 & 0 & 0 & -1 \\ \gamma_3 & 0 & -1 & 0 & 1 & 1 & 1 & 1 \\ \gamma_4 & 1 & -1 & -1 & 0 & 1 & 1 & 2 \\ \gamma_5 & 1 & 0 & -1 & -1 & 0 & 0 & 1 \\ \gamma_6 & 1 & 0 & -1 & -1 & 0 & 0 & 1 \\ \gamma_7 & 1 & 1 & -1 & -2 & -1 & -1 & 0 \end{pmatrix} , \tag{11.25}$$

where the 1-loops satisfying the commutation relations can be written in terms of the canonical variables as follows,

$$\gamma_1 = e^{-Q-P} z_3 z_5 \ , \ \ \gamma_2 = e^{-P} z_3 z_5 \ , \ \ \gamma_3 = e^{Q+P} z_2 z_4 z_5^{-1} \ ,$$

$$\gamma_4 = e^{Q+2P} z_2 z_4 z_5^{-1} \ , \ \ \gamma_5 = e^{P} z_5^{-1} z_6^{-1} \ , \ \ \gamma_6 = e^{P} z_2 \ , \ \ \gamma_7 = e^{-Q} z_4^{-1} z_6^{-1} \ . \tag{11.26}$$
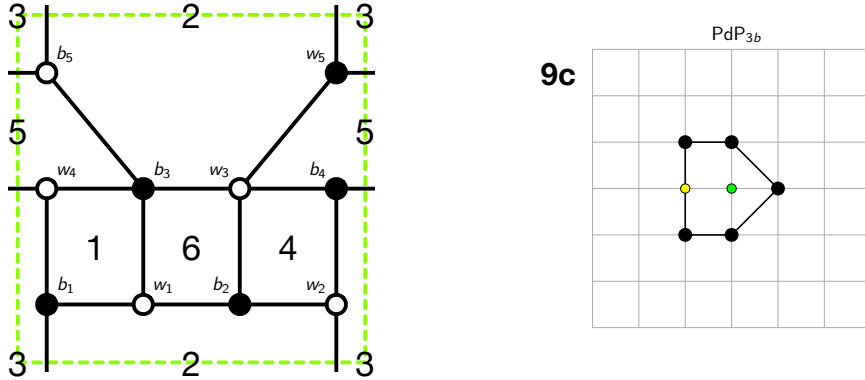
11.3 Model 9c

Figure 25: The brane tiling and toric diagram of Model 9c.

The brane tiling for Model 9c can be expressed in terms of the following pair of permutation tuples

$$\sigma_B = (e_{11} \; e_{41} \; e_{51}) \; (e_{12} \; e_{22} \; e_{32}) \; (e_{13} \; e_{33} \; e_{53} \; e_{43}) \; (e_{24} \; e_{44} \; e_{34})$$
$$(e_{25} \; e_{35} \; e_{55})$$
$$\sigma_W = (e_{11} \; e_{13} \; e_{12}) \; (e_{22} \; e_{24} \; e_{25}) \; (e_{32} \; e_{33} \; e_{35} \; e_{34}) \; (e_{41} \; e_{44} \; e_{43})$$
$$(e_{51} \; e_{53} \; e_{55}) \tag{11.27}$$

which correspond to black and white nodes in the brane tiling, respectively.

The brane tiling for Model 9c has 6 zig-zag paths given by,

$$z_1 = (e_{11}^+ \; e_{41}^- \; e_{44}^+ \; e_{34}^- \; e_{32}^+ \; e_{12}^-) \; , \quad z_2 = (e_{43}^+ \; e_{13}^- \; e_{12}^+ \; e_{22}^- \; e_{24}^+ \; e_{44}^-) \; ,$$
$$z_3 = (e_{13}^+ \; e_{33}^- \; e_{35}^+ \; e_{55}^- \; e_{51}^+ \; e_{11}^-) \; , \quad z_4 = (e_{25}^+ \; e_{35}^- \; e_{34}^+ \; e_{24}^-) \; ,$$
$$z_5 = (e_{41}^+ \; e_{51}^- \; e_{53}^+ \; e_{43}^-) \; , \quad z_6 = (e_{22}^+ \; e_{32}^- \; e_{33}^+ \; e_{53}^- \; e_{55}^+ \; e_{25}^-) \; , \tag{11.28}$$

and 6 face paths given by,

$$f_1 = (e_{41}^+ \; e_{11}^- \; e_{13}^+ \; e_{43}^-) \; , \quad f_2 = (e_{11}^+ \; e_{51}^- \; e_{53}^+ \; e_{33}^- \; e_{35}^+ \; e_{25}^- \; e_{22}^+ \; e_{12}^-) \; ,$$
$$f_3 = (e_{51}^+ \; e_{41}^- \; e_{44}^+ \; e_{24}^- \; e_{25}^+ \; e_{55}^-) \; , \quad f_4 = (e_{24}^+ \; e_{34}^- \; e_{32}^+ \; e_{22}^-) \; ,$$
$$f_5 = (e_{43}^+ \; e_{53}^- \; e_{55}^+ \; e_{35}^- \; e_{34}^+ \; e_{44}^-) \; , \quad f_6 = (e_{33}^+ \; e_{13}^- \; e_{12}^+ \; e_{32}^-) \; , \tag{11.29}$$

which satisfy the following relations,

$$f_5 f_6 = z_2 z_4 z_6 \; , \quad f_3 f_6^{-1} = z_1 z_3 z_4 \; , \quad f_1 f_4^{-1} = z_1^{-1} z_2^{-1} \; ,$$
$$f_2 f_4^2 f_5^{-1} = z_1^3 z_2^2 z_3^2 z_5^3 z_6 \; , \quad f_1 f_2 f_3 f_4 f_5 f_6 = 1 \; . \tag{11.30}$$

The face paths can be written in terms of the canonical variables as follows,

$$f_1 = e^P \; , \quad f_2 = e^{Q-2P} z_2^{-1} z_3 z_5 \; , \quad f_3 = e^{-Q} \; , \quad f_4 = e^P z_1 z_2 \; ,$$
$$f_5 = e^Q z_4 z_5^{-1} \; , \quad f_6 = e^{-Q} z_2 z_5 z_6 \; , \tag{11.31}$$

The Kasteleyn matrix of the brane tiling for Model 9b in Figure 25 is given by,

$$K = \begin{pmatrix}
 & b_1 & b_2 & b_3 & b_4 & b_5 \\
\hline
w_1 & e_{11} & e_{12} & e_{13} & 0 & 0 \\
w_2 & 0 & e_{22} & 0 & e_{24} & e_{25}y^{-1} \\
w_3 & 0 & e_{32} & e_{33} & e_{34} & e_{35} \\
w_4 & e_{41} & 0 & e_{43} & e_{44}x^{-1} & 0 \\
w_5 & e_{51}y & 0 & e_{53} & 0 & e_{55}x^{-1}
\end{pmatrix} \; . \tag{11.32}$$

By taking the permanent of the Kasteleyn matrix in (11.32) with a $GL(2, \mathbb{Z})$ transformation $M : (x, y) \mapsto (\frac{1}{x}, y)$, we obtain the spectral curve of the dimer integrable system for Model 9c as follows,

$$0 = \bar{p}_0 \cdot x \cdot \left[\delta_{(-1,-1)} \frac{1}{xy} + \delta_{(-1,0)} \frac{1}{x} + \delta_{(-1,1)} \frac{y}{x} \right.$$
$$\left. + \delta_{(0,-1)} \frac{1}{y} + \delta_{(0,1)} y + \delta_{(1,0)} x + H \right] , \tag{11.33}$$

where $\bar{p}_0 = e_{11}^+ e_{22}^+ e_{33}^+ e_{44}^+ e_{55}^+$. The Casimirs $\delta_{(m,n)}$ in (11.33) can be written in terms of the zig-zag paths in (11.28) as shown below,

$$\delta_{(-1,-1)} = z_1^{-1} z_6^{-1} , \quad \delta_{(-1,-0)} = z_2 z_3 z_4 + z_2 z_3 z_5 , \quad \delta_{(-1,1)} = z_2 z_3 ,$$
$$\delta_{(0,-1)} = z_6^{-1} , \quad \delta_{(0,1)} = z_3 , \quad \delta_{(1,0)} = 1 , \tag{11.34}$$

such that the spectral curve for Model 9c takes the following form,

$$\Sigma \; : \; (z_2 z_3 z_4 + z_2 z_3 z_5) \frac{1}{x} + \frac{1}{z_6 y} + \frac{1}{z_1 z_6 xy} + z_2 z_3 \frac{y}{x} + z_3 y + x + H = 0 . \tag{11.35}$$

The Hamiltonian is a sum over all 8 1-loops γ_i,

$$H = \sum_{i=1}^{8} \gamma_i , \tag{11.36}$$

where the 1-loops γ_i can be expressed in terms of zig-zag paths and face paths as follows,

$$\gamma_1 = z_4^{-1} z_6^{-1} f_4^{-1} , \; \gamma_2 = z_2 f_4^{-1} f_6^{-1} , \; \gamma_3 = z_1^{-1} f_6^{-1} , \; \gamma_4 = z_2 f_6^{-1} ,$$
$$\gamma_5 = z_2 f_1 f_6^{-1} , \; \gamma_6 = z_5^{-1} z_6^{-1} f_1 , \; \gamma_7 = z_2 f_1 , \; \gamma_8 = z_5^{-1} z_6^{-1} f_1 f_6 . \tag{11.37}$$

The commutation matrix C for Model 9c is given by,

$$C = \begin{pmatrix}
 & \gamma_1 & \gamma_2 & \gamma_3 & \gamma_4 & \gamma_5 & \gamma_6 & \gamma_7 & \gamma_8 \\
\hline
\gamma_1 & 0 & 1 & 1 & 1 & 1 & 0 & 0 & -1 \\
\gamma_2 & -1 & 0 & 1 & 1 & 2 & 1 & 1 & 0 \\
\gamma_3 & -1 & -1 & 0 & 0 & 1 & 1 & 1 & 1 \\
\gamma_4 & -1 & -1 & 0 & 0 & 1 & 1 & 1 & 1 \\
\gamma_5 & -1 & -2 & -1 & -1 & 0 & 1 & 1 & 2 \\
\gamma_6 & 0 & -1 & -1 & -1 & -1 & 0 & 0 & 1 \\
\gamma_7 & 0 & -1 & -1 & -1 & -1 & 0 & 0 & 1 \\
\gamma_8 & 1 & 0 & -1 & -1 & -2 & -1 & -1 & 0
\end{pmatrix} . \tag{11.38}$$

The 1-loops satisfying the commutation relations can be written in terms of the canonical variables as follows,

$$\gamma_1 = e^{-P} z_3 z_5 \ , \ \ \gamma_2 = e^{Q-P} z_3 z_4 \ , \ \ \gamma_3 = e^Q z_3 z_4 \ , \ \ \gamma_4 = e^Q z_1 z_2 z_3 z_4 \ ,$$
$$\gamma_5 = e^{Q+P} z_1 z_2 z_3 z_4 \ , \ \ \gamma_6 = e^P z_5^{-1} z_6^{-1} \ , \ \ \gamma_7 = e^P z_2 \ , \ \ \gamma_8 = e^{-Q+P} z_2 \ . \tag{11.39}$$

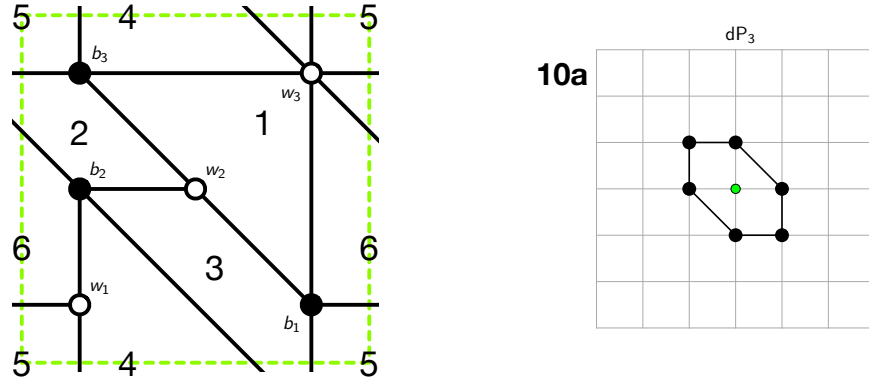## 12 Model 10: dP$_3$

12.1 Model 10a

Figure 26: The brane tiling and toric diagram of Model 10a.

The brane tiling for Model 10a can be expressed in terms of the following pair of permutation tuples

$$\sigma_B = (e_{11} \ e_{31}^2 \ e_{21} \ e_{31}^1) \ (e_{12} \ e_{32}^2 \ e_{22} \ e_{32}^1) \ (e_{13} \ e_{33}^2 \ e_{23} \ e_{33}^1) \ ,$$
$$\sigma_W^{-1} = (e_{11} \ e_{12} \ e_{13}) \ (e_{21} \ e_{22} \ e_{23}) \ (e_{31}^1 \ e_{33}^2 \ e_{32}^1 \ e_{31}^2 \ e_{33}^1 \ e_{32}^2) \ , \tag{12.1}$$

which correspond to black and white nodes in the brane tiling, respectively.

The brane tiling for Model 10a has 6 zig-zag paths given by,

$$z_1 = (e_{31}^{2,+}, e_{21}^- \ e_{22}^+ \ e_{32}^{1,-}) \ , \ \ z_2 = (e_{23}^+ \ e_{33}^{1,-}, e_{32}^{2,+}, e_{22}^-) \ ,$$
$$z_3 = (e_{21}^+ \ e_{31}^{1,-}, e_{33}^{2,+}, e_{23}^-) \ , \ \ z_4 = (e_{31}^{1,+}, e_{11}^- \ e_{12}^+ \ e_{32}^{2,-}) \ ,$$
$$z_5 = (e_{33}^{1,+}, e_{13}^- \ e_{11}^+ \ e_{31}^{2,-}) \ , \ \ z_6 = (e_{32}^{1,+}, e_{12}^- \ e_{13}^+ \ e_{33}^{2,-}) \ , \tag{12.2}$$

and 6 face paths given by,

$$f_1 = (e_{21}^{1,+}, e_{31}^{2,-}, e_{33}^{1,+}, e_{23}^{1,-}) \ , \ f_2 = (e_{23}^{1,+}, e_{33}^{2,-}, e_{32}^{1,+}, e_{22}^{1,-}) \ ,$$
$$f_3 = (e_{22}^{1,+}, e_{32}^{2,-}, e_{31}^{1,+}, e_{21}^{1,-}) \ , \ f_4 = (e_{32}^{2,+}, e_{12}^{1,-}, e_{13}^{1,+}, e_{33}^{1,-}) \ ,$$
$$f_5 = (e_{33}^{2,+}, e_{13}^{1,-}, e_{11}^{1,+}, e_{31}^{1,-}) \ , \ f_6 = (e_{31}^{2,+}, e_{11}^{1,-}, e_{12}^{1,+}, e_{32}^{1,-}) \ , \tag{12.3}$$

which satisfy the following relations,

$$f_4 f_5 f_6 = z_1 z_2 z_3 \ , \ f_3 f_6 = z_1 z_4 \ , \ f_2 f_5^{-1} f_6^{-1} = z_2 z_4 z_5 z_6^2 \ ,$$
$$f_1 f_5 = z_3 z_5 \ , \ f_1 f_2 f_3 f_4 f_5 f_6 = 1 \ . \tag{12.4}$$

The face paths can be written in terms of the canonical variables as shown below,

$$f_1 = e^P, \ f_2 = e^Q, \ f_3 = z_4 z_5 z_6 e^{-Q-P}, \ f_4 = z_2 z_6 e^{-Q},$$
$$f_5 = z_3 z_5 e^{-P}, \ f_6 = z_1 z_5^{-1} z_6^{-1} e^{Q+P} \ . \tag{12.5}$$

The Kasteleyn matrix of the brane tiling for Model 10a in Figure 26 is given by,

$$K = \begin{pmatrix} e_{11} x^{-1} & e_{12} & e_{13} y^{-1} \\ e_{21} & e_{22} & e_{23} \\ e_{31}^1 y + e_{31}^2 & e_{32}^1 x + e_{32}^2 y & e_{33}^1 + e_{33}^2 x \end{pmatrix} \ . \tag{12.6}$$

By taking the permanent of the Kasteleyn matrix in (12.6), we obtain the spectral curve of the dimer integrable system for Model 10a as shown below,

$$0 = \text{perm } K = \bar{p}_0 \cdot \left[\delta_{(1,-1)} \frac{x}{y} + \delta_{(0,-1)} \frac{1}{y} + \delta_{(1,0)} x + \delta_{(-1,0)} \frac{1}{x} + \delta_{(-1,1)} \frac{y}{x} + \delta_{(0,1)} y + H \right] \ , \tag{12.7}$$

where $\bar{p}_0 = e_{12} e_{21} e_{33}^2$.

The Casimirs $\delta_{(m,n)}$ in (12.7) can be written in terms of the zig-zag paths in (12.2) as follows,

$$\delta_{(1,0)} = 1 \ , \ \delta_{(-1,0)} = z_1 z_5 z_6 \ , \ \delta_{(0,1)} = z_3^{-1} \ ,$$
$$\delta_{(0,-1)} = z_1 z_6 \ , \ \delta_{(1,-1)} = z_6 \ , \ \delta_{(-1,1)} = z_1 z_2 z_5 z_6 \ . \tag{12.8}$$

Accordingly, we can express the spectral curve for Model 10a in the following form,

$$\Sigma \ : \ z_6 \frac{x}{y} + z_1 z_6 \frac{1}{y} + x + z_1 z_5 z_6 \frac{1}{x} + z_1 z_2 z_5 z_6 \frac{y}{x} + z_3^{-1} y + H = 0 \ . \tag{12.9}$$

The Hamiltonian is a sum over all 6 1-loops γ_i,

$$H = \gamma_1 + \gamma_2 + \gamma_3 + \gamma_4 + \gamma_5 + \gamma_6 \ , \tag{12.10}$$

where the 1-loops γ_i can be expressed in terms of zig-zag paths and face paths as follows,

$$\gamma_1 = z_5 z_6 f_1^{-1} \ , \ \ \gamma_2 = z_5 z_6 f_1^{-1} f_6 \ , \ \ \gamma_3 = z_5 z_6 f_6 \ ,$$
$$\gamma_4 = z_1 z_2 z_6 f_1 \ , \ \ \gamma_5 = z_1 z_2 z_6 f_1 f_3 \ , \ \ \gamma_6 = z_4^{-1} f_3 \ . \tag{12.11}$$

The commutation matrix for Model 10a is given by,

$$
C = \left(
\begin{array}{c|cccccc}
 & \gamma_1 & \gamma_2 & \gamma_3 & \gamma_4 & \gamma_5 & \gamma_6 \\
\hline
\gamma_1 & 0 & 1 & 1 & 0 & -1 & -1 \\
\gamma_2 & -1 & 0 & 1 & 1 & 0 & -1 \\
\gamma_3 & -1 & -1 & 0 & 1 & 1 & 0 \\
\gamma_4 & 0 & -1 & -1 & 0 & 1 & 1 \\
\gamma_5 & 1 & 0 & -1 & -1 & 0 & 1 \\
\gamma_6 & 1 & 1 & 0 & -1 & -1 & 0
\end{array}
\right) \ . \tag{12.12}
$$

The 1-loops satisfying the commutation relations can be written in terms of the canonical variables as shown below,

$$\gamma_1 = z_5 z_6 e^{-P} \ , \ \ \gamma_2 = z_1 e^{Q} \ , \ \ \gamma_3 = z_1 e^{Q+P} \ ,$$
$$\gamma_4 = z_1 z_2 z_6 e^{P} \ , \ \ \gamma_5 = z_3^{-1} z_6 e^{-Q} \ , \ \ \gamma_6 = z_5 z_6 e^{-Q-P} \ . \tag{12.13}$$
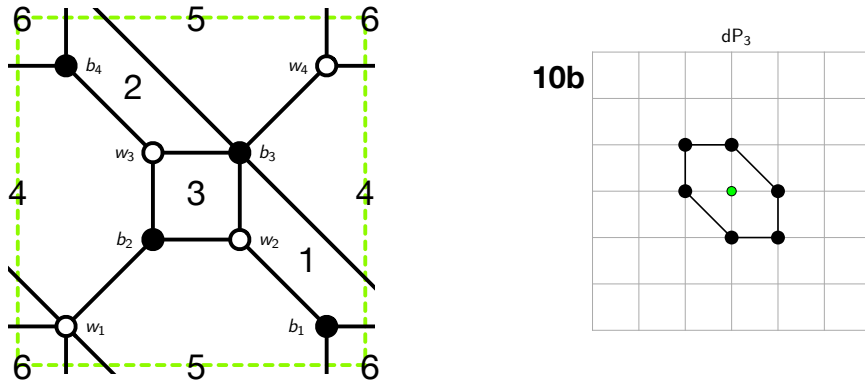
12.2 Model 10b

Figure 27: The brane tiling and toric diagram of Model 10b.

The brane tiling for Model 10b can be expressed in terms of the following pair of permutation tuples

$$\sigma_B = (e_{11}\ e_{21}\ e_{41})\ (e_{12}\ e_{22}\ e_{32})\ (e_{23}\ e_{13}^1\ e_{43}\ e_{13}^2\ e_{33})\ (e_{14}\ e_{44}\ e_{34})\ ,$$
$$\sigma_W^{-1} = (e_{11}\ e_{13}^2\ e_{12}\ e_{13}^1\ e_{14})\ (e_{21}\ e_{22}\ e_{23})\ (e_{32}\ e_{34}\ e_{33})\ (e_{41}\ e_{44}\ e_{43})\ ,\qquad (12.14)$$

which correspond to black and white nodes in the brane tiling, respectively.

The brane tiling for Model 10b has 6 zig-zag paths given by,

$$z_1 = (e_{23}^+\ e_{13}^{2,-}, e_{12}^+\ e_{22}^-)\ ,\quad z_2 = (e_{11}^+\ e_{21}^-\ e_{22}^+\ e_{32}^-\ e_{34}^+\ e_{14}^-)\ ,$$
$$z_3 = (e_{13}^{1,+}, e_{33}^-\ e_{32}^+\ e_{12}^-)\ ,\quad z_4 = (e_{21}^+\ e_{41}^-\ e_{44}^+\ e_{34}^-\ e_{33}^+\ e_{23}^-)\ ,$$
$$z_5 = (e_{14}^+\ e_{44}^-\ e_{43}^+\ e_{13}^{1,-})\ ,\quad z_6 = (e_{13}^{2,+}, e_{43}^-\ e_{41}^+\ e_{11}^-)\ ,\qquad (12.15)$$

and 6 face paths given by,

$$f_1 = (e_{13}^{2,+}, e_{23}^-\ e_{21}^+\ e_{11}^-)\ ,\quad f_2 = (e_{33}^+\ e_{13}^{1,-}, e_{14}^+\ e_{34}^-)\ ,$$
$$f_3 = (e_{23}^+\ e_{33}^-\ e_{32}^+\ e_{22}^-)\ ,\quad f_4 = (e_{34}^+\ e_{44}^-\ e_{43}^+\ e_{13}^{2,-}, e_{12}^+\ e_{32}^-)\ ,$$
$$f_5 = (e_{13}^{1,+}, e_{43}^-\ e_{41}^+\ e_{21}^-\ e_{22}^+\ e_{12}^-)\ ,\quad f_6 = (e_{11}^+\ e_{41}^-\ e_{44}^+\ e_{14}^-)\ .\qquad (12.16)$$

which satisfy the following constraints,

$$f_1 f_2 f_3 f_4 f_5 f_6 = 1\ ,\quad f_3 f_6^{-1} = z_1 z_3 z_5 z_6\ ,\quad f_2 f_5^{-1} f_6^{-1} = z_1 z_4 z_5^2 z_6\ ,$$
$$f_1 f_4^{-1} f_6^{-1} = z_3 z_4 z_5 z_6^2\ ,\quad f_4 f_5 f_6^2 = z_1 z_2^2 z_3 z_4\ .\qquad (12.17)$$

The face paths can be written in terms of the canonical variables as follows,

$$f_1 = z_4 z_5 z_6 e^P,\ \ f_2 = e^{-P},\ \ f_3 = e^Q,\ \ f_4 = z_1 z_5 e^{-Q+P},$$
$$f_5 = z_3 z_4^{-1} z_5^{-1} e^{-Q-P},\ \ f_6 = z_2 z_4 e^Q\qquad (12.18)$$

The Kasteleyn matrix of the brane tiling for Model 10b in Figure 27 is given by,

$$K = \begin{pmatrix} e_{11}x^{-1} & e_{12} & e_{13}^1 y^{-1} + e_{13}^2 x^{-1} & e_{14}y^{-1} \\ e_{21} & e_{22} & e_{23} & 0 \\ 0 & e_{32} & e_{33} & e_{34} \\ e_{41}y & 0 & e_{43} & e_{44}x \end{pmatrix}\ .\qquad (12.19)$$

The permanent of the Kasteleyn matrix gives the spectral curve of the dimer integrable system for Model 10b as follows,

$$0 = \operatorname{perm} K = \bar{p}_0 \cdot \left[\delta_{(1,-1)}\frac{x}{y} + \delta_{(0,-1)}\frac{1}{y} + \delta_{(1,0)}x + \delta_{(-1,0)}\frac{1}{x} + \delta_{(-1,1)}\frac{y}{x} + \delta_{(0,1)}y + H \right]\ ,$$
$$(12.20)$$

where $\bar{p}_0 = e_{12}e_{21}e_{33}e_{44}$. The Casimirs $\delta_{(m,n)}$ in (12.20) can be written in terms of the zig-zag paths in (12.15) as shown below,

$$\delta_{(1,0)} = 1 \ , \ \delta_{(-1,0)} = z_2 z_3 z_5 \ , \ \delta_{(0,1)} = z_4^{-1} \ ,$$
$$\delta_{(0,-1)} = z_3 z_5 \ , \ \delta_{(1,-1)} = z_3 \ , \ \delta_{(-1,1)} = z_2 z_3 z_5 z_6 \ , \tag{12.21}$$

such that the spectral curve for Model 10b takes the following form,

$$\Sigma \ : \ z_3 \frac{x}{y} + z_3 z_5 \frac{1}{y} + x + z_2 z_3 z_5 \frac{1}{x} + z_2 z_3 z_5 z_6 \frac{y}{x} + z_4^{-1} y + H = 0 \ . \tag{12.22}$$

The Hamiltonian is a sum over all 7 1-loops γ_i,

$$H = \gamma_1 + \gamma_2 + \gamma_3 + \gamma_4 + \gamma_5 + \gamma_6 + \gamma_7 \ , \tag{12.23}$$

where the 1-loops γ_i can be expressed in terms of zig-zag paths and face paths as follows,

$$\gamma_1 = z_5 f_1 f_3 f_5 f_6 \ , \ \gamma_2 = z_1 z_2 z_3 z_5 f_1 \ , \ \gamma_3 = z_3 z_4^{-2} z_5^{-1} z_6^{-1} f_1 f_2 f_3^{-1} \ ,$$
$$\gamma_4 = z_3 z_4^{-1} f_2 f_3^{-1} \ , \ \gamma_5 = z_5 f_3 f_5 \ , \ \gamma_6 = z_2 z_3 f_2 \ , \ \gamma_7 = z_5 f_3 f_5 f_6 \ , \tag{12.24}$$

The commutation matrix for Model 10b is given by,

$$C = \begin{pmatrix}
 & \gamma_1 & \gamma_2 & \gamma_3 & \gamma_4 & \gamma_5 & \gamma_6 & \gamma_7 \\
\hline
\gamma_1 & 0 & 1 & 0 & -1 & -1 & -1 & -1 \\
\gamma_2 & -1 & 0 & 1 & 1 & 0 & 0 & -1 \\
\gamma_3 & 0 & -1 & 0 & 1 & 1 & 1 & 1 \\
\gamma_4 & 1 & -1 & -1 & 0 & 1 & 1 & 2 \\
\gamma_5 & 1 & 0 & -1 & -1 & 0 & 0 & 1 \\
\gamma_6 & 1 & 0 & -1 & -1 & 0 & 0 & 1 \\
\gamma_7 & 1 & 1 & -1 & -2 & -1 & -1 & 0
\end{pmatrix} \ , \tag{12.25}$$

where the 1-loops satisfying the commutation relations can be written in terms of the canonical variables as follows,

$$\gamma_1 = z_1^{-1} e^Q \ , \ \gamma_2 = z_5 e^P \ , \ \gamma_3 = z_3 z_4^{-1} e^{-Q} \ ,$$
$$\gamma_4 = z_3 z_4^{-1} e^{-Q-P} \ , \ \gamma_5 = z_3 z_4^{-1} e^{-P} \ , \ \gamma_6 = z_2 z_3 e^{-P} \ , \ \gamma_7 = z_2 z_3 e^{Q-P} \ , \tag{12.26}$$
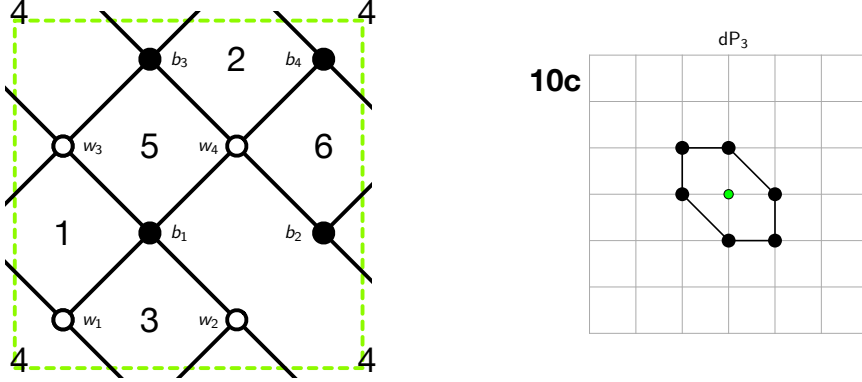
12.3 Model 10c

Figure 28: The brane tiling and toric diagram of Model 10c.

The brane tiling for Model 10c can be expressed in terms of the following pair of permutation tuples

$$\sigma_B = (e_{11} \ e_{21} \ e_{41} \ e_{31}) \ (e_{12} \ e_{32} \ e_{42}) \ (e_{13} \ e_{33} \ e_{43} \ e_{23}) \ (e_{24} \ e_{44} \ e_{34})$$
$$\sigma_W^{-1} = (e_{11} \ e_{13} \ e_{12}) \ (e_{21} \ e_{24} \ e_{23}) \ (e_{31} \ e_{32} \ e_{34} \ e_{33}) \ (e_{41} \ e_{43} \ e_{44} \ e_{42}) \ , \qquad (12.27)$$

which correspond to black and white nodes in the brane tiling, respectively.

The brane tiling for Model 10c has 6 zig-zag paths given by,

$$z_1 = (e_{31}^+ \ e_{11}^- \ e_{13}^+ \ e_{33}^-) \ , \quad z_2 = (e_{12}^+ \ e_{32}^- \ e_{34}^+ \ e_{24}^- \ e_{23}^+ \ e_{13}^-) \ ,$$
$$z_3 = (e_{43}^+ \ e_{23}^- \ e_{21}^+ \ e_{41}^-) \ , \quad z_4 = (e_{11}^+ \ e_{21}^- \ e_{24}^+ \ e_{44}^- \ e_{42}^+ \ e_{12}^-) \ ,$$
$$z_5 = (e_{32}^+ \ e_{42}^- \ e_{41}^+ \ e_{31}^-) \ , \quad z_6 = (e_{44}^+ \ e_{34}^- \ e_{33}^+ \ e_{43}^-) \ , \qquad (12.28)$$

and 6 face paths given by,

$$f_1 = (e_{11}^+ \ e_{31}^- \ e_{32}^+ \ e_{12}^-) \ , \quad f_2 = (e_{23}^+ \ e_{43}^- \ e_{44}^+ \ e_{24}^-) \ ,$$
$$f_3 = (e_{21}^+ \ e_{11}^- \ e_{13}^+ \ e_{23}^-) \ , \quad f_4 = (e_{12}^+ \ e_{42}^- \ e_{41}^+ \ e_{21}^- \ e_{24}^+ \ e_{34}^- \ e_{33}^+ \ e_{13}^-) \ ,$$
$$f_5 = (e_{31}^+ \ e_{41}^- \ e_{43}^+ \ e_{33}^-) \ , \quad f_6 = (e_{34}^+ \ e_{44}^- \ e_{42}^+ \ e_{32}^-) \ . \qquad (12.29)$$

which satisfy the following relations,

$$f_5 f_6 = z_1 z_2 z_3 z_4 \ , \quad f_3 f_6^{-1} = z_1 z_3 z_5 z_6 \ , \quad f_1 f_2^{-1} = z_3 z_4 z_5 \ ,$$
$$f_2^2 f_4 f_5^{-1} = z_2 z_3^{-1} z_5 z_6^2 \ , \quad f_1 f_2 f_3 f_4 f_5 f_6 = 1 \qquad (12.30)$$

The face paths can be written in terms of the canonical variables as shown below,

$$f_1 = e^P \ , \ f_2 = e^P z_1 z_2 z_6 \ , \ f_3 = e^{-Q} z_1 z_3 \ ,$$
$$f_4 = e^{Q-2P} z_1^{-1} z_4 z_5^2 z_6 \ , \ f_5 = e^Q \ , \ f_6 = e^{-Q} z_1 z_2 z_3 z_4 \ , \tag{12.31}$$

The Kasteleyn matrix of the brane tiling for Model 10c in Figure 28 is given by,

$$K = \begin{pmatrix} & b_1 & b_2 & b_3 & b_4 \\ \hline w_1 & e_{11} & e_{12}x^{-1} & e_{13}y^{-1} & 0 \\ w_2 & e_{21} & 0 & e_{23}y^{-1} & e_{24}y^{-1} \\ w_3 & e_{31} & e_{32}x^{-1} & e_{33} & e_{34}x^{-1} \\ w_4 & e_{41} & e_{42} & e_{43} & e_{44} \end{pmatrix} . \tag{12.32}$$

By taking the permanent of the Kasteleyn matrix, we obtain the spectral curve of the dimer integrable system for Model 10c as follows,

$$0 = \text{perm } K = \bar{p}_0 \cdot x^{-1} y^{-1} \cdot \left[\delta_{(-1,0)} \frac{1}{x} + \delta_{(-1,1)} \frac{y}{x} + \delta_{(0,-1)} \frac{1}{y} + \delta_{(0,1)} y \right.$$
$$\left. + \delta_{(1,-1)} \frac{x}{y} + \delta_{(1,0)} x + H \right] , \tag{12.33}$$

where $\bar{p}_0 = e_{11}^+ e_{24}^+ e_{33}^+ e_{42}^+$. The Casimirs $\delta_{(m,n)}$ in (12.33) can be written in terms of the zig-zag paths in (12.28) as shown below,

$$\delta_{(-1,0)} = z_1 z_2 z_5 \ , \ \delta_{(-1,1)} = z_1 z_2 z_3 z_5 \ , \ \delta_{(0,-1)} = z_1 z_5 \ ,$$
$$\delta_{(0,1)} = z_1 z_2 z_3 z_5 z_6 \ , \ \delta_{(1,-1)} = z_1 \ , \ \delta_{(1,0)} = 1 \ , \tag{12.34}$$

allows us to express the spectral curve for Model 10c in the following form,

$$\Sigma \ : \ \left(1 + \frac{z_1}{y} \right) x + \frac{y}{z_4} + \frac{z_1 z_5}{y} + (1 + z_3 y) \frac{z_1 z_2 z_5}{x} + H = 0 \ . \tag{12.35}$$

The Hamiltonian is a sum over all 8 1-loops γ_i,

$$H = \gamma_1 + \gamma_2 + \gamma_3 + \gamma_4 + \gamma_5 + \gamma_6 + \gamma_7 + \gamma_8 \ , \tag{12.36}$$

where the 1-loops γ_i can be written in terms of zig-zag paths and face paths as follows,

$$\gamma_1 = z_1 z_2 f_1 f_3 f_4 \ , \ \gamma_2 = z_1 z_3 z_5 f_2 f_4 f_5 f_6 \ , \ \gamma_3 = z_5 f_5 \ , \ \gamma_4 = z_1 z_2 z_5 z_6 f_5 \ ,$$
$$\gamma_5 = z_1 z_2 z_5 z_6 f_1 f_5 \ , \ \gamma_6 = z_1 z_4^{-1} f_1 \ , \ \gamma_7 = z_1 z_2 f_1 \ , \ \gamma_8 = z_1 z_4^{-1} f_1 f_6 \ , \tag{12.37}$$

The commutation matrix C for Model 10c is given by,

$$
C = \begin{pmatrix}
 & \gamma_1 & \gamma_2 & \gamma_3 & \gamma_4 & \gamma_5 & \gamma_6 & \gamma_7 & \gamma_8 \\
\hline
\gamma_1 & 0 & 1 & 1 & 1 & 1 & 0 & 0 & -1 \\
\gamma_2 & -1 & 0 & 1 & 1 & 2 & 1 & 1 & 0 \\
\gamma_3 & -1 & -1 & 0 & 0 & 1 & 1 & 1 & 1 \\
\gamma_4 & -1 & -1 & 0 & 0 & 1 & 1 & 1 & 1 \\
\gamma_5 & -1 & -2 & -1 & -1 & 0 & 1 & 1 & 2 \\
\gamma_6 & 0 & -1 & -1 & -1 & -1 & 0 & 0 & 1 \\
\gamma_7 & 0 & -1 & -1 & -1 & -1 & 0 & 0 & 1 \\
\gamma_7 & 1 & 0 & -1 & -1 & -2 & -1 & -1 & 0
\end{pmatrix} . \tag{12.38}
$$

The 1-loops satisfying the commutation relations can be written in terms of the canonical variables as follows,

$$
\gamma_1 = e^{-P} z_5 \ , \ \ \gamma_2 = e^{Q-P} z_5 \ , \ \ \gamma_3 = e^Q z_5 \ , \ \ \gamma_4 = e^Q z_3^{-1} z_4^{-1} \ ,
$$
$$
\gamma_5 = e^{Q+P} z_3^{-1} z_4^{-1} \ , \ \ \gamma_6 = e^P z_1 z_4^{-1} \ , \ \ \gamma_7 = e^P z_1 z_2 \ , \ \ \gamma_8 = e^{-Q+P} z_1^2 z_2 z_3 \ , \tag{12.39}
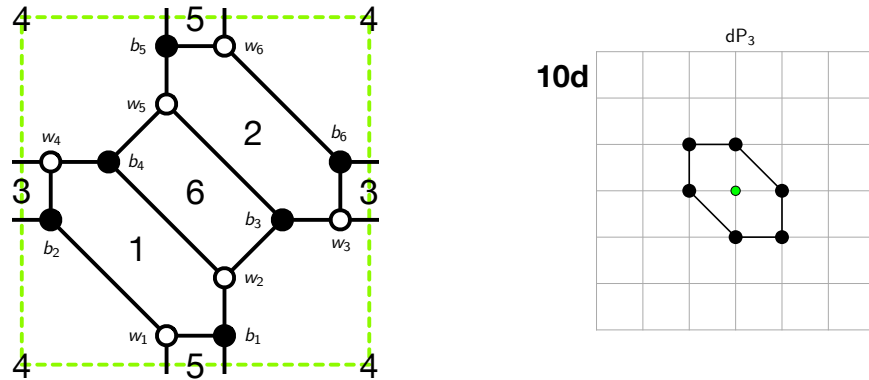$$

12.4 Model 10d

Figure 29: The brane tiling and toric diagram of Model 10d.

The brane tiling for Model 10d can be expressed in terms of the following pair of permutation tuples

$$
\begin{aligned}
\sigma_B =\ & (e_{11}\ e_{61}\ e_{21})\ (e_{12}\ e_{42}\ e_{32})\ (e_{23}\ e_{33}\ e_{53})\ (e_{24}\ e_{54}\ e_{44}) \\
& (e_{15}\ e_{55}\ e_{65})\ (e_{36}\ e_{46}\ e_{66}) \\
\sigma_W^{-1} =\ & (e_{11}\ e_{15}\ e_{12})\ (e_{21}\ e_{24}\ e_{23})\ (e_{32}\ e_{33}\ e_{36})\ (e_{42}\ e_{46}\ e_{44}) \\
& (e_{53}\ e_{54}\ e_{55})\ (e_{61}\ e_{66}\ e_{65})
\end{aligned}
\tag{12.40}
$$

which correspond to black and white nodes in the brane tiling, respectively.

The brane tiling for Model 10d has 6 zig-zag paths given by,

$$
\begin{aligned}
z_1 &= (e_{12}^+\ e_{42}^-\ e_{46}^+\ e_{66}^-\ e_{65}^+\ e_{15}^-)\ , \quad z_2 = (e_{21}^+\ e_{11}^-\ e_{15}^+\ e_{55}^-\ e_{53}^+\ e_{23}^-)\ , \\
z_3 &= (e_{44}^+\ e_{24}^-\ e_{23}^+\ e_{33}^-\ e_{36}^+\ e_{46}^-)\ , \quad z_4 = (e_{11}^+\ e_{61}^-\ e_{66}^+\ e_{36}^-\ e_{32}^+\ e_{12}^-)\ , \\
z_5 &= (e_{24}^+\ e_{54}^-\ e_{55}^+\ e_{65}^-\ e_{61}^+\ e_{21}^-)\ , \quad z_6 = (e_{42}^+\ e_{32}^-\ e_{33}^+\ e_{53}^-\ e_{54}^+\ e_{44}^-)\ ,
\end{aligned}
\tag{12.41}
$$

and 6 face paths given by,

$$
\begin{aligned}
f_1 &= (e_{42}^+\ e_{12}^-\ e_{11}^+\ e_{21}^-\ e_{24}^+\ e_{44}^-)\ , \quad f_2 = (e_{36}^+\ e_{66}^-\ e_{65}^+\ e_{55}^-\ e_{53}^+\ e_{33}^-)\ , \\
f_3 &= (e_{32}^+\ e_{42}^-\ e_{46}^+\ e_{36}^-)\ , \quad f_4 = (e_{44}^+\ e_{54}^-\ e_{55}^+\ e_{15}^-\ e_{12}^+\ e_{32}^-\ e_{33}^+\ e_{23}^-\ e_{21}^+\ e_{61}^-\ e_{66}^+\ e_{46}^-)\ , \\
f_5 &= (e_{15}^+\ e_{65}^-\ e_{61}^+\ e_{11}^-)\ , \quad f_6 = (e_{23}^+\ e_{53}^-\ e_{54}^+\ e_{24}^-)\ .
\end{aligned}
\tag{12.42}
$$

which satisfy the following relations,

$$
\begin{aligned}
f_1^{-1} f_2 &= z_1 z_2 z_3\ , \quad f_3 f_5^{-1} = z_1 z_4\ , \quad f_5^{-1} f_6 = z_2^{-1} z_5^{-1}\ , \\
f_1^2 f_4 f_5^3 &= z_1^{-1} z_2 z_5^2 z_6\ , \quad f_1 f_2 f_3 f_4 f_5 f_6 = 1\ .
\end{aligned}
\tag{12.43}
$$

The face paths can be written in terms of the canonical variables as follows,

$$
\begin{aligned}
f_1 &= e^P\ , \quad f_2 = e^P z_1 z_2 z_3\ , \quad f_3 = e^Q z_1 z_4\ , \\
f_4 &= e^{-3Q-2P} z_1^{-1} z_2 z_5^2 z_6\ , \quad f_5 = e^Q\ , \quad f_6 = e^Q z_2^{-1} z_5^{-1}\ ,
\end{aligned}
\tag{12.44}
$$

The Kasteleyn matrix of the brane tiling for Model 10d in Figure 29 is given by,

$$
K = \begin{pmatrix}
e_{11} & e_{12} & 0 & 0 & e_{15}y^{-1} & 0 \\
e_{21} & 0 & e_{23} & e_{24} & 0 & 0 \\
0 & e_{32}x & e_{33} & 0 & 0 & e_{36} \\
0 & e_{42} & 0 & e_{44} & 0 & e_{46}x^{-1} \\
0 & 0 & e_{53} & e_{54} & e_{55} & 0 \\
e_{61}y & 0 & 0 & 0 & e_{65} & e_{66}
\end{pmatrix}\ .
\tag{12.45}
$$

By taking the permanent of the Kasteleyn matrix in (12.45), we obtain the spectral curve of the dimer integrable system for Model 10d as shown below,

$$0 = \text{perm } K = \bar{p}_0 \cdot \left[\delta_{(-1,0)} \frac{1}{x} + \delta_{(-1,1)} \frac{y}{x} + \delta_{(0,-1)} \frac{1}{y} + \delta_{(0,1)} y \right.$$

$$\left. + \delta_{(1,-1)} \frac{x}{y} + \delta_{(1,0)} x + H \right] , \tag{12.46}$$

where $\bar{p}_0 = e_{11}^+ e_{23}^+ e_{32}^+ e_{44}^+ e_{55}^+ e_{66}^+$. The Casimirs $\delta_{(m,n)}$ in (12.46) can be expressed in terms of the zig-zag paths in (12.41) as follows,

$$\delta_{(-1,0)} = z_1 z_2 z_6 , \quad \delta_{(-1,1)} = z_1 z_2 z_5 z_6 , \quad \delta_{(0,-1)} = z_2 z_6 ,$$

$$\delta_{(0,1)} = z_4^{-1} , \quad \delta_{(1,-1)} = z_2 , \quad \delta_{(1,0)} = 1 , \tag{12.47}$$

such that the spectral curve for Model 10d takes the following form,

$$\Sigma \; : \; \left(1 + \frac{z_2}{y} \right) x + \frac{y}{z_4} + \frac{z_2 z_6}{y} + (1 + z_5 y) \frac{z_1 z_2 z_6}{x} + H = 0 . \tag{12.48}$$

The Hamiltonian is a sum over all 11 1-loops γ_i,

$$H = \sum_{i=1}^{11} \gamma_i , \tag{12.49}$$

where the 1-loops γ_i's can be expressed in terms of zig-zag paths and face paths as follows,

$$\gamma_1 = z_3^{-1} f_1^{-1} f_3^{-1} , \quad \gamma_2 = z_3^{-1} f_3^{-1} , \quad \gamma_3 = z_2 z_4^{-1} f_1 ,$$

$$\gamma_4 = z_2 z_4^{-1} f_1 f_3 , \quad \gamma_5 = z_2 z_3 z_4^{-1} z_6 f_1 f_3 , \quad \gamma_6 = z_1 z_2 f_1 f_5 f_6 ,$$

$$\gamma_7 = z_1 z_2 f_3^{-1} , \quad \gamma_8 = z_1 z_2 f_1 f_3^{-1} , \quad \gamma_9 = z_1 z_2 f_1 ,$$

$$\gamma_{10} = z_1 z_2 z_3 z_6 f_1 , \quad \gamma_{11} = z_1 z_2 z_3 z_6 f_1 f_3 . \tag{12.50}$$

The commutation matrix C for Model 10d is given by,

$$C = \begin{pmatrix}
 & \gamma_1 & \gamma_2 & \gamma_3 & \gamma_4 & \gamma_5 & \gamma_6 & \gamma_7 & \gamma_8 & \gamma_9 & \gamma_{10} & \gamma_{11} \\
\hline
\gamma_1 & 0 & -1 & -1 & 0 & 0 & 1 & -1 & -2 & -1 & -1 & 0 \\
\gamma_2 & 1 & 0 & -1 & -1 & -1 & -1 & 0 & -1 & -1 & -1 & -1 \\
\gamma_3 & 1 & 1 & 0 & -1 & -1 & -2 & 1 & 1 & 0 & 0 & -1 \\
\gamma_4 & 0 & 1 & 1 & 0 & 0 & -1 & 1 & 2 & 1 & 1 & 0 \\
\gamma_5 & 0 & 1 & 1 & 0 & 0 & -1 & 1 & 2 & 1 & 1 & 0 \\
\gamma_6 & -1 & 1 & 2 & 1 & 1 & 0 & 1 & 3 & 2 & 2 & 1 \\
\gamma_7 & 1 & 0 & -1 & -1 & -1 & -1 & 0 & -1 & -1 & -1 & -1 \\
\gamma_8 & 2 & 1 & -1 & -2 & -2 & -3 & 1 & 0 & -1 & -1 & -2 \\
\gamma_9 & 1 & 1 & 0 & -1 & -1 & -2 & 1 & 1 & 0 & 0 & -1 \\
\gamma_{10} & 1 & 1 & 0 & -1 & -1 & -2 & 1 & 1 & 0 & 0 & -1 \\
\gamma_{11} & 0 & 1 & 1 & 0 & 0 & -1 & 1 & 2 & 1 & 1 & 0
\end{pmatrix} . \tag{12.51}$$

The 1-loops satisfying the commutation relations can be written in terms of the canonical variables as follows,

$$\gamma_1 = e^{-Q-P} z_2 z_5 z_6 \ , \ \ \gamma_2 = e^{-Q} z_2 z_5 z_6 \ , \ \ \gamma_3 = e^P z_2 z_4^{-1} \ , \ \ \gamma_4 = e^{Q+P} z_1 z_2 \ ,$$

$$\gamma_5 = e^{Q+P} z_4^{-1} z_5^{-1} \ , \ \ \gamma_6 = e^{2Q+P} z_1 z_5^{-1} \ , \ \ \gamma_7 = e^{-Q} z_2 z_4^{-1} \ , \ \ \gamma_8 = e^{-Q+P} z_2 z_4^{-1} \ ,$$

$$\gamma_9 = e^P z_1 z_2 \ , \ \ \gamma_{10} = e^P z_4^{-1} z_5^{-1} \ , \ \ \gamma_{11} = e^{Q+P} z_1 z_5^{-1} \ . \tag{12.52}$$

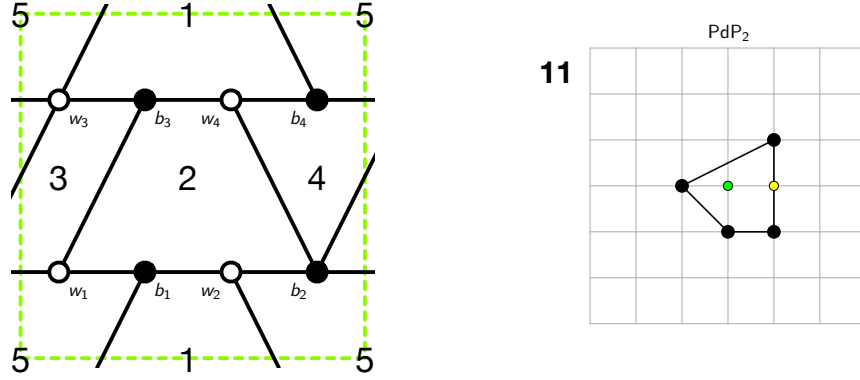# 13   Model 11: PdP$_2$

Figure 30: The brane tiling and toric diagram of Model 11.

The brane tiling for Model 11 can be expressed in terms of the following pair of permutation tuples

$$\sigma_B = (e_{11} \ e_{31} \ e_{21}) \ (e_{22} \ e_{12} \ e_{32} e_{42}) \ (e_{13} \ e_{43} \ e_{33}) \ (e_{44} \ e_{34} \ e_{24}) \ ,$$

$$\sigma_W^{-1} = (e_{11} \ e_{12} \ e_{13}) \ (e_{21} \ e_{22} \ e_{24}) \ (e_{31} \ e_{33} \ e_{32} \ e_{34}) \ (e_{42} \ e_{43} \ e_{44}) \ , \tag{13.1}$$

which correspond to black and white nodes in the brane tiling, respectively.

The brane tiling for Model 11 has 5 zig-zag paths given by,

$$z_1 = (e_{31}^+ \ e_{21}^- \ e_{22}^+ \ e_{12}^- \ e_{13}^+ \ e_{43}^- \ e_{44}^+ \ e_{34}^-) \ , \ \ z_2 = (e_{43}^+ \ e_{33}^- \ e_{32}^+ \ e_{42}^-) \ ,$$

$$z_3 = (e_{24}^+ \ e_{44}^- \ e_{42}^+ \ e_{22}^-) \ , \ \ z_4 = (e_{33}^+ \ e_{13}^- \ e_{11}^+ \ e_{31}^-) \ ,$$

$$z_5 = (e_{21}^+ \ e_{11}^- \ e_{12}^+ \ e_{32}^- \ e_{34}^+ \ e_{24}^-) \ , \tag{13.2}$$

and 5 face paths given by,

$$f_1 = (e_{21}^+ \ e_{31}^- \ e_{33}^+ \ e_{43}^- \ e_{44}^+ \ e_{24}^-) , \quad f_2 = (e_{43}^+ \ e_{13}^- \ e_{11}^+ \ e_{21}^- \ e_{22}^+ \ e_{42}^-) ,$$
$$f_3 = (e_{13}^+ \ e_{33}^- \ e_{32}^+ \ e_{12}^-) , \quad f_4 = (e_{42}^+ \ e_{32}^- \ e_{34}^+ \ e_{44}^-) ,$$
$$f_5 = (e_{31}^+ \ e_{11}^- \ e_{12}^+ \ e_{22}^- \ e_{24}^+ \ e_{34}^-) , \tag{13.3}$$

which satisfy the following relations,

$$f_1 f_2 f_3 f_4 f_5 = 1 , \quad f_3 f_4 f_5 = z_3 z_4^{-1} ,$$
$$f_2 f_4^{-2} f_5^{-1} = z_1 z_2^2 z_3^{-1} z_4^2 , \quad f_1 f_3^{-2} f_5^{-1} = z_1 z_4^3 z_5^2 . \tag{13.4}$$

The face paths can be written in terms of the canonical variables as shown below,

$$f_1 = z_2^{-1} z_4 z_5 e^{-2Q+P}, \ f_2 = z_1 z_2^2 z_4 e^{2Q-P}, \ f_3 = e^{-Q}$$
$$f_4 = e^{q-p}, \ f_5 = z_3 z_4^{-1} e^p \tag{13.5}$$

The Kasteleyn matrix of the brane tiling for Model 11 in Figure 30 is given by,

$$K = \begin{pmatrix} e_{11} & e_{12}x^{-1} & e_{13} & 0 \\ e_{21} & e_{22} & 0 & e_{24}y^{-1} \\ e_{31}y & e_{32}x^{-1} & e_{33} & e_{34}x^{-1} \\ 0 & e_{42} & e_{43} & e_{44} \end{pmatrix} . \tag{13.6}$$

By taking the permanent of the Kasteleyn matrix in (13.6), we obtain the spectral curve of the dimer integrable system for Model 11 as follows,

$$0 = \text{perm } K = \bar{p}_0 \cdot x^{-1} \cdot \left[\delta_{(-1,0)}x^{-1} + \delta_{(1,0)}x + \delta_{(0,-1)}y^{-1} \right.$$
$$\left. + \delta_{(1,-1)}xy^{-1} + \delta_{(1,1)}xy + H \right] , \tag{13.7}$$

where $\bar{p}_0 = e_{13}e_{24}e_{31}e_{42}$. The Casimirs $\delta_{(m,n)}$ in (13.7) can be written in terms of the zig-zag paths in (13.2) as follows,

$$\delta_{(-1,0)} = z_1^{-1} z_3^{-1} , \ \delta_{(1,0)} = \delta_{(1,0)}^1 + \delta_{(1,0)}^2 = 1 + z_3^{-1} z_4 , \ \delta_{(0,-1)} = z_2 z_4 ,$$
$$\delta_{(1,-1)} = z_4 , \ \delta_{(1,1)} = z_3^{-1} , \tag{13.8}$$

such that the spectral curve for Model 11 takes the following form,

$$\Sigma \ : \ z_1^{-1} z_3^{-1} x^{-1} + (1 + z_3^{-1} z_4)x + z_2 z_4 y^{-1} + z_4 xy^{-1} + z_3^{-1} xy + H = 0 . \tag{13.9}$$

The Hamiltonian is a sum over all 5 1-loops γ_i,

$$H = \gamma_1 + \gamma_2 + \gamma_3 + \gamma_4 + \gamma_5 , \tag{13.10}$$

where the 1-loops γ_i can be expressed in terms of zig-zag paths and face paths as follows,

$$\gamma_1 = z_2 f_3^{-1} \ , \ \ \gamma_2 = z_3^{-1} z_4^2 z_5 f_3 f_5 \ , \ \ \gamma_3 = z_2 f_1 \ ,$$
$$\gamma_4 = z_4 z_5 f_3 \ , \ \ \gamma_5 = z_2 f_3^{-1} f_5^{-1} \ , \tag{13.11}$$

The commutation matrix C for Model 11 is given by,

$$C = \begin{pmatrix}
 & \gamma_1 & \gamma_2 & \gamma_3 & \gamma_4 & \gamma_5 \\
\hline
\gamma_1 & 0 & 1 & 1 & 0 & -1 \\
\gamma_2 & -1 & 0 & 1 & 1 & 0 \\
\gamma_3 & -1 & -1 & 0 & 1 & 1 \\
\gamma_4 & 0 & -1 & -1 & 0 & 1 \\
\gamma_5. & 1 & 0 & -1 & -1 & 0
\end{pmatrix} \ , \tag{13.12}$$

where the 1-loops satisfying the commutation relations can be written in terms of the canonical variables as follows,

$$\gamma_1 = e^Q z_2 \ , \ \ \gamma_2 = e^{-Q+P} z_4 z_5 \ , \ \ \gamma_3 = e^{-2Q+P} z_4 z_5 \ ,$$
$$\gamma_4 = e^{-Q} z_4 z_5 \ , \ \ \gamma_5 = e^{Q-P} z_2 z_3^{-1} z_4 \ . \tag{13.13}$$

14 Model 12: dP$_2$
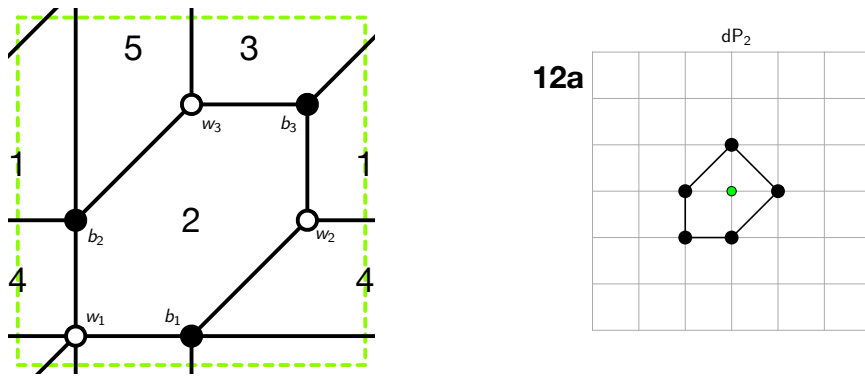
14.1 Model 12a

Figure 31: The brane tiling and toric diagram of Model 12a.

The brane tiling for Model 12a can be expressed in terms of the following pair of permutation tuples

$$\sigma_B = (e_{11}^1 \ e_{31} \ e_{11}^2 \ e_{21}) \ (e_{12}^1 \ e_{22} \ e_{12}^2 \ e_{32}) \ (e_{13} \ e_{33} \ e_{23}) \ ,$$
$$\sigma_W^{-1} = (e_{13} \ e_{11}^2 \ e_{12}^2 \ e_{11}^1 \ e_{12}^1) \ (e_{21} \ e_{23} \ e_{22}) \ (e_{31} \ e_{33} \ e_{32}) \ , \tag{14.1}$$

which correspond to black and white nodes in the brane tiling, respectively.

The brane tiling for Model 12a has 6 zig-zag paths given by,

$$z_1 = (e_{23}^+ \ e_{13}^- \ e_{11}^{2,+}, e_{21}^-) \ , \quad z_2 = (e_{12}^{1,+}, e_{22}^- \ e_{21}^+ \ e_{11}^{1,-}) \ ,$$
$$z_3 = (e_{22}^+ \ e_{12}^{2,-}, e_{11}^{1,+}, e_{31}^- \ e_{33}^+ \ e_{23}^-) \ , \quad z_4 = (e_{13}^+ \ e_{33}^- \ e_{32}^+ \ e_{12}^{1,-}) \ ,$$
$$z_5 = (e_{31}^+ \ e_{11}^{2,-}, e_{12}^{2,+}, e_{32}^-) \ , \tag{14.2}$$

and 5 face paths given by,

$$f_1 = (e_{13}^+ \ e_{23}^- \ e_{22}^+ \ e_{12}^{1,-}) \ , \quad f_2 = (e_{23}^+ \ e_{33}^- \ e_{32}^+ \ e_{12}^{2,-}, e_{11}^{1,+}, e_{21}^-) \ ,$$
$$f_3 = (e_{33}^+ \ e_{13}^- \ e_{11}^{2,+}, e_{31}^-) \ , \quad f_4 = (e_{21}^+ \ e_{11}^{2,-}, e_{12}^{2,+}, e_{22}^-) \ ,$$
$$f_5 = (e_{12}^{1,+}, e_{32}^- \ e_{31}^+ \ e_{11}^{1,-}) \ , \tag{14.3}$$

which satisfy the following relations,

$$f_1 f_2 f_3 f_4 f_5 = 1 \ , \quad f_4 f_5 = z_2 z_5 \ , \quad f_2 f_3^2 f_4^{-1} = z_1^3 z_2 z_3^2 z_4 \ , \quad f_1 f_3^{-1} f_5^{-1} = z_3 z_4^2 z_5 \ . \tag{14.4}$$

The face paths can be written in terms of the canonical variables as follows,

$$f_1 = e^{Q-P} z_1^{-1} z_4 z_5, \ f_2 = e^{-2Q+P} z_1^2 z_3 z_5^{-1}, \ f_3 = e^Q, \ f_4 = e^P, \ f_5 = e^{-P} z_2 z_5 \ . \tag{14.5}$$

The Kasteleyn matrix of the brane tiling for Model 12a in Figure 31 is given by,

$$K = \begin{pmatrix} e_{11}^1 + e_{11}^2 x^{-1} & e_{12}^1 y^{-1} + e_{12}^2 & e_{13} x^{-1} y^{-1} \\ e_{21} & e_{22} x & e_{23} \\ e_{31} y & e_{32} & e_{33} \end{pmatrix} \ . \tag{14.6}$$

The permanent of the Kasteleyn matrix gives the spectral curve of the dimer integrable system, which for Model 12a takes the following form,

$$0 = \text{perm } K = \bar{p}_0 \cdot \left[\delta_{(-1,0)} x^{-1} + \delta_{(1,0)} x + \delta_{(0,-1)} y^{-1} \right.$$
$$\left. + \delta_{(-1,-1)} x^{-1} y^{-1} + \delta_{(0,1)} y + H \right] \ , \tag{14.7}$$

where $\bar{p}_0 = e_{11}e_{22}e_{33}$. The Casimirs $\delta_{(m,n)}$ in (14.7) can be expressed in terms of the zig-zag paths in (14.2) as follows,

$$\delta_{(-1,0)} = z_1 z_2 z_4 \ , \ \ \delta_{(1,0)} = 1 \ , \ \ \delta_{(0,-1)} = z_2 \ ,$$
$$\delta_{(-1,-1)} = z_2 z_4 \ , \ \ \delta_{(0,1)} = z_3^{-1} \ , \tag{14.8}$$

such that the spectral curve for Model 12a takes the following form,

$$\Sigma \ : \ z_1 z_2 z_4 x^{-1} + x + z_2 y^{-1} + z_2 z_4 x^{-1} y^{-1} + z_3^{-1} y + H = 0 \ . \tag{14.9}$$

The Hamiltonian is a sum over all 4 1-loops γ_i,

$$H = \gamma_1 + \gamma_2 + \gamma_3 + \gamma_4 + \gamma_5 \ , \tag{14.10}$$

where the 1-loops γ_i can be expressed in terms of zig-zag paths and face paths as follows,

$$\gamma_1 = z_4 f_1^{-1} \ , \ \ \gamma_2 = z_4 f_1^{-1} f_5 \ , \ \ \gamma_3 = z_4 f_5 \ ,$$
$$\gamma_4 = z_1 z_2 f_1 \ , \ \ \gamma_5 = z_1 z_2 f_1 f_4. \tag{14.11}$$

The commutation matrix C for Model 12a is given by,

$$C = \begin{pmatrix} \begin{array}{c|ccccc} & \gamma_1 & \gamma_2 & \gamma_3 & \gamma_4 & \gamma_5 \\ \hline \gamma_1 & 0 & 1 & 1 & 0 & -1 \\ \gamma_2 & -1 & 0 & 1 & 1 & 0 \\ \gamma_3 & -1 & -1 & 0 & 1 & 1 \\ \gamma_4 & 0 & -1 & -1 & 0 & 1 \\ \gamma_5. & 1 & 0 & -1 & -1 & 0 \end{array} \end{pmatrix} \ , \tag{14.12}$$

where the 1-loops satisfying the commutation relations can be written in terms of the canonical variables as follows,

$$\gamma_1 = e^{-Q+P} z_1 z_5^{-1} \ , \ \ \gamma_2 = e^{-Q} z_1 z_2 \ , \ \ \gamma_3 = e^{-P} z_2 z_4 z_5 \ ,$$
$$\gamma_4 = e^{Q-P} z_2 z_4 z_5 \ , \ \ \gamma_5 = e^{Q} z_2 z_4 z_5 \ . \tag{14.13}$$
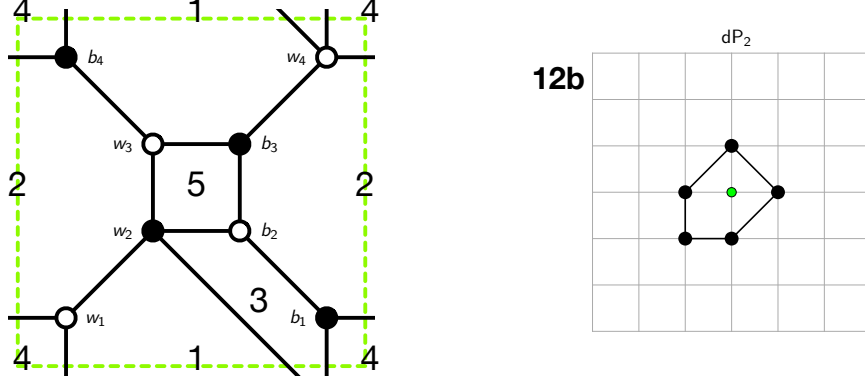
14.2 Model 12b

Figure 32: The brane tiling and toric diagram of Model 12b.

The brane tiling for Model 12b can be expressed in terms of the following pair of permutation tuples

$$\sigma_B = (e_{11}\ e_{21}\ e_{41})\ (e_{12}\ e_{42}\ e_{22}\ e_{32})\ (e_{23}\ e_{43}\ e_{33})\ (e_{14}\ e_{44}\ e_{34})\ ,$$
$$\sigma_W^{-1} = (e_{11}\ e_{12}\ e_{14})\ (e_{21}\ e_{22}\ e_{23})\ (e_{32}\ e_{34}\ e_{33})\ (e_{41}\ e_{44}\ e_{43}\ e_{42})\ , \tag{14.14}$$

which correspond to black and white nodes in the brane tiling, respectively.

The brane tiling for Model 12b has 5 zig-zag paths given by,

$$z_1 = (e_{12}^+\ e_{42}^-\ e_{41}^+\ e_{11}^-)\ ,\quad z_2 = (e_{34}^+\ e_{14}^-\ e_{11}^+\ e_{21}^-\ e_{22}^+\ e_{32}^-)\ ,$$
$$z_3 = (e_{14}^+\ e_{44}^-\ e_{43}^+\ e_{33}^-\ e_{32}^+\ e_{12}^-)\ ,\quad z_4 = (e_{33}^+\ e_{23}^-\ e_{21}^+\ e_{41}^-\ e_{44}^+\ e_{34}^-)\ ,$$
$$z_5 = (e_{42}^+\ e_{22}^-\ e_{23}^+\ e_{43}^-)\ , \tag{14.15}$$

and 5 face paths given by,

$$f_1 = (e_{42}^+\ e_{12}^-\ e_{14}^+\ e_{34}^-\ e_{33}^+\ e_{43}^-)\ ,\quad f_2 = (e_{12}^+\ e_{32}^-\ e_{34}^+\ e_{44}^-\ e_{43}^+\ e_{23}^-\ e_{21}^+\ e_{11}^-)\ ,$$
$$f_3 = (e_{41}^+\ e_{21}^-\ e_{22}^+\ e_{42}^-)\ ,\quad f_4 = (e_{11}^+\ e_{41}^-\ e_{44}^+\ e_{14}^-)\ ,$$
$$f_5 = (e_{23}^+\ e_{33}^-\ e_{32}^+\ e_{22}^-) \tag{14.16}$$

satisfying the following relations,

$$f_1 f_2 f_3 f_4 f_5 = 1\ ,\quad f_4 f_5^{-1} = z_2 z_4\ ,$$
$$f_2 f_3^2 f_5 = z_1 z_4^{-1} z_5^{-1}\ ,\quad f_1 f_2^{-1} f_3^{-3} = z_1^{-1} z_3 z_4^2 z_5^3\ . \tag{14.17}$$

The face paths can be written in terms of the canonical variables as follows,

$$f_1 = z_3 z_4 z_5^2 e^{-Q+P}, \ \ f_2 = z_1 z_4^{-1} z_5^{-1} e^{-Q-2P}, \ \ f_3 = e^P,$$

$$f_4 = z_2 z_4 e^Q, \ \ f_5 = e^Q . \tag{14.18}$$

The Kasteleyn matrix of the brane tiling for Model 12b in Figure 32 is given by,

$$K = \begin{pmatrix} e_{11} x^{-1} & e_{12} & 0 & e_{14} y^{-1} \\ e_{21} & e_{22} & e_{23} & 0 \\ 0 & e_{32} & e_{33} & e_{34} \\ e_{41} y & e_{42} y & e_{43} & e_{44} x \end{pmatrix} . \tag{14.19}$$

By taking the permanent of the Kasteleyn matrix in (14.19) with a $GL(2, \mathbb{Z})$ transformation $M : (x, y) \mapsto (x, \frac{1}{y})$, we obtain the spectral curve of the dimer integrable system for Model 12b as follows,

$$0 = \bar{p}_0 \cdot \left[\delta_{(-1,0)} x^{-1} + \delta_{(1,0)} x + \delta_{(0,-1)} y^{-1} + \delta_{(-1,-1)} x^{-1} y^{-1} + \delta_{(0,1)} y + H \right] , \tag{14.20}$$

where $\bar{p}_0 = e_{12} e_{21} e_{33} e_{44}$. The Casimirs $\delta_{(m,n)}$ in (14.20) can be written in terms of the zig-zag paths in (14.15) as shown below,

$$\delta_{(-1,0)} = z_2 z_3 , \ \ \delta_{(1,0)} = 1 , \ \ \delta_{(0,-1)} = z_4^{-1} , \ \ \delta_{(-1,-1)} = z_2 z_3 z_5 , \ \ \delta_{(0,1)} = z_3 , \tag{14.21}$$

such that the spectral curve for Model 12b takes the following form,

$$\Sigma \ : \ x + z_2 z_3 \frac{1}{x} + z_2 z_3 z_5 \frac{1}{xy} + z_3 y + \frac{1}{z_4 y} + H = 0 . \tag{14.22}$$

The Hamiltonian is a sum over all 6 1-loops γ_i,

$$H = \gamma_1 + \gamma_2 + \gamma_3 + \gamma_4 + \gamma_5 + \gamma_6 , \tag{14.23}$$

where the 1-loops γ_i can be expressed in terms of zig-zag paths and face paths as follows,

$$\gamma_1 = z_1^{-1} f_3 , \ \ \gamma_2 = z_3 z_5 f_3 f_4 , \ \ \gamma_3 = z_1 z_2 z_3 f_1 ,$$

$$\gamma_4 = z_1 z_3 z_4^{-1} f_1 f_4 , \ \ \gamma_5 = z_1 z_2 z_3 f_1 f_3^{-1} , \ \ \gamma_6 = z_1^{-1} f_1^{-1} f_4^{-1} . \tag{14.24}$$

The commutation matrix C for Model 12b is given by,

$$C = \begin{pmatrix} \begin{array}{c|cccccc} & \gamma_1 & \gamma_2 & \gamma_3 & \gamma_4 & \gamma_5 & \gamma_6 \\ \hline \gamma_1 & 0 & -1 & 1 & 0 & 1 & 0 \\ \gamma_2 & 1 & 0 & 2 & 1 & 1 & -1 \\ \gamma_3 & -1 & -2 & 0 & -1 & 1 & 1 \\ \gamma_4 & 0 & -1 & 1 & 0 & 1 & 0 \\ \gamma_5 & -1 & -1 & -1 & -1 & 0 & 1 \\ \gamma_6 & 0 & 1 & -1 & 0 & -1 & 0 \end{array} \end{pmatrix} . \tag{14.25}$$

The 1-loops satisfying the commutation relations can be written in terms of the canonical variables as shown below,

$$\gamma_1 = e^P z_1^{-1} \ , \ \ \gamma_2 = e^{Q+P} z_1^{-1} \ , \ \ \gamma_3 = e^{-Q+P} z_3 z_5 \ ,$$
$$\gamma_4 = e^P z_3 z_5 \ , \ \ \gamma_5 = e^{-Q} z_3 z_5 \ , \ \ \gamma_5 = e^{-P} z_1 z_2 z_3 \ . \tag{14.26}$$

15 Model 13: $\mathbb{C}^3/\mathbb{Z}_4$ $(1,2,2)$, $Y^{2,2}$
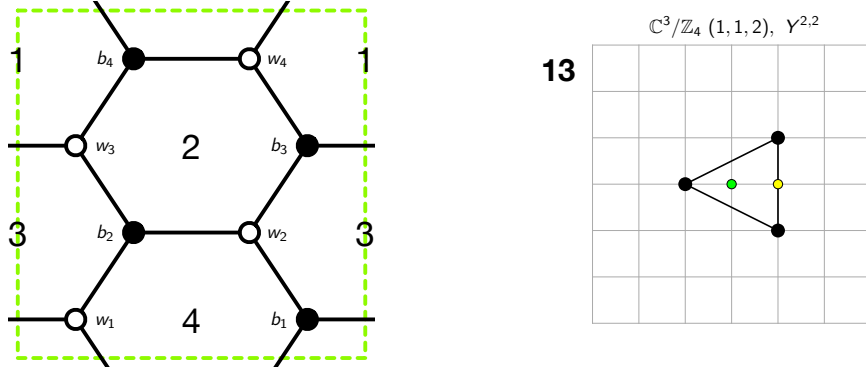
Figure 33: The brane tiling and toric diagram of Model 13.

The brane tiling for Model 13 can be expressed in terms of the following pair of permutation tuples

$$\sigma_B = (e_{11} \ e_{21} \ e_{41}) \ (e_{12} \ e_{22} \ e_{32}) \ (e_{23} \ e_{33} \ e_{43}) \ (e_{14} \ e_{34} \ e_{44}) \ ,$$
$$\sigma_W^{-1} = (e_{11} \ e_{12} \ e_{14}) \ (e_{21} \ e_{22} \ e_{23}) \ (e_{32} \ e_{33} \ e_{34}) \ (e_{41} \ e_{43} \ e_{44}) \ , \tag{15.1}$$

which correspond to black and white nodes in the brane tiling, respectively.

The brane tiling for Model 13 has 4 zig-zag paths given by,

$$z_1 = (e_{33}^+ \ e_{43}^- \ e_{44}^+ \ e_{14}^- \ e_{11}^+ \ e_{21}^- \ e_{22}^+ \ e_{32}^-) \ , \ \ z_2 = (e_{41}^+ \ e_{11}^- \ e_{12}^+ \ e_{22}^- \ e_{23}^+ \ e_{33}^- \ e_{34}^+ \ e_{44}^-) \ ,$$
$$z_3 = (e_{43}^+ \ e_{23}^- \ e_{21}^+ \ e_{41}^-) \ , \ \ z_4 = (e_{32}^+ \ e_{12}^- \ e_{14}^+ \ e_{34}^-) \ , \tag{15.2}$$

and 4 face paths given by,

$$f_1 = (e_{43}^+ \ e_{33}^- \ e_{34}^+ \ e_{14}^- \ e_{11}^+ \ e_{41}^-) \ , \quad f_2 = (e_{23}^+ \ e_{43}^- \ e_{44}^+ \ e_{34}^- \ e_{32}^+ \ e_{22}^-) \ ,$$
$$f_3 = (e_{33}^+ \ e_{23}^- \ e_{21}^+ \ e_{11}^- \ e_{12}^+ \ e_{32}^-) \ , \quad f_4 = (e_{41}^+ \ e_{21}^- \ e_{22}^+ \ e_{12}^- \ e_{14}^+ \ e_{44}^-) \ , \tag{15.3}$$

which satisfy the following relations,

$$f_1 f_3 = z_3 z_4^{-1} \ , \quad f_2 f_4 = z_3^{-1} z_4 \ , \quad f_1 f_2 f_3 f_4 = 1 \tag{15.4}$$

The face paths can be written in terms of the canonical variables as shown below,

$$f_1 = e^{-Q}, \ f_2 = e^{2P}, \ f_3 = z_3 z_4^{-1} e^Q, \ f_4 = z_3^{-1} z_4 e^{-2P} \ . \tag{15.5}$$

The Kasteleyn matrix of the brane tiling for Model 13 in Figure 33 is given by,

$$K = \begin{pmatrix} e_{11} x^{-1} & e_{12} & 0 & e_{14} y^{-1} \\ e_{21} & e_{22} & e_{23} & 0 \\ 0 & e_{32} & e_{33} x^{-1} & e_{34} \\ e_{41} y & 0 & e_{43} & e_{44} \end{pmatrix} \ . \tag{15.6}$$

By taking the permanent of the Kasteleyn matrix in (15.6), we obtain the spectral curve of the dimer integrable system for Model 13 as follows,

$$0 = \text{perm } K = \bar{p}_0 \cdot x^{-1} \cdot \left[\delta_{(1,0)} x + \delta_{(-1,0)} \frac{1}{x} + \delta_{(1,1)} xy + \delta_{(1,-1)} \frac{x}{y} + H \right] \ , \tag{15.7}$$

where $\bar{p}_0 = e_{11} e_{22} e_{33} e_{44}$. The Casimirs $\delta_{(m,n)}$ in (15.7) can be expressed in terms of the zig-zag paths in (15.2) as follows,

$$\delta_{(-1,0)} = 1 \ , \quad \delta_{(1,0)} = z_2 z_3 + z_2 z_4 \ , \quad \delta_{(1,-1)} = z_2 z_3 z_4 \ , \quad \delta_{(1,1)} = z_2 \ , \tag{15.8}$$

allowing us to express the spectral curve for Model 13 in the following form,

$$\Sigma \ : \ \frac{1}{x} + z_2 (z_3 + z_4) x + z_2 xy + z_2 z_3 z_4 \frac{x}{y} + H = 0 \ . \tag{15.9}$$

The Hamiltonian is a sum over all 4 1-loops γ_i,

$$H = \gamma_1 + \gamma_2 + \gamma_3 + \gamma_4 \ , \tag{15.10}$$

where the 1-loops γ_i can be expressed in terms of zig-zag paths and face paths as follows,

$$\gamma_1 = z_2^{1/2} z_4^{1/2} f_3^{1/2} f_4^{-1/2} \ , \quad \gamma_2 = z_2^{1/2} z_4^{1/2} f_1^{1/2} f_2^{1/2} \ ,$$
$$\gamma_3 = z_2^{1/2} z_4^{1/2} f_1^{1/2} f_2^{-1/2} \ , \quad \gamma_4 = z_2^{1/2} z_4^{1/2} f_3^{1/2} f_4^{1/2} \ . \tag{15.11}$$

The commutation matrix C for Model 13 is given by,

$$
C = \begin{pmatrix}
 & \gamma_1 & \gamma_2 & \gamma_3 & \gamma_4 \\
\hline
\gamma_1 & 0 & 1 & 0 & -1 \\
\gamma_2 & -1 & 0 & 1 & 0 \\
\gamma_3 & 0 & -1 & 0 & 1 \\
\gamma_4 & 1 & 0 & -1 & 0
\end{pmatrix} \ , \tag{15.12}
$$

where the 1-loops satisfying the commutation relations can be written in terms of the canonical variables as shown below,

$$
\gamma_1 = e^{Q/2+P} z_2^{1/2} z_3 z_4^{-1/2} \ , \quad \gamma_2 = e^{-Q/2+P} z_2^{1/2} z_4^{1/2} \ ,
$$
$$
\gamma_3 = e^{-Q/2-P} z_2^{1/2} z_4^{1/2} \ , \quad \gamma_4 = e^{Q/2-P} z_2^{1/2} z_4^{1/2} \ . \tag{15.13}
$$

16 Model 14: dP$_1$

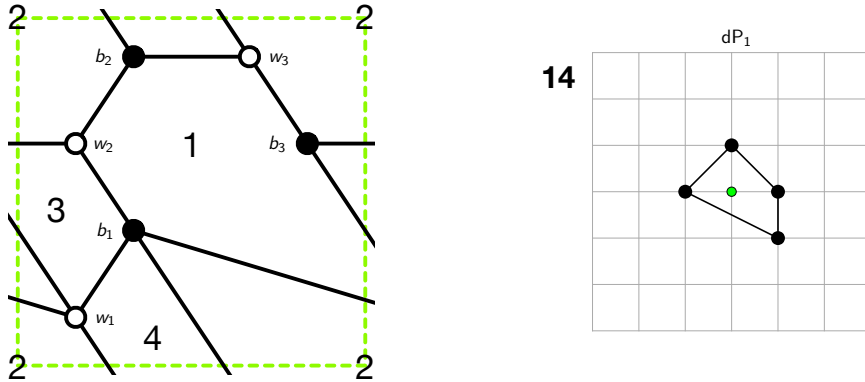**Figure 34**: The brane tiling and toric diagram of Model 14.

The brane tiling for Model 14 can be expressed in terms of the following pair of permutation tuples

$$
\sigma_B = (e_{11}^1 \ e_{31} \ e_{11}^2 \ e_{21}) \ (e_{12} \ e_{22} \ e_{32}) \ (e_{13} \ e_{23} \ e_{33}) \ ,
$$
$$
\sigma_W^{-1} = (e_{11}^1 \ e_{12} \ e_{11}^2 \ e_{13}) \ (e_{21} \ e_{23} \ e_{22}) \ (e_{31} \ e_{33} \ e_{32}) \ , \tag{16.1}
$$

which correspond to black and white nodes in the brane tiling, respectively.

The brane tiling for Model 14 has 4 zig-zag paths given by,

$$z_1 = (e_{33}^+ \ e_{13}^- \ e_{11}^{1,+}, e_{31}^-) \ , \ \ z_2 = (e_{13}^+ \ e_{23}^- \ e_{22}^+ \ e_{32}^- \ e_{31}^+ \ e_{11}^{2,-}) \ ,$$
$$z_3 = (e_{32}^+ \ e_{12}^- \ e_{11}^{2,+}, e_{21}^- \ e_{23}^+ \ e_{33}^-) \ , \ \ z_4 = (e_{21}^+ \ e_{11}^{1,-}, e_{12}^+ \ e_{22}^-) \ , \tag{16.2}$$

and 4 face paths given by,

$$f_1 = (e_{13}^+ \ e_{33}^- \ e_{32}^+ \ e_{22}^- \ e_{21}^+ \ e_{11}^{2,-}) \ , \ \ f_2 = (e_{33}^+ \ e_{23}^- \ e_{22}^+ \ e_{12}^- \ e_{11}^{2,+}, \ e_{31}^-) \ ,$$
$$f_3 = (e_{23}^+ \ e_{13}^- \ e_{11}^{1,+}, e_{21}^-) \ , \ \ f_4 = (e_{31}^+ \ e_{11}^{1,-}, e_{12}^+ \ e_{32}^-) \ , \tag{16.3}$$

which satisfy the following relations,

$$f_1^2 f_2 f_4^3 = z_2^2 z_3 z_4^3 \ , \ \ f_1 f_2^2 f_3^3 = z_1 z_2^{-1} z_4^{-2} \ , \ \ f_1 f_2 f_3 f_4 = 1 \tag{16.4}$$

The face paths can be written in terms of the canonical variables as follows,

$$f_1 = z_2 e^{2Q-P}, \ \ f_2 = z_3 e^{-Q-P}, \ \ f_3 = z_1 e^{P}, \ \ f_4 = z_4 e^{-Q+P} \ . \tag{16.5}$$

The Kasteleyn matrix of the brane tiling for Model 14 in Figure 34 is given by,

$$K = \begin{pmatrix} e_{11}^1 + e_{11}^2 x^{-1} & e_{12} y^{-1} & e_{13} x^{-1} \\ e_{21} & e_{22} & e_{23} x^{-1} \\ e_{31} y & e_{32} & e_{33} \end{pmatrix} \ . \tag{16.6}$$

By taking a permanent of the Kasteleyn matrix in (16.6), we obtain the spectral curve of the dimer integrable system for Model 14 as shown below,

$$0 = \text{perm} \ K = \bar{p}_0 \cdot x^{-1} \cdot \left[\delta_{(1,0)} x + \delta_{(-1,0)} \frac{1}{x} + \delta_{(0,1)} y + \delta_{(1,-1)} \frac{x}{y} + H \right] \ , \tag{16.7}$$

where $\bar{p}_0 = e_{11}^1 e_{22} e_{33}$. The Casimirs $\delta_{(m,n)}$ in (16.7) can be written in terms of the zig-zag paths in (16.2) as shown below,

$$\delta_{(1,0)} = 1 \ , \ \ \delta_{(-1,0)} = z_3 z_4 \ , \ \ \delta_{(0,1)} = z_2 z_3 z_4 \ , \ \ \delta_{(1,-1)} = z_4 \ , \tag{16.8}$$

such that the spectral curve for Model 14 can be expressed in the following form,

$$\Sigma \ : \ z_4 \frac{x}{y} + x + z_3 z_4 \frac{1}{x} + z_2 z_3 z_4 y + H = 0 \ . \tag{16.9}$$

The Hamiltonian is a sum over all 4 1-loops γ_i,

$$H = \gamma_1 + \gamma_2 + \gamma_3 + \gamma_4 \ , \tag{16.10}$$

where the 1-loops γ_i's can be expressed in terms of zig-zag paths and face paths as follows,

$$\gamma_1 = z_1 z_3 f_1 f_4 \ , \ \ \gamma_2 = z_1^{-1} z_4 f_3 \ , \ \ \gamma_3 = z_1 z_3 f_3^{-1} f_4 \ , \ \ \gamma_4 = z_1^{-1} z_4 f_4^{-1} \ . \tag{16.11}$$

The commutation matrix C for Model 14 is given by,

$$C = \begin{pmatrix} \begin{array}{c|cccc} & \gamma_1 & \gamma_2 & \gamma_3 & \gamma_4 \\ \hline \gamma_1 & 0 & 1 & 0 & -1 \\ \gamma_2 & -1 & 0 & 1 & -1 \\ \gamma_3 & 0 & -1 & 0 & 1 \\ \gamma_4 & 1 & 1 & -1 & 0 \end{array} \end{pmatrix} \ , \tag{16.12}$$

where the 1-loops satisfying the commutation relations can be written in terms of the canonical variables as follows,

$$\gamma_1 = e^Q \ , \ \ \gamma_2 = z_4 e^P \ , \ \ \gamma_3 = z_3 z_4 e^{-Q} \ , \ \ \gamma_4 = z_2 z_3 z_4 e^{Q-P} \ . \tag{16.13}$$

17 Model 15: $\mathcal{C}/\mathbb{Z}_2 \ (1,1,1,1)$, F_0
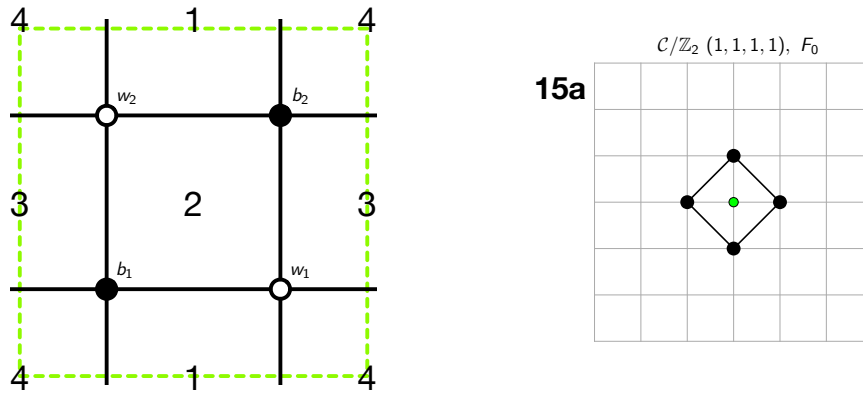
17.1 Model 15a

Figure 35: The brane tiling and toric diagram of Model 15a.

The brane tiling for Model 15a can be expressed in terms of the following pair of permutation tuples

$$\sigma_B = (e_{11}^1 \ e_{21}^1 \ e_{11}^2 \ e_{21}^2) \ (e_{12}^1 \ e_{22}^1 \ e_{12}^2 \ e_{22}^2) \ ,$$
$$\sigma_W^{-1} = (e_{11}^1 \ e_{12}^1 \ e_{11}^2 \ e_{12}^2) \ (e_{21}^1 \ e_{22}^1 \ e_{21}^2 \ e_{22}^2) \ , \tag{17.1}$$

which correspond to black and white nodes in the brane tiling, respectively.

The brane tiling for Model 15a has 4 zig-zag paths given by,

$$z_1 = (e_{12}^{2,+}, e_{22}^{2,-}, e_{21}^{1,+}, e_{11}^{2,-}) \ , \ z_2 = (e_{11}^{1,+}, e_{21}^{1,-}, e_{22}^{1,+}, e_{12}^{2,-}) \ ,$$
$$z_3 = (e_{21}^{2,+}, e_{11}^{1,-}, e_{12}^{1,+}, e_{22}^{1,-}) \ , \ z_4 = (e_{22}^{2,+}, e_{12}^{1,-}, e_{11}^{2,+}, e_{21}^{2,-}) \ , \tag{17.2}$$

and 4 face paths given by,

$$f_1 = (e_{22}^{2,+}, e_{12}^{2,-}, e_{11}^{1,+}, e_{21}^{2,-}) \ , \ f_2 = (e_{21}^{1,+}, e_{11}^{1,-}, e_{12}^{1,+}, e_{22}^{2,-}) \ ,$$
$$f_3 = (e_{11}^{2,+}, e_{21}^{1,-}, e_{22}^{1,+}, e_{12}^{1,-}) \ , \ f_4 = (e_{12}^{2,+}, e_{22}^{1,-}, e_{21}^{2,+}, e_{11}^{2,-}) \ , \tag{17.3}$$

which satisfy the following constraints,

$$f_2 f_4 = z_1 z_3, \ \ f_1 f_3 = z_2 z_4, \ \ f_1 f_2 f_3 f_4 = 1 \ . \tag{17.4}$$

The face paths can be written in terms of the canonical variables as follows,

$$f_1 = e^Q, \ f_2 = e^{2P}, \ f_3 = z_2 z_4 e^{-Q}, \ f_4 = z_1 z_3 e^{-2P} \ . \tag{17.5}$$

The Kasteleyn matrix of the brane tiling for Model 15a in Figure 35 is given by,

$$K = \begin{pmatrix} e_{11}^1 + e_{11}^2 x \ e_{21}^1 + e_{21}^2 y \\ e_{12}^1 + e_{12}^2 \frac{1}{y} \ e_{22}^1 \frac{1}{x} + e_{22}^2 \end{pmatrix} \ . \tag{17.6}$$

The permanent of the Kasteleyn matrix gives the expression for the spectral curve of the dimer integrable system for Model 15a as follows,

$$0 = \text{perm } K = \bar{p}_0 \cdot \left[\delta_{(1,0)} x + \delta_{(-1,0)} \frac{1}{x} + \delta_{(0,1)} y + \delta_{(0,-1)} \frac{1}{y} + H \right] \ , \tag{17.7}$$

where $\bar{p}_0 = e_{11}^{2,+} e_{22}^{2,+}$. The Casimirs $\delta_{(m,n)}$ in (17.7) can be written in terms of the zig-zag paths in (17.2) as shown below,

$$\delta_{(1,0)} = 1 \ , \ \delta_{(-1,0)} = z_1 z_2 \ , \ \delta_{(0,1)} = z_1 z_2 z_3 \ , \ \delta_{(0,-1)} = z_1 \ , \tag{17.8}$$

such that the spectral curve for Model 15a can be written in the following form,

$$\Sigma \; : \; z_1 \frac{1}{y} + x + z_1 z_2 \frac{1}{x} + z_1 z_2 z_3 y + H = 0 \; . \tag{17.9}$$

The Hamiltonian is a sum over all 4 1-loops γ_i,

$$H = \gamma_1 + \gamma_2 + \gamma_3 + \gamma_4 \; , \tag{17.10}$$

where the 1-loops γ_i can be expressed in terms of zig-zag paths and face paths as follows,

$$\begin{aligned}
\gamma_1 &= z_1^{1/2} z_4^{-1/2} f_1^{1/2} f_2^{1/2} \; , \quad \gamma_2 = z_1^{1/2} z_4^{-1/2} f_1^{1/2} f_2^{-1/2} \; , \\
\gamma_3 &= z_1^{1/2} z_4^{-1/2} f_3^{1/2} f_4^{1/2} \; , \quad \gamma_4 = z_1^{1/2} z_4^{-1/2} f_3^{1/2} f_4^{-1/2} \; .
\end{aligned} \tag{17.11}$$

The commutation matrix C for Model 15a is given by,

$$C = \begin{pmatrix}
 & \gamma_1 & \gamma_2 & \gamma_3 & \gamma_4 \\
\hline
\gamma_1 & 0 & 1 & 0 & -1 \\
\gamma_2 & -1 & 0 & 1 & 0 \\
\gamma_3 & 0 & -1 & 0 & 1 \\
\gamma_4 & 1 & 0 & -1 & 0
\end{pmatrix} \; . \tag{17.12}$$

The 1-loops satisfying the commutation relations can be written in terms of the canonical variables as follows,

$$\begin{aligned}
\gamma_1 &= z_1^{1/2} z_4^{-1/2} e^{Q/2+P} \; , \quad \gamma_2 = z_1^{1/2} z_4^{-1/2} e^{Q/2-P} \; , \\
\gamma_3 &= z_1^{1/2} z_4^{-1/2} e^{-Q/2-P} \; , \quad \gamma_4 = z_2^{1/2} z_3^{-1/2} e^{-Q/2+P} \; .
\end{aligned} \tag{17.13}$$
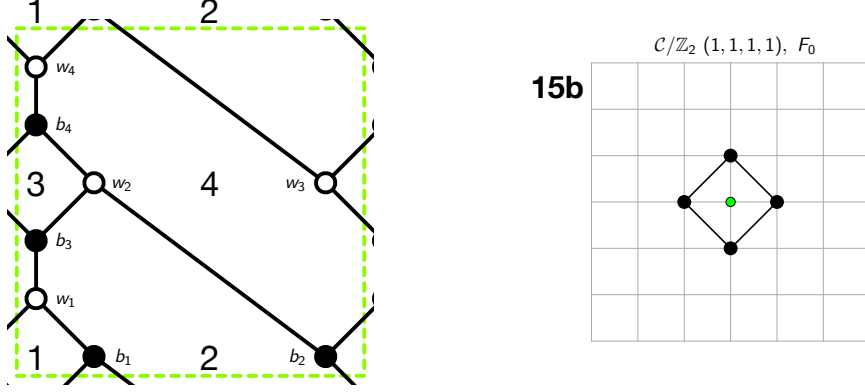
17.2 Model 15b

Figure 36: The brane tiling and toric diagram of Model 15b.

The brane tiling for Model 15b can be expressed in terms of the following pair of permutation tuples

$$\sigma_B = (e_{11} \ e_{41} \ e_{31}) \ (e_{22} \ e_{42} \ e_{12}) \ (e_{13} \ e_{23} \ e_{33}) \ (e_{24} \ e_{44} \ e_{34}) \ ,$$
$$\sigma_W^{-1} = (e_{11} \ e_{12} \ e_{13}) \ (e_{22} \ e_{23} \ e_{24}) \ (e_{31} \ e_{34} \ e_{33}) \ (e_{41} \ e_{44} \ e_{42}) \ , \qquad (17.14)$$

which correspond to black and white nodes in the brane tiling, respectively.

The brane tiling for Model 15b has 4 zig-zag paths given by,

$$z_1 = (e_{12}^+ \ e_{22}^- \ e_{23}^+ \ e_{33}^- \ e_{31}^+ \ e_{11}^-) \ , \ \ z_2 = (e_{42}^+ \ e_{12}^- \ e_{13}^+ \ e_{23}^- \ e_{24}^+ \ e_{44}^-) \ ,$$
$$z_3 = (e_{11}^+ \ e_{41}^- \ e_{44}^+ \ e_{34}^- \ e_{33}^+ \ e_{13}^-) \ , \ \ z_4 = (e_{22}^+ \ e_{42}^- \ e_{41}^+ \ e_{31}^- \ e_{34}^+ \ e_{24}^-) \ , \qquad (17.15)$$

and 4 face paths given by,

$$f_1 = (e_{12}^+ \ e_{42}^- \ e_{41}^+ \ e_{11}^-) \ , \ \ f_2 = (e_{11}^+ \ e_{31}^- \ e_{34}^+ \ e_{44}^- \ e_{42}^+ \ e_{22}^- \ e_{23}^+ \ e_{13}^-) \ ,$$
$$f_3 = (e_{24}^+ \ e_{34}^- \ e_{33}^+ \ e_{23}^-) \ , \ \ f_4 = (e_{22}^+ \ e_{12}^- \ e_{13}^+ \ e_{33}^- \ e_{31}^+ \ e_{41}^- \ e_{44}^+ \ e_{24}^-) \ , \qquad (17.16)$$

satisfying the following relations,

$$f_2 f_3^2 f_4 = z_2 z_3 \ , \ \ f_1 f_3^{-1} = z_1 z_4 \ , \ \ f_1 f_2 f_3 f_4 = 1 \ . \qquad (17.17)$$

The face paths can be written in terms of the canonical variables as shown below,

$$f_1 = e^{2Q}, \ \ f_2 = e^P, \ \ f_3 = z_2 z_3 e^{2Q}, \ \ f_4 = z_1 z_4 e^{-4Q-P} \quad . \qquad (17.18)$$

The Kasteleyn matrix of the brane tiling for Model 15b in Figure 36 is given by,

$$
K = \begin{pmatrix} e_{11} & e_{12}x^{-1} & e_{13} & 0 \\ 0 & e_{22} & e_{23} & e_{24} \\ e_{31}y & 0 & e_{33}x & e_{34}x \\ e_{41}y & e_{42}x^{-1}y & 0 & e_{44} \end{pmatrix} . \tag{17.19}
$$

The permanent of the Kasteleyn matrix in (17.19) gives the following expression,

$$
0 = \mathrm{perm}\, K = \bar{p}_0 \cdot xy^{-1} \cdot \left[\delta_{(1,0)}x + \delta_{(-1,0)}\frac{1}{x} + \delta_{(1,-1)}\frac{x}{y} + \delta_{(-1,1)}\frac{y}{x} + H \right] ,
$$

where $\bar{p}_0 = e_{13}e_{22}e_{34}e_{41}$. Under a $GL(3,\mathbb{Z})$ transformation $(x,y) \mapsto (x, \frac{x}{y})$, we obtain the following form of the spectral curve of the dimer integrable system for Model 15b,

$$
\Sigma \; : \; \delta_{(1,0)}x + \delta_{(-1,0)}\frac{1}{x} + \delta_{(0,1)}y + \delta_{(0,-1)}\frac{1}{y} + H = 0 . \tag{17.20}
$$

The Casimirs $\delta_{(m,n)}$ in (17.20) can be written in terms of the 4 zig-zag paths in (17.15) as follows,

$$
\delta_{(1,0)} = 1 , \; \delta_{(-1,0)} = z_1 z_3 , \; \delta_{(0,1)} = z_3 , \; \delta_{(0,-1)} = z_4^{-1} , \tag{17.21}
$$

allowing us to express the spectral curve for Model 15b in the following form,

$$
\Sigma \; : \; \frac{1}{z_4 y} + x + z_1 z_3 \frac{1}{x} + z_3 y + H = 0 . \tag{17.22}
$$

The Hamiltonian is a sum over all 5 1-loops γ_i,

$$
H = \gamma_1 + \gamma_2 + \gamma_3 + \gamma_4 + \gamma_5 , \tag{17.23}
$$

where the 1-loops γ_i can be expressed in terms of zig-zag paths and face paths as follows,

$$
\gamma_1 = z_1^{1/2} z_3^{1/2} f_1^{1/2} f_2^{1/2} , \; \gamma_2 = z_1^{1/2} z_3^{1/2} f_3^{1/2} f_4^{-1/2} , \; \gamma_3 = z_3^{1/2} z_4^{-1/2} f_2^{1/2} f_3^{-1/2} ,
$$
$$
\gamma_4 = z_3^{1/2} z_4^{-1/2} f_2^{1/2} f_3^{1/2} , \; \gamma_5 = z_1^{1/2} z_3^{1/2} f_3^{1/2} f_4^{1/2} , \tag{17.24}
$$

The commutation matrix C for Model 15b is given by,

$$
C = \begin{pmatrix}
 & \gamma_1 & \gamma_2 & \gamma_3 & \gamma_4 & \gamma_5 \\
\hline
\gamma_1 & 0 & -1 & 1 & 0 & 0 \\
\gamma_2 & 1 & 0 & 2 & 1 & -1 \\
\gamma_3 & -1 & -2 & 0 & -1 & 1 \\
\gamma_4 & 0 & -1 & 1 & 0 & 0 \\
\gamma_5 & 0 & 1 & -1 & 0 & 0
\end{pmatrix} . \tag{17.25}
$$

The 1-loops satisfying the commutation relations can be written in terms of the canonical variables as follows,

$$\gamma_1 = z_1^{1/2} z_3^{1/2} e^{Q+P/2} \ , \ \ \gamma_2 = z_2^{1/2} z_3 z_4^{-1/2} e^{3Q+P/2} \ , \ \ \gamma_3 = z_1^{1/2} z_3^{1/2} e^{-Q+P/2} \ ,$$
$$\gamma_4 = z_2^{1/2} z_3 z_4^{-1/2} e^{Q+P/2} \ , \ \ \gamma_5 = z_1^{1/2} z_3^{1/2} e^{-Q-P/2} \ . \tag{17.26}$$

18 Model 16: $\mathbb{C}^3/\mathbb{Z}_3$ $(1,1,1)$, $\mathbf{dP}_0$
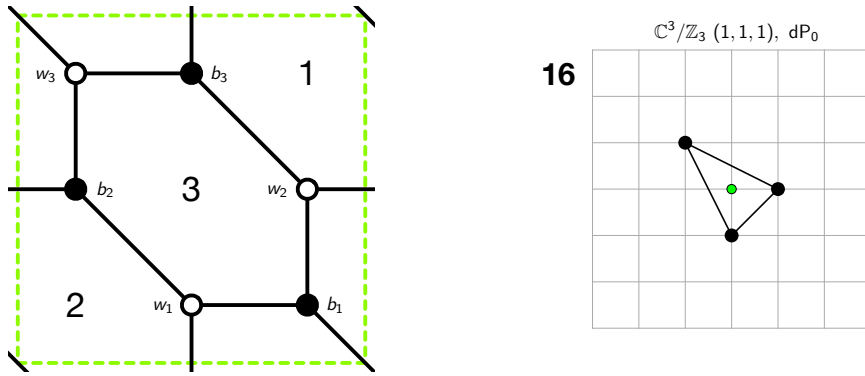
Figure 37: The brane tiling and toric diagram of Model 16.

The brane tiling for Model 16 can be expressed in terms of the following pair of permutation tuples

$$\sigma_B = (e_{11} \ e_{31} \ e_{21}) \ (e_{12} \ e_{32} \ e_{22}) \ (e_{13} \ e_{33} \ e_{23}) \ ,$$
$$\sigma_W^{-1} = (e_{11} \ e_{13} \ e_{12}) \ (e_{21} \ e_{23} \ e_{22}) \ (e_{31} \ e_{33} \ e_{32}) \ , \tag{18.1}$$

which correspond to black and white nodes in the brane tiling, respectively.

The brane tiling for Model 16 has 3 zig-zag paths given by,

$$z_1 = (e_{13}^+ \ e_{33}^- \ e_{32}^+ \ e_{22}^- \ e_{21}^+ \ e_{11}^-) \ , \ \ z_2 = (e_{11}^+ \ e_{31}^- \ e_{33}^+ \ e_{23}^- \ e_{22}^+ \ e_{12}^-) \ ,$$
$$z_3 = (e_{12}^+ \ e_{32}^- \ e_{31}^+ \ e_{21}^- \ e_{23}^+ \ e_{13}^-) \ , \tag{18.2}$$

and 3 face paths given by,

$$f_1 = (e_{13}^+ \ e_{23}^- \ e_{22}^+ \ e_{32}^- \ e_{31}^+ \ e_{11}^-) \ , \ \ f_2 = (e_{12}^+ \ e_{22}^- \ e_{21}^+ \ e_{31}^- \ e_{33}^+ \ e_{13}^-) \ ,$$
$$f_3 = (e_{11}^+ \ e_{21}^- \ e_{23}^+ \ e_{33}^- \ e_{32}^+ \ e_{12}^-) \ , \tag{18.3}$$

which satisfy the following relation,

$$f_1 f_2 f_3 = 1 \ . \tag{18.4}$$

The face paths can be written in terms of the canonical variables as follows,

$$f_1 = e^Q, \ f_2 = e^{-Q+3P}, \ f_3 = e^{-3P} \ . \tag{18.5}$$

The Kasteleyn matrix of the brane tiling for Model 16 in Figure 37 is given by,

$$K = \begin{pmatrix} e_{11} & e_{12} & e_{13}y^{-1} \\ e_{21} & e_{22}x & e_{23} \\ e_{31}\frac{y}{x} & e_{32} & e_{33} \end{pmatrix} \ . \tag{18.6}$$

By taking the permanent of the Kasteleyn matrix in (18.6), we obtain the spectral curve of the dimer integrable system for Model 16 as follows,

$$0 = \mathrm{perm}\ K = \bar{p}_0 \cdot \left[\delta_{(0,-1)}\frac{1}{y} + \delta_{(1,0)}x + \delta_{(-1,1)}\frac{y}{x} + H \right] \ , \tag{18.7}$$

where $\bar{p}_0 = e_{11}e_{22}e_{33}$. The Casimirs $\delta_{(m,n)}$ in (18.7) can be written in terms of the 3 zig-zag paths in (13.2) as shown below,

$$\delta_{(0,-1)} = z_1 \ , \ \ \delta_{(1,0)} = 1 \ , \ \ \delta_{(-1,1)} = z_1 z_3 \ , \tag{18.8}$$

allowing us to express the spectral curve of Model 16 in the following form,

$$\Sigma \ : \ z_1\frac{1}{y} + x + z_1 z_3\frac{y}{x} + H = 0 \ . \tag{18.9}$$

The Hamiltonian is a sum over all 3 1-loops γ_i,

$$H = \gamma_1 + \gamma_2 + \gamma_3 \ , \tag{18.10}$$

where the 1-loops γ_i can be expressed in terms of zig-zag paths and face paths as follows,

$$\gamma_1 = z_1^{1/3} z_2^{-1/3} f_1^{1/3} f_2^{-1/3} \ , \ \ \gamma_2 = z_1^{1/3} z_2^{-1/3} f_1^{1/3} f_2^{2/3} \ , \ \ \gamma_3 = z_1^{1/3} z_2^{-1/3} f_1^{-1/3} f_3^{1/3} \ . \tag{18.11}$$

The commutation matrix C for Model 16 is given by,

$$C = \left(\begin{array}{c|ccc} & \gamma_1 & \gamma_2 & \gamma_3 \\ \hline \gamma_1 & 0 & 1 & -1 \\ \gamma_2 & -1 & 0 & 1 \\ \gamma_3 & 1 & -1 & 0 \end{array} \right) \, , \tag{18.12}$$

where the 1-loops satisfying the commutation relations can be written in terms of the canonical variables as follows,

$$\gamma_1 = z_1^{1/3} z_2^{-1/3} e^{\frac{2}{3}Q-P} \, , \quad \gamma_2 = z_1^{1/3} z_2^{-1/3} e^{-\frac{Q}{3}+2P} \, , \quad \gamma_3 = z_1^{1/3} z_2^{-1/3} e^{-\frac{Q}{3}-P} \, . \tag{18.13}$$

19 Bucket 1
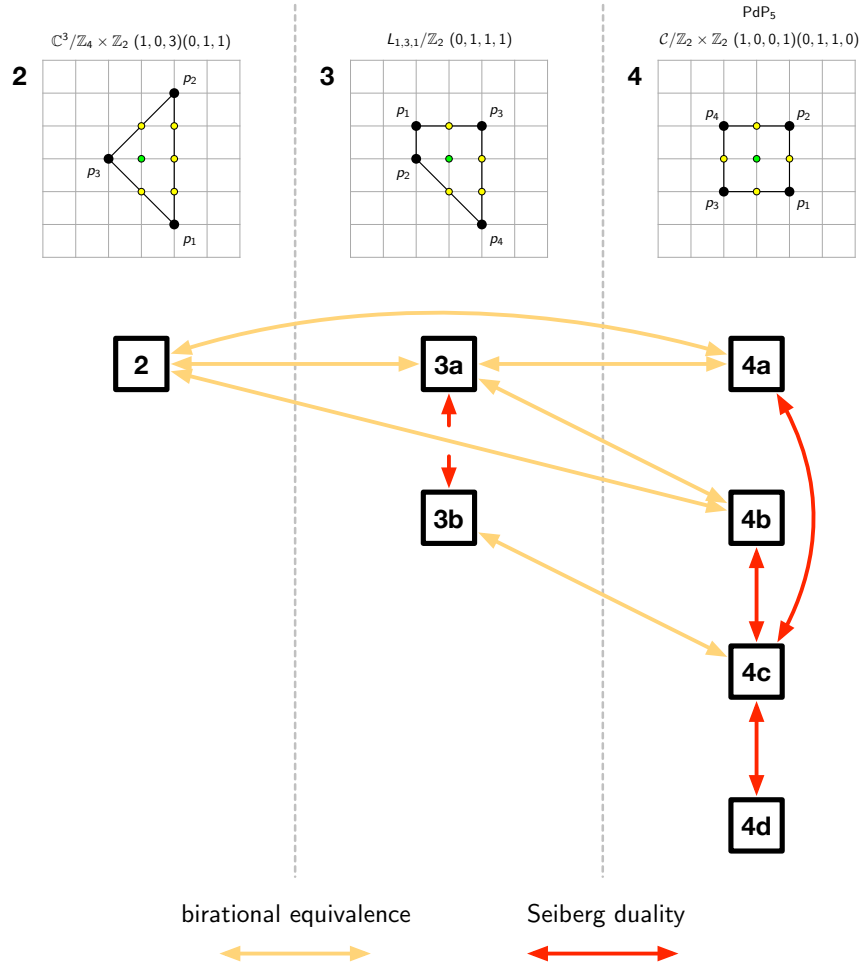

Figure 38: Brane tilings and toric diagrams in Bucket 1.

19.1 Hilbert series and generators of the mesonic moduli spaces

Figure 38 summarizes the brane tilings related by birational transformations in bucket 1. From the results in [15], we have the refined Hilbert series of the mesonic moduli spaces of these models in terms of fugacities t_a corresponding to GLSM fields p_a as

follows,

$$g(t_a; \mathcal{M}^{mes}_{\text{Model 2}}) = \frac{(1 - t_1^4 t_2^4)(1 - t_1^2 t_2^2 t_3^2)}{(1 - t_1^4)(1 - t_1^2 t_2^2)(1 - t_2^4)(1 - t_1 t_2 t_3)(1 - t_3^2)} \ ,$$

$$g(t_a; \mathcal{M}^{mes}_{\text{Model 3a, 3b}}) = \frac{(1 - t_1^2 t_2^2 t_3^2 t_4^2)(1 - t_1 t_2 t_3^3 t_4^3)}{(1 - t_1^2 t_2^2)(1 - t_1 t_3^3)(1 - t_1 t_2 t_3 t_4)(1 - t_3^2 t_4^2)(1 - t_2 t_4^3)} \ ,$$

$$g(t_a; \mathcal{M}^{mes}_{\text{Model 4a, 4b, 4c, 4d}}) = \frac{(1 - t_1^2 t_2^2 t_3^2 t_4^2)^2}{(1 - t_1^2 t_2^2)(1 - t_1^2 t_3^2)(1 - t_1 t_2 t_3 t_4)(1 - t_2^2 t_4^2)(1 - t_3^2 t_4^2)} \ .$$

$$(19.1)$$

We note here that brane tilings related by Seiberg duality have the same mesonic moduli space and therefore have the same associated Hilbert series.

Model 2		
GLSM	$U(1)_R$	fugacity
p_1	r	$t_1 = \bar{t}$
p_2	r	$t_2 = \bar{t}$
p_3	$2r$	$t_3 = \bar{t}^2$

Model 3a, 3b		
GLSM	$U(1)_R$	fugacity
p_1	r	$t_1 = \bar{t}$
p_2	r	$t_2 = \bar{t}$
p_3	r	$t_3 = \bar{t}$
p_4	r	$t_4 = \bar{t}$

Model 4a, 4b, 4c, 4d		
GLSM	$U(1)_R$	fugacity
p_1	r	$t_1 = \bar{t}$
p_2	r	$t_2 = \bar{t}$
p_3	r	$t_3 = \bar{t}$
p_4	r	$t_4 = \bar{t}$

Table 4: $U(1)_R$ charge assignment on GLSM fields of birationally related brane tilings in bucket 1 such that the $U(1)_R$ charge of the superpotentials is $4r = 2$ and that the generators of the mesonic moduli spaces have all $U(1)_R$ charge $4r$.

Table 4 summarizes the $U(1)_R$ charge assignment on the GLSM fields for the brane tilings in bucket 1 in terms of a $U(1)_R$ charge r, ensuring that the superpotentials of the brane tilings have all $U(1)_R$ charge $4r = 2$ and the generators of the mesonic moduli spaces have all $U(1)_R$ charge $4r$. In terms of the fugacity $\bar{t}$ corresponding to $U(1)_R$ charge r, the refined Hilbert series in (19.1) all become,

$$g(\bar{t}; \mathcal{M}^{mes}_{\text{bucket 1}}) = \frac{(1 - \bar{t}^8)^2}{(1 - \bar{t}^4)^5} \ , \tag{19.2}$$

confirming that the birational transformations relating the brane tilings in bucket 1 leave the $U(1)_R$-refined Hilbert series of the associated mesonic moduli spaces invariant.

We also note here based on the results in [15] that the brane tilings in bucket 1 have all mesonic moduli spaces with 5 generators confirming that birational transformations also leave the number of generators invariant. This can be seen by taking the plethystic logarithm [60–64] of the Hilbert series in (19.2), which takes the form,

$$PL[g(\bar{t}; \mathcal{M}^{mes}_{\text{bucket 1}})] = 5\bar{t} - 2\bar{t}^8 , \tag{19.3}$$

confirming the number of mesonic moduli space generators to be 5.

In the following sections, we illustrate how birational transformations in bucket 1 map between birationally equivalent dimer integrable systems defined by the corresponding brane tilings.

19.2   Model 2 to Model 3a

Let us refer to the spectral curve in (4.9) for Model 2 as $\Sigma^{(2)}$ and the spectral curve in (5.9) for Model 3a as $\Sigma^{(3a)}$.

Under the following birational transformation,

$$\varphi_{A;M;N} = M \circ \varphi_A \circ N \; : \; (x, y) \mapsto \left(\frac{1}{xy(1 + \frac{z_5^{(2)}}{y})(1 + \frac{z_6^{(2)}}{y})(1 + \frac{z_8^{(2)}}{y})}, y \right) , \tag{19.4}$$

where

$$M \; : \; (x, y) \mapsto \left(\frac{1}{x}, y \right) , \; N \; : \; (x, y) \mapsto \left(xy, y \right) ,$$

$$\varphi_A \; : \; (x, y) \mapsto \left(\left(1 + \frac{z_5^{(2)}}{y} \right) \left(1 + \frac{z_6^{(2)}}{y} \right) \left(1 + \frac{z_8^{(2)}}{y} \right) x, y \right) , \tag{19.5}$$

we discover that the spectral curve $\Sigma^{(2)}$ in (4.9) is mapped to $\Sigma^{(3a)}$ in (5.9),

$$\varphi_{A;M;N} \Sigma^{(2)} = \Sigma^{(3a)} . \tag{19.6}$$

Based on this map, we have the following identifications between the zig-zag paths,

$$z_1^{(2)} = \frac{1}{z_3^{(3a)}} , \; z_2^{(2)} = \frac{1}{z_4^{(3a)}} , \; z_3^{(2)} = z_1^{(3a)} z_3^{(3a)} z_4^{(3a)} z_7^{(3a)} ,$$

$$z_4^{(2)} = z_3^{(3a)} z_4^{(3a)} z_5^{(3a)} z_7^{(3a)} , \; z_5^{(2)} = z_2^{(3a)} , \; z_6^{(2)} = z_6^{(3a)} ,$$

$$z_7^{(2)} = \frac{1}{z_7^{(3a)}} , \; z_8^{(2)} = z_8^{(3a)} , \tag{19.7}$$

as well as between the face paths,

$$f_1^{(2)} = f_4^{(3a)} \ , \ \ f_2^{(2)} = f_6^{(3a)} \ , \ \ f_3^{(2)} = f_2^{(3a)} \ , \ \ f_4^{(2)} = f_5^{(3a)} \ ,$$
$$f_5^{(2)} = f_3^{(3a)} \ , \ \ f_6^{(2)} = f_7^{(3a)} \ , \ \ f_7^{(2)} = f_8^{(3a)} \ , \ \ f_8^{(2)} = f_1^{(3a)} \ . \tag{19.8}$$

Moreover, the 1-loops of the two dimer integrable systems are identified as follows,

$$\gamma_u^{(2)} = \gamma_u^{(3a)} \ , \tag{19.9}$$

for all $u = 1, \dots, 12$. This implies that the two Hamiltonians of the dimer integrable systems are identical under the birational transformation in (19.4),

$$H^{(2)} = H^{(3a)} \ . \tag{19.10}$$

By identifying (4.5) with (5.5), we also obtain the following canonical transformation,

$$e^{Q^{(2)}} = \frac{1}{z_2^{(3a)} z_4^{(3a)} z_5^{(3a)}} e^{-Q^{(3a)}} \ , \ \ e^{P^{(2)}} = \frac{z_2^{(3a)}}{z_6^{(3a)}} e^{-P^{(3a)}} \ . \tag{19.11}$$

We conclude that the dimer integrable systems for Model 2 and Model 3a are birationally equivalent to each other.

19.3   Model 2 to Model 4a

Let us refer to the spectral curve in (4.9) for Model 2 as $\Sigma^{(2)}$ and the spectral curve in (6.9) for Model 4a as $\Sigma^{(4a)}$.

Under the following birational transformation,

$$\varphi_A \ : \ (x, y) \mapsto$$
$$\left(\left(\frac{y}{1 + \frac{y}{z_6^{(2)}}} \right) \left(\frac{y}{1 + \frac{y}{z_8^{(2)}}} \right) \frac{1}{z_6^{(2)} y} x \ , \ y \right) \ , \tag{19.12}$$

we discover that the spectral curve $\Sigma^{(2)}$ in (4.9) is mapped to $\Sigma^{(4a)}$ in (6.9),

$$\varphi_A \Sigma^{(2)} = \Sigma^{(4a)} \ . \tag{19.13}$$

Based on this map, we have the following identifications between the zig-zag paths,

$$z_1^{(2)} = z_1^{(4a)} z_8^{(4a)} \ , \ \ z_2^{(2)} = z_3^{(4a)} z_8^{(4a)} \ , \ \ z_3^{(2)} = z_4^{(4a)} z_6^{(4a)} \ ,$$
$$z_4^{(2)} = z_2^{(4a)} z_6^{(4a)} \ , \ \ z_5^{(2)} = z_5^{(4a)} \ , \ \ z_6^{(2)} = \frac{1}{z_6^{(4a)}} \ ,$$
$$z_7^{(2)} = z_7^{(4a)} \ , \ \ z_8^{(2)} = \frac{1}{z_8^{(4a)}} \ , \tag{19.14}$$

as well as between the face paths,

$$f_1^{(2)} = f_8^{(4a)} \ , \ f_2^{(2)} = f_6^{(4a)} \ , \ f_3^{(2)} = f_3^{(4a)} \ ,$$
$$f_4^{(2)} = f_1^{(4a)} \ , \ f_5^{(2)} = f_2^{(4a)} \ , \ f_6^{(2)} = f_4^{(4a)} \ ,$$
$$f_7^{(2)} = f_5^{(4a)} \ , \ f_8^{(2)} = f_7^{(4a)} \ . \tag{19.15}$$

Moreover, the 1-loops of the two dimer integrable systems are identified as follows,

$$\gamma_u^{(2)} = \gamma_u^{(4a)} \ , \tag{19.16}$$

for all $u = 1, \dots, 12$. This implies that the two Hamiltonians of the dimer integrable systems are identical under the birational transformation in (19.12),

$$H^{(2)} = H^{(4a)} \ . \tag{19.17}$$

By identifying (4.5) with (6.5), we also obtain the following canonical transformation,

$$e^{Q^{(2)}} = e^{Q^{(4a)}} z_3^{(4a)} z_4^{(4a)} z_6^{(4a)} z_7^{(4a)} \ , \ e^{P^{(2)}} = e^{P^{(4a)}} \tag{19.18}$$

We conclude that the dimer integrable systems for Model 2 and Model 4a are birationally equivalent to each other.

19.4 Model 2 to Model 4b

Let us refer to the spectral curve in (4.9) for Model 2 as $\Sigma^{(2)}$ and the spectral curve in (6.22) for Model 4b as $\Sigma^{(4b)}$.

Under the following birational transformation,

$$\varphi_{A:N} = \varphi_A \circ N \ : \ (x, y) \mapsto \left(\frac{1}{(1 + \frac{1}{z_6^{(2)} y})(1 + \frac{1}{z_7^{(2)} y})} \frac{1}{xy} \ , \ \frac{1}{y} \right) \ , \tag{19.19}$$

where

$$\varphi_A \ : \ (x, y) \mapsto \left(\left(\frac{x}{1 + \frac{y}{z_6^{(2)}}} \right) \left(\frac{x}{1 + \frac{y}{z_7^{(2)}}} \right) x, y \right) \ , \ N \ : \ (x, y) \mapsto \left(\frac{y}{x}, \frac{1}{y} \right) \ , \tag{19.20}$$

we discover that the spectral curve $\Sigma^{(2)}$ in (4.9) is mapped to $\Sigma^{(4b)}$ in (6.22),

$$\varphi_A \Sigma^{(2)} = \Sigma^{(4b)} \ . \tag{19.21}$$

Based on this map, we have the following identifications between the zig-zag paths,

$$z_1^{(2)} = z_2^{(4b)} z_4^{(4b)} z_8^{(4b)} \ , \ z_2^{(2)} = z_2^{(4b)} z_3^{(4b)} z_4^{(4b)} \ , \ z_3^{(2)} = z_5^{(4b)} \ ,$$
$$z_4^{(2)} = z_6^{(4b)} \ , \ z_5^{(2)} = z_7^{(4b)} \ , \ z_6^{(2)} = \frac{1}{z_4^{(4b)}} \ , \ z_7^{(2)} = \frac{1}{z_2^{(4b)}} \ , \ z_8^{(2)} = z_1^{(4b)} \ , \tag{19.22}$$

as well as between the face paths,

$$f_1^{(2)} = f_7^{(4b)} \ , \ f_2^{(2)} = f_1^{(4b)} \ , \ f_3^{(2)} = f_8^{(4b)} \ ,$$
$$f_4^{(2)} = f_2^{(4b)} \ , \ f_5^{(2)} = f_3^{(4b)} \ , \ f_6^{(2)} = f_5^{(4b)} \ ,$$
$$f_7^{(2)} = f_6^{(4b)} \ , \ f_8^{(2)} = f_4^{(4b)} \ . \tag{19.23}$$

Moreover, the 1-loops of the two dimer integrable systems are identified as follows,

$$\gamma_u^{(2)} = \gamma_u^{(4b)} \ , \tag{19.24}$$

for all $u = 1, \ldots, 12$. This implies that the two Hamiltonians of the dimer integrable systems are identical under the birational transformation in (19.19),

$$H^{(2)} = H^{(4b)} \ . \tag{19.25}$$

By identifying (4.5) with (6.5), we also obtain the following canonical transformation,

$$e^{Q^{(2)}} = e^{Q^{(4b)}} \ , \ e^{P^{(2)}} = e^{P^{(4b)}} \ . \tag{19.26}$$

We conclude that the dimer integrable systems for Model 2 and Model 4b are birationally equivalent to each other.

19.5 Model 3a to Model 4a

Let us refer to the spectral curve in (5.9) for Model 3a as $\Sigma^{(3a)}$ and the spectral curve in (6.9) for Model 4a as $\Sigma^{(4a)}$.

Under the following birational transformation,

$$\varphi_{A;M;N} = M \circ \varphi_A \circ N \ :$$
$$(x, y) \mapsto \left(\frac{1}{(y + z_2^{(3a)}) z_8^{(3a)}} \frac{y}{x} \ , \ y \right) \ , \tag{19.27}$$

where

$$M \ : \ (x, y) \mapsto \left(\frac{x}{y}, y \right) \ , \ N \ : \ (x, y) \mapsto \left(\frac{1}{x}, y \right) \ ,$$
$$\varphi_A \ : \ (x, y) \mapsto \left(\frac{y^2}{(y + z_2^{(3a)}) z_8^{(3a)}} x, y \right) \ , \tag{19.28}$$

we discover that the spectral curve $\Sigma^{(3a)}$ in (5.9) is mapped to $\Sigma^{(4a)}$ in (6.9),

$$\varphi_A \Sigma^{(3a)} = \Sigma^{(4a)} \ . \tag{19.29}$$

Based on this map, we have the following identifications between the zig-zag paths,

$$z_1^{(3a)} = \frac{z_8^{(4a)}}{z_2^{(4a)} z_5^{(4a)}} \; , \; z_2^{(3a)} = z_5^{(4a)} \; , \; z_3^{(3a)} = \frac{1}{z_1^{(4a)} z_8^{(4a)}} \; , \; z_4^{(3a)} = \frac{1}{z_3^{(4a)} z_8^{(4a)}} \; ,$$

$$z_5^{(3a)} = \frac{z_8^{(4a)}}{z_4^{(4a)} z_5^{(4a)}} \; , \; z_6^{(3a)} = \frac{1}{z_6^{(4a)}} \; , \; z_7^{(3a)} = \frac{1}{z_7^{(4a)}} \; , \; z_8^{(3a)} = \frac{1}{z_8^{(4a)}} \; , \tag{19.30}$$

as well as between the face paths,

$$f_1^{(3a)} = f_7^{(4a)} \; , \; f_2^{(3a)} = f_3^{(4a)} \; , \; f_3^{(3a)} = f_2^{(4a)} \; ,$$
$$f_4^{(3a)} = f_8^{(4a)} \; , \; f_5^{(3a)} = f_1^{(4a)} \; , \; f_6^{(3a)} = f_6^{(4a)} \; ,$$
$$f_7^{(3a)} = f_4^{(4a)} \; , \; f_8^{(3a)} = f_5^{(4a)} \; . \tag{19.31}$$

Moreover, the 1-loops of the two dimer integrable systems are identified as follows,

$$\gamma_u^{(3a)} = \gamma_u^{(4a)} \; , \tag{19.32}$$

for all $u = 1, \ldots, 12$. This implies that the two Hamiltonians of the dimer integrable systems are identical under the birational transformation in (19.27),

$$H^{(3a)} = H^{(4a)} \; . \tag{19.33}$$

By identifying (5.5) with (6.5), we also obtain the following canonical transformation,

$$e^{Q^{(3a)}} = \frac{1}{z_6^{(4a)} z_7^{(4a)}} e^{-Q^{(4a)}} \; , \; e^{P^{(3a)}} = z_5^{(4a)} z_6^{(4a)} e^{-P^{(4a)}} \; . \tag{19.34}$$

We conclude that the dimer integrable systems for Model 3a and Model 4a are birationally equivalent to each other.

19.6   Model 3a to Model 4b

Let us refer to the spectral curve in (5.9) for Model 3a as $\Sigma^{(3a)}$ and the spectral curve in (6.22) for Model 4b as $\Sigma^{(4b)}$.

Under the following birational transformation,

$$\varphi_{A;M;N} = M \circ \varphi_A \circ N \; :$$
$$(x, y) \mapsto \left(\frac{(y + z_7^{(3a)})}{(1 + z_2^{(3a)} y)(1 + z_8^{(3a)} y) z_6^{(3a)}} x \; , \; \frac{1}{y} \right) \; , \tag{19.35}$$

where

$$M \; : \; (x, y) \mapsto \left(\frac{x}{y}, y \right) \; , \; N \; : \; (x, y) \mapsto \left(\frac{x}{y}, \frac{1}{y} \right) \; ,$$
$$\varphi_A \; : \; (x, y) \mapsto \left(\frac{1 + z_7^{(3a)} y}{(y + z_2^{(3a)})(y + z_8^{(3a)}) z_6^{(3a)}} xy, y \right) \; , \tag{19.36}$$

we discover that the spectral curve $\Sigma^{(3a)}$ in (5.9) is mapped to $\Sigma^{(4b)}$ in (6.22),

$$\varphi_A \Sigma^{(3a)} = \Sigma^{(4b)} \ . \tag{19.37}$$

Based on this map, we have the following identifications between the zig-zag paths,

$$z_1^{(3a)} = z_2^{(4b)} z_3^{(4b)} z_4^{(4b)2} z_5^{(4b)} z_8^{(4b)} \ , \quad z_2^{(3a)} = z_7^{(4b)} \ , \quad z_3^{(3a)} = \frac{1}{z_2^{(4b)} z_4^{(4b)} z_8^{(4b)}} \ ,$$

$$z_4^{(3a)} = \frac{1}{z_2^{(4b)} z_3^{(4b)} z_4^{(4b)}} \ , \quad z_5^{(3a)} = z_2^{(4b)} z_3^{(4b)} z_4^{(4b)2} z_6^{(4b)} z_8^{(4b)} \ ,$$

$$z_6^{(3a)} = \frac{1}{z_4^{(4b)}} \ , \quad z_7^{(3a)} = z_2^{(4b)} \ , \quad z_8^{(3a)} = z_1^{(4b)} \ , \tag{19.38}$$

as well as between the face paths,

$$
\begin{aligned}
f_1^{(2)} &= f_4^{(4b)} \ , \quad f_2^{(2)} = f_8^{(4b)} \ , \quad f_3^{(2)} = f_3^{(4b)} \ , \\
f_4^{(2)} &= f_7^{(4b)} \ , \quad f_5^{(2)} = f_2^{(4b)} \ , \quad f_6^{(2)} = f_1^{(4b)} \ , \\
f_7^{(2)} &= f_5^{(4b)} \ , \quad f_8^{(2)} = f_6^{(4b)} \ .
\end{aligned} \tag{19.39}
$$

Moreover, the 1-loops of the two dimer integrable systems are identified as follows,

$$\gamma_u^{(3a)} = \gamma_u^{(4b)} \ , \tag{19.40}$$

for all $u = 1, \ldots, 12$. This implies that the two Hamiltonians of the dimer integrable systems are identical under the birational transformation in (19.35),

$$H^{(3a)} = H^{(4b)} \ . \tag{19.41}$$

By identifying (5.5) with (6.18), we also obtain the following canonical transformation,

$$e^{Q^{(3a)}} = z_1^{(4b)} z_2^{(4b)} z_3^{(4b)} z_5^{(4b)} e^{-Q^{(4b)}} \ , \quad e^{P^{(3a)}} = z_4^{(4b)} z_7^{(4b)} e^{-P^{(4b)}} \ . \tag{19.42}$$

We conclude that the dimer integrable systems for Model 3a and Model 4b are birationally equivalent to each other.

19.7 Model 3b to Model 4c

Let us refer to the spectral curve in (5.22) for Model 3b as $\Sigma^{(3b)}$ and the spectral curve in (6.35) for Model 4c as $\Sigma^{(4c)}$.

Under the following birational transformation,

$$
\begin{aligned}
\varphi_{A;M;N} &= M \circ \varphi_A \circ N \ : \\
(x, y) &\mapsto \left(\frac{x}{(1 + \frac{z_2^{(3b)}}{y})y} \ , \ \frac{1}{y} \right) \ ,
\end{aligned} \tag{19.43}
$$

where

$$M \; : \; (x,y) \mapsto \left(\tfrac{x}{y}, y\right) , \; N \; : \; (x,y) \mapsto \left(\tfrac{x}{y}, \tfrac{1}{y}\right) ,$$

$$\varphi_A \; : \; (x,y) \mapsto \left(\frac{x}{(1+z_2^{(3b)}y)}x, y\right) , \tag{19.44}$$

we discover that the spectral curve $\Sigma^{(3b)}$ in (5.22) is mapped to $\Sigma^{(4c)}$ in (6.35),

$$\varphi_A \Sigma^{(3b)} = \Sigma^{(4c)} . \tag{19.45}$$

Based on this map, we have the following identifications between the zig-zag paths,

$$z_1^{(3b)} = z_4^{(4c)} z_8^{(4c)} , \; z_2^{(3b)} = \tfrac{1}{z_4^{(4c)}} , \; z_3^{(3b)} = z_7^{(4c)} ,$$

$$z_4^{(3b)} = z_2^{(4c)} , \; z_5^{(3b)} = z_1^{(4c)} ,$$

$$z_6^{(3b)} = z_4^{(4c)} z_5^{(4c)} , \; z_7^{(3b)} = z_6^{(4c)} , \; z_8^{(3b)} = z_3^{(4c)} . \tag{19.46}$$

as well as between the face paths,

$$f_1^{(3b)} = f_5^{(4c)} , \; f_2^{(3b)} = f_1^{(4c)} , \; f_3^{(3b)} = f_8^{(4c)} ,$$

$$f_4^{(3b)} = f_6^{(4c)} , \; f_5^{(3b)} = f_7^{(4c)} , \; f_6^{(3b)} = f_4^{(4c)} ,$$

$$f_7^{(3b)} = f_2^{(4c)} , \; f_8^{(3b)} = f_3^{(4c)} . \tag{19.47}$$

Moreover, the 1-loops of the two dimer integrable systems are identified as follows,

$$\gamma_u^{(3b)} = \gamma_u^{(4c)} , \tag{19.48}$$

for all $u = 1, \ldots, 14$. This implies that the two Hamiltonians of the dimer integrable systems are identical under the birational transformation in (19.43),

$$H^{(3b)} = H^{(4c)} . \tag{19.49}$$

By identifying (5.5) with (6.18), we also obtain the following canonical transformation,

$$e^{Q^{(3b)}} = z_2^{(4c)} z_5^{(4c)} z_6^{(4c)} z_7^{(4c)} e^{Q^{(4c)}} , \; e^{P^{(3b)}} = z_4^{(4c)} z_6^{(4c)} z_7^{(4c)} z_8^{(4c)} e^{P^{(4c)}} . \tag{19.50}$$

We conclude that the dimer integrable systems for Model 3b and Model 4c are birationally equivalent to each other.
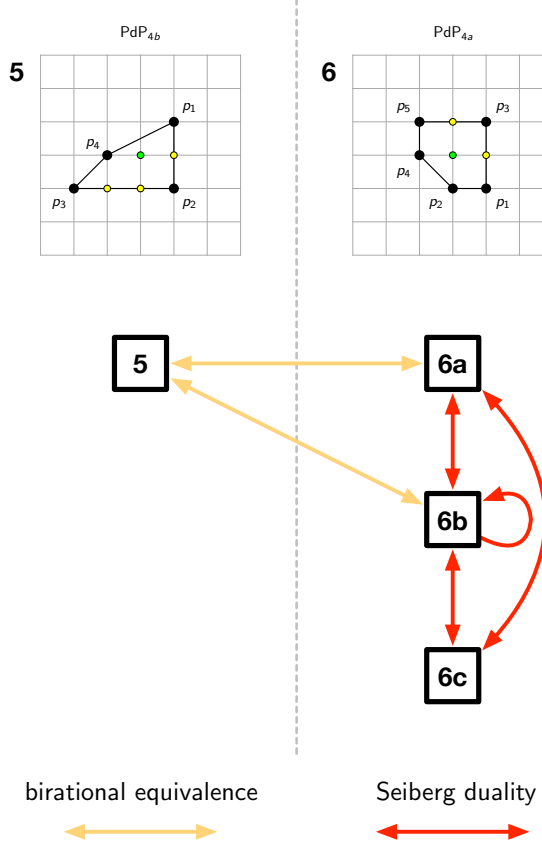
20 Bucket 2

Figure 39: Brane tilings and toric diagrams in Bucket 2.

20.1 Hilbert series and generators of the mesonic moduli spaces

Figure 39 summarizes the brane tilings in bucket 2 that are related by birational transformations. Based on the results in [15], the refined Hilbert series of the mesonic moduli spaces of these brane tilings in terms of fugacities t_a corresponding to GLSM fields p_a are given as follows,

$$g(t_a; \mathcal{M}^{mes}_{\text{Model 5}}) = \frac{1 + t_1 t_2 t_3 t_4 - t_1^2 t_2^4 t_3 t_4 + t_2^2 t_3^2 t_4 - t_1 t_2^5 t_3^2 t_4 - t_1^2 t_2^6 t_3^3 t_4^2}{(1 - t_1 t_2^3)(1 - t_2^4 t_3)(1 - t_1^2 t_4)(1 - t_3^3 t_4^2)} \ ,$$

$$\begin{aligned}
g(t_a; \mathcal{M}^{mes}_{\text{Model 6a, 6b, 6c}}) &= \frac{1}{(1 - t_1^2 t_2 t_3^2)(1 - t_1^2 t_2^2 t_4)(1 - t_1 t_3^3 t_5)(1 - t_3^2 t_4 t_5^2)(1 - t_2 t_4^2 t_5^2)} \\
&\quad \times (1 + t_1 t_2 t_3 t_4 t_5 - t_1^3 t_2^2 t_3^3 t_4 t_5 - t_1^2 t_2 t_3^3 t_4^4 t_5^2 \\
&\quad - t_1^2 t_2^2 t_3^2 t_4^2 t_5^2 - t_1 t_2 t_3^3 t_4^2 t_5^3 + t_1^3 t_2^2 t_3^5 t_4^2 t_5^3 + t_1^4 t_2^3 t_3^6 t_4^3 t_5^4) \ , \quad (20.1)
\end{aligned}$$

where we note that brane tilings related by Seiberg duality have the same mesonic moduli space and therefore have the same corresponding Hilbert series.

Model 5		
GLSM	$U(1)_R$	fugacity
p_1	$2r$	$t_1 = \bar{t}^2$
p_2	r	$t_2 = \bar{t}$
p_3	r	$t_3 = \bar{t}$
p_4	r	$t_4 = \bar{t}$

Model 6a, 6b, 6c		
GLSM	$U(1)_R$	fugacity
p_1	r	$t_1 = \bar{t}$
p_2	r	$t_2 = \bar{t}$
p_3	r	$t_3 = \bar{t}$
p_4	r	$t_4 = \bar{t}$
p_5	r	$t_5 = \bar{t}$

Table 5: $U(1)_R$ charge assignment on GLSM fields of birationally related brane tilings in bucket 2 such that the $U(1)_R$ charge of the superpotentials is $5r = 2$ and that the generators of the mesonic moduli spaces have all $U(1)_R$ charge $5r$.

Table 5 summarizes the $U(1)_R$ charge assignment on the GLSM fields in terms of a $U(1)_R$ charge r, ensuring that the superpotentials of the brane tilings in bucket 2 have all $U(1)_R$ charge $5r = 2$ and the generators of the mesonic moduli spaces have all $U(1)_R$ charge $5r$. Based on this $U(1)_R$ charge assignment, in terms of a fugacity $\bar{t}$ corresponding to $U(1)_R$ charge r, the refined Hilbert series in (20.1) all become,

$$g(\bar{t}; \mathcal{M}^{mes}_{\text{bucket 2}}) = \frac{1 + 3\bar{t}^5 + \bar{t}^{10}}{(1 - \bar{t}^5)^3} \ . \tag{20.2}$$

This confirms that the birational transformations relating the brane tilings in bucket 2 keep the $U(1)_R$-refined Hilbert series of the associated mesonic moduli spaces invariant.

Based on the results in [15], we also note here that the brane tilings in bucket 2 have all mesonic moduli spaces with 6 generators. This can also be seen by taking the plethystic logarithm [60–64] of the Hilbert series in (20.2), giving us,

$$PL[g(\bar{t}; \mathcal{M}^{mes}_{\text{bucket 2}})] = 6\bar{t}^5 - 5\bar{t}^{10} + 5\bar{t}^{15} + \dots \ , \tag{20.3}$$

which confirms the number of generators to be 6 for all brane tilings in bucket 2.

In the following sections, we illustrate how the brane tilings in bucket 2 define dimer integrable systems that are equivalent under birational transformations.

20.2 Model 5 to Model 6a

Let us refer to the spectral curve in (7.9) for Model 5 as $\Sigma^{(5)}$ and the spectral curve in (8.9) for Model 6a as $\Sigma^{(6a)}$.

Under the following birational transformation,

$$\varphi_{A;N} = \varphi_A \circ N \ : \ (x, y) \mapsto \left(x, z_3^{(5)} z_7^{(5)} \frac{(x + z_2^{(5)})}{xy} \right) , \tag{20.4}$$

where

$$\varphi_A \ : \ (x, y) \mapsto \left(x, z_3^{(5)} z_7^{(5)} \frac{(x + z_2^{(5)})}{x} y \right) , \quad N \ : \ (x, y) \mapsto \left(x, \frac{1}{y} \right) , \tag{20.5}$$

we discover that the spectral curve $\Sigma^{(5)}$ in (7.9) is mapped to $\Sigma^{(6a)}$ in (8.9),

$$\varphi_{A;N} \Sigma^{(5)} = \Sigma^{(6a)} . \tag{20.6}$$

Based on this map, we have the following identifications between the zig-zag paths,

$$z_1^{(5)} = z_2^{(6a)} z_3^{(6a)} z_4^{(6a)} \ , \ z_2^{(5)} = z_1^{(6a)} \ , \ z_3^{(5)} = z_7^{(6a)} \ , \ z_4^{(5)} = z_2^{(6a)} z_3^{(6a)} z_6^{(6a)} \ ,$$
$$z_5^{(5)} = \frac{1}{z_3^{(6a)}} \ , \ z_6^{(5)} = \frac{1}{z_2^{(6a)}} \ , \ z_7^{(5)} = z_5^{(6a)} \ , \tag{20.7}$$

as well as between the face paths,

$$f_1^{(5)} = f_5^{(6a)} \ , \ f_2^{(5)} = f_4^{(6a)} \ , \ f_3^{(5)} = f_6^{(6a)} \ , \ f_4^{(5)} = f_2^{(6a)} \ ,$$
$$f_5^{(5)} = f_7^{(6a)} \ , \ f_6^{(5)} = f_3^{(6a)} \ , \ f_7^{(5)} = f_1^{(6a)} . \tag{20.8}$$

Moreover, the 1-loops of the two dimer integrable systems are identified as follows,

$$\gamma_u^{(5)} = \gamma_u^{(6a)} , \tag{20.9}$$

for all $u = 1, \ldots, 9$. This implies that the two Hamiltonians of the dimer integrable systems are identical under the birational transformation in (20.4),

$$H^{(5)} = H^{(6a)} . \tag{20.10}$$

By identifying (7.5) with (8.5), we also obtain the following canonical transformation,

$$e^{Q^{(5)}} = \frac{1}{z_2^{(6a)} z_4^{(6a)} z_5^{(6a)}} e^{Q^{(6a)}} \ , \ e^{P^{(5)}} = e^{P^{(6a)}} . \tag{20.11}$$

We conclude that the dimer integrable systems for Model 5 and Model 6a are birationally equivalent to each other.

20.3 Model 5 to Model 6b

Let us refer to the spectral curve in (7.9) for Model 5 as $\Sigma^{(5)}$ and the spectral curve in (8.22) for Model 6b as $\Sigma^{(6b)}$.

Under the following birational transformation,

$$\varphi_{A;N} = \varphi_A \circ N \ : \ (x,y) \mapsto \left(x, z_3^{(5)} z_7^{(5)} \frac{(x + z_5^{(5)})}{xy} \right) \ , \tag{20.12}$$

where

$$\varphi_A \ : \ (x,y) \mapsto \left(x, z_3^{(5)} z_7^{(5)} \frac{(x + z_5^{(5)})}{x} y \right) \ , \quad N \ : \ (x,y) \mapsto \left(x, \frac{1}{y} \right) \ , \tag{20.13}$$

we discover that the spectral curve $\Sigma^{(5)}$ in (7.9) is mapped to $\Sigma^{(6b)}$ in (8.22),

$$\varphi_{A;N} \Sigma^{(5)} = \Sigma^{(6b)} \ . \tag{20.14}$$

Based on this map, we have the following identifications between the zig-zag paths,

$$z_1^{(5)} = z_2^{(6b)} z_5^{(6b)} z_7^{(6b)} \ , \quad z_2^{(5)} = \frac{1}{z_2^{(6b)}} \ , \quad z_3^{(5)} = z_4^{(6b)} \ , \quad z_4^{(5)} = z_2^{(6b)} z_3^{(6b)} z_7^{(6b)} \ ,$$
$$z_5^{(5)} = z_1^{(6b)} \ , \quad z_6^{(5)} = \frac{1}{z_7^{(6b)}} \ , \quad z_7^{(5)} = z_6^{(6b)} \ , \tag{20.15}$$

as well as between the face paths,

$$f_1^{(5)} = f_7^{(6b)} \ , \quad f_2^{(5)} = f_1^{(6b)} \ , \quad f_3^{(5)} = f_2^{(6b)} \ , \quad f_4^{(5)} = f_3^{(6b)} \ ,$$
$$f_5^{(5)} = f_4^{(6b)} \ , \quad f_6^{(5)} = f_5^{(6b)} \ , \quad f_7^{(5)} = f_6^{(6b)} \ . \tag{20.16}$$

Moreover, the 1-loops of the two dimer integrable systems are identified as follows,

$$\gamma_u^{(5)} = \gamma_u^{(6b)} \ , \tag{20.17}$$

for all $u = 1, \ldots, 9$. This implies that the two Hamiltonians of the dimer integrable systems are identical under the birational transformation in (20.12),

$$H^{(5)} = H^{(6b)} \ . \tag{20.18}$$

By identifying (7.5) with (8.18), we also obtain the following canonical transformation,

$$e^{Q^{(5)}} = z_3^{(6b)} z_4^{(6b)} e^{Q^{(6b)}} \ , \quad e^{P^{(5)}} = e^{P^{(6b)}} \ . \tag{20.19}$$

We conclude that the dimer integrable systems for Model 5 and Model 6b are birationally equivalent to each other.

21 Bucket 3

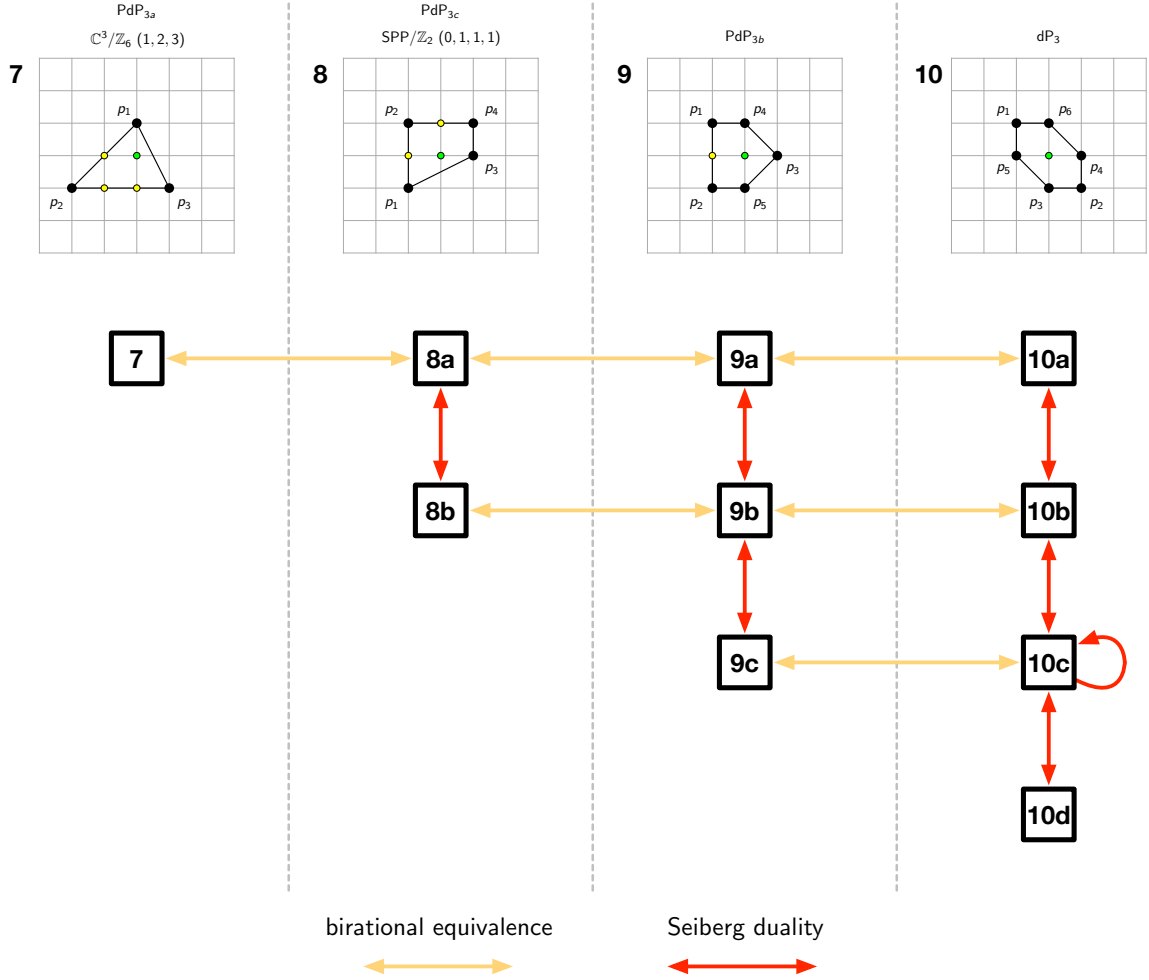**Figure 40**: Brane tilings and toric diagrams in Bucket 3.

21.1 Hilbert series and generators of the mesonic moduli spaces

Figure 40 summarizes the brane tilings in bucket 3 that are related by birational transformations. Taking the results in [15], the refined Hilbert series of the mesonic moduli spaces of these brane tilings in terms of fugacities t_a corresponding to GLSM fields p_a

are given by,

$$g(t_a; \mathcal{M}^{mes}_{\text{Model 7}}) = \frac{1 + t_1 t_2^3 + t_1 t_2 t_3 + t_2^4 t_3 + t_2^2 t_3^2 + t_1 t_2^5 t_3^2}{(1 - t_1^2)(1 - t_2^6)(1 - t_3^3)} \,,$$

$$g(t_a; \mathcal{M}^{mes}_{\text{Model 8a, 8b}}) = \frac{1}{(1 - t_1^2 t_2^2)(1 - t_1^2 t_3^4)(1 - t_2 t_4^2)(1 - t_3^2 t_4^2)}$$
$$\times (1 + t_1^2 t_2 t_3^2 + t_1 t_2 t_3 t_4 + t_1 t_3^3 t_4 - t_1^2 t_2^2 t_3^2 t_4^2 - t_1^2 t_2 t_3^4 t_4^2$$
$$- t_1 t_2 t_3^3 t_4^3 - t_1^3 t_2^2 t_3^5 t_4^3) \,,$$

$$g(t_a; \mathcal{M}^{mes}_{\text{Model 9a, 9b, 9c}}) = \frac{1}{(1 - t_1^3 t_2 t_4^2)(1 - t_1^2 t_3 t_4^2)(1 - t_3^2 t_4 t_5)(1 - t_1 t_3^3 t_5^2)(1 - t_2^2 t_3 t_5^2)}$$
$$\times (1 + t_1^2 t_2^2 t_4 t_5 + t_1 t_2 t_3 t_4 t_5 - t_1^4 t_2^2 t_3 t_4^3 t_5 - t_1^3 t_2 t_3^2 t_4^3 t_5$$
$$- t_1^3 t_2^3 t_3 t_4^2 t_5^2 - t_1^2 t_2^2 t_3^2 t_4^2 t_5^2 - t_1^2 t_2^4 t_3 t_4 t_5^3 - t_1 t_2^3 t_3^2 t_4 t_5^3$$
$$+ t_1^4 t_2^4 t_3^2 t_4^3 t_5^3 + t_1^3 t_2^3 t_3^3 t_4^3 t_5^3 + t_1^5 t_2^5 t_3^3 t_4^4 t_5^4) \,,$$

$$g(t_a; \mathcal{M}^{mes}_{\text{Model 10a, 10b, 10c, 10d}}) = \frac{(1 - t_1 t_2 t_3 t_4 t_5 t_6)}{(1 - t_2^2 t_3^2 t_4 t_5)(1 - t_1 t_2 t_3^2 t_5^2)(1 - t_2^2 t_3 t_4^2 t_6)(1 - t_1^2 t_3 t_5^2 t_6)}$$
$$\times \frac{1}{(1 - t_1 t_2 t_4^2 t_6^2)(1 - t_1^2 t_4 t_5 t_6^2)} \times (1 + 2 t_1 t_2 t_3 t_4 t_5 t_6$$
$$- t_1 t_2^3 t_3^3 t_4^2 t_5^2 t_6 - t_1^2 t_2^2 t_3^3 t_4 t_5^3 t_6 - t_1 t_2^3 t_3^2 t_4^3 t_5 t_6^2$$
$$- t_1^3 t_2 t_3^2 t_4 t_5^3 t_6^2 - t_1^2 t_2^2 t_3 t_4^3 t_5 t_6^3 - t_1^3 t_2 t_3 t_4^2 t_5^2 t_6^3$$
$$+ 2 t_1^3 t_2^3 t_3^3 t_4^3 t_5^3 t_6^3 + t_1^4 t_2^4 t_3^4 t_4^4 t_5^4 t_6^4) \,. \tag{21.1}$$

Here, we note that brane tilings related by Seiberg duality have the same mesonic moduli space and associated Hilbert series.

Table 6 summarizes the $U(1)_R$ charge assignment on the GLSM fields in terms of a $U(1)_R$ charge r, which ensures that the superpotentials of the brane tilings in bucket 3 have all $U(1)_R$ charge $6r = 2$ and the generators of the mesonic moduli spaces have all $U(1)_R$ charge $6r$. Using this $U(1)_R$ charge assignment, we see that the refined Hilbert series in (21.1) expressed in terms of a single fugacity $\bar{t}$ corresponding to $U(1)_R$ charge r all become,

$$g(\bar{t}; \mathcal{M}^{mes}_{\text{bucket 3}}) = \frac{1 + 4\bar{t}^6 + \bar{t}^{12}}{(1 - \bar{t}^6)^3} \,. \tag{21.2}$$

This confirms that the birational transformations relating the brane tilings in bucket 3 preserve the Hilbert series of the mesonic moduli spaces when refined only under the $U(1)_R$ symmetry.

Model 7		
GLSM	$U(1)_R$	fugacity
p_1	$3r$	$t_1 = \bar{t}^3$
p_2	r	$t_2 = \bar{t}$
p_3	$2r$	$t_3 = \bar{t}^2$

Model 8a, 8b		
GLSM	$U(1)_R$	fugacity
p_1	r	$t_1 = \bar{t}$
p_2	$2r$	$t_2 = \bar{t}^2$
p_3	r	$t_3 = \bar{t}$
p_4	$2r$	$t_4 = \bar{t}^2$

Model 9a, 9b, 9c		
GLSM	$U(1)_R$	fugacity
p_1	r	$t_1 = \bar{t}$
p_2	r	$t_2 = \bar{t}$
p_3	$2r$	$t_3 = \bar{t}^2$
p_4	r	$t_4 = \bar{t}$
p_5	r	$t_5 = \bar{t}$

Model 10a, 10b, 10c, 10d		
GLSM	$U(1)_R$	fugacity
p_1	r	$t_1 = \bar{t}$
p_2	r	$t_2 = \bar{t}$
p_3	r	$t_3 = \bar{t}$
p_4	r	$t_4 = \bar{t}$
p_5	r	$t_5 = \bar{t}$
p_6	r	$t_6 = \bar{t}$

Table 6: $U(1)_R$ charge assignment on GLSM fields of birationally related brane tilings in bucket 3 such that the $U(1)_R$ charge of the superpotentials is $6r = 2$ and that the generators of the mesonic moduli spaces have all $U(1)_R$ charge $6r$.

Moreover, by further referring to the results in [15], we note here that the brane tilings in bucket 3 all have mesonic moduli spaces with 7 generators. This can also be seen through the plethystic logarithm [60–64] of the Hilbert series in (21.2), which takes the following form,

$$PL[g(\bar{t}; \mathcal{M}^{mes}_{\text{bucket 3}})] = 7\bar{t}^6 - 9\bar{t}^{12} + 16\bar{t}^{18} + \dots . \tag{21.3}$$

This confirms the mesonic moduli spaces in bucket 3 all have 7 generators.

The following sections illustrate how the brane tilings in bucket 3 define dimer integrable systems that are birationally equivalent to each other.

21.2 Model 7 to Model 8a

Let us refer to the spectral curve in (9.9) for Model 7 as $\Sigma^{(7)}$ and the spectral curve in (10.9) for Model 8a as $\Sigma^{(8a)}$.

Under the following birational transformation,

$$\varphi_{A;N} = \varphi_A \circ N \; : \; (x,y) \mapsto \left(\frac{1}{y}, z_3^{(7)} z_6^{(7)} \frac{(y + z_4^{(7)})(y + z_5^{(7)})}{xy} \right) , \qquad (21.4)$$

where

$$\varphi_A \; : \; (x,y) \mapsto \left(x, z_3^{(7)} z_6^{(7)} (x + z_4^{(7)})(x + z_5^{(7)}) y \right) , \quad N \; : \; (x,y) \mapsto \left(\frac{1}{y}, \frac{y}{x} \right) , \quad (21.5)$$

we discover that the spectral curve $\Sigma^{(7)}$ in (9.9) is mapped to $\Sigma^{(8a)}$ in (10.9),

$$\varphi_{M;N} \Sigma^{(7)} = \Sigma^{(8a)} . \qquad (21.6)$$

Based on this map, we have the following identifications between the zig-zag paths,

$$z_1^{(7)} = \frac{1}{z_1^{(8a)2} z_3^{(8a)}} \; , \; z_2^{(7)} = z_1^{(8a)} \; , \; z_3^{(7)} = \frac{1}{z_5^{(8a)}} \; , \; z_4^{(7)} = \frac{1}{z_2^{(8a)}} \; , \; z_5^{(7)} = \frac{1}{z_6^{(8a)}} \; , \; z_6^{(7)} = \frac{1}{z_4^{(8a)}} \; ,$$
$$(21.7)$$

as well as between the face paths,

$$f_1^{(7)} = f_1^{(8a)} \; , \; f_2^{(7)} = f_6^{(8a)} \; , \; f_3^{(7)} = f_3^{(8a)} \; ,$$
$$f_4^{(7)} = f_2^{(8a)} \; , \; f_5^{(7)} = f_4^{(8a)} \; , \; f_6^{(7)} = f_5^{(8a)} . \qquad (21.8)$$

Moreover, the 1-loops of the two dimer integrable systems are identified as follows,

$$\gamma_u^{(7)} = \gamma_u^{(8a)} , \qquad (21.9)$$

for all $u = 1, \ldots, 6$. This implies that the two Hamiltonians of the dimer integrable systems are identical under the birational transformation in (21.4),

$$H^{(7)} = H^{(8a)} . \qquad (21.10)$$

By identifying (9.5) with (10.5), we also obtain the following canonical transformation,

$$e^{Q^{(7)}} = \frac{1}{z_1 z_2} e^{-P^{(8a)}} \; , \; e^{P^{(7)}} = e^{Q^{(8a)}} . \qquad (21.11)$$

We conclude that the dimer integrable systems for Model 7 and Model 8a are birationally equivalent to each other.

21.3 Model 8a to Model 9a

Let us refer to the spectral curve in (10.9) for Model 8a as $\Sigma^{(8a)}$ and the spectral curve in (11.9) for Model 9a as $\Sigma^{(9a)}$.

Under the following birational transformation,

$$\varphi_{M;A;N} = M \circ \varphi_A \circ N \ : \ (x,y) \mapsto \left(\frac{x}{z_1^{(8a)}}, \frac{1}{y + \frac{z_4^{(8a)}xy}{z_1^{(8a)}}} \right) , \tag{21.12}$$

where

$$M \ : \ (x,y) \mapsto \left(x, \tfrac{1}{y} \right) , \ \varphi_A \ : \ (x,y) \mapsto \left(x, (1 + z_4^{(8a)}x)y \right) ,$$
$$N \ : \ (x,y) \mapsto \left(\tfrac{x}{z_1^{(8a)}}, y \right) , \tag{21.13}$$

we discover that the spectral curve $\Sigma^{(8a)}$ in (10.9) is mapped to $\Sigma^{(9a)}$ in (11.9),

$$\varphi_{M;A;N}\Sigma^{(8a)} = \Sigma^{(9a)} . \tag{21.14}$$

Based on this map, we have the following identifications between the zig-zag paths,

$$z_1^{(8a)} = \frac{1}{z_2^{(9a)}z_4^{(9a)}} \ , \ z_2^{(8a)} = \frac{1}{z_3^{(9a)}} \ , \ z_3^{(8a)} = \frac{z_2^{(9a)}z_4^{(9a)2}}{z_5^{(9a)}} \ ,$$
$$z_4^{(8a)} = \frac{1}{z_4^{(9a)}} \ , \ z_5^{(8a)} = \frac{1}{z_1^{(9a)}z_2^{(9a)}z_4^{(9a)}} \ , \ z_6^{(8a)} = \frac{1}{z_6^{(9a)}} \ , \tag{21.15}$$

as well as between the face paths,

$$f_1^{(8a)} = f_6^{(9a)} \ , \ f_2^{(8a)} = f_4^{(9a)} \ , \ f_3^{(8a)} = f_5^{(9a)} \ ,$$
$$f_4^{(8a)} = f_3^{(9a)} \ , \ f_5^{(8a)} = f_2^{(9a)} \ , \ f_6^{(8a)} = f_1^{(9a)} \ . \tag{21.16}$$

Moreover, the 1-loops of the two dimer integrable systems are identified as follows,

$$\gamma_u^{(8a)} = \gamma_u^{(9a)} , \tag{21.17}$$

for all $u = 1, \ldots, 6$. This implies that the two Hamiltonians of the dimer integrable systems are identical under the birational transformation in (21.12),

$$H^{(8a)} = H^{(9a)} . \tag{21.18}$$

By identifying (10.5) with (11.5), we also obtain the following canonical transformation,

$$e^{Q^{(8a)}} = \frac{z_5^{(9a)}z_6^{(9a)}}{z_2^{(9a)}}e^{Q^{(9a)}-P^{(9a)}} \ , \ e^{P^{(8a)}} = e^{Q^{(9a)}} . \tag{21.19}$$

We conclude that the dimer integrable systems for Model 8a and Model 9a are birationally equivalent to each other.

21.4 Model 8b to Model 9b

Let us refer to the spectral curve in (10.22) for Model 8b as $\Sigma^{(8b)}$ and the spectral curve in (11.22) for Model 9b as $\Sigma^{(9b)}$.

Under the following birational transformation,

$$\varphi_{M;A;N} = M \circ \varphi_A \circ N \ : \ (x,y) \mapsto \left(\frac{x}{z_5^{(8b)}}, \frac{1}{(1 + \frac{z_1^{(8b)}}{z_5^{(8b)}}x)y} \right) , \qquad (21.20)$$

where

$$M \ : \ (x,y) \mapsto \left(x, \frac{1}{y} \right) , \quad \varphi_A \ : \ (x,y) \mapsto \left(x, (1 + z_1^{(8a)}x)y \right) ,$$
$$N \ : \ (x,y) \mapsto \left(\frac{x}{z_5^{(8a)}}, y \right) , \qquad (21.21)$$

we discover that the spectral curve $\Sigma^{(8b)}$ in (10.22) is mapped to $\Sigma^{(9b)}$ in (11.22),

$$\varphi_{M;A;N}\Sigma^{(8b)} = \Sigma^{(9b)} . \qquad (21.22)$$

Based on this map, we have the following identifications between the zig-zag paths,

$$z_1^{(8b)} = z_6^{(9b)} , \ z_2^{(8b)} = z_2^{(9b)-1}z_3^{(9b)}z_6^{(9b)-2} , \ z_3^{(8b)} = z_1^{(9b)}z_2^{(9b)}z_6^{(9b)} ,$$
$$z_4^{(8b)} = z_5^{(9b)} , \ z_5^{(8b)} = z_2^{(9b)}z_6^{(9b)} , \ z_6^{(8b)} = z_4^{(9b)} , \qquad (21.23)$$

as well as between the face paths,

$$f_1^{(8b)} = f_6^{(9b)} , \ f_2^{(8b)} = f_4^{(9b)} , \ f_3^{(8b)} = f_5^{(9b)} ,$$
$$f_4^{(8b)} = f_3^{(9b)} , \ f_5^{(8b)} = f_2^{(9b)} , \ f_6^{(8b)} = f_1^{(9b)} . \qquad (21.24)$$

Moreover, the 1-loops of the two dimer integrable systems are identified as follows,

$$\gamma_u^{(8b)} = \gamma_u^{(9b)} , \qquad (21.25)$$

for all $u = 1, \ldots, 7$. This implies that the two Hamiltonians of the dimer integrable systems are identical under the birational transformation in (21.20),

$$H^{(8b)} = H^{(9b)} . \qquad (21.26)$$

By identifying (10.18) with (11.18), we also obtain the following canonical transformation,

$$e^{Q^{(8b)}} = z_1^{(9b)}z_3^{(9b)}z_5^{(9b)}e^{-Q^{(9b)}-P^{(9b)}} , \ e^{P^{(8b)}} = e^{Q^{(9b)}} . \qquad (21.27)$$

We conclude that the dimer integrable systems for Model 8b and Model 9b are birationally equivalent to each other.

21.5 Model 9a to Model 10a

Let us refer to the spectral curve in (11.9) for Model 9a as $\Sigma^{(9a)}$ and the spectral curve in (12.9) for Model 10a as $\Sigma^{(10a)}$.

Under the following birational transformation,

$$\varphi_{A;N} = \varphi_A \circ N \; : \; (x, y) \mapsto \left(z_1^{(9a)} z_3^{(9a)} z_4^{(9a)} \frac{(1 + z_6^{(9a)} y)}{x}, y \right) , \qquad (21.28)$$

where

$$\varphi_A \; : \; (x, y) \mapsto \left(z_1^{(9a)} z_3^{(9a)} z_4^{(9a)} (1 + z_6^{(9a)} y) x, y \right) , \; N \; : \; (x, y) \mapsto \left(\frac{1}{x}, y \right) , \quad (21.29)$$

we discover that the spectral curve $\Sigma^{(9a)}$ in (11.9) is mapped to $\Sigma^{(10a)}$ in (12.9),

$$\varphi_{A;N} \Sigma^{(9a)} = \Sigma^{(10a)} . \qquad (21.30)$$

Based on this map, we have the following identifications between the zig-zag paths,

$$z_1^{(9a)} = z_5^{(10a)} z_6^{(10a)} \; , \; z_2^{(9a)} = z_4^{(10a)} \; , \; z_3^{(9a)} = \frac{1}{z_6^{(10a)}} \; ,$$
$$z_4^{(9a)} = z_1^{(10a)} z_6^{(10a)} \; , \; z_5^{(9a)} = z_3^{(10a)} \; , \; z_6^{(9a)} = z_2^{(10a)} \; , \qquad (21.31)$$

as well as between the face paths,

$$f_1^{(9a)} = f_4^{(10a)} \; , \; f_2^{(9a)} = f_2^{(10a)} \; , \; f_3^{(9a)} = f_3^{(10a)} \; ,$$
$$f_4^{(9a)} = f_5^{(10a)} \; , \; f_5^{(9a)} = f_1^{(10a)} \; , \; f_6^{(9a)} = f_6^{(10a)} \; . \qquad (21.32)$$

Moreover, the 1-loops of the two dimer integrable systems are identified as follows,

$$\gamma_u^{(9a)} = \gamma_u^{(10a)} , \qquad (21.33)$$

for all $u = 1, \ldots, 6$. This implies that the two Hamiltonians of the dimer integrable systems are identical under the birational transformation in (21.28),

$$H^{(9a)} = H^{(10a)} . \qquad (21.34)$$

By identifying (11.5) with (12.5), we also obtain the following canonical transformation,

$$e^{Q^{(9a)}} = z_4^{(10a)} z_5^{(10a)} z_6^{(10a)} e^{-Q^{(10a)} - P^{(10a)}} \; , \; e^{P^{(9a)}} = z_3^{(10a)} z_5^{(10a)} e^{-P^{(10a)}} \; . \qquad (21.35)$$

We conclude that the dimer integrable systems for Model 9a and Model 10a are birationally equivalent to each other.

21.6 Model 9b to Model 10b

Let us refer to the spectral curve in (11.22) for Model 9b as $\Sigma^{(9b)}$ and the spectral curve in (12.22) for Model 10b as $\Sigma^{(10b)}$.

Under the following birational transformation,

$$\varphi_{A;N} = \varphi_A \circ N \ : \ (x, y) \mapsto \left(\frac{(\frac{1}{y} + z_5^{(9b)})x}{z_5^{(9b)}}, \frac{1}{y} \right) , \tag{21.36}$$

where

$$\varphi_A \ : \ (x, y) \mapsto \left(x, \frac{(y + z_5^{(9b)})}{z_5^{(9b)}} x \right) , \ N \ : \ (x, y) \mapsto \left(x, \frac{1}{y} \right) , \tag{21.37}$$

we discover that the spectral curve $\Sigma^{(9b)}$ in (11.22) is mapped to $\Sigma^{(10b)}$ in (12.22),

$$\varphi_{A;N} \Sigma^{(9b)} = \Sigma^{(10b)} . \tag{21.38}$$

Based on this map, we have the following identifications between the zig-zag paths,

$$z_1^{(9b)} = z_1^{(10b)} \ , \ z_2^{(9b)} = z_2^{(10b)} z_3^{(10b)} \ , \ z_3^{(9b)} = z_3^{(10b)} z_5^{(10b)} \ ,$$
$$z_4^{(9b)} = z_6^{(10b)} \ , \ z_5^{(9b)} = \frac{1}{z_3^{(10b)}} \ , \ z_6^{(9b)} = z_4^{(10b)} . \tag{21.39}$$

as well as between the face paths,

$$f_1^{(9b)} = f_2^{(10b)} \ , \ f_2^{(9b)} = f_4^{(10b)} \ , \ f_3^{(9b)} = f_3^{(10b)} \ ,$$
$$f_4^{(9b)} = f_1^{(10b)} \ , \ f_5^{(9b)} = f_5^{(10b)} \ , \ f_6^{(9b)} = f_6^{(10b)} . \tag{21.40}$$

Moreover, the 1-loops of the two dimer integrable systems are identified as follows,

$$\gamma_u^{(9b)} = \gamma_u^{(10b)} , \tag{21.41}$$

for all $u = 1, \ldots, 7$. This implies that the two Hamiltonians of the dimer integrable systems are identical under the birational transformation in (21.20),

$$H^{(9b)} = H^{(10b)} . \tag{21.42}$$

By identifying (11.18) with (12.18), we also obtain the following canonical transformation,

$$e^{Q^{(9b)}} = z_1^{(10b)} z_5^{(10b)} e^{-Q^{(10b)} + P^{(10b)}} \ , \ e^{P^{(9b)}} = e^{-P^{(10b)}} . \tag{21.43}$$

We conclude that the dimer integrable systems for Model 9b and Model 10b are birationally equivalent to each other.

21.7 Model 9c to Model 10c

Let us refer to the spectral curve in (11.35) for Model 9c as $\Sigma^{(9c)}$ and the spectral curve in (12.35) for Model 10c as $\Sigma^{(10c)}$.

Under the following birational transformation,

$$\varphi_{A;N} = \varphi_A \circ N \ : \ (x,y) \mapsto \left(\frac{(\frac{1}{y} + z_5^{(9c)})x}{z_5^{(9c)}}, \frac{1}{y} \right) , \tag{21.44}$$

where

$$\varphi_A \ : \ (x,y) \mapsto \left(x, \frac{(y + z_5^{(9c)})}{z_5^{(9c)}}x \right) , \quad N \ : \ (x,y) \mapsto \left(x, \frac{1}{y} \right) , \tag{21.45}$$

we discover that the spectral curve $\Sigma^{(9c)}$ in (11.35) is mapped to $\Sigma^{(10c)}$ in (12.35),

$$\varphi_{A;N} \Sigma^{(9c)} = \Sigma^{(10c)} . \tag{21.46}$$

Based on this map, we have the following identifications between the zig-zag paths,

$$\begin{aligned} z_1^{(9c)} = z_6^{(10c)} \ &, \ z_2^{(9c)} = z_1^{(10c)} z_2^{(10c)} \ , \ z_3^{(9c)} = z_1^{(10c)} z_5^{(10c)} \ , \\ z_4^{(9c)} = z_3^{(10c)} \ &, \ z_5^{(9c)} = \frac{1}{z_1^{(10c)}} \ , \ z_6^{(9c)} = z_4^{(10c)} \ , \end{aligned} \tag{21.47}$$

as well as between the face paths,

$$\begin{aligned} f_1^{(9c)} = f_1^{(10c)} \ , \ f_2^{(9c)} = f_4^{(10c)} \ , \ f_3^{(9c)} = f_3^{(10c)} \ , \\ f_4^{(9c)} = f_2^{(10c)} \ , \ f_5^{(9c)} = f_5^{(10c)} \ , \ f_6^{(9c)} = f_6^{(10c)} \ . \end{aligned} \tag{21.48}$$

Moreover, the 1-loops of the two dimer integrable systems are identified as follows,

$$\gamma_u^{(9c)} = \gamma_u^{(10c)} , \tag{21.49}$$

for all $u = 1, \ldots, 8$. This implies that the two Hamiltonians of the dimer integrable systems are identical under the birational transformation in (21.20),

$$H^{(9c)} = H^{(10c)} . \tag{21.50}$$

By identifying (11.31) with (12.31), we also obtain the following canonical transformation,

$$e^{Q^{(9c)}} = \frac{1}{z_1^{(10c)} z_3^{(10c)}} e^{Q^{(10c)}} \ , \ e^{P^{(9c)}} = e^{P^{(10c)}} . \tag{21.51}$$

We conclude that the dimer integrable systems for Model 9c and Model 10c are birationally equivalent to each other.
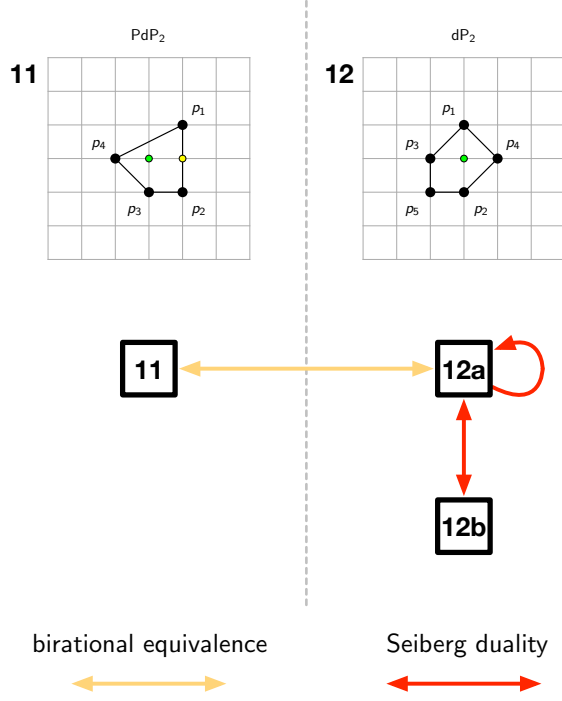
22 Bucket 4

Figure 41: Brane tilings and toric diagrams in Bucket 4.

22.1 Hilbert series and generators of the mesonic moduli spaces

Figure 41 illustrates how birational transformations relate brane tilings in bucket 4. From [15], we have the refined Hilbert series of the mesonic moduli spaces of these brane tilings in bucket 4 in terms of fugacities t_a corresponding to GLSM fields p_a. These refined Hilbert series take the following form,

$$
\begin{aligned}
g(t_a; \mathcal{M}^{mes}_{\text{Model 11}}) = & \frac{1}{(1 - t_1^3 t_2)(1 - t_2^4 t_3^3)(1 - t_1^2 t_4)(1 - t_3 t_4^2)} \\
& \times (1 + t_1^2 t_2^2 t_3 + t_1 t_2^3 t_3^2 + t_1 t_2 t_3 t_4 - t_1^4 t_2^2 t_3 t_4 + t_2^2 t_3^2 t_4 \\
& \quad - t_1^3 t_2^3 t_3^2 t_4 - t_1^3 t_2 t_3 t_4^2 - t_1^2 t_2^2 t_3^2 t_4^2 - t_1^4 t_2^4 t_3^3 t_4^2) \ , \\
g(t_a; \mathcal{M}^{mes}_{\text{Model 12a, 12b}}) = & \frac{1}{(1 - t_1^2 t_3 t_4)(1 - t_1 t_2 t_4^2)(1 - t_1^2 t_3^2 t_5)(1 - t_2^2 t_4^2 t_5)(1 - t_2^2 t_3^2 t_5^3)} \\
& \times (1 + t_1 t_2 t_3 t_4 t_5 - t_1^3 t_2 t_3^2 t_4^2 t_5 - t_1^2 t_2^2 t_3 t_4^3 t_5 + t_1 t_2 t_3^2 t_5^2 + t_2^2 t_3 t_4 t_5^2 \\
& \quad - t_1^3 t_2 t_3^3 t_4 t_5^2 - 2 t_1^2 t_2^2 t_3^2 t_4^2 t_5^2 - t_1 t_2^3 t_3 t_4^3 t_5^2 + t_1^4 t_2^2 t_3^3 t_4^3 t_5^2 + t_1^3 t_2^3 t_3^2 t_4^4 t_5^2 \\
& \quad - t_1^2 t_2^2 t_3^3 t_4 t_5^3 - t_1 t_2^3 t_3^2 t_4^2 t_5^3 + t_1^3 t_2^3 t_3^3 t_4^3 t_5^3 + t_1^4 t_2^4 t_3^4 t_4^4 t_5^4) \ , \quad (22.1)
\end{aligned}
$$

where we note that brane tilings related by Seiberg duality have the same mesonic moduli space and therefore the same corresponding Hilbert series.

Model 11		
GLSM	$U(1)_R$	fugacity
p_1	$2r$	$t_1 = \bar{t}^2$
p_2	r	$t_2 = \bar{t}$
p_3	r	$t_3 = \bar{t}$
p_4	$3r$	$t_4 = \bar{t}^3$

Model 12a, 12b		
GLSM	$U(1)_R$	fugacity
p_1	$2r$	$t_1 = \bar{t}^2$
p_2	r	$t_2 = \bar{t}$
p_3	r	$t_3 = \bar{t}$
p_4	$2r$	$t_4 = \bar{t}^2$
p_5	r	$t_5 = \bar{t}$

Table 7: $U(1)_R$ charge assignment on GLSM fields of birationally related brane tilings in bucket 4 such that the $U(1)_R$ charge of the superpotentials is $7r = 2$ and that the generators of the mesonic moduli spaces have all $U(1)_R$ charge $7r$.

Under the $U(1)_R$ charge assignment on the GLSM fields summarized in Table 7, the superpotentials of the brane tilings in bucket 4 have all $U(1)_R$ charge $7r = 2$ and the generators of the mesonic moduli spaces have all $U(1)_R$ charge $7r$. Using this $U(1)_R$ charge assignment, the refined Hilbert series in (22.1) can be rewritten in terms of a single fugacity $\bar{t}$ corresponding to $U(1)_R$ charge r. We note here that the Hilbert series in terms of the fugacity $\bar{t}$ takes the following form for all brane tilings in bucket 4,

$$g(\bar{t}; \mathcal{M}^{mes}_{\text{bucket 4}}) = \frac{1 + 5\bar{t}^7 + \bar{t}^{14}}{(1 - \bar{t}^7)^3} \ , \tag{22.2}$$

confirming that birational transformations relating brane tilings in bucket 4 preserve the Hilbert series when it is refined only under $U(1)_R$.

Using the results in [15], we also note that the brane tilings in bucket 4 all have mesonic moduli spaces with 8 generators. This can be seen by taking the plethystic logarithm [60–64] of the Hilbert series in (22.2), which gives,

$$PL[g(\bar{t}; \mathcal{M}^{mes}_{\text{bucket 4}})] = 8\bar{t}^7 - 14\bar{t}^{14} + 35\bar{t}^{21} + \dots \ . \tag{22.3}$$

This confirms that the number of generators is 8 for all mesonic moduli spaces in bucket 4.

In the following sections, we illustrate how brane tilings in bucket 4 define dimer integrable systems that are equivalent under birational transformations.

22.2 Model 11 to Model 12a

Let us refer to the spectral curve in (13.9) for Model 11 as $\Sigma^{(11)}$ and the spectral curve in (14.9) for Model 12a as $\Sigma^{(12a)}$.

Under the following birational transformation,

$$\varphi_{A;M;N} = M \circ \varphi_A \circ N \ : \ (x,y) \mapsto \left(\frac{z_3^{(11)}x}{z_3^{(11)} + xy}, xy \right) , \qquad (22.4)$$

where

$$M \ : \ (x,y) \mapsto \left(\frac{1}{x}, y \right) , \quad \varphi_A \ : \ (x,y) \mapsto \left(\frac{(y + z_3^{(11)})}{z_3^{(11)}}x, y \right) , \quad N \ : \ (x,y) \mapsto \left(\frac{1}{x}, xy \right) , \qquad (22.5)$$

we discover that the spectral curve $\Sigma^{(11)}$ in (13.9) is mapped to $\Sigma^{(12a)}$ in (14.9),

$$\varphi_{A;M;N}\Sigma^{(11)} = \Sigma^{(12a)} . \qquad (22.6)$$

Based on this map, we have the following identifications between the zig-zag paths,

$$z_1^{(11)} = \frac{z_5^{(12a)}}{z_1^{(12a)}z_2^{(12a)}z_4^{(12a)}} \ , \quad z_2^{(11)} = z_4^{(12a)} \ , \quad z_3^{(11)} = \frac{1}{z_5^{(12a)}} \ , \quad z_4^{(11)} = z_2^{(12a)} \ , \quad z_5^{(11)} = z_1^{(12a)} \ , \qquad (22.7)$$

as well as between the face paths,

$$f_1^{(11)} = f_5^{(12a)} \ , \quad f_2^{(11)} = f_4^{(12a)} \ , \quad f_3^{(11)} = f_1^{(12a)} \ , \quad f_4^{(11)} = f_3^{(12a)} \ , \quad f_5^{(11)} = f_2^{(12a)} \ . \qquad (22.8)$$

Moreover, the 1-loops of the two dimer integrable systems are identified as follows,

$$\gamma_u^{(11)} = \gamma_u^{(12a)} \ , \qquad (22.9)$$

for all $u = 1, \ldots, 5$. This implies that the two Hamiltonians of the dimer integrable systems are identical under the birational transformation in (22.4),

$$H^{(11)} = H^{(12a)} . \qquad (22.10)$$

By identifying (13.5) with (14.5), we also obtain the following canonical transformation,

$$e^{Q^{(11)}} = e^{-Q^{(12a)}+P^{(12a)}} \frac{z_1^{(12a)}}{z_4^{(12a)}z_5^{(12a)}} \ , \quad e^{P^{(11)}} = e^{-2Q^{(12a)}+P^{(12a)}} \frac{z_1^{(12a)}}{z_4^{(12a)}z_5^{(12a)}} \ . \qquad (22.11)$$

We conclude that the dimer integrable systems for Model 11 and Model 12a are birationally equivalent to each other.
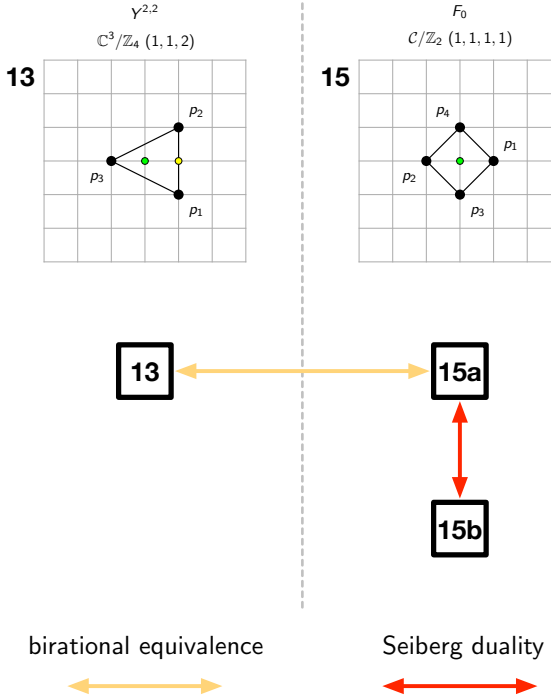
23 Bucket 5

Figure 42: Brane tilings and toric diagrams in Bucket 5.

23.1 Hilbert series and generators of the mesonic moduli spaces

Figure 42 illustrates how brane tilings in bucket 5 are related by birational transformations. Using the results in [15], we have the refined Hilbert series of the mesonic moduli spaces of the brane tilings in bucket 4 in terms of fugacities t_a corresponding to GLSM fields p_a. These refined Hilbert series are as follows,

$$
g(t_a; \mathcal{M}^{mes}_{\text{Model 13}}) = \frac{1 + t_1^3 t_2 + t_1^2 t_2^2 + t_1 t_2^3 + t_1^2 t_3 + t_1 t_2 t_3 + t_2^2 t_3 + t_1^3 t_2^3 t_3}{(1 - t_1^4)(1 - t_2^4)(1 - t_3^2)} ,
$$
$$
\begin{aligned}
g(t_a; \mathcal{M}^{mes}_{\text{Model 15a, 15b}}) = &\frac{1 - t_1 t_2 t_3 t_4}{(1 - t_1^2 t_3^2)(1 - t_2^2 t_3^2)(1 - t_1^2 t_4^2)(1 - t_2^2 t_4^2)} \\
&\times (1 + t_1 t_2 t_3^2 + t_1^2 t_3 t_4 + 2 t_1 t_2 t_3 t_4 + t_2^2 t_3 t_4 \\
&\quad + t_1 t_2 t_4^2 + t_1^2 t_2^2 t_3^2 t_4^2) ,
\end{aligned} \tag{23.1}
$$

where we note that brane tilings related by Seiberg duality have the same mesonic moduli space and Hilbert series.

Model 13		
GLSM	$U(1)_R$	fugacity
p_1	r	$t_1 = \bar{t}$
p_2	r	$t_2 = \bar{t}$
p_3	$2r$	$t_3 = \bar{t}^2$

Model 15a, 15b		
GLSM	$U(1)_R$	fugacity
p_1	r	$t_1 = \bar{t}$
p_2	r	$t_2 = \bar{t}$
p_3	r	$t_3 = \bar{t}$
p_4	r	$t_4 = \bar{t}$

Table 8: $U(1)_R$ charge assignment on GLSM fields of birationally related brane tilings in bucket 5 such that the $U(1)_R$ charge of the superpotentials is $4r = 2$ and that the generators of the mesonic moduli spaces have all $U(1)_R$ charge $4r$.

Table 8 summarizes a $U(1)_R$ charge assignment in terms of $U(1)_R$ charge r on the GLSM fields such that the superpotentials of the brane tilings in bucket 5 all have $U(1)_R$ charge $4r = 2$ and the generators of the mesonic moduli spaces have all $U(1)_R$ charge $4r$. In terms of this $U(1)_R$ charge assignment, the refined Hilbert series in (23.1) can be expressed in terms of a single fugacity $\bar{t}$ corresponding to $U(1)_R$ charge r. We note here that the Hilbert series in terms of $\bar{t}$ all become,

$$g(\bar{t}; \mathcal{M}^{mes}_{\text{bucket 5}}) = \frac{1 + 6\bar{t}^4 + \bar{t}^8}{(1 - \bar{t}^4)^3} \ , \tag{23.2}$$

which confirms that brane tilings related by birational transformations in bucket 5 share the same Hilbert series refined only under $U(1)_R$.

By further using the results in [15], we note that the brane tilings in bucket 5 all have mesonic moduli spaces with 9 generators. We can see this also by taking the plethystic logarithm [60–64] of the Hilbert series in (23.2), which takes the form,

$$PL[g(\bar{t}; \mathcal{M}^{mes}_{\text{bucket 5}})] = 9\bar{t}^4 - 20\bar{t}^8 + 64\bar{t}^{12} + \dots \ . \tag{23.3}$$

We note here that the above plethystic logarithm confirms that the number of generators is 9 for all mesonic moduli spaces of brane tilings in bucket 5.

The following sections illustrate how brane tilings in bucket 5 define dimer integrable systems that are equivalent under birational transformations.

23.2 Model 13 to Model 15a

Let us refer to the spectral curve in (15.9) for Model 13 as $\Sigma^{(13)}$ and the spectral curve in (17.9) for Model 15a as $\Sigma^{(15a)}$.

Under the following birational transformation,

$$\varphi_{A;M;N} = M \circ \varphi_A \circ N \ : \ (x,y) \mapsto \left(\frac{z_4^{(13)}}{(\frac{y}{x} + z_4^{(13)})x}, \frac{y}{x} \right) , \tag{23.4}$$

where

$$M \ : \ (x,y) \mapsto \left(\frac{1}{x}, y \right) , \ N \ : \ (x,y) \mapsto \left(x, \frac{y}{x} \right) ,$$

$$\varphi_A \ : \ (x,y) \mapsto \left(\frac{(y+z_4^{(13)})}{z_4^{(13)}}x, y \right) , \tag{23.5}$$

we discover that the spectral curve $\Sigma^{(13)}$ in (15.9) is mapped to $\Sigma^{(15a)}$ in (17.9),

$$\varphi_{A;M;N}\Sigma^{(13)} = \Sigma^{(15a)} . \tag{23.6}$$

Based on this map, we have the following identifications between the zig-zag paths,

$$z_1^{(13)} = \frac{1}{z_1^{(15a)}} \ , \ z_2^{(13)} = \frac{z_1^{(15a)}z_2^{(15a)}}{z_4^{(15a)}} \ , \ z_3^{(13)} = \frac{1}{z_2^{(15a)}} \ , \ z_4^{(13)} = z_4^{(15a)} \ , \tag{23.7}$$

as well as between the face paths,

$$f_1^{(13)} = f_4^{(15a)} \ , \ f_2^{(13)} = f_1^{(15a)} \ , \ f_3^{(13)} = f_2^{(15a)} \ , \ f_4^{(13)} = f_3^{(15a)} \ . \tag{23.8}$$

Moreover, the 1-loops of the two dimer integrable systems are identified as follows,

$$\gamma_u^{(13)} = \gamma_u^{(15a)} \ , \tag{23.9}$$

for all $u = 1, \ldots, 4$. This implies that the two Hamiltonians of the dimer integrable systems are identical under the birational transformation in (23.4),

$$H^{(13)} = H^{(15a)} . \tag{23.10}$$

By identifying (15.13) with (17.13), we also obtain the following canonical transformation,

$$e^{Q^{(13)}} = e^{2P^{(15a)}} z_2^{(15a)} z_4^{(15a)} \ , \ e^{P^{(13)}} = \left(e^{Q^{(15a)}} \right)^{1/2} . \tag{23.11}$$

We conclude that the dimer integrable systems for Model 13 and Model 15a are birationally equivalent to each other.
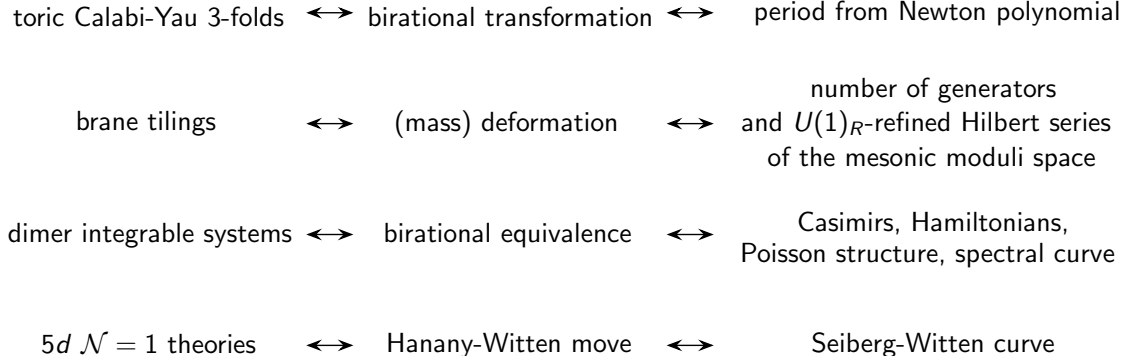
24 Conclusions and Discussions

toric Calabi-Yau 3-folds   ⟷   birational transformation   ⟷   period from Newton polynomial

brane tilings   ⟷   (mass) deformation   ⟷   number of generators
and $U(1)_R$-refined Hilbert series
of the mesonic moduli space

dimer integrable systems   ⟷   birational equivalence   ⟷   Casimirs, Hamiltonians,
Poisson structure, spectral curve

$5d$ $\mathcal{N} = 1$ theories   ⟷   Hanany-Witten move   ⟷   Seiberg-Witten curve

Figure 43: The correspondence between birational transformations of toric Calabi-Yau 3-folds and their toric varieties, deformations of brane tilings, birational equivalence between dimer integrable systems, and Hanany-Witten moves for $5d$ $\mathcal{N} = 1$ theories.

In this work, we present a complete classification of dimer integrable systems that correspond to the 16 reflexive polygons in 2 dimensions. The reflexive polygons are toric diagrams of toric Calabi-Yau 3-folds and each of the dimer integrable systems in the classification correspond to a brane tiling associated to these toric Calabi-Yau 3-folds. The classification contains 30 dimer integrable systems and is based on the 30 brane tilings in the classification in [15]. There are more brane tilings and associated dimer integrable systems than toric Calabi-Yau 3-folds because when the associated brane tilings are related by Seiberg duality then they correspond to the same toric Calabi-Yau 3-fold and the corresponding dimer integrable systems are equivalent under a canonical transformation [4].

In our classification, we present for each dimer integrable system the Casimirs, the single Hamiltonian, the spectral curve and the Poisson commutation relations. In order to express these, we make use of directed paths along edges in the bipartite periodic graph on the 2-torus given by the associated brane tiling, including zig-zag paths and paths around faces of the brane tiling. The dimer integrable systems in our classification contain only a single Hamiltonian because the corresponding toric diagrams are reflexive and have a single internal vertex corresponding to the Hamiltonian.

As part of our classification, we identify 16 pairs of birationally equivalent dimer integrable systems. Equivalence between dimer integrable systems via birational transformations between the associated toric Calabi-Yau 3-folds and brane tilings has been first studied in [13]. In our work, we give explicit expressions for the birational transformations that map the Casimirs, the Hamiltonian, the spectral curve and the Poisson commutation relations between birationally equivalent dimer integrable systems. Combined with equivalence due to Seiberg duality of the associated brane tilings, birational equivalence subdivides the dimer integrable systems in our classification into 5 equivalence classes that we call buckets [38].

Similar to observations made in [59] in the context of generalized toric polygons (GTPs) and in [41, 42] in the context of brane brick models corresponding to $2d$ $(0, 2)$ supersymmetric gauge theories and toric Calabi-Yau 4-folds [45–50], we have shown in our work that birational transformations between brane tilings and dimer integrable systems preserve the number of generators of the mesonic moduli spaces associated to the brane tilings as well as the Hilbert series of the mesonic moduli space refined under the $U(1)_R$ symmetry. We note that deformations of brane tilings [53–55] that also include mass deformations [56–58] correspond to these birational transformations.

As a final comment, we note here that the deformations of the brane tilings corresponding to birational transformations of the associated toric Calabi-Yau 3-folds and toric varieties have an interpretation in terms of $5d$ superconformal field theories defined by the dual (p, q) web of the toric diagrams [17, 54, 59, 80–87]. The deformation of the brane tilings [53–55, 58] associated to birational transformations is realized as a Hanany-Witten move [88] in the dual (p, q) web diagram which reverses a semi-infinite 5-brane. With our work, we further strengthen the correspondence between the $5d$ $\mathcal{N} = 1$ theories associated to (p, q) web diagrams, brane tilings associated to toric Calabi-Yau 3-folds, and dimer integrable systems. The Hanany-Witten move on the (p, q) web diagram associated to birational transformations of corresponding brane tilings and dimer integrable systems preserves based on our classification not only the number of generators and $U(1)_R$-refined Hilbert series of the mesonic moduli space, but also the dimer integrable system itself with its Casimirs, Hamiltonians, spectral curve and Poisson commutation relations. We note here that the spectral curve of birationally equivalent dimer integrable systems are mapped to each other by birational transformations and correspond to Seiberg-Witten curves [89–93] of the $5d$ $\mathcal{N} = 1$ theories related by a Hanany-Witten move. We summarize the relationships in Figure 43.

Acknowledgments

References

[1] A. Hanany and K. D. Kennaway, *Dimer models and toric diagrams*, `hep-th/0503149`.

[2] S. Franco, A. Hanany, K. D. Kennaway, D. Vegh and B. Wecht, *Brane dimers and quiver gauge theories*, *JHEP* **01** (2006) 096, [`hep-th/0504110`].

[3] S. Franco, A. Hanany, D. Martelli, J. Sparks, D. Vegh and B. Wecht, *Gauge theories from toric geometry and brane tilings*, *JHEP* **01** (2006) 128, [`hep-th/0505211`].

[4] A. B. Goncharov and R. Kenyon, *Dimers and cluster integrable systems*, 2012.

[5] R. Eager, S. Franco and K. Schaeffer, *Dimer Models and Integrable Systems*, *JHEP* **06** (2012) 106, [`1107.1244`].

[6] R. Kenyon, *Local statistics of lattice dimers*, *Annales de l'Institut Henri Poincare (B) Probability and Statistics* **33** (1997) 591–618.

[7] R. Kenyon, *An introduction to the dimer model*, 2003.

[8] M. Bershtein, P. Gavrylenko and A. Marshakov, *Cluster integrable systems, q-Painlevé equations and their quantization*, *JHEP* **02** (2018) 077, [`1711.02063`].

[9] A. Marshakov and M. Semenyakin, *Cluster integrable systems and spin chains*, *JHEP* **10** (2019) 100, [`1905.09921`].

[10] N. Lee, *New dimer integrable systems and defects in five dimensional gauge theory*, *JHEP* **12** (2024) 050, [`2312.13133`].

[11] K. Lee and N. Lee, *Dimers for type D relativistic Toda model*, *JHEP* **09** (2024) 198, [`2406.00925`].

[12] M. Bershtein, P. Gavrylenko, A. Marshakov and M. Semenyakin, *Cluster Reductions, Mutations, and q-Painlevé Equations*, `2411.00325`.

[13] M. Kho, N. Lee and R.-K. Seong, *Birational transformations on dimer integrable systems*, *Phys. Rev. D* **112** (2025) L041901, [`2504.21081`].

[14] K. Lee and N. Lee, *Dimers for Relativistic Toda Models with Reflective Boundaries*, 2510.01768.

[15] A. Hanany and R.-K. Seong, *Brane Tilings and Reflexive Polygons*, *Fortsch. Phys.* **60** (2012) 695–803, [1201.2614].

[16] W. Fulton, *Introduction to toric varieties*. No. 131. Princeton university press, 1993.

[17] N. C. Leung and C. Vafa, *Branes and toric geometry*, *Adv. Theor. Math. Phys.* **2** (1998) 91–118, [hep-th/9711013].

[18] Y.-H. He, R.-K. Seong and S.-T. Yau, *Calabi–Yau Volumes and Reflexive Polytopes*, *Commun. Math. Phys.* **361** (2018) 155–204, [1704.03462].

[19] D. Krefl and R.-K. Seong, *Machine Learning of Calabi-Yau Volumes*, *Phys. Rev. D* **96** (2017) 066014, [1706.03346].

[20] E. Choi and R.-K. Seong, *Machine learning regularization for the minimum volume formula of toric Calabi-Yau 3-folds*, *Phys. Rev. D* **109** (2024) 046015, [2310.19276].

[21] J. Bao, E. Choi, Y.-H. He, R.-K. Seong and S.-T. Yau, *Futaki Invariants and Reflexive Polygons*, 2410.18476.

[22] V. V. Batyrev, *Dual Polyhedra and Mirror Symmetry for Calabi-Yau Hypersurfaces in Toric Varieties*, *arXiv e-prints* (Oct., 1993) alg–geom/9310003, [alg-geom/9310003].

[23] V. V. Batyrev and L. A. Borisov, *Dual Cones and Mirror Symmetry for Generalized Calabi-Yau Manifolds*, *arXiv e-prints* (Feb., 1994) alg–geom/9402002, [alg-geom/9402002].

[24] M. Kreuzer and H. Skarke, *Classification of reflexive polyhedra in three-dimensions*, *Adv. Theor. Math. Phys.* **2** (1998) 853–871, [hep-th/9805190].

[25] M. Kreuzer and H. Skarke, *Reflexive polyhedra, weights and toric Calabi-Yau fibrations*, *Rev. Math. Phys.* **14** (2002) 343–374, [math/0001106].

[26] M. Kreuzer and H. Skarke, *Complete classification of reflexive polyhedra in four-dimensions*, *Adv. Theor. Math. Phys.* **4** (2000) 1209–1230, [hep-th/0002240].

[27] B. Feng, A. Hanany and Y.-H. He, *Phase structure of D-brane gauge theories and toric duality*, *JHEP* **08** (2001) 040, [hep-th/0104259].

[28] B. Feng, A. Hanany and Y.-H. He, *D-brane gauge theories from toric singularities and toric duality*, *Nucl. Phys. B* **595** (2001) 165–200, [hep-th/0003085].

[29] B. Feng, S. Franco, A. Hanany and Y.-H. He, *UnHiggsing the del Pezzo*, *JHEP* **08** (2003) 058, [hep-th/0209228].

[30] B. Feng, S. Franco, A. Hanany and Y.-H. He, *Symmetries of toric duality*, *JHEP* **12** (2002) 076, [hep-th/0205144].

[31] J. Davey, A. Hanany and R.-K. Seong, *Counting Orbifolds*, *JHEP* **06** (2010) 010, [1002.3609].

[32] A. Hanany and R.-K. Seong, *Symmetries of Abelian Orbifolds*, *JHEP* **01** (2011) 027, [1009.3017].

[33] N. Seiberg, *Electric - magnetic duality in supersymmetric nonAbelian gauge theories*, *Nucl. Phys. B* **435** (1995) 129–146, [hep-th/9411149].

[34] B. Feng, A. Hanany, Y.-H. He and A. M. Uranga, *Toric duality as Seiberg duality and brane diamonds*, *JHEP* **12** (2001) 035, [hep-th/0109063].

[35] C. E. Beasley and M. R. Plesser, *Toric duality is Seiberg duality*, *JHEP* **12** (2001) 001, [hep-th/0109053].

[36] S. Galkin and A. Usnich, *Mutations of potentials*, preprint IPMU **10** (2010) 0100.

[37] N. O. Ilten, *Mutations of Laurent Polynomials and Flat Families with Toric Fibers*, *SIGMA* **8** (July, 2012) 047, [1205.4664].

[38] M. Akhtar, T. Coates, S. Galkin, A. M. Kasprzyk et al., *Minkowski polynomials and mutations*, SIGMA. Symmetry, Integrability and Geometry: Methods and Applications **8** (2012) 094.

[39] C. Birkar, *Birational geometry of algebraic varieties*, *arXiv e-prints* (Dec., 2017) arXiv:1801.00013, [1801.00013].

[40] T. Coates, A. M. Kasprzyk, G. Pitton and K. Tveiten, *Maximally mutable Laurent polynomials*, *Proceedings of the Royal Society of London Series A* **477** (Sept., 2021) 20210584, [2107.14253].

[41] D. Ghim, M. Kho and R.-K. Seong, *Combinatorial and algebraic mutations of toric Fano 3-folds and mass deformations of 2d(0,2) quiver gauge theories*, *Phys. Rev. D* **110** (2024) 086001, [2407.19924].

[42] D. Ghim, M. Kho and R.-K. Seong, *Birational transformations and 2d (0, 2) quiver gauge theories beyond toric Fano 3-folds*, *JHEP* **06** (2025) 032, [2502.08741].

[43] M. Ciucu, *A complementation theorem for perfect matchings of graphs having a cellular completion*, *Journal of Combinatorial Theory, Series A* **81** (1998) 34–68.

[44] R. W. Kenyon, J. G. Propp and D. B. Wilson, *Trees and Matchings*, *arXiv Mathematics e-prints* (Mar., 1999) math/9903025, [math/9903025].

[45] S. Franco, D. Ghim, S. Lee, R.-K. Seong and D. Yokoyama, *2d (0,2) Quiver Gauge Theories and D-Branes*, *JHEP* **09** (2015) 072, [1506.03818].

[46] S. Franco, S. Lee and R.-K. Seong, *Brane Brick Models, Toric Calabi-Yau 4-Folds and 2d (0,2) Quivers*, *JHEP* **02** (2016) 047, [1510.01744].

[47] S. Franco, S. Lee and R.-K. Seong, *Brane brick models and 2d (0, 2) triality*, *JHEP* **05** (2016) 020, [`1602.01834`].

[48] S. Franco, S. Lee, R.-K. Seong and C. Vafa, *Brane Brick Models in the Mirror*, *JHEP* **02** (2017) 106, [`1609.01723`].

[49] S. Franco and R.-K. Seong, *Fano 3-folds, reflexive polytopes and brane brick models*, *JHEP* **08** (2022) 008, [`2203.15816`].

[50] M. Kho and R.-K. Seong, *On the master space for brane brick models*, *JHEP* **09** (2023) 150, [`2306.16616`].

[51] S. Franco, D. Ghim, G. P. Goulas and R.-K. Seong, *Mass deformations of brane brick models*, *JHEP* **09** (2023) 176, [`2307.03220`].

[52] M. Carcamo, S. Franco, D. Ghim, G. P. Goulas and R.-K. Seong, *Relevant Deformations, Brane Brick Models and Triality*, `2510.05517`.

[53] A. Higashitani and Y. Nakajima, *Deformations of Dimer Models*, *SIGMA* **18** (Apr., 2022) 030, [`1903.01636`].

[54] S. Franco and R.-K. Seong, *Twin theories, polytope mutations and quivers for GTPs*, *JHEP* **07** (2023) 034, [`2302.10951`].

[55] S. Cremonesi and J. Sá, *Zig-zag deformations of toric quiver gauge theories. Part I. Reflexive polytopes*, *JHEP* **05** (2024) 114, [`2312.13909`].

[56] I. R. Klebanov and E. Witten, *Superconformal field theory on three-branes at a Calabi-Yau singularity*, *Nucl. Phys. B* **536** (1998) 199–218, [`hep-th/9807080`].

[57] S. Gubser, N. Nekrasov and S. Shatashvili, *Generalized conifolds and 4-Dimensional N=1 SuperConformal Field Theory*, *JHEP* **05** (1999) 003, [`hep-th/9811230`].

[58] M. Bianchi, S. Cremonesi, A. Hanany, J. F. Morales, D. Ricci Pacifici and R.-K. Seong, *Mass-deformed Brane Tilings*, *JHEP* **10** (2014) 027, [`1408.1957`].

[59] G. Arias-Tamargo, S. Franco and D. Rodríguez-Gómez, *The geometry of GTPs and 5d SCFTs*, *JHEP* **07** (2024) 159, [`2403.09776`].

[60] S. Benvenuti, B. Feng, A. Hanany and Y.-H. He, *Counting BPS Operators in Gauge Theories: Quivers, Syzygies and Plethystics*, *JHEP* **11** (2007) 050, [`hep-th/0608050`].

[61] A. Hanany and C. Romelsberger, *Counting BPS operators in the chiral ring of N=2 supersymmetric gauge theories or N=2 braine surgery*, *Adv. Theor. Math. Phys.* **11** (2007) 1091–1112, [`hep-th/0611346`].

[62] A. Butti, D. Forcella, A. Hanany, D. Vegh and A. Zaffaroni, *Counting Chiral Operators in Quiver Gauge Theories*, *JHEP* **11** (2007) 092, [`0705.2771`].

[63] B. Feng, A. Hanany and Y.-H. He, *Counting gauge invariants: The Plethystic program*, *JHEP* **03** (2007) 090, [`hep-th/0701063`].

[64] A. Hanany, *Counting BPS operators in the chiral ring: The plethystic story*, *AIP Conf. Proc.* **939** (2007) 165–175.

[65] D. Forcella, A. Hanany, Y.-H. He and A. Zaffaroni, *The Master Space of N=1 Gauge Theories*, *JHEP* **08** (2008) 012, [`0801.1585`].

[66] D. Forcella, A. Hanany, Y.-H. He and A. Zaffaroni, *Mastering the Master Space*, *Lett. Math. Phys.* **85** (2008) 163–171, [`0801.3477`].

[67] A. Hanany and A. Zaffaroni, *The master space of supersymmetric gauge theories*, *Adv. High Energy Phys.* **2010** (2010) 427891.

[68] A. Hanany and R.-K. Seong, *Brane Tilings and Specular Duality*, *JHEP* **08** (2012) 107, [`1206.2386`].

[69] M. R. Douglas, B. R. Greene and D. R. Morrison, *Orbifold resolution by D-branes*, *Nucl. Phys. B* **506** (1997) 84–106, [`hep-th/9704151`].

[70] M. R. Douglas and G. W. Moore, *D-branes, quivers, and ALE instantons*, `hep-th/9603167`.

[71] K. Hori, A. Iqbal and C. Vafa, *D-branes and mirror symmetry*, `hep-th/0005247`.

[72] K. Hori and C. Vafa, *Mirror symmetry*, `hep-th/0002222`.

[73] K. Hori, S. Katz, A. Klemm, R. Pandharipande, R. Thomas, C. Vafa et al., *Mirror symmetry*, vol. 1 of *Clay mathematics monographs*. AMS, Providence, USA, 2003.

[74] P. Kasteleyn, *Graph theory and crystal physics*, *Graph theory and theoretical physics* (1967) 43–110.

[75] E. Witten, *Phases of N=2 theories in two-dimensions*, *Nucl. Phys. B* **403** (1993) 159–222, [`hep-th/9301042`].

[76] V. Jejjala, S. Ramgoolam and D. Rodriguez-Gomez, *Toric CFTs, Permutation Triples and Belyi Pairs*, *JHEP* **03** (2011) 065, [`1012.2351`].

[77] A. Hanany, V. Jejjala, S. Ramgoolam and R.-K. Seong, *Consistency and Derangements in Brane Tilings*, *J. Phys. A* **49** (2016) 355401, [`1512.09013`].

[78] A. Marshakov, *Lie Groups, Cluster Variables and Integrable Systems*, *J. Geom. Phys.* **67** (2013) 16–36, [`1207.1869`].

[79] V. V. Fock and A. Marshakov, *Loop groups, Clusters, Dimers and Integrable systems*, `1401.1606`.

[80] K. A. Intriligator, D. R. Morrison and N. Seiberg, *Five-dimensional supersymmetric gauge theories and degenerations of Calabi-Yau spaces*, *Nucl. Phys. B* **497** (1997) 56–100, [`hep-th/9702198`].

[81] O. Aharony, A. Hanany and B. Kol, *Webs of (p,q) five-branes, five-dimensional field theories and grid diagrams*, *JHEP* **01** (1998) 002, [`hep-th/9710116`].

[82] F. Benini, S. Benvenuti and Y. Tachikawa, *Webs of five-branes and N=2 superconformal field theories*, *JHEP* **09** (2009) 052, [0906.0359].

[83] P. Jefferson, H.-C. Kim, C. Vafa and G. Zafrir, *Towards classification of 5d SCFTs: Single gauge node*, *SciPost Phys.* **14** (2023) 122, [1705.05836].

[84] C. Closset, M. Del Zotto and V. Saxena, *Five-dimensional SCFTs and gauge theory phases: an M-theory/type IIA perspective*, *SciPost Phys.* **6** (2019) 052, [1812.10451].

[85] C. Closset and M. Del Zotto, *On 5D SCFTs and their BPS quivers. Part I: B-branes and brane tilings*, *Adv. Theor. Math. Phys.* **26** (2022) 37–142, [1912.13502].

[86] S. Franco and D. Rodriguez-Gomez, *Quiver tails and brane webs*, *JHEP* **10** (2024) 118, [2310.10724].

[87] A. Bourget, A. Collinucci and S. Schafer-Nameki, *Generalized Toric Polygons, T-branes, and 5d SCFTs*, *SciPost Phys.* **18** (2025) 079, [2301.05239].

[88] A. Hanany and E. Witten, *Type IIB superstrings, BPS monopoles, and three-dimensional gauge dynamics*, *Nucl. Phys. B* **492** (1997) 152–190, [hep-th/9611230].

[89] R. Donagi and E. Witten, *Supersymmetric Yang-Mills theory and integrable systems*, *Nucl. Phys. B* **460** (1996) 299–334, [hep-th/9510101].

[90] N. Nekrasov, *Five dimensional gauge theories and relativistic integrable systems*, *Nucl. Phys. B* **531** (1998) 323–344, [hep-th/9609219].

[91] A. Gorsky, S. Gukov and A. Mironov, *Multiscale N=2 SUSY field theories, integrable systems and their stringy / brane origin. 1.*, *Nucl. Phys. B* **517** (1998) 409–461, [hep-th/9707120].

[92] A. Gorsky and A. Mironov, *Solutions to the reflection equation and integrable systems for N=2 SQCD with classical groups*, *Nucl. Phys. B* **550** (1999) 513–530, [hep-th/9902030].

[93] A. Gorsky and A. Mironov, *Integrable many body systems and gauge theories*, hep-th/0011197.